



UNIVERSITÀ
di **VERONA**

UNIVERSITA' DEGLI STUDI DI VERONA

DEPARTMENT OF

Neuroscience biomedicine and movement sciences

GRADUATE SCHOOL OF

Health and life sciences

DOCTORAL PROGRAM IN

Applied life and health sciences

WITH THE FINANCIAL CONTRIBUTION OF

Ateneo-University of Verona

Cycle XXXII / year 2016

***Development of new edited cell models to analyze pros and cons
of the CRISPR/Cas9 technique***

S.S.D. Bio/11

Coordinator: Prof. Giovanni Malerba




Tutor: Prof. Donato Zipeto

Co-tutor Prof. Maria Grazia Romanelli

Doctoral Student: Dr. Simona Mutascio

Quest'opera è stata rilasciata con licenza Creative Commons Attribuzione – non commerciale
Non opere derivate 3.0 Italia . Per leggere una copia della licenza visita il sito web:

<http://creativecommons.org/licenses/by-nc-nd/3.0/it/>

-  **Attribuzione** Devi riconoscere una menzione di paternità adeguata, fornire un link alla licenza e indicare se sono state effettuate delle modifiche. Puoi fare ciò in qualsiasi maniera ragionevole possibile, ma non con modalità tali da suggerire che il licenziante avalli te o il tuo utilizzo del materiale.
-  **NonCommerciale** Non puoi usare il materiale per scopi commerciali.
-  **Non opere derivate** —Se remixi, trasformi il materiale o ti basi su di esso, non puoi distribuire il materiale così modificato.

*Development of new edited cell models to analyze pros and cons
of the CRISPR/Cas9 technique*

To my family

SOMMARIO

Il sistema CRISPR/Cas9 è un potente strumento di manipolazione del genoma. Dal 2012, la tecnica CRISPR/Cas9 è stata utilizzata per diverse applicazioni, dall'ingegnerizzazione delle piante, allo sviluppo di nuovi modelli *in vitro* e *in vivo* per lo studio di specifiche patologie.

Brevemente, la tecnica CRISPR/Cas9 basa la sua attività sulla presenza di una piccola guida a RNA in grado di dirigere l'endonucleasi Cas9 sulla sequenza genomica bersaglio dove introduce un taglio al doppio filamento di DNA. Il danno al DNA è poi riparato dai sistemi cellulari di ricombinazione non omologa e ricombinazione omologa. Il primo meccanismo congiunge le estremità interrotte del DNA con conseguenti inserzioni e/o delezioni casuali e viene principalmente utilizzato per ottenere knock out genici. La ricombinazione omologa, diversamente, permette il riparo del danno al DNA impiegando uno stampo, introducendo così specifiche e volute mutazioni nella sequenza genomica bersaglio.

Nel presente lavoro, abbiamo impiegato la tecnica CRISPR/Cas9 per analizzarne pro e contro sviluppando nuovi modelli *in vitro* utilizzati per studiare il coinvolgimento di specifici fattori in diverse patologie umane. In particolare infezioni virali, tumori e malattie neurodegenerative costituiscono un importante problema per la sanità pubblica. La tecnologia CRISPR/Cas9 ci ha permesso di generare nuovi modelli cellulari utili per indagare interazioni cellula-retrovirus, il coinvolgimento di specifiche proteine nella tumorigenesi e nella progressione tumorale, ma anche l'importanza di particolari proteine nell'insorgenza di malattie neurodegenerative.

Interazioni retrovirus-ospite

I due maggiori retrovirus umani, HIV-1 e HTLV-1, sono responsabili di importanti patologie nell'uomo, ma ancora oggi i meccanismi pato-molecolari sono sconosciuti. Per investigare come specifiche proteine cellulari modulano l'infezione da HIV-1, la tecnica CRISPR/Cas9 è stata impiegata per sviluppare

nuove cellule di packaging virale difettive per le proteine ACOT8, HDAC6 e HLA-C.

Per indagare il meccanismo molecolare esercitato dalla proteina virale di HTLV-1 Tax1, e il coinvolgimento del fattore cellulare TRAF3, nella deregolazione della trasduzione del segnale di NF- κ B, la tecnica CRISPR/Cas9 è stata applicata per lo sviluppo di una linea cellulare KO per TRAF3.

Malattie tumorali

Il melanoma e l'adenocarcinoma del pancreas sono tra i tumori più frequenti nella popolazione.

Per analizzare il potenziale oncogenico della proteina RUNX2 e il suo coinvolgimento nello sviluppo e nella progressione del melanoma, la tecnologia CRISPR/Cas9 è stata impiegata per lo sviluppo di una linea cellulare RUNX2 KO. Per chiarire il ruolo della proteina GNA15 nel meccanismo molecolare responsabile dell'insorgenza dell'adenocarcinoma del pancreas, è stato generato un modello cellulare di adenocarcinoma pancreatico GNA15 KO.

Malattie neurodegenerative

I disordini neurodegenerativi stanno diventando sempre più frequenti, specialmente a causa dell'aumentata età media della popolazione. Al giorno d'oggi non sono disponibili terapie risolutive.

Per investigare il meccanismo molecolare con cui la proteina GPR3 induce la deposizione di placche β amiloidi, la tecnica CRISPR/Cas9 è stata impiegata per produrre una linea cellulare di neuroglioma GPR3 KO, caratterizzata dalla mutazione Swe, tipica dell'Alzheimer familiare.

Per comprendere pienamente il coinvolgimento di PPT1 nella lipofusinosi ceroidi neuronale, il sistema CRISPR/Cas9 è stato impiegato per lo sviluppo di una linea cellulare di neuroblastoma PPT1 KO.

Nel presente lavoro, sono discussi pro e contro della tecnica CRISPR/Cas9, con particolare riguardo ai suoi potenziali limiti, quali effetti off-target, la manipolazione *in vitro* del genoma, i sistemi di veicolo del sistema CRISPR/Cas9 e le tecniche di screening.

Come ogni rivoluzione tecnologica, il sistema CRISPR/Cas9 è attualmente al centro di un acceso dibattito che coinvolge scienziati e ricercatori nel tentativo di stabilire un codice etico e dettare delle linee guida per il suo impiego nella terapia genica, nella manipolazione della linea germinale e di embrioni umani.

ABSTRACT

The CRISPR/Cas9 system is a powerful genome-editing tool and its great potential is thoroughly recognized. CRISPR/Cas9 has been applied in several fields, such as plant engineering, development of new cell lines, and animal models.

CRISPR/Cas9 exploits a small single guide RNA to direct the Cas9 endonuclease activity against a specific genome sequence, where it introduces a double strand break. The DNA damage is then repaired by the non-homologous end joining or the homology direct repair processes. While the first one allows a gene knock out, the homology direct repair bases its activity on a repair template, thus allowing the introduction of specific modification within a gene target.

In the present work, we aimed to analyze the pros and cons of the CRISPR/Cas9 system by developing new edited cell models, that will be useful to study the involvement of specific factors in different human diseases. Particularly, viral infections, cancer diseases, and neurodegenerative disorders represent a major issue for public health.

The CRISPR/Cas9 system was fundamental to develop new cell lines useful to study host-retrovirus interaction, the involvement of specific proteins in tumorigenesis and cancer progression, and the importance of particular proteins in the onset of neurodegenerative disorders.

Retroviral infection: host-virus interaction

HIV-1 and HTLV-1 represent the two major human retroviruses. To assess how specific host proteins modulate HIV-1 infection, different 293T packaging cell lines were developed. Specifically, CRISPR/Cas9 was used to produce 293T ACOT8, HDAC6 Δ BUZ, and HLA-C KO cell lines.

To investigate the involvement of TRAF3 in the deregulation of the NF- κ B pathway mediated by the HTLV protein Tax1, a TRAF3 KO cell model was developed.

Cancer diseases

Malignant melanoma and pancreatic cancer are two of the most frequent morbidities.

To analyze the oncogenic potential of RUNX2 in the development and progression of malignant melanoma, the Mel-HO RUNX2 KO melanoma cell line was developed through CRISPR/Cas9.

To clarify the role of GNA15 in the molecular mechanisms leading to pancreatic adenocarcinoma, CRISPR/Cas9 was employed to generate PT45 GNA15 KO adenocarcinoma cells.

Neurodegenerative diseases

Neurodegenerative disorders are becoming even more frequent especially due to the increase in the average age of the population. Nowadays no effective cures are available.

To understand the molecular mechanism by which GPR3 induces amyloid β deposition in Alzheimer's disease, CRISPR/Cas9 was used to develop H4 Swe GPR3 KO neuroglioma cells.

To fully investigate the involvement of the palmitoyl-protein thioesterase 1 PPT1, in the neuronal ceroid lipofuscinoses neurological disorder, SH-SY5Y PPT1 KO neuroblastoma cell line was developed.

The CRISPR/Cas9 pros and cons are analyzed for a full technique understanding, with particular regard to its potential limits, such as off-targets, *in vitro* genome manipulation, delivery systems, and editing screening.

As any technology revolution, CRISPR/Cas9 represents the linchpin of fierce debates involving many scientists and researchers to regulate its employment for gene therapy, germline, and human embryos manipulation.

INDEX

1. INTRODUCTION.....	1
1.1 Genome manipulation	1
1.2 Artificial restriction enzymes: ZFNs and TALENs	2
1.3 Brief history: discovery of the CRISPR/Cas9 system, a case of serendipity, from the dairy industry to biotechnology.....	5
1.4 Classification of CRISPR/Cas system	6
1.5 CRISPR/Cas adaptive immune system in prokaryotes	7
1.6 CRISPR/Cas9 system engineering.....	10
1.6.1 CRISPR/Cas9 as a genome editing tool.....	11
1.6.2 CRISPR/Cas9 system for eukaryotic genome engineering.....	12
1.7 Development of alternative CRISPR/Cas systems	15
1.7.1 Engineering of CRISPR/Cpf1 (Cas12a).....	15
1.7.2 Engineering of CRISPR/C2c2 (Cas13a)	16
1.8 CRISPR/Cas9 delivery systems	18
1.9 Application of CRISPR/Cas9 system.....	21
1.9.1 CRISPR/Cas9 in cancer	22
1.9.2 CRISPR/Cas9 against viral infections	22
1.9.3 CRISPR/Cas9 in neurological disorders	23
1.10 CRISPR/Cas9 for gene editing.....	24
1.11 Ethical concerns in genome editing	25
2. MATERIALS AND METHODS	24

Buffers and solutions.....	24
Cell culture	26
Vectors	27
sgRNA design and cloning.....	27
sgRNA off-targets prediction.....	27
Polymerase chain reaction (PCR) for sequencing.....	28
Transfection.....	28
Production of pseudoviruses and infection	28
RNA extraction and Real-Time PCR.....	29
Flow cytometry analysis of HLA-C cell surface expression	29
Flow cytometry analysis of HLA-C binding stability to β_2 microglobulin	30
Immunofluorescence analysis	30
Western Blot analyses	30
Primary antibodies	31
HLA-C genotyping.....	32
Statistical Analyses	32
3. AIM OF THE THESIS	34
4. RESULTS.....	35
4.1 CRISPR/Cas9 to study host-retrovirus interaction	36
4.1.1 HIV-1 – host factors interaction.....	36
Development of ACOT8 KO cell lines to study the HIV-1 Nef/ACOT8 interaction in HIV-1 infection.....	37
Development of HDAC6 edited cell lines to study the role of HDAC6 in HIV-1 infection	40

a) Development of 293T HDAC6 KO cell line	41
b) Development of 293T HDAC6 Δ BUZ cell line	43
Development of HLA-C KO cell line to study the involvement of the different HLA-C variants in HIV-1 infection outcome.....	45
4.1.2 HTLV-1 – host factors interaction	52
4.2 CRISPR/Cas9 to study cancer diseases.....	56
4.2.1 Development of RUNX2 KO cell line to study its involvement in malignant melanoma	56
4.2.2 Development of GNA15 KO cell line to study its involvement in pancreatic carcinoma.....	59
4.2.3 CRISPR/Cas9 to study the involvement of PTPRG in Chronic myeloid leukemia	63
4.3 CRISPR/Cas9 to study neurological disorders	66
4.3.1 Development of PPT1 KO cell line to investigate its involvement in CLN1 disease	66
4.3.2 CRISPR/Cas9 to study the involvement of GPR3 in Alzheimer’s disease	69
5. DISCUSSION	74
5.1 CRISPR/Cas9 targeted cell lines.....	74
5.2 CRISPR/Cas9 delivery.....	76
5.3 Evaluation of Cas9 off-target activity	77
5.4 Screening of CRISPR/Cas9-edited cells	81
5.5 Final considerations	83
BIBLIOGRAPHY	86

ACKNOWLEDGEMENTS.....	118
ATTACHMENTS	119

ABBREVIATIONS

A20	TNF Alpha Induced Protein 3
AAV	Adeno-associated viral
ABL	Abelson gene
ACOT8	Acyl-CoA Thioesterase 8
AD	Alzheimer's disease
ADC	AIDS dementia complex
AIDS	Acquired immune deficiency syndrome
AKT/PKB	Protein Kinase B
ANXA1	Annexin A1
APOBEC3G	Apolipoprotein B mRNA editing enzyme catalytic subunit 3G
APP	β -amyloid precursor
AsCas12a	<i>Acidaminococcus</i> species Cas12a
ATLL	Adult T-cell Leukemia/Lymphoma
A β	amyloid- β
BAFF	B-cell Activating Factor
BCL2	B-cell lymphoma 2
BCR	breakpoint cluster region
BLESS	Breaks labeling enrichment on streptavidin and next generation sequencing
BUZ	Bound to ubiquitin zinc finger
CAR	Chimeric antigen receptor
CCL20	C-C motif chemokine ligand 20
CCR5	C-C chemokine receptor type 5
CD40L	CD40 ligand
CFTR	Cystic fibrosis transmembrane conductance regulator
CIRCLE-Seq	Circularization for in vitro reporting of cleavage effects by sequencing
CLN	ceroid lipofuscinosis
CML	Chronic Myeloid Leukemia
CNS	Central nervous system

CRISPR/Cas	Clustered Regularly Interspaced Short Palindromic Repeats/CRISPR associated genes
crRNA	CRISPR RNA
CSF	Cerebrospinal fluid
Cul5	Cullin 5
CXCL5	C-X-C Motif Chemokine Ligand 5
CXCR4	C-X-C motif chemokine receptor 4
DDR	DNA damage repair
DSB	Double strand break
EDNRA	Endothelin Receptor Type A
EGFR	Epidermal Growth Factor Receptor
EMT	Epithelial-Mesenchymal Transition
Env	Envelope
ERK	Extracellular signal regulated kinase
EV	Extracellular vesicles
F2R	Coagulation Factor II Thrombin Receptor
FAK	Focal adhesion kinase
FDA	Food and drug administration
FKBP12	Peptidyl-prolyl cis-trans isomerase
FRB	FKBP-Rapamycin Binding Domain
Gag	Group Antigens
GFP	Green fluorescent protein
GNA15	G Protein subunit alpha 15
gp41	Glycoprotein 41
gp120	Glycoprotein 120
GPCR	G protein coupled receptors
GPR3	G protein coupled receptor 3
GPR6	G protein coupled receptor 6
GPR12	G protein coupled receptor 12
HAND	HIV-associated neurocognitive disorders
HBZ	HTLV-1 bZIP factor
HDAC6	Histone Deacetylase 6

HDR	Homologous Direct Repair
HEPN	Higher eukaryotes and prokaryotes nucleotide
HIF	Hypoxia-inducible factor 1
HIV-1	Human Immunodeficiency Virus-1
HLA-A	Human Leukocyte Antigen-A
HLA-B	Human Leukocyte Antigen-B
HLA-C	Human Leukocyte Antigen-C
hPSCs	human Pluripotent Stem Cells
HTLV-1	Human T-lymphotropic virus-1
HTR2C	Hydroxytryptamine receptor 2c
IDT	Integrated DNA technologies
IL-1	Interleukin-1
IL-6	Interleukin
KO	Knock out
Lamp2	Lysosome associated membrane protein 2
LentiSLICES	Self-Limiting Cas9 circuitry delivered through a lentiviral vector for Enhanced Safety and specificity
LPAR6	Lysophosphatidic Acid Receptor 6
LPS	Lipopolysaccharides
LTR	Long terminal repeats
LV	Lentiviral
MAPK	Mitogen activated protein kinase
MHC I	Major histocompatibility complex-I
MHC-II	Major histocompatibility complex-II
MIT	Massachusetts institute of technology
MLV	Murine Leukemia Virus
MM	Multiple myeloma
NCL	Neuronal ceroid lipofuscinoses
Nef	Negative regulatory factor
NF-kB	Nuclear factor kappa light chain enhancer of activated B cells
NanoMEDIC	Nanomembrane-derived extracellular vesicles for the delivery of macromolecular cargo

NGS	Next generation sequencing
NHEJ	Non homologous end joining
NIK	NF-kB Inducing Kinase
NK	Natural killer
NLS	Nuclear Localization Sequence
NMDA	N-methyl D-aspartate
NMDARs	N-methyl-d-aspartate receptors
NMU	Neuromedin U
PAM	Protospacer adjacent motif
PBMC	Peripheral blood mononuclear cell
PD-L1	Programmed death-ligand 1
PDAC	Pancreatic ductal adenocarcinoma
PFS	Protospacer flanking sequences
PI-3	Phosphatidyl inositol 3
PI3K	Phosphoinositide 3-kinase
PKC	Protein kinase C
PKD	Protein kinase
PKD1	Protein kinase D1
PNKP	Polynucleotide kinase/phosphatase
Pol	Polymerase
PPT1	Palmitoyl protein thioesterase 1
PTEN	Phosphatase and tensin homolog
PTGER2	Prostaglandin e receptor 2
PTK2	Protein tyrosine kinase 2
PTP	Protein tyrosine phosphatase
PTPRG	Protein tyrosine phosphatase receptor type G
RLP0	Ribosomal Protein Lateral Stalk Subunit P0
RMD	Rhythmic movement disorder
RNAi	RNA interference
RNP	Ribonucleoprotein
RUNX1	Runt related transcription factor 1
RUNX2	Runt related transcription factor 2

RUNX3	Runt related transcription factor 3
saCas9	<i>Staphylococcus aureus</i> Cas9
SCD	Sickle Cell Disease
sgRNA	Single guide RNA
spCas9	<i>Streptococcus pyogenes</i> Cas9
STAT3	Signal transducer and activator of transcription 3
STMN1	Stathmin 1
TALE	Transcription activator-like effector
TALEN	Transcription activator-like effector nucleases
TCID50	Tissue Culture Infectious Doses 50
TDT	Transfusion-dependent β -thalassaemia
TKIs	Tyrosine kinase inhibitors
TLN1	Talin 1
TNF	Tumor necrosis factor
TNF- α	Tumor necrosis factor- α
TRAC	T Cell Receptor Alpha Constant
TracrRNA	Transactivating RNA
TRAF	TNF receptor-associated factor
TRAF3	TNF receptor-associated factor 3
TSP/HAM	Tropical Spastic Paraparesis/HTLV-1 Associated Myelopathy
VEGF	Vascular endothelial growth factor
Vif	Virion infectivity factor
WHO	World Health Organization
XRCC4	X-ray repair cross complementing 4
ZF	Zinc finger
ZFN	Zinc finger endonucleases
ZFP	Zinc finger protein
β -arr2	β -arrestin 2
β 2m	β 2-microglobulin

1. INTRODUCTION

1.1 Genome manipulation

The major challenge in biomedicine is the development of an optimal and safe system for gene manipulation, to study specific gene mutations responsible for human pathologies, and to correct gene alterations causing disease.

Many efforts have been directed to develop new biological tools to manipulate the human genome directly within cells and tissues affected by pathologies.

Gene therapy exploits delivery vectors for inserting nucleic acid into cells to correct genome alterations causing pathological conditions. Based on delivery vectors, the exogenous nucleic acid remains in an episomal form or integrates into the host DNA (Kay 2011).

Gene modifications can be obtained through different mechanisms: gene addition, gene substitution, and gene ablation. Gene addition is used to supply a specific functional gene into the host. Gene substitution allows the replacement of a defective gene with a wild type and functional one. Gene ablation avoids or reduced protein expression (Kay 2011).

Gene therapy techniques, such as RNA interference (RNAi), Zinc Finger Nucleases (ZFNs), Transcription Activator-Like Effector Nucleases (TALENs), and the promising Clustered Regularly Interspaced Short Palindromic Repeat (CRISPR)/CRISPR-associated genes (Cas), represent a great promise in biomedicine research, although they have different limitations for their successful employment. Particularly, RNA interference is limited to mRNA knockdown, thus circumscribing its usage only to pathological conditions that get benefits by gene expression reduction (Cox, Platt, and Zhang 2015). Moreover, RNAi may display low target specificity, making the treatment unsafe and risky (Jackson and Linsley 2010). In gene therapy, enzymes able to modify the target genome are widely used. To reach this aim, the most employed are ZFNs, TALENs, and the promising CRISPR/Cas technique (Chandrasegaran and Carroll 2016).

From the discovery of the CRISPR/Cas9 system and its engineering for biomedical applications, a real revolution has begun.

1.2 Artificial restriction enzymes: ZFNs and TALENs

Restriction endonucleases are not suitable for direct manipulation of genomic DNA since they recognize a sequence of only 4-8 bp, that frequently occur in most genomes. For instance, the human genome, having a length of 3×10^9 bp, would undergo different undesired cleavages, due to the repetition of the short sequence recognized by restriction enzymes (Chandrasegaran and Carroll 2016).

In the past years, artificial restriction enzymes have been developed, to bypass repetitive cleavages within the target genome, thus increasing their specificity (Bhakta et al. 2013).

Typically, a restriction enzyme shows a dual function for the presence of a DNA binding domain, to recognize the target sequence, and a DNA restriction domain, exerting the catalytic function introducing a DBS (Chandrasegaran and Carroll 2016). These two functions overlap creating issues for genome manipulation. To bypass this problem, artificial restriction enzymes were generated, based on Type IIS FokI endonuclease. FokI recognizes the non-palindromic sequences 5'-GGATG-3' and 5'-CATCC-3' and cleaves 12-13 bp downstream the duplex target DNA.

The crystal structure of FokI was published in 1998 by Wah et al., showing that this endonuclease can form a catalytically active restriction domain only as homodimer and that at the interface between the two monomers is formed the pocket holding the target DNA (Wah et al. 1998).

ZFNs are constituted of ZF moieties, each one composed of 30 aminoacids, where the Cys₂His₂ motif forms a $\beta\beta\alpha$ structure stabilized by a zinc cation (Pavletich and Pabo 1991). Each ZF binds DNA in the major groove where recognizes selectively 3-4 bp. Consequently, to ensure high specificity and avoid undesired off-target cleavages, ZFNs are built in a modular assembly of 3 or 4 ZF domains, and since each one recognizes a sequence of 3-4 bp, each ZF monomer can recognize 12 bp, increasing the specificity.

The crystal structure clarified that for ZFN assembly it is necessary to maintain unaltered the backbone, modifying just the aminoacids in the α helix to change the ZFN specificity. Accordingly, Zinc Finger Proteins (ZFPs) design is carried on in

a context-dependent manner to ensure the optimal recognition of the target sequence.

To generate new ZFNs two strategies can be applied: the sequential and the bipartite techniques.

The sequential selection needs ZFP libraries, identifying each ZF in a context-dependent manner for a modular assembly (Greisman and Pabo 1997). The bipartite approach is based on two ZFP libraries, selecting the N-terminal part of the ZFP using one library, instead, the C-terminal is selected with the other one (Moore, Klug, and Choo 2001). Both the selection methods are based on a phage display, so the ZFP detection requires several rounds of analyses. An alternative strategy of ZFNs construction occurs in an *in vivo* strategy based on bacterial or yeast one- or two-hybrid system (Chandrasegaran and Carroll 2016; Joung, Ramm, and Pabo 2000).

Once ZFPs are assembled, they are fused to the FokI cleavage domain, obtaining a catalytic functional ZFN.

As shown in Figure 1.1, to obtain a DSB, two ZFNs are fused, to ensure the right orientation of the restriction site within the target genome (Smith et al. 2000).

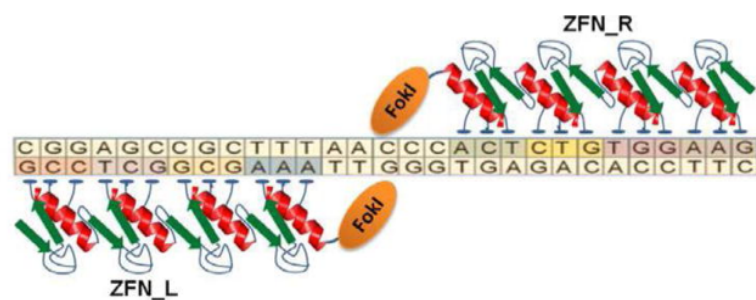


Figure 1.1: ZFN is assembled by fusing both the FokI nucleases to one ZFN, referred to ZFN_L and ZFN_R, each one constituted of 4 ZFPs. Each ZFP is able to recognize 3 nucleotide into the target genome (Ramalingam et al 2013).

Moscou MJ and Boch in 2009 discovered the transcription activator-like effector (TALE) from *Xanthomonas* bacteria. Based on the TALE DNA binding module, transcription activator-like effector endonucleases (TALEN) have been engineered fusing each DNA binding portion to the FokI endonuclease (Figure 1.2), resulting in a DNA artificial endonuclease.

Each TALE motif is formed by 33-34 aminoacids and each one recognizes a single nucleotide (Figure 1.2). As ZFNs, TALENs are generated in a modular way, but while ZFNs recognize the target DNA using the ZF domain, the TALENs DNA binding domain is based on the TALE motif. A common feature between these two artificial restriction enzymes is the FokI endonuclease activity (Deng et al. 2012). Different groups have shown that ZFNs and TALENs cleavage efficiencies are comparable, instead, the cytotoxicity typical of ZFNs, due to the off-target effects, is reduced with TALENs (Ramalingam et al. 2013, 2014), however, since TALENs are three times larger than ZFNs (Chandrasegaran and Carroll 2016), their employment may be cytotoxic.

ZFNs and TALENs are assembled in a modular way, making their production not only extremely difficult but also time-consuming. Instead, the most recent CRISPR/Cas9 system results easier and more effective, and for its employment only the Cas9 endonuclease and a short single strand RNA are required.



Figure 1.2: The TALEN modular assembly is obtained by fusing both the FokI endonucleases to two TALE motifs, i.e. TALEN_L and TALEN_R. Each TALE motif is constituted of 33-34 aminoacids, represented by squares, each one able to recognize a specific nucleotide within the target genome (Ramalingam et al 2013).

1.3 Brief history: discovery of the CRISPR/Cas9 system, a case of serendipity, from the dairy industry to biotechnology

The history of clustered regularly interspaced short palindromic repeat (CRISPR)/CRISPR-associated genes (Cas) began at the end of the '80s when, independently, different research groups found in bacteria and archaea unknown repeated sequences. In 1987, in Japan, while Ishino et al. were studying iap (alkaline phosphatase isozyme) isozyme conversion activity of alkaline phosphatase, they found a particular sequence-structure flanking the 3' end of the iap gene in *Escherichia coli* K12. Specifically, five homologous repeated sequences of 29 nucleotides were found interspaced by variable sequences (Ishino et al. 1987).

In 1989, in Santa Pola, Spain, Mojica et al. were analyzing the salt tolerance of the archaeal microbe *Haloferax mediterranei*. It was known that in the presence of high salt concentration in the growth medium, *H. mediterranei* genome underwent restriction. The analyses of those fragments revealed a particular structure: they were constituted by multiple palindromic copies of 30 nucleotides, divided by variable sequences of 36 nucleotides (Mojica, Juez, and Rodriguez-Valera 1993). The same repeated structure was also found in other archaea and bacteria.

In 2000 Horvath, during its Ph.D. studies in Dange'-Saint-Romain, France, was studying lactic acid bacteria, such as *Streptococcus thermophilus*, used in the dairy industry for cheese and yogurt production. Its efforts were especially focused to develop DNA-based methods to bypass phage infection compromising dairy derivatives production. Soon it was clear the existing correlation between the variable sequence found in many archaea and bacteria and the resistance against phage infection. By performing structural and functional analyses of CRISPR associated (Cas) genes, their crucial role in the resistance against phages became clear, suggesting that CRISPR/Cas system originally evolved in archaea, and then it was horizontally transmitted to bacteria (Makarova et al. 2006).

Its molecular mechanism was unclear until 2007. To finally prove that CRISPR is a bacterial acquired immune system against bacteriophages, two different *S. thermophilus* strains were infected by two different phages. Bacteria able to counteract phage infection were isolated and through sequencing of CRISPR loci,

it has become clear that the variable sequences found in many archaea and bacteria derived from phage genomes. Researchers started to think that these phage-derived sequences were probably responsible for prokaryotic resistance against phage infection. The demonstration of CRISPR locus and phage resistance correlation was finally obtained by removing these integrated viral sequences from CRISPR locus, and observing that bacteria lost their ability to counteract phage infection. In prokaryotes, CRISPR/Cas is defined as an adaptive immune systems, due to their function in fighting viral infection (Barrangou et al. 2007).

From discovery and understanding the CRISPR system, its great potential became immediately clear for biomedical applications.

1.4 Classification of CRISPR/Cas system

Over the year, different efforts have been directed to discovery different kinds of CRISPR/Cas systems (Figure 1.3).

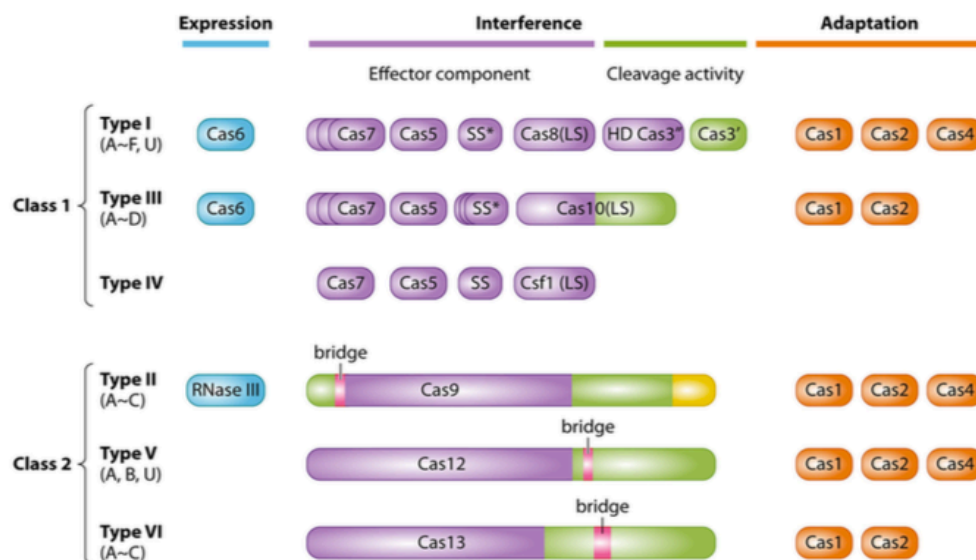


Figure 1.3: Based on the sequence analyses and Cas genes organization, two major classes of CRISPR/Cas can be identified, depending on the effector complex. Class 1 includes CRISPR/Cas Type I, III, and IV; class 2 includes CRISPR/Cas types IV and V. each type of CRISPR/Cas presets different Cas protein for the interference process and the adaptation (Ishino et al., 2018).

Nowadays, 6 types of CRISPR/Cas systems are known. Based on the encoded Cas protein effectors, these systems are grouped into two main classes (Burstein et al. 2017).

Each class includes 3 types of CRISPR/Cas systems: types I, III and IV are grouped in class 1, instead type II, V and VI are grouped in class 2. CRISPR/Cas type I, II and III present specific signatures: type I is characterized by Cas3 effector, type II by Cas9, and type III by Cas10. Type I and III share a common architecture of effector complexes referred to as CRISPR-associated complex for antiviral defense (Cascade) and the Csm/Cmr complexes, respectively (Makarova et al. 2011). Also, each CRISPR/Cas type is distinguished into different subtypes for the presence of additional characteristic genes (Koonin, Makarova, and Zhang 2017).

The simple architecture of the CRISPR/Cas system class 2 has represented a starting point for the development of new genome engineering technology. Indeed, the most studied and used Cas proteins for genome editing belong to class 2: the type II Cas9, both the type V Cas12a (Cpf1) and Cas12b (C2c1), and both the type VI Cas13a (C2c2) and Cas13b (C2c3) (Shmakov et al. 2017).

1.5 CRISPR/Cas adaptive immune system in prokaryotes

Typically, a CRISPR locus shows a well-conserved architecture (Figure 1.4).

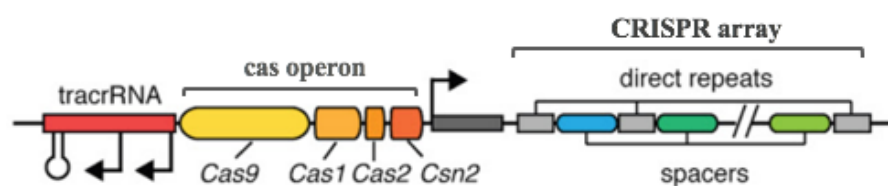


Figure 1.4: A CRISPR locus is composed of tracrRNA; Cas operon, encoding for Cas proteins involved in interference and adaptation processes; CRISPR array, formed by spacers, deriving from phage genome, and direct repeats (modified from Cong et al., 2013).

Starting from the 5' end, the CRISPR locus is composed by the noncoding transactivating RNA (tracrRNA), necessary for the processing of the CRISPR RNA (crRNA) in short RNA sequences (Garneau et al. 2010); the Cas operon, encoding the Cas effector proteins; the CRISPR array, formed by repeated sequences, referred to as direct repeats, interspaced by short spacers, variable sequences derived from phage protospacers, due to the acquisition machinery encoded by Cas operon (Cas1, Cas2, Csn2) (Jiang and Doudna 2017).

When a phage infects a bacterium, injects its genome into the host. Archaea and bacteria counteract viral infections disrupting the phage DNA through restriction enzymes, thus producing small fragments of the viral genome. Whether bacteria survive to this first infection acquire a sort of immunity against this specific phage. In detail, stretches of the viral genome, called protospacers, are inserted into the bacterial genome, becoming part of the CRISPR locus, within the CRISPR array, as spacers. To acquire phage genome portions, they need to be flanked by a protospacer adjacent motif (PAM). The PAM sequence is unique for each type of CRISPR system.

As shown in Figure 1.5, this adaptive immune system can be summarized in three steps: 1) immunization against specific phage, 2) expression of CRISPR/non-coding RNA effectors, and 3) defense itself leading to viral DNA degradation.

- 1) First, when a bacterium is infected by a bacteriophage, the viral genome is released into the host. Short viral genome sequences, called protospacers, flanked by PAM motif, are cleaved and incorporated into the CRISPR locus as spacers, providing a memory of phage infection (Amitai and Sorek 2016).
- 2) The second step leads to the expression of the CRISPR locus. In this phase, the CRISPR-precursor (pre-crRNA), transcribed from spacer sequences is processed through different cleavages, generating a mature crRNA able to form complex with tracrRNA and Cas protein effector (Brouns et al. 2008).
- 3) The third step occurs when the bacterium is newly infected by the same phage. tracrRNA/crRNAs/Cas function as surveyor complexes, able to recognize the viral genome injected again into the host. Thanks to this recognition, carried out by base pairing between spacers, included in the tracrRNA/crRNAs/Cas complexes, and viral protospacers, the Cas effector

proteins mediate the degradation of the invading genome (Garneau et al. 2010).

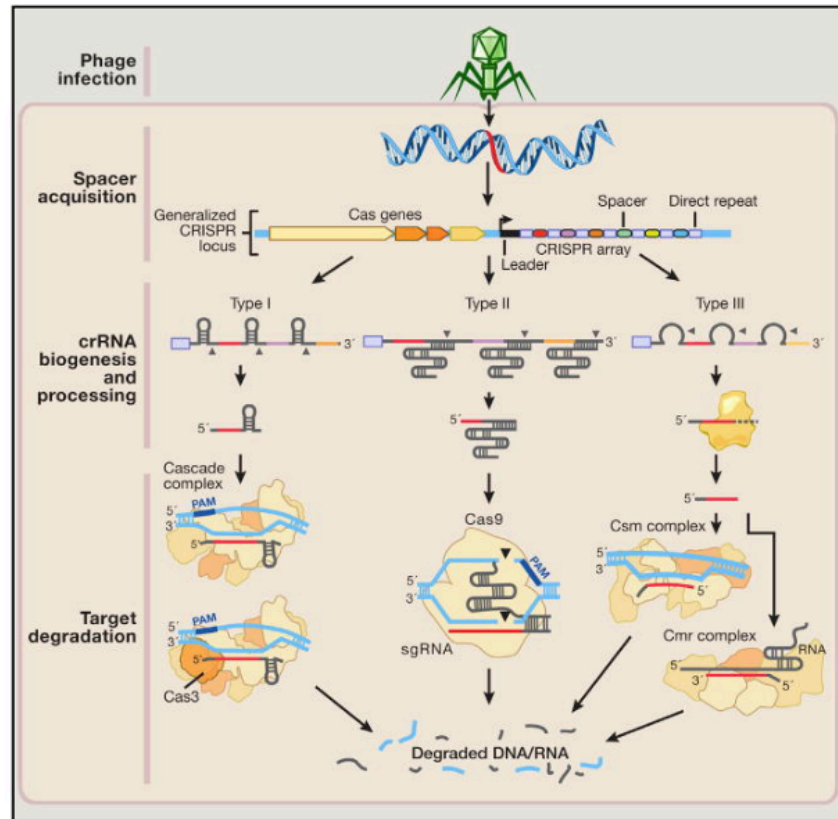


Figure 1.5: Following the entry of a phage genome into a bacterium, the CRISPR/Cas immune adaptive response is carried out in three steps. Spacer acquisition is the first step, shown at the top, when portions of the phage genome (protospacers) are acquired into the CRISPR array as spacers. The second step, in the middle, is the crRNA biogenesis and processing, that leads to the CRISPR locus expression producing surveyor complexes composed of Cas effector proteins and sgRNA. The third step, at the bottom, is the target degradation, indeed wheatear a surveyor complex recognizes an invading viral genome, thanks to sgRNA-phage genome base pairing, the CRISPR/Cas immune response leads to viral genome degradation (from Hsu et al., 2014).

1.6 CRISPR/Cas9 system engineering

The most known CRISPR/Cas system is the CRISPR/Cas9 type II, extensively studied from *Streptococcus pyogenes*, characterized by the NGG-trinucleotide protospacer adjacent motif (PAM), meaning that *S. pyogenes* can mediate its defense against phage infection by incorporating in its genome protospacers adjacent to the NGG PAM. Structurally, spCas9 is composed of a recognition (REC) lobe, which is able to recognize the target DNA, and by a nuclease (NUC) lobe, containing both HNH and RuvC nuclease domains, and PAM interacting (PI) domain (Figure 1.6). The endonuclease spCas9 works in a crRNA-dependent manner: indeed thanks to the crRNA it is guided at the target sequence, recognized through the REC lobe and the PI domain. Once the target is recognized and the PAM sequence is individuated, HNH and RuvC endonuclease domains cleave the foreign target genome (Nishimasu et al. 2014).

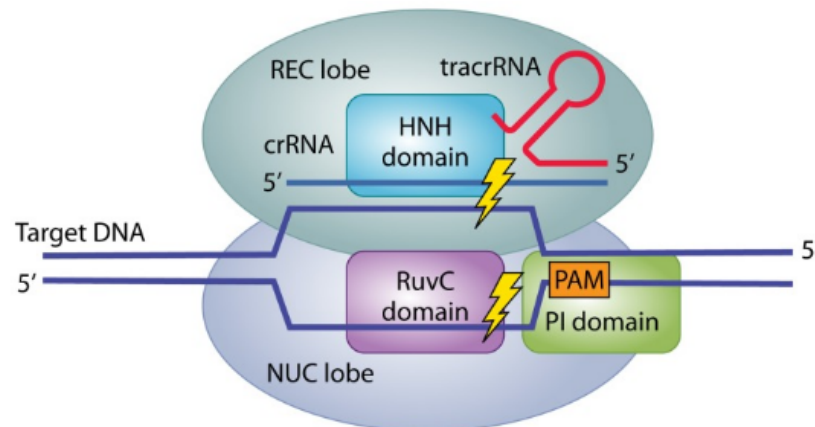


Figure 1.6: The Cas9-crRNA-tracrRNA complex binds the DNA target. The Cas9 consists of REC (recognition) and the NUC (nuclease) lobes. The REC lobe allows DNA recognition, instead, the NUC lobe holds the HNH and RuvC nuclease domains and a PAM-interacting (PI) domain. The DNA is cleaved by HNH and RuvC nuclease domains (Ishino et al., 2018).

1.6.1 CRISPR/Cas9 as a genome editing tool

The CRISPR/Cas9 system quickly replaced artificial restriction enzymes for genome engineering. As ZFNs and TALENs, CRISPR/Cas9 introduces DSB at the target locus, due to the spCas9 endonuclease activity. The DNA damage is then repaired by NHEJ or HDR. The CRISPR/Cas9 system would work in mammalian cells just engineering spCas9. Specifically, spCas9 needs to translocate into the nucleus and, to replace the spacer function, a 20 nt single guide RNA (sgRNA) has to be provided to the endonuclease to direct its activity. It has been reported that tracrRNA, crRNA, and Cas9 are fundamental for an efficient DNA target breaking (Gasiunas et al. 2012; Jinek et al. 2012).

Zhang and coworkers improved the CRISPR/Cas9 system to allow gene manipulation. To this aim, Cong, in 2013, has extensively analyzed how to employ this prokaryotic system in mammalian cells. By fusing the Cas9 coding region to two nuclear localization sequences (NLS), the Cas9 activity can be efficiently directed into the nucleus. Moreover, the reconstitution of CRISPR non-coding RNA and tracrRNA were placed under the U6 promoter to express the pre-crRNA containing also the single guide RNA (sgRNA). Since spCas9 recognizes the target genome via Watson-Crick base pairing, it is indispensable to design the sgRNA immediately adjacent to an NGG-PAM sequence. It was demonstrated that, for an optimal genome editing in human cells, just these three elements were required (Cong et al. 2013).

Ran and colleagues in 2013 published guidelines to use CRISPR/Cas9 all-in-one plasmid (Figure 1.7).

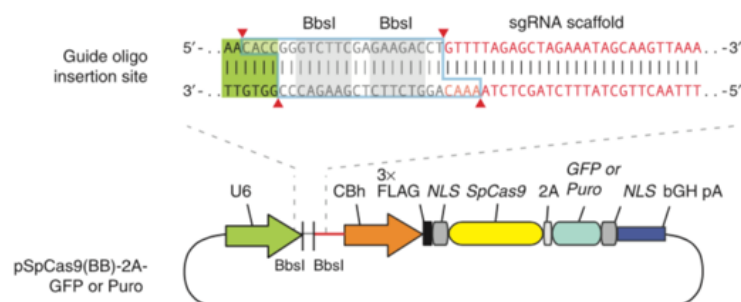


Figure 1.7: Schematic representation of the sgRNA cloned into a Cas9 expressing plasmid (pSpCas9(BB)-2A-GFP/Puro; Ran et al., 2013).

The pSpCas9(BB)-2A-GFP/Puro vector encodes SpCas9 fused to two NLS and it is characterized by the U6 RNA polymerase promoter controlling both sgRNA and gRNA scaffold expression, which replaces the CRISPR non-coding RNAs, necessary for Cas9/sgRNA proper assembly (Ran et al. 2013). The feasibility to manipulate a target genome has become easier and quicker compared to the development of modular ZFNs and TALENs, indeed it needs the design of an appropriate sgRNA, based on the target sequence, cloned into the Cas9 expressing vector and, lastly, provided to the cells.

1.6.2 CRISPR/Cas9 system for eukaryotic genome engineering

It is possible to direct the Cas9 endonuclease activity against a specific gene of interest, simply by providing to the nuclease an appropriate sgRNA. The sgRNA is 20 nt length and its sequence is complementary to the target genome sequence. Many *in silico* tools have been developed for sgRNA design, such as guide design resources, IDT Integrated DNA Technologies (https://eu.idtdna.com/site/order/designtool/index/CRISPR_SEQUENCE), and CHOPCHOP (<https://chopchop.cbu.uib.no/>). These tools share a common workflow for sgRNA identification. Based on the target DNA sequence, all the possible NGG PAM sequences are sought on both the DNA strands. A list of predicted sgRNAs is returned, and generally, each one associated with score indicating its quality and its specificity referred to the target sequence.

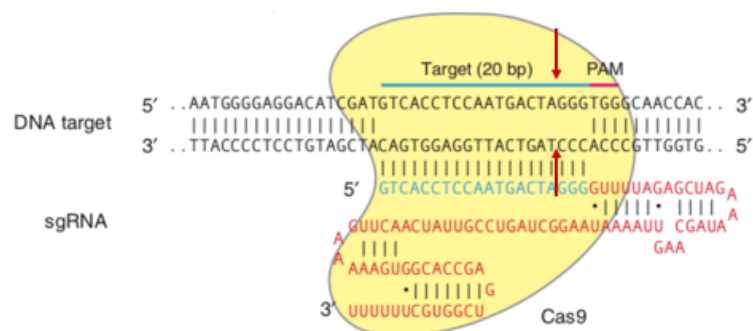


Figure 1.8: The Cas9 nuclease (in yellow) is guided at the target genome sequence by a 20 nt sgRNA (blue line) and a scaffold (red). The red arrows indicate the DSB introduced by Cas9 3 bp upstream of the PAM (modified from Ran et al., 2013).

Since Cas9 is directed by a 20 nt sgRNA and for its cleavage-activity it needs the presence of a PAM sequence immediately after the complementarity region of the sgRNA, the off-target cuttings are significantly reduced, compared to those produced by artificial restriction enzymes. Anyhow, the sgRNA selection must be carefully conducted. Considering that sgRNA-genome target sequence base pairing occurs also in the presence of mismatches, the selected sgRNA must guarantee specific on-target cleavage, avoiding off-target cuts.

The Cas9 ability to cleave eukaryotic genomes occurs when it recognizes the PAM sequence within the target sequence and cleaves both the DNA strands. Specifically, once Cas9 has individuated the NGG sequence within the target genome, it cleaves 3 nt upstream the PAM sequence itself (Figure 1.8).

Once the DSB has been introduced, the DNA damage is repaired by the cell repair mechanisms. As schematically shown in figure 1.9, to obtain a gene knock out (KO), the Non Homologous and Joining (NHEJ) pathway is exploited because, being an error-prone mechanism, the DNA damage is repaired by joining the interrupted DNA ends. Through the NHEJ, indel mutations are introduced and, in most cases, these lead to a frameshift, inserting a premature STOP codon that does not allow the gene expression. Conversely, to obtain a specific mutation into a target gene, a donor template is provided with the CRISPR/Cas9 system. The repair template brings the desired mutation and, once Cas9 introduced the DBS, the Homologous Directed Repair (HDR) process can repair it exploiting the donor template, allowing the gene editing (Figure 1.9 on the right).

Briefly, eukaryotic cells respond to DNA damage activating the DNA damage repair (DDR) pathways. Once the DNA damage has been introduced, the triggering event for its repair is the phosphorylation of the γ H2AX histone at the DSB locus, necessary to activate the appropriate repair mechanism, based on the DNA damage entity and the cell cycle phase (Rogakou et al. 1998)

The NHEJ DNA damage repair pathway takes place in G0 and G1 cell cycle phases (Chiruvella, Liang, and Wilson 2013; Karanam et al. 2012). The recognition of the DNA interrupted ends occurs thanks to Ku70/80 heterodimeric complex, that binds the DNA ends and recruits the phosphatidylinositol-3 kinase-like (PKcs) to the DSB (Singleton et al. 1999). PKcs mediates its autophosphorylation (Meek et al.

2007), crucial for the DNA damage pathway repair choice, suppressing HDR and allowing the NHEJ progression (Cui et al. 2005). For DNA ends processing different factors can be recruited, forming exonuclease/endonuclease complexes, as well as DNA polymerase μ and λ to fill-in the gap and polynucleotide kinase/phosphatase (PNKP), which removes 3' phosphate groups and/or adds 5' phosphate groups to DNA interrupted ends. The DNA ligation is then carried out by the XRCC4/DNA ligase IV complex (Ahnesorg, Smith, and Jackson 2006; J. Gu et al. 2010; Niewolik et al. 2006).

Differently, the HDR process occurs in S and G2 cell cycle phases (Kato et al. 1993). In the HDR process, a 5'-3' directional degradation of the DNA damaged ends occurs, generating a 3' ssDNA tail, that functions as a platform for the formation of the HDR complexes. Once the 3' ssDNA is generated, it is bound by the RAD51 recombinase producing the RAD51/ssDNA-nucleofilament able to search for the homologous strand. The DNA lost portion is then faithfully synthesized, based on the DNA template, and ligated to the DNA break sites (Ayoub et al. 2009; Esashi et al. 2007).

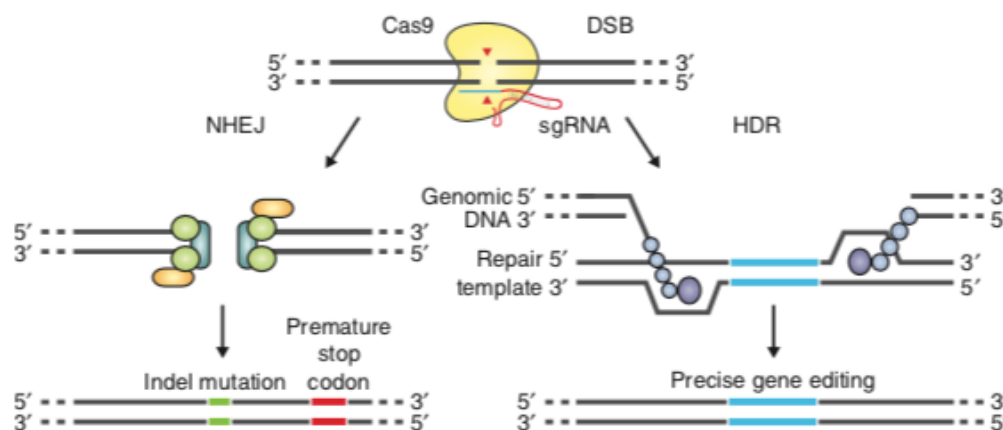


Figure 1.9: Cas9 cleaves the target genome sequence guided by sgRNA. Once Cas9 has recognized the PAM sequence, it introduces a DSB. The DNA damage, in the absence of a repair template, is repaired by NHEJ (in the left), thus leading to random indel mutations, that in most cases cause a frameshift inserting a premature STOP codon. Providing to the target cells both Cas9/sgRNA and a repair template, the DSB can be repaired by HDR (on the right), inserting desired mutations into the target gene, thus obtaining a precise gene editing (Ran et al., 2013).

1.7 Development of alternative CRISPR/Cas systems

Different CRISPR/Cas systems have been engineered, to make the system fitting to various fields and to allow genome manipulation in different experimental contexts.

1.7.1 Engineering of CRISPR/Cpf1 (Cas12a)

Recently, Zhang and coworkers have engineered a new type of CRISPR/Cas system, based on Cpf1 (also known as Cas12a) derived from *Prevotella* and *Francisella* (Zetsche et al. 2015). Cpf1 belongs to class 2 type V. Peculiar characteristic of Cpf1 is its RNase and DNase activity, thus, for the pre-crRNA maturation, it does not require tracrRNA, since Cpf1 itself mediated its recognition and cleavage to produce a mature crRNA (Chylinski, Le Rhun, and Charpentier 2013; Deltcheva et al. 2011). Structurally, Cpf1 is slightly different from Cas9: it presents a RuvC endonuclease domain divided into three catalytically active parts (RuvC-I, -II, and -III) and lacks HNH domain (Figure 1.10), allowing Cpf1 to cleave one strand DNA one at a time (Yamano et al. 2016).

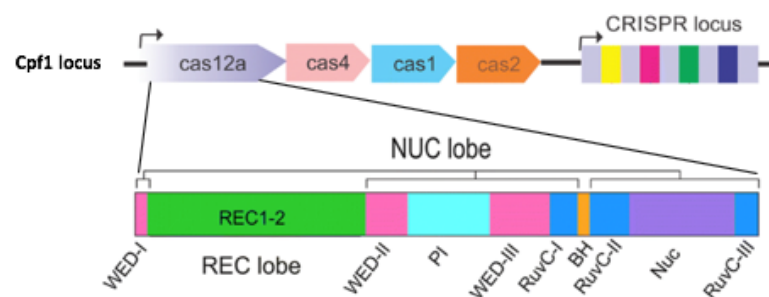


Figure 1.10: The Cpf1 locus encodes for the Cpf1 (Cas12a) effector protein and for Cas4, Cas1, and Cas2 interference proteins, located upstream the CRISPR array into the Cpf1 locus (upper part). In the lower part a schematic representation of Cpf1 protein is shown (modified from Safari et al., 2019).

For Cpf1 activity a particular PAM sequence 5'-TTTN-3' is required. Once Cpf1 recognizes the PAM sequence, it can mediate the DNA target cleavage. Particularly, Cpf1 recognizes and cleaves firstly the target DNA base-paired with the sgRNA, and subsequently the other strand (Swarts, van der Oost, and Jinek 2017).

The employment of Cpf1 shows some advantages over Cas9. Firstly, since Cpf1 does not require a specific PAM sequence, its activity results in a very low off-targets rate (Gao et al. 2017; Kleinstiver et al. 2016). Moreover, after the target cleavage, Cpf1 introduces sticky ends, useful for increasing the yield of HDR (Mali et al. 2013).

Compared to the Cas9 activity, Cpf1 is a powerful instrument for introducing gene deletion (Kleinstiver et al. 2016), a feature that makes it suitable for genome sequence replacement. Furthermore, due to Cpf1 RNase activity, it results particularly eligible for multiplex gene editing by delivering just one all-in-one plasmid (Gao et al. 2017).

The Cpf1 applications are increasing. For instance, the Cpf1 engineering allowed to correct the dystrophin gene mutations, through HDR, responsible for Duchenne muscular dystrophy in *in vivo* model (Y. Zhang et al. 2017), as well as the study of BRAF cancer-driving mutations (BRAF-V600E, 1799 T > A) in *in vitro* cell model (M. Yang et al. 2017).

1.7.2 Engineering of CRISPR/C2c2 (Cas13a)

C2c2 (Cas13a) is a type VI effector protein belonging to class 2. Contrarily to Cas9 and Cpf1, C2c2 does not possess any DNA nuclease domain, but it presents RNase function due to the presence of two Higher Eukaryotes and Prokaryotes Nucleotide-binding (HEPN) domains (Shmakov et al. 2015). The HEPN domains associate to form a catalytically active RNase domain (East-Seletsky et al. 2017). The best characterized CRISPR type VI system derives from *Leptotrichia shahii*. The C2c2 CRISPR locus comprises Cas1 and Cas2, involved in spacer acquisition, and C2c2 encoding the effector protein (Figure 1.11) (Abudayyeh et al. 2016).

C2c2 is able to cleave ssRNA when its target takes a particular secondary structure. Contrarily to the other Cas proteins, C2c2 does not need a PAM sequence to

recognize its target (Elmore et al. 2016; Gootenberg et al. 2017), but its RNase activity can be directed by building a specific crRNA of 28 nt complementary to the ssRNA to target (Abudayyeh et al. 2016). Anyway, the ssRNA cleavage is ensured not only for the complementary crRNA-ssRNA, but it is also modulated by Protospacer Flanking Sequences (PFSs) (Abudayyeh et al. 2016; Gootenberg et al. 2017). The activity of the C2c2-crRNA effector complex is triggered by the complementary between crRNA and the target ssRNA. ssRNA cleavage occurs outside the region base-paired with the crRNA (Knott et al. 2017; L. Liu et al. 2017).

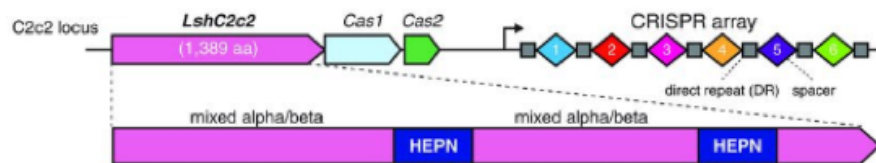


Figure 1.11: The C2c2 locus includes C2c2, Cas1, and Cas2 encoding genes and the CRISPR array (upper part). The lower part shows the C2c2 protein domains. C2c2 is characterized by two RNase HEPN domain (blue boxes; modified from Abudayyeh et al., 2016)

1.8 CRISPR/Cas9 delivery systems

Based on the CRISPR/Cas9 application, it is strictly necessary to individuate the proper delivery system to maximize the genome editing yield and minimize off-target cleavages. The delivery system is chosen evaluating the target cell line or the animal model and what kind of mutation will be inserted within the genome.

CRISPR/Cas9 system can be provided exploiting the following approaches:

- 1) DNA plasmid encoding both Cas9 protein and sgRNA;
- 2) Cas9 mRNA and sgRNA;
- 3) Ribonucleoprotein complex (RNP) composed of Cas protein and sgRNA;
- 4) Viral vector providing both Cas9 and sgRNA.

CRISPR/Cas9 can be delivered employing different strategies, which are selected according to the CRISPR/Cas9 provided system and the target to edit.

The most used delivery system is based on lipid nanoparticles. In this system, exogenous material negatively charged interacts with lipids positively charged, thus generating liposomes, that once transfected into the target cells lead to the expression of the delivered material. This system is particularly suitable for *in vitro* gene manipulation of easy-to-transfect cells (Miller et al. 2017).

Microinjection allows the insertion of the CRISPR/Cas9 system in a single cell. It allows the CRISPR/Cas9 delivery with an efficiency of about 100%. It is particularly recommended as a vehicle of Cas9 mRNA and sgRNA. By introducing directly Cas9 mRNA and sgRNA into the cytoplasm, the Cas9 mRNA can be translated and then the Cas9 protein can associate with sgRNA and the RNP complex newly formed move into the nucleus. Because microinjection permits single-cell manipulation, it is often employed for zygotes gene editing (Raveux, Vandormael-Pournin, and Cohen-Tannoudji 2017).

Electroporation and nucleofection open nanopores on the cell membrane through voltage change, permitting CRISPR/Cas9 delivery. Those approaches are suitable for delivering DNA plasmid encoding Cas9 and sgRNA, as well as Cas9 mRNA and RNP complex. Although electroporation and nucleofection efficiently transport exogenous material within the target cells, they are not suitable for *in vivo* application (S. Kim et al. 2014; Schumann et al. 2015).

The hydrodynamic method permits the delivering of material in *in vivo* systems, allowing to convey DNA plasmid encoding for both Cas9 and sgRNA directly into the vein, not requiring any other exogenous components (Guan et al. 2016; F. Liu, Song, and Liu 1999; Xue et al. 2014).

Viral systems are used for delivering exogenous materials both for *in vitro* and *in vivo* gene editing. Lentiviral (LV) and Adeno-associated Viral (AAV) vectors are the most employed delivery systems, allowing gene editing through cell target transduction (Maggio et al. 2014; Shalem et al. 2014). Both AAV and LV particles are packaged in HEK 293T cells, then harvested and used for infection. An important feature to consider is the DNA quantity that can be included in these two viral delivery systems, indeed while AAV can contain a smaller DNA amount, it is possible to vehicle a higher DNA amount with LV. Particularly, since Cas9 and sgRNA are 4.2 Kb and AAV may include 4.5-5 Kb of genomic materials, this system requires other vectors for delivering other components, such as multiple sgRNAs or template DNA, making difficult the AAV packaging (Z. Wu, Yang, and Colosi 2010). To bypass this size packaging limit, the smaller SaCas9 (from *Staphylococcus aureus*) can be exploited instead of SpCas9 (Friedland et al. 2015). Moreover, it is also possible to split the N-terminal and the C-terminal parts of Cas9 in two different AAV vectors. Then with the transduction, the two protein portions can auto-assemble producing a complete and functional Cas9 (Zetsche, Volz, and Zhang 2015).

Lentiviral vectors lead to the insertion into the target genome of both the Cas9 gene and sgRNA. To produce lentiviral particles, second generation or third generation packaging plasmids can be employed, encoding for Cas9, sgRNA, and HIV related genes necessary for the viral replication cycle (Naldini et al. 1996). Second generation vectors are now basically replaced by third generation ones to increase the biosafety level since these vectors are built by physical separation of minimal HIV genetic elements in two different vectors. This system includes a third vector encoding both the Cas9 and the sgRNA (Shearer and Saunders 2015). AAV and LV particles can infect both dividing and non-dividing cells, characteristic which make this delivery system suitable for genome editing in particular cell lines, such as neurons (Dever et al. 2019).

Recently, the innovative Nanoblade viral-delivery method, has been described (Mangeot et al. 2019). The Nanoblade method allows the Cas9/sgRNA RNP complex shuttling, exploiting the Murine Leukemia Virus (MLV). This nanotechnology is based on two main components: a plasmid encoding the Cas9-Gag (MLV) fusion protein and a sgRNA expressing plasmid. Nanoblades are produced in 293T packaging cells, then harvested and used for viral transduction of the target cells. Compared with other CRISPR/Cas9 delivery methods, Nanoblades result in the efficient induction of DNA DSB in immortalized cell lines, but also in primary cells, such as human primary fibroblasts, human hepatocytes, human induced pluripotent stem cells, macrophages, and human hematopoietic progenitors. Intriguingly, nanoblades show a comparable CRISPR/Cas9 delivery and efficiency, and in some cases even higher, compared to Cas9/sgRNA RNP electroporation. Nanoblades can be also packaged with a DNA donor template, thus permitting a more precise gene editing both *in vitro* and *in vivo* models (Mangeot et al. 2019). Likewise, the new CRISPR/Cas9 vehicle method NanoMEDIC (nanomembrane-derived extracellular vesicles for the delivery of macromolecular cargo) has been developed (Gee et al. 2020). NanoMEDIC is an RNP convey system exploiting 293T cells for the packaging of Cas9 through two vectors expressing the dimerization of Peptidyl-prolyl cis-trans isomerase (FKBP12) fused to Gag (HIV) and FKBP-Rapamycin Binding Domain (FRB) fused to Cas9 is exploited, to direct the Cas9 protein into Extracellular vesicles (EV). The sgRNA is then loaded in the Cas9-bearing-EV after the treatment of 293T cells with a retroviral construct carrying the sgRNA flanked by Ψ and HH and HDV ribozymes, both essentials to release the sgRNA into the EV. The novel NanoMEDIC system shows higher RNP delivery compared to other RNP convey method (Mangeot et al. 2019) and off-target analysis revealed that this shuttle system is characterized by a very low off-target rate, as the other RNP delivery method (S. Kim et al. 2014). NanoMEDIC might be a very promising CRISPR/Cas9 vehicle method in human pluripotent stem cells and in *in vivo* model (Gee et al. 2020). Both Nanoblades and NanoMEDIC allow the delivery of RNP complex avoiding the Cas9/sgRNA prolonged expression, thus reducing off-target cuts (Mangeot et al. 2019; Gee et al. 2020).

1.9 Application of CRISPR/Cas9 system

One of the major challenges in biotechnology is the capability to modify a specific genome for desired purposes. Over the year several researchers have developed different systems trying to make gene manipulation easier and less harmful, starting with the improvement of artificial nuclease systems up to the employment of CRISPR/Cas technologies. Making easier and safer the genome manipulation, several advantages can be reached in many fields (Figure 1.12).

Overall, the CRISPR/Cas9 system has an important impact on basic research and medicine against cancer, viral infection and neurological disorders.



Figure 1.12: CRISPR/Cas9 system permits to improve genome editing in biology, allowing the development of appropriate animal models, as well as in vitro gene manipulation; biotechnology, with its application aimed to develop new materials important for drug delivery, plants resistant to pathogen, and fuel, by modifying microorganisms and algae to produce renewable energy; medicine, making feasible gene surgery, thus correcting aberrant genetic and epigenetic mutations; drug development, exploiting bacteria to produce new generation drugs reducing their costs and increasing their accessibility (Hsu et al., 2014).

1.9.1 CRISPR/Cas9 in cancer

CRISPR/Cas9 represents a very powerful tool for cancer research and therapy. CRISPR/Cas9 system may be applied in controlling gene expression in cancer cells. Recently, a work on the activation of the tumor suppressor PTEN (phosphatase and tensin homolog) mediated by CRISPR/dCas9, has been published (Moses et al. 2019). PTEN results inactivated in many tumors, such as melanoma and breast cancer (J. S. Lee et al. 2004; Tsao et al. 1998). It has been reported that by activating PTEN in breast cancer and melanoma, cell proliferation and migration pathways are inhibited, revealing the dead Cas9 potential in counteracting uncontrolled cell growth and invasiveness (Moses et al. 2019). Another relevant application of CRISPR/Cas9 has been the prevention of the chromosome translocation that generates the constitutive active oncogene BCR/ABL in hematopoietic stem cells (Lugo et al. 1990). BCR/ABL is responsible for chronic myeloid leukemia (CML) pathogenesis by increasing cell survival (Brightbill and Schlissel 2009; Colicelli 2010), avoiding apoptosis (Bedi et al. 1994), and promoting genomic instability through the inhibition of DDR pathways (Deutsch et al. 2001). Exploiting the CRISPR/Cas9 approach, BCR/ABL KO cells were developed. Interestingly, this new cell model restored a high level of apoptosis and, by injecting BCR/ABL negative cells in mice, tumors were not induced due to the loss of their onco-transformation ability (García-Tuñón et al. 2017).

1.9.2 CRISPR/Cas9 against viral infections

CRISPR/Cas9 system has important antiviral potential. Currently, no therapy is effective against human viruses that have a latent stage in their life-cycle, such as human immunodeficiency virus-1 (HIV-1). HIV is the etiological agent of acquired immunodeficiency syndrome (AIDS). It integrates its genome within the host DNA, making antiretroviral drugs ineffective for its eradication. Many researchers focused their efforts on CRISPR/Cas9 application against HIV-1 (Ebina et al. 2013; Rafal Kaminski et al. 2016; Yin et al. 2017). Anti-HIV-1 CRISPR/Cas9 systems target viral LTR, gag, pol, env, and other HIV-1 accessory genes. Despite initial

observation of decreased HIV-1 copy number (R. Kaminski et al. 2016), reduction of viral p24 protein (Zhu et al. 2015), and significant reduction of HIV-1 latency activation (Ebina et al. 2013), HIV-1 is able to generate escape mutants by modifying the viral genome sequence recognized by sgRNA, exploiting the same viral mechanism that confers drug resistance to HIV-1 (Ueda et al. 2016; G. Wang et al. 2016). Recently it has been reported that the combinatorial CRISPR/Cas9 approach targeting two viral genes did not lead to HIV-1 CRISPR/Cas9 resistant variants. Particularly, sgRNAs were designed to target viral protease and reverse transcriptase and when provided with a LentiCRISPR system, viral replication and infection were abrogated (Lebbink et al. 2017). Another anti-HIV-1 approach affects viral entry, by using CRISPR/Cas9 to mutate HIV-1 co-receptor CCR5 (chemokine receptor type 5). Cell transduction with LentiCRISPR vector expressing both Cas9 and sgRNA to target CCR5 induced CCR5 KO, thus generating CCR5 defective cells resistant to infection by CCR5-tropic HIV-1 (W. Wang et al. 2014).

1.9.3 CRISPR/Cas9 in neurological disorders

Neurological disorders include several types of neuropathies affecting the central nervous system (CNS), such as neurodegenerative diseases. Although therapies are not yet available, patients affected by neurodegenerative disorders are treated with drugs able to reduce pathological symptoms or delay the pathology progression, but definitively an effective cure is still lacking. Alzheimer's disease (AD) is a very severe neurodegenerative disorder. World Health Organization estimated that 50 million people suffer from dementia worldwide and that 60-70% of dementia cases are caused by AD. AD is mainly due to mutations in amyloid precursor protein (APP) leading to amyloid- β ($A\beta$) deposition (Bertram et al. 2007). The most frequent APP mutation is the Swedish mutation (APP_{swe}), which causes an increase of APP enzymatic cleavage by β -secretase, which in turn leads to high $A\beta$ levels in the brain and peripheral tissues (Citron et al. 1994; Johnston et al. 1994). Recently CRISPR/Cas9 has been used to evaluate whether it can target the APP_{swe} mutation. To this aim, mice expressing the APP_{swe} allele were treated with

CRISPR/Cas9 exploiting the AAV delivery system, resulting in the introduction of indel mutations, thus leading to a frameshift and lacking of APP expression (György et al. 2018).

CRISPR/Cas9 has found applications also for studying rare neurological disorders, such as Neuronal Ceroid Lipofuscinosis (NCLs), a class of autosomal recessive pathologies, characterized by progressive mental and motor deterioration, blindness, epileptic seizures, and death (Haltia 2003). 85% of NCL patients show a 1.02 Kb deletion in the *CLN3* gene (Haskell 2000). In a recent work, successfully CRISPR/Cas9 was employed to correct the *CLN3* deletion in induced pluripotent stem cells obtained from NCL patients, thus giving new input in understanding the molecular mechanisms causing NCL pathologies (Burnight et al. 2018).

1.10 CRISPR/Cas9 for gene editing

For the development of new knock out cell lines, as well as for the introduction of a more precise gene editing, some important issues need to be addressed for getting optimal results by using CRISPR/Cas9.

After the introduction of DBS, the CRISPR/Cas9 activity must be followed by the proper DNA damage repair mechanism. Since NHEJ inserts unpredictable gene mutations, it cannot be exploited for introducing specific modifications within a target locus. In this case, the most suitable process is the HDR pathway.

For HDR induction it is essential to provide to the target cell line both the CRISPR/Cas9 system and a DNA donor template to be used for recombination. The donor template has to be designed with the appropriate length of homology arms, as well as it must hold specific silent mutations to avoid consecutive and undesired Cas9 cleavages (Paquet et al. 2016). It is necessary to underline that HDR occurs at a very low rate and, specifically, during the S and G2 cell cycle phases (Shrivastav, De Haro, and Nickoloff 2008). To overcome this limitation, efforts have been directed for enhancing the HDR activity and suppressing the NHEJ pathway (Mateos-Gomez et al. 2017; Zelensky et al. 2017). For instance, as reported by Chu et al. (2015), by using the *src7* DNA ligase IV inhibitor, the NHEJ is suppressed and the HDR rate increases 4-5 folds (Chu et al. 2015). Interestingly, the treatment

of mouse zygotes with the src7 inhibitor induces a HDR increase of even 19 folds (Maruyama et al. 2015). To favor the HDR pathway, it may also be convenient to synchronize the cell cycle. Different compounds can be administered to the target cell line for this purpose. For example, nocodazole synchronizes cells in the G2/M phase and mimosine arrests the cell cycle before DNA replication, leading to increased HDR efficiency of about 2 folds (D. Yang et al. 2016).

1.11 Ethical concerns in genome editing

CRISPR/Cas9 is quickly establishing compared to other technologies, such as ZFN, TALEN, and RNAi. The great potential of CRISPR/Cas9 for genome manipulation is accompanied by ethical debates, mostly regarding the feasibility to manipulate human germline and human embryos.

The most debated concern is referred to off-targets, indeed although off-targets have been reported to be very low in animal models, such as zebrafish and mice, they present a high frequency in CRISPR/Cas9-edited human cells (Fu et al. 2013; Hwang et al. 2013; H. Yang et al. 2013). Efforts are directed to improve the CRISPR/Cas9 system to eliminate off-target risks (Hsu et al. 2013).

Generally, gene therapy is widely accepted to correct mutations in somatic cells, but issues arise about the possibility to employ this new genome editing tool in the human germline, because of unpredictable side effects that would be genetically transmitted to the following generations (Mulvihill et al. 2017). In 2015 researchers from America, Britain and China scientific academies participated to the International Summit on Human Gene Editing, debating the ethical issues of human germline manipulation, concluding that CRISPR/Cas9 is a powerful tool for basic and clinical research, but its application to modify human beings is to consider irresponsible.

Ihry et al. (2018), recently published a refined work evaluating the potential of CRISPR/Cas9 for human pluripotent stem cells (hPSCs) engineering. hPSCs are reluctant to genome manipulation and, after CRISPR/Cas9 treatment they show a higher percentage of mortality, compared to transformed cells (Ihry et al. 2018). By performing RNA-seq, it emerged that after CRISPR/Cas9, DNA damage and pro-apoptotic proteins increased in hPSCs. Interestingly, by analyzing the cell

interactome, Ihry et al. found that the proteins overexpressed in response to the Cas9-induced DSB interact with p53, thus explaining the difficulty in obtaining gene editing in hPSCs. Moreover, by providing a p53 inhibitor, the efficiency of CRISPR/Cas9 improved 16-19 folds. Following the DNA damage, the p53 activity in hPSCs is fundamental to avoid the development of mutated and transformed cells. It is worth noting that the edited stem cells presented a non-functioning p53 protein, which in turn reflects their tumorigenic potential. This represents a pivotal point to consider especially before *ex vivo* patient cell manipulation. Pro and cons, risks and benefits need to be carefully addressed to avoid the onset of a serious pathology after transplantation of manipulated cells.

Concerning the employment of CRISPR/Cas9 for human genome handling, the most fierce debate, related to germline and embryos gene editing, emerged in 2015 with the Nature publication entitled “Don't edit the human germline” (Lanphier et al. 2015). In this comment, the importance and the value of the CRISPR/Cas9 system employment for the treatment of human diseases, such as hemophilia, AIDS, sickle cell diseases, and many types of cancers are strongly highlighted. Conversely, the authors condemn the potential application of CRISPR/Cas9 to human sperm, eggs, and embryos, mainly for the unknown effects on the following generations. Unfortunately, only three years later, the scientific community was shocked to hear about the CRISPR/Cas9 application on human embryos. Indeed, in November 2018 He Jiankui, from Southern University of Science and Technology in Shenzhen (China), during the genome-editing summit in Hong Kong, reported that he edited the CCR5 gene to make two twin embryos resistant to HIV infection. The scientific community has widely condemned this experimental intervention, raising several concerns: the lack of appropriate parents' information, the complete absence of ethics committees, and the unknown future effects on the twins (Lovell-Badge 2019). On the 3rd December 2019, an interesting article on MIT technology review was published, highlighting the absence of new information on the two edited twins and the lack of a peer-reviewed scientific publication. Moreover, the article reported that the Chinese government seized all the data regarding the manipulation of the human embryos, thus not allowing them to perform further experiments that may be required by a journal scientific review. Additionally,

Fyodor Urnov, a geneticist at the UC Berkeley, reported that this embryos editing did not insert the desired mutation into the CCR5 gene, but rather produced unwanted mutations in the genome with unknown consequences.

Recently, regarding the development of new CRISPR/Cas9-based strategies to cure HIV-1 infection, Xu et al. reported that a HIV-1 infected patient was treated with allogenic CCR5-edited hematopoietic stem and progenitor cells (HSPCs). After CCR5 KO induction through CRISPR/Cas9, the HSPCs CCR5 edited cells were engrafted into the HIV-1 infected patients. After treatment, opportunistic infections occurred, such as cytomegalovirus infection and herpes simplex virus reactivation (Xu et al. 2019). Even if after few months from treatment, the patient recovered from these infections, this work underlines the importance of a full understanding and control of the CRISPR/Cas9 technique. Indeed, despite great advances achieved in the CRISPR/Cas9 employment, many fundamental responses to the CRISPR/Cas9 treatment escape.

CRISPR/Cas9 is accompanied by a fierce debated on its potential application on the human being. So far, reliable evidence about CRISPR/Cas9-associated risks in human embryos are not available. It results necessary to consider the possible scenarios. In fact, besides off-targets, mosaicism due to incomplete gene editing, and limited CRISPR efficiency, the genome manipulation of the human germline may induce heritable harmful and unpredictable gene modifications with important consequences on the future generations. Therefore, it is extremely difficult to certainly predict the potential risks and benefits associated with CRISPR/Cas9 application

Moreover, being CRISPR/Cas9 a revolutionary technology, it has been subjected to patent claims from Zhang of the Broad Institute, which first engineered the microbial CRISPR/Cas9 system to be applied in animal and human cells (Cong et al. 2013), and from Doudna of University of California, which supports to be the first to adapt CRISPR/Cas9 system in eukaryotic cells. On 15th February 2017, the US Patent and Trademark Office has assigned the CRISPR/Cas9 patent to the Broad Institute of MIT. Therefore on 10th September 2018, the US Court of Appeals for the Federal Circuit has confirmed that the intellectual property of the CRISPR/Cas9 technique belongs to the Broad Institute of MIT.

2. MATERIALS AND METHODS

Buffers and solutions

Laemmli buffer	50mM Tris-HCl pH 6.8 6% v/v glycerol 3% v/v β -mercaptoethanol 1% w/v SDS 0.001% w/v bromophenol blue
RIPA buffer	50mM Tris-HCl pH 7.5 150mM NaCl 2mM EDTA 1mM PMSF 1% v/v Triton X-100 1% v/v Sodium deoxycholate Protease inhibitors cocktail (Roche)
Running buffer	25mM Tris 192mM Glycine 0.1% w/v SDS
Transfer buffer	25mM Tris 192mM Glycine 0.1% w/v SDS 20/ v/v methanol

Stripping acid wash buffer	300mM Glycin 1% w/v BSA in PBS, pH 2.5
TBS-T	20 mM Tris 150mM NaCl 0.05% v/v Tween-20 pH 7.6
TAE	40 mM Tris 20 mM Acetic acid 1 mM EDTA

Cell culture

Human embryonic kidney (HEK) 293T cells were purchased from the American Type Culture Collection (ATCC) and grown in Dulbecco's Modified Eagle Medium (DMEM, Euroclone) completed by 10% Fetal Bovine Serum (FBS, Euroclone), 2mM L-glutamine (Lonza), 100 U/mL Penicillin G, and 100 U/mL Streptomycin (Lonza).

The HeLa derived TZM-bl cells were provided by EU Programme EVA Centre for AIDS (NIBSC) and grown in Dulbecco's Modified Eagle Medium (DMEM, Euroclone) completed by 10% Fetal Bovine Serum (FBS, Euroclone), 2mM L-glutamine (Lonza), 100 U/mL Penicillin G, and 100 U/mL Streptomycin (Lonza).

Malignant melanoma Mel-HO cells were kindly provided by Dott. Maria Teresa Valenti (University of Verona, Italy) and grown in Dulbecco's Modified Eagle Medium (DMEM, Euroclone) completed by 10% Fetal Bovine Serum (FBS, Euroclone), 2mM L-glutamine (Lonza), 100 U/mL Penicillin G, and 100 U/mL Streptomycin (Lonza).

Pancreatic adenocarcinoma PT45 cells were kindly provided by Dott. Giulio Innamorati (University of Verona, Italy) and grown in Roswell Park Memorial Institute (RPMI 1640, Euroclone) medium supplemented with 10% FBS (Euroclone), 2mM L-glutamine (Lonza), 100 U/mL Penicillin G, and 100 U/mL Streptomycin (Lonza).

Chronic myeloid leukemia LAMA84 cells were kindly provided by Prof. Claudio Sorio (University of Verona, Italy) and grown in RPMI 1640 (Euroclone) supplemented with 10% FBS (Euroclone) and 2mM L-glutamine (Lonza).

Neuroblastoma SH-SY5Y cells were kindly provided by Prof. Alessandro Simonati (University of Verona, Italy) and grown in Dulbecco's Modified Eagle Medium (DMEM, Euroclone) completed by 10% Fetal Bovine Serum (FBS, Euroclone), 2mM L-glutamine (Lonza), 100 U/mL Penicillin G, and 100 U/mL Streptomycin (Lonza).

The neuroglioma H4 Swe cells were kindly provided by Prof. Mario Buffelli (University of Verona, Italy) and grown in Dulbecco's Modified Eagle Medium (DMEM, Euroclone) completed by 10% Fetal Bovine Serum (FBS, Euroclone),

2mM L-glutamine (Lonza), 100 U/mL Penicillin G, and 100 U/mL Streptomycin (Lonza).

Vectors

pSpCas9(BB)-2A-Puro (PX459) V2.0 (#62988), psPAX2(#12260), and pVSVg (#8454) were purchased from Addgene.

LentiCRISPR v2 was kindly provided by Prof. Massimo Pizzato.

The plasmid expressing HIV-1 envelope QHO protein (ARP2043) was purchased from EU Program EVA Centre for AIDS (NIBSC).

The pSG3 Δ env backbone plasmid (#11051) was purchased from the NIH AIDS Research and Reference Reagent Program.

The pNF-kB-Luc and pHRG-TK plasmids were purchased from Stratagene.

The pJFE-Tax-1 plasmid was constructed by Tax-1 PCR amplification (Lamsoul et al. 2005).

The HLA-C pcDNA6.2 (Invitrogen) expressing plasmids were constructed by HLA-C RT-PCR amplification.

sgRNA design and cloning

Following the Zhang's protocol (Ran et al. 2013), sgRNAs were designed using MIT guide design resource (<https://zlab.bio/guide-design-resources>) and Chopchop (<https://chopchop.cbu.uib.no/>). 5'-CACC and 3'-AAAC overhangs were added to each sgRNA for their cloning in the Cas9 expressing vector. The sgRNA sequences are reported in the table 2.1.

Briefly, forward (Fw) and reverse (Rev) sgRNAs were annealed and cloned into the Cas9 expressing plasmid. Top10 and X11-blue were transformed with the sgRNA-Cas9 (PX459 2.0) and sgRNA-LentiCRISPRv2 expressing plasmids, respectively, and DNA was extracted and purified by MIDIprep (QIAGEN).

sgRNA off-targets prediction

For each sgRNA, eventual off-targets were analyzed using the CRISPR RGEN tool (<http://www.rgenome.net/cas-offfinder/>). Only sgRNAs able to specifically target the desired gene sequence have been selected.

Polymerase chain reaction (PCR) for sequencing

All the CRISPR/Cas9 targeted exons were amplified through PCR for sequencing, in a final concentration of 1X Wonder Taq Buffer (New England Biolab), 10 µM primer forward and reverse; 0,05 U Wonder Taq (New England Biolab). The primer pairs used are reported in Table 2.2.

PCR products were purified (QIAquick PCR Purification Kit) and Sanger sequenced (BMR genomics), and analyzed through both BLASTN alignment (https://blast.ncbi.nlm.nih.gov/Blast.cgi?PAGE_TYPE=BlastSearch&BLAST_SPEC=blast2seq&LINK_LOC=align2seq) and *in silico* translation Expasy tool (<https://web.expasy.org/translate/>).

Transfection

293T were transfected using TransIT LT1 transfection reagent (Temaricerca), following the manufacture's protocol.

Mel-HO, PT45, and LAMA84 were transfected using Lipofectamine 3000 (ThermoFisher), following the manufacture's protocol.

SH-SY5Y were transfected by nucleofection following the Amaxa's guideline (kit V, Lonza, program G-004).

Production of pseudoviruses and infection

HIV-1 pseudotyped viruses were packaged in 293T cells by transfecting the QHO-env expressing plasmid and the pSG3Δenv backbone plasmid in a ratio 1:2, respectively.

LentiCRISPRv2 pseudoviruses were packaged in 293T cells by transfecting the sgRNA-LentiCRISPRv2 plasmid and the psPAX2 and pVSVg plasmids in a ratio 4:3:2.

After 48 hours from transfection the culture medium containing pseudoviruses was filtered through 0,45 µm filter and collected by adjusting the FBS concentration at 20%.

The QHO-env viral concentration was quantified by detecting the HIV-1 antigen p24 concentration (One-Wash Lentivirus Titer Kit, p24 ELISA, Origene).

TZM-bl infectivity assay, according to Montefiori's protocol (2009), was performed by titrating QHO-env pseudoviruses starting from 1000 pg/mL. 1×10^3 TZM-bl cells were infected for each condition in the presence of 15 μ /mL dextran. 48 hours from infection the luminescence was measured using the Victo 3 luminometer (Perkin Elmer). The infectivity values were analyzed as Median Tissue Culture Infectious Dose (TCID₅₀).

The H4 Swe cells and the LAMA84 cells were infected by titrating sgRNA-LentiCRISPRv2 viruses (1:1, 1:100, 1:1000, and 1:10000).

RNA extraction and Real-Time PCR

RNA extraction was performed using TRIzol (Invitrogen), according to the manufacturers' protocol. Total RNA was retrotranscribed using oligo dT primers and the SuperScript™ III First-Strand Synthesis System (Invitrogen).

Real-Time PCR were performed with the Power SYBR Green PCR Master Mix (Applied Biosystems) and ran on CFX Connect™ Real-Time Detection System (Bio-Rad). Primer pairs for TNF Alpha Induced Protein 3 (A20), Apoptosis Regulator Bcl-2 (BCL2), Interleukin 6 (IL-6), and Ribosomal Protein Lateral Stalk Subunit P0 (RPLP0) mRNA expression quantification are listed in Table 2. The $2^{-\Delta\Delta C_t}$ method was used to calculate the relative fold change (Livak and Schmittgen 2001). As internal reference gene RPLP0 was used.

Flow cytometry analysis of HLA-C cell surface expression

293T HLA-C KO cells were stably transfected with HLA-C pcDNA 6.2 expressing plasmids and grown by adding 8 μ g/mL of Blasticidin to the culture medium.

293T HLA-C KO CRISPR/Cas9 treated cells and stably transfected 293T HLA-C expressing cells were surface labeled with DT9 antibody (1 μ g/ 1×10^6 cells, EDM Millipore) for 1 hour on ice. After Phosphate Buffered Saline (PBS) washing the cells were incubated with Alexa Fluor 488 anti mouse antibody (Cell Signaling) for 30 minutes on ice (1:1000 in 1% w/v BSA in PBS) and washed in PBS. HLA-C detection was performed using the FACSCanto Flow cytometer.

Flow cytometry analysis of HLA-C binding stability to β_2 microglobulin

Stably transfected 293T HLA-C expressing cells were incubated in 0.3 M glycine HCl stripping acid buffer (pH 2.5) for 0 sec, 30 sec, and 60 sec, followed by extensive PBS washing to neutralize the pH. The cells were labeled with the L31 antibody (1 μ g/mL, 1% w/v BSA in PBS) for 40 minutes, to specifically detect HLA-C free chains. After PBS washing the cells were incubated with Alexa Fluor 488 anti mouse antibody (Cell Signaling) for 30 minutes on ice (1:1000, 1% w/v BSA in PBS).

The flow cytometry analysis was performed using the FACSCanto Flow cytometer. The results were analyzed as fluorescence increase (RMFI fluorescence intensity ratio between stripped/non-stripped). The amount of HLA-C free chains was analyzed as slope of interpolated curve.

Immunofluorescence analysis

SH-SY5Y wt and SH-SY5Y PPT1 KO cells were incubated in a PBS blocking with 1% BSA, incubated with 4% paraformaldehyde and then incubated overnight at 4°C with the rabbit polyclonal anti-PPT1 (Sigma Aldrich, 1:50) and mouse monoclonal anti-Lamp2 (1:400, Abcam) primary antibodies. Goat anti-mouse AlexaFluor 488 and goat anti-rabbit AlexaFluor 594 secondary antibodies were incubated for 1 hour at room temperature. Nuclei were stained with 5 μ g/ml DAPI (Sigma- Aldrich). Immunofluorescence were detected using the Zeiss LSM 710 fluorescence microscopy.

Western Blot analyses

Proteins were extracted with the RIPA buffer and quantified with Coomassie Plus Bradford Protein Assay Reagent (ThermoScientific) at the spectrophotometer (Eppendorf). Proteins were treated with Laemmli buffer and resolved by SDS-PAGE on acrylamide gel. After protein transfer on PVDF membrane (GE Healthcare), the PVDF membrane was saturated with 5% milk TBS-Tween buffer and incubated over night with primary antibody (for more details see antibody section). Anti-rabbit, anti-mouse, or anti-goat HRP-conjugated secondary

antibodies (Promega) were diluted 1:10000 in 5% milk TBS-Tween buffer and incubated 1 hour at room temperature.

The protein signal was detected using the ECL Advanced Western Blotting Detection kit (Amersham) at the Azure 300. The densitometric analyses were performed using ImageJ software.

Primary antibodies

The mouse monoclonal anti-HLA-C L31 antibody was kindly provided by Dr Patrizio Giacomini (Regina Elena Hospital, Rome, Italy), used 1:1. The mouse monoclonal anti-HLA-C DT9 antibody (EMD Millipore) was used 1:500. The rabbit polyclonal anti-GPR3 antibody (Sigma Aldrich) was used diluted 1:1000. The rabbit polyclonal anti-PPT1 antibody (Sigma Aldrich) was used 1:1000 for western blot analysis and 1:50 for IF analysis. The rabbit polyclonal anti-TRAF3 antibody (ProteinTech) was used 1:1000. The rabbit monoclonal anti-NF- κ B p100/p52 antibody (Cell Signaling Technology) was used 1:1000. The mouse monoclonal anti-Tax-1 derives from hybridoma 168-A51 (AIDS research and Reagent Program). The rabbit polyclonal anti I κ B- α antibody (Cell Signaling) was used 1:1000. The rabbit polyclonal anti-HDAC6 antibody (Santa Cruz Biotechnology) was used 1:1000. The mouse monoclonal anti-p62/SQSTM1 antibody (Santa Cruz Biotechnology) was used 1:1000. The rabbit polyclonal anti-acetylated tubulin antibody (Sigma-Aldrich) was used 1:1000. The goat polyclonal anti-TROP2 antibody (R&D system) was used 1:1000. The rabbit polyclonal anti GNA15 antibody (Torrey Pines Biolabs) was used 1:1000. The rabbit monoclonal anti-RUNX2 antibody (Cell Signaling Technology) was used 1:1000. The mouse monoclonal anti- β tubulin and anti- β actin antibodies (Cell Signaling) were used 1:1000. The rabbit polyclonal anti GAPDH antibody (Cell Signaling) was used 1:1000.

HLA-C genotyping

For HLA-C typing, DNA was extracted from whole blood of HIV-no-ADC and HIV-ADC patients using the QIAamp DNA Blood Kit (Qiagen).

HLA-C typing was performed at the HLA laboratory of tissue typing at Azienda Ospedaliera Universitaria Integrata (AOUI) of Verona.

Statistical Analyses

The association between stable and unstable HLA-C alleles with HIV-ADC and HIV-no-ADC was examined using the Fisher's exact test.

Statistical significance was assessed by the Student's t-test. Differences were considered to be significant when $P < 0.05$ (*), and strongly significant when $P < 0.01$ (**), and $P < 0.001$ (**).

Table 2.1: sgRNA sequences

Target gene	Mutation	sgRNA	Cas9 expressing plasmid
ACOT8	KO	Fw CACCGCGT CGTGACCAAGACGCTA Rev AAACTAGCGT CTTGGTCACGACCGC	PX459 v2.0
HDAC6	KO	Fw(A) CACCGCCG CTCTATCCCAATCTAG Rev(A) AAACTAG ATTGGGGATAGAGCGGC Fw(B) CACCGAC CTAATCGTGGGACTGCAA Rev(B) AAACTTG CAGTCCACGATTAGGTC	PX459 v2.0
HDAC6	BUZ deletion	Fw(A) CACCGAT CTAGGGCCCTCACTGATC Rev(A) AAACGAT CAGTGAGGCCCTAGATC Fw(B) CACCGAT CGCCACCAGAACAAGTT Rev(B) AAACA ACTTTGTTCTGGTGGCGATC	PX459 v2.0
HLA-C	KO	Fw CACCGAC ACAGAAGTACAAGCGCC Rev AAACGGC GCTGTACTTCTGTGTC	PX459 v2.0
TRAF3	KO	Fw CACCGCA GTTTTTGTCCCTGAACA Rev AAACTGT CAGGGACAAAAGTGGC	PX459 v2.0
RUNX2	KO	Fw(A) CACCGCC CTCGGAGAGGTACCAGA Rev(A) AAACTCT GTGACTCTCCGAGGGC Fw(B) CACCGCC ATCTGGTACTCTCCGA Rev(B) AAACTCG GAGAGGTACCAGATGGGC	PX459 v2.0
GNA15	KO	Fw(A) CACCGAG GATGAGAAGGCCGCCGCC Rev(A) AAACGGC GGCGGCCTTCTCATCCTC Fw(B) CACCGTG TCTTCCCGTCTCGCC Rev(B) AAACGGC GAGAGCGGGAAGAGCAC	PX459 v2.0
PTPRG	KO	Fw CACCGAG GCTTCAGGCGACCCGTAC Rev AAACGT ACGGGTGCGCTGAAGCCTC	PX459 v2.0/LentiCRISPrv2
PPT1	KO	Fw CACCGAT CAATCTGATCTCGGTTG Rev AAACCA CCGAGATCAGATTGATC	LentiCRISPrv2
GPR3	KO	Fw CACCGCT GCGCGTGGCAGACTGC Rev AAACGCA GGTCTGCCACGGCCAGGC	PX459 v2.0

The overhangs added for sgRNA cloning in the Cas9 expressing plasmid are reported in red.

Table 2.2: Primer sequences

Target gene	Primers
HLA-C KO	Fw ATCTCAGTGGGCTACGTGGA Rev GGGGTCACTACCGTCCTC
HDAC6 KO	Fw GGA CTCCAGTGTCACTTCGG Rev AAACCCAAAGGTTCCCCACC
HDAC6 ΔBUZ	Fw(A) CCCAGGAGAGGAGAACCTA Rev(A) GGAGTGGGTGGGTGAAACTA
RUNX2 KO	Fw TGAAGTGGCATCACAAACCA Rev AGTCAGAGACCTACCTCGTC
GNA15 KO	Fw AGCGGTTCTGCTGCTCCATC Rev GGGCCTGCTGAATGGAATC
PPT1 KO	Fw TGGGGAGTCACAGAGGATGA Rev TCAGGTGGTCATGTGGGTTA
GPR3 KO	Fw CCTGGTGTCTGCGAGAATG Rev ACAGAGAAAGGTAGCGGTCCG

3. AIM OF THE THESIS

The present thesis work aims to analyze and review critical and crucial aspects concerning the CRISPR/Cas9 employment for the development of new cell models. The application of CRISPR/Cas9 faced us to important issues linked to the technique, to the manipulation of particular cell lines, and the screening of specific gene domain deletion and knock out.

To deeply analyze questions and limits concerning the CRISPR/Cas9 technology, as well as the genome manipulation of different cell lines, we generated new *in vitro* cell models.

Particular attention was paid to the target cell lines for selecting the best CRISPR/Cas9 shuttling method. With this regard, cell lines easy to transfect were edited exploiting the all-in-one CRISPR/Cas9 plasmid, whereas for cells tricky to manipulate the third generation LentiCRISPR viral vector was engineered. On the base of the CRISPR/Cas9-targeted gene, the most suitable screening detection assay was performed.

The CRISPR/Cas9 technique led us to generate new cell models useful for elucidating the patho-molecular mechanisms involved in retrovirus-host interactions, melanoma and pancreatic tumorigenesis and progression, as well as neurological disorders.

4. RESULTS

I applied the CRISPR/Cas9 technique to develop new edited cell lines to study 3 main topics (table 4.1):

- 1) the molecular mechanism involved in the modulation of retroviral infections caused by HIV-1 and HTLV-1;
- 2) cancer diseases, such as melanoma, pancreatic cancer, and chronic myeloid leukemia;
- 3) neurological disorders, such as neuronal ceroid lipofuscinoses and Alzheimer's disease.

Table 4.1: CRISPR/Cas9 application

Project	Target gene	Cell line
HIV-1/host factors interaction	ACOT8	HEK 293T
	HDAC6	HEK 293T
	HDAC6 ΔBUZ	HEK 293T
	HLA-C	HEK 293T
HTLV1/host factors interaction	TRAF3	HEK 293T
Cancer diseases	RUNX2	Mel-Ho
	GNA15	PT45
	PTPRG	LAMA84
Neurological diseases	PPT1	SH-SY5Y
	GPR3	H4 Swe

4.1 CRISPR/Cas9 to study host-retrovirus interaction

4.1.1 HIV-1 – host factors interaction

HIV is an enveloped retrovirus. Its genome is composed of two molecules of negative single-stranded RNA encoding for both structural and regulatory genes. The structural genes are *gag*, *pol* and *env*. The core and matrix proteins are encoded by the *gag* gene. The *env* gene encodes the HIV gp120 and gp41 envelope glycoproteins. HIV reverse transcriptase and integrase are encoded by the *pol* gene. While the structural genes produce structural viral proteins, the regulatory proteins are mainly involved in the modulation of the HIV-1 infection cycle (Fanales-Belasio et al. 2010).

HIV-1 infects CD4⁺ immune cells such as T-lymphocytes, macrophages, monocytes, and dendritic cells. Since CD4⁺ T-lymphocytes play a central role in immune response, their depletion leads to lacking the immune response, a condition known as Acquired Immune Deficiency Syndrome (AIDS). The viral entry in the host cell is mediated by the binding of HIV-1 gp120 to the CD4 receptor. The gp120-CD4 interaction induces a conformational change in HIV-1 gp41 protein, leading to its binding with the host coreceptors CXCR4 and CCR5 (Clapham and McKnight 2002).

70-80% of HIV-1 infected subjects show a very long period of viral latency lasting 8-10 years before developing AIDS. Instead, 10% of infected patients are defined as rapid progressors, since the AIDS onset occurs in 3 years or even less. On the contrary, 5% of patients are classified as long term non-progressors, since they do not show AIDS-related symptoms for more than 10 years, maintaining normal CD4 cell count and low viremia. Interestingly, some people, referred to as exposed uninfected, even if exposed to HIV-1 result resistant to the infection (Sharma, Kaur, and Mehra 2011).

Although antiretroviral therapy significantly decreases the viral load, about 1 million people still die of AIDS every year (UNAIDS data 2018 | UNAIDS n.d.). Since a definitive cure and a vaccine against HIV-1 is not yet available, it is important to focus the research in understanding how HIV-1 and specific host factors are involved in the crucial steps of viral infection, latency, and persistence

to individuate the key factors involved in AIDS pathogenesis, to the aim of understanding the molecular mechanisms driving the HIV-1 pathogenesis to develop new specific HIV-1 inhibitory compounds.

Development of ACOT8 KO cell lines to study the HIV-1 Nef/ACOT8 interaction in HIV-1 infection

The negative regulatory factor (Nef) is one of the main HIV-1 accessory proteins, fundamental in viral replication and infectivity. Nef is involved in HIV-1 pathology by modulating different cell pathways involved in host protein trafficking, apoptosis, T-cell development and viral replication (Lamers et al. 2012). Moreover, Nef is involved in the remodeling of different host surface proteins. Specifically, HIV-1 Nef positively regulates membrane proteins important in the modulation of the immune system, such as TNF and immature major histocompatibility complex class II (MHC-II); instead, it negatively modulates other immune factors, such as CD4, CD8, CXCR4, CCR5, and mature MHC-II.

It is known that the Nef N-terminal part removal causes the decrease of HIV-1 infectivity and failure in CD4⁺ and MHC I down-regulation (Bentham, Mazaleyrat, and Harris 2006).

The Nef N-terminal portion can be myristoylated, thus ensuring its association with lipid raft on the cell surface. Moreover, myristoylated Nef shows different tertiary and quaternary structures, allowing its interaction with different host proteins (Arold et al. 2000). An important key host factor interacting with HIV-1 Nef is the human Acyl-Coenzyme A Thioesterase 8 (ACOT8) (L. X. Liu et al. 1997; Watanabe et al. 1997), a peroxisomal enzyme involved in the fatty acids β oxidation, by controlling the peroxisomal acyl-CoA/CoASH balance. Our research group reported that Nef/ACOT8 association may be involved in maintaining Nef stability, avoiding its proteasome degradation (Serena et al. 2016). Different evidences have revealed that the N-terminal portion of ACOT8 play a crucial role in Nef-mediated down-modulation of CD4 and MHC-I (Cohen et al. 2000; Gondim et al. 2015; L. X. Liu et al. 2000; Peng and Robert-Guroff 2001), thus underlying the central role of ACOT8 in the regulation of CD4 surface expression level.

Moreover, being ACOT8 involved in the modulation of protein acylation, ACOT8 may be fundamental for HIV-1 particles budding from the plasma membrane (Benichou et al. 1994).

To study the involvement of ACOT8 in the modulation of HIV-1 infectivity, the CRISPR/Cas9 technique has been employed to generate 293T ACOT8 KO cell lines.

ACOT8 gene is located on chromosome 20 and its transcription leads to 13 predicted transcripts generated by both canonical and alternative splicing (http://www.ensembl.org/Homo_sapiens/Gene/Summary?db=core;g=ENSG00000101473;r=20:45841721-45857405).

The ACOT8 splice variants were analyzed and the exon 1 was found to be common to all the splice variants; thus, a sgRNA was designed to target this common exon, and cloned into the PX450 2.0 Cas9 expressing plasmid.

293T packaging cells and TZM-bl HIV-1 receptor and co-receptor expressing cells were transfected and selected with puromycin. To isolate clonal 293T and TZM-bl ACOT8 KO cell lines, a single cell cloning was performed. The expression of ACOT8 was analyzed by western blot (Figure 4.1).

The western blot analyses revealed that all the tested CRISPR/Cas9 clonal cell lines did not express ACOT8, compared to 293T and TZM-bl parental cells (Figures 4.1 A and B).

The role of ACOT8 in the modulation of HIV-1 infectivity was preliminarily evaluated. Following the Montefiori's protocol (2009), HIV-1 QHO pseudotyped viruses were produced in 293T ACOT8 wt and 293T ACOT8 KO packaging cells and their infectivity was analyzed performing a Luc-reporter gene assay on TZM-bl ACOT8 wt and ACOT8 KO cells (Figure 4.2).

The infectivity assay showed that HIV-1 QHO pseudotyped viruses produced in the absence of ACOT8 (red bar in Figure 4.2) resulted less infectious compared to the viruses produced in 293T wt cells (black bar on the left in Figure 4.2). Instead, no differences were detected by infecting either TZM-bl wt or TZM-bl ACOT8 KO cells (black and grey bars, respectively, reported on the right in Figure 4.2).

Our preliminary results suggest that ACOT8 may be necessary to generate infectious viruses, but it is not involved in the post-viral entry mechanism.

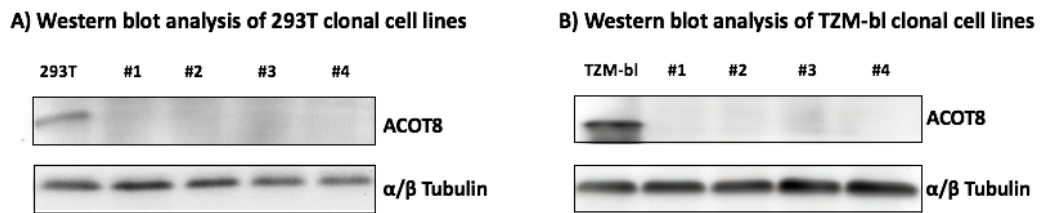


Figure 4.1: Western blot analysis of ACOT8 KO cell clones after CRISPR/Cas9. (A) Western blot analysis performed on 293T ACOT8 KO cell clones (#1-#4). (B) Western blot analysis conducted on TZM-bl cell clones (#1-#4). The ACOT8 protein expression was normalized using α/β Tubulin.

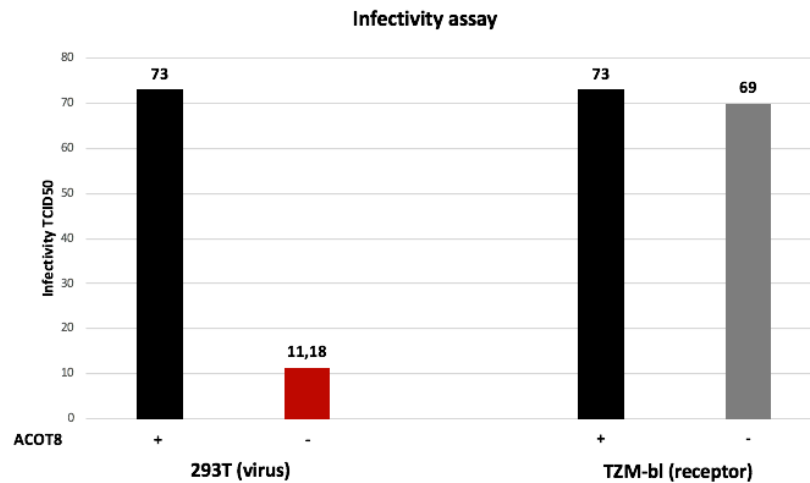


Figure 4.2: Luciferase gene reporter infectivity assay. HIV-1 QHO pseudotyped viruses were packaged in 293T wt and 293T ACOT8 KO cell lines and used to infect TZM-bl wt and TZM-bl ACOT8 KO cell lines. The infectivity values are reported as 50% Tissue Culture Infective Dose (TCID₅₀). Black bars refer to the control conditions (HIV-1 pseudotyped viruses produced in 293T wt cells and used to infect TZM-bl wt cells; red bar refers to HIV-1 pseudotyped viruses produced in 293T ACOT8 KO cells and used to infect TZM-bl wt cell; grey bar refers to HIV-1 pseudotyped viruses produced in 293T wt cells and used to infect TZM-bl ACOT8 KO cells).

Development of HDAC6 edited cell lines to study the role of HDAC6 in HIV-1 infection

The human histone deacetylase 6 (HDAC6) protein belongs to the human histone deacetylase family. Differently from other HDAC proteins, mainly located into the nucleus, HDAC6 is located into the cytoplasm (Hubbert et al. 2002), where it associates to the microtubules motor complex, taking part in the cytoskeleton remodeling by regulating the α -tubulin acetylation (Hubbert et al. 2002; Piperno, LeDizet, and Chang 1987). Its activity is crucial in the modulation of different cell pathways, such as cell migration (Palazzo, Ackerman, and Gundersen 2003), membrane proteins organization, and T-cell activation (Serrador et al. 2004).

The apolipoprotein B mRNA-editing enzyme-catalytic polypeptide-like 3G (APOBEC3G) is a cytidine deaminase (Jarmuz et al. 2002), involved in counteraction of retroviral infection. APOBEC3G exerts its anti-HIV-1 activity leading to cytidine deamination in uracil within the RNA viral genome, thus producing G-to-A point mutations in the mature HIV-1 RNA genome (Newman et al. 2005). APOBEC3G impairs retroviral infection also in a deaminase-independent manner, indeed it compromises the retroviral reverse transcription and integration steps (Mbisa et al. 2007; Mbisa, Bu, and Pathak 2010). However, due to the hypermutations induced by APOBEC3G into the viral genome, retroviruses undergo an important selection pressure that may be responsible for the generation of new variants (Berkhout and de Ronde 2004; E.-Y. Kim et al. 2010).

HIV-1 can escape from this defense mechanism through the viral infectivity factor (Vif) accessory protein (Henriet et al. 2009). Specifically, HIV-1 Vif binds the host factor Cullin 5 (Cul5), thus generating a ubiquitin ligase (E3)-like complex able to ubiquitinate APOBEC3G and leading to Vif proteasome-mediated degradation (Guo et al. 2014; Marin et al. 2003).

HDAC6 plays a crucial role in Vif degradation. At the C terminal portion, HDAC6 presents the bound to ubiquitin zinc finger (BUZ) domain (Ouyang et al. 2012; Pai et al. 2007). The HDAC6-BUZ domain is essential for HDAC6-APOBEC3G interaction, thus counteracting the Vif activity. Interestingly, the BUZ domain is

also involved in HIV-1 Vif degradation in a BUZ-dependent manner exploiting autophagy (Valera et al. 2015).

a) Development of 293T HDAC6 KO cell line

To investigate the role of HDAC6 in HIV-1 counteraction, CRISPR/Cas9 was induced to target the exon 3. Specifically, HDAC6 shows 43 splice variants (https://www.ensembl.org/Homo_sapiens/Gene/Summary?db=core;g=ENSG00000094631;r=X:48801377-48824982) and to knock out all of them, two specific sgRNAs were designed to direct the Cas9 activity on the exon 3, common to all of them.

293T cells were treated with sgRNA(HDAC6)-Cas9 expressing plasmids, selected with puromycin and single cell cloned.

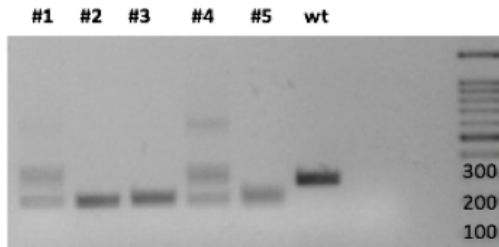
A preliminary screening was carried out by PCR to evaluate whether the employment of two sgRNAs induced a deletion on the exon 3. As shown in Figure 4.3 A the PCR product obtained after HDAC6 genomic amplification from the clones #2, #3, and #5 resulted lower than that obtained from 293T wt cells. Clones #1, #3, and #4, instead, showed different PCR products, probably due to different indel mutations inserted in the two DNA strands, leading to heterozygous clonal cell lines.

For addressing the HDAC6 gene mutation introduced by CRISPR/Cas9, the HDAC6 exon 3 of the clone #5 was analyzed by Sanger sequencing, which revealed a 74 bp deletion responsible for a frameshift (Figure 4.3 B).

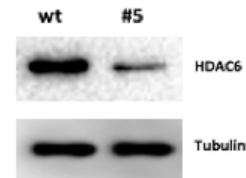
Intriguingly, western blot analysis showed that, despite the frameshift mutation, the HDAC6 expression was still detected in the clone #5, compared to the control, even if lower (Figure 4.3 C).

These contradictory results are probably due to a response mechanism carried out after CRISPR/Cas9 treatment (Smits et al. 2019).

A) PCR analysis of CRISPR/Cas9 HDAC6 edited clones



C) Western blot analysis of HDAC6 expression



B) BLAST alignment of CRISPR/Cas9 HDAC6 edited cells

```

HDAC6_WT      GGACTCCAGTGTCACTTCGGTGAGGCCCTAGACCCGCCCTGATGAGGGGGAGAGGGAGCA
HDAC6_KO      GGACTCCAGTGTCACTTCGGTGAGGCCCTAGACCCGCCCTGATGAGGGGGAGAGGGAGCA
*****

HDAC6_WT      AGTTGGTCATGCCCTGGACTCTGACCCCTTCTCTCTGATTCACAGAAGCGAAATATTAATA
HDAC6_KO      AGTTGGTCATGCCCTGGACTCTGACCCCTTCTCTCTGATTCACAGAAGCGAAATATTAATA
*****

HDAC6_WT      AGGGAGCCGTTCCCGCTCTATCCCAATCTAGCGGAGGTAAGAAGAAAGGCAAAATGA
HDAC6_KO      AGGGAGCCGTTCCCGCTCTATCCCAATC-----
*****

HDAC6_WT      AGAAGCTCGGCCAAGCAATGGAAGAAGACCTAATCGTGGGACTGCAAGGGATGGTGAGCA
HDAC6_KO      -----CAAGGGATGGTGAGCA
*****

HDAC6_WT      GGGCCTGGCTGCAGTTTAGCCTCGTATGACAATCAAAACCCAAAGGTTCCCCACC
HDAC6_KO      GGGCCTGGCTGCAGTTTAGCCTCGTATGAAATCAAAACCCAAAGGTTCCCCACC
*****
    
```

Figure 4.3: HDAC6 expression analyses after CRISPR/Cas9. (A) genomic PCR amplification on the edited clones obtained after CRISPR/Cas9. (B) Sanger sequence alignment revealed a 74bp deletion (in red is highlighted the premature STOP codon). (C) Western blot analysis of the HDAC6 expression, normalized with β Tubulin.

b) Development of 293T HDAC6 Δ BUZ cell line

To develop 293T HDAC6 Δ BUZ packaging cells, two sgRNAs were designed to specifically induce the deletion of the HDAC6 BUZ domain (Figure 4.4).

Bioinformatic analysis of the HDAC6 gene sequence was conducted to target the first and the last exon (exons 26 and 29, respectively) encoding the BUZ domain, thus inducing its deletion. The two sgRNAs were used for Cas9 expressing plasmid engineering and transfected into 293T packaging cells. After puromycin selection and single-cell cloning, the new 293T clonal cell lines were analyzed by western blot (Figure 4.4 A) to evaluate the BUZ domain deletion, revealing that only in three clones the BUZ domain deletion was achieved.

Of note, the p62 protein connects ubiquitinated proteins to autophagosomes. Ubiquitinated proteins are charged into autophagic vesicles and, then, HDAC6 induces the degradation of p62 (Bjørkøy et al. 2005; Pankiv et al. 2007). p62 protein expression was assessed too (Figure 4.5 A), indicating that the 293T clones with a lower HDAC6 protein presented a higher p62 expression. Instead, as expected, the acetylated α -tubulin levels did not correlate with the modulation of α -tubulin deacetylation, since the BUZ domain is not involved in the tubulin remodeling (Figure 4.5 A).

The deletion of the BUZ domain was further confirmed by performing a Sanger sequencing, that revealed the presence of indels responsible for the BUZ domain deletion (Figure 4.5 B).

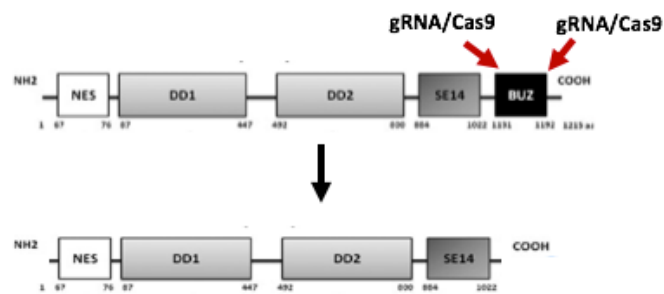
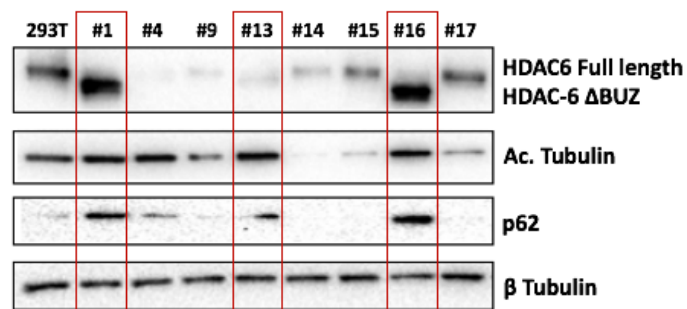


Figure 4.4: HDAC6 protein structure and CRISPR/Cas9 approach. Starting from the N terminal part, HDAC6 presents a Nuclear Export Signal (NES) domain, two Deacetylase Domains (DD1 and DD2), SE14, and the bound to ubiquitin zinc finger (BUZ) domain. To delete the BUZ domain, gRNA/Cas9 activity was directed at the beginning and at the end of the BUZ domain, as shown with the red arrow (Modified from Yan 2014).

A) Western blot analysis of 293T HDAC6 expression



B) BLAST alignment of CRISPR/Cas9 HDAC-6 ΔBUZ edited cells

```

HDAC6_WT          TGGAGGTCAGGACATGGCTGATTCGATGCTGATGCAGGGATCTAGGGCCTCACTGATCA
HDAC-6_deltaBUZ  TGGAGGTCAGGACATGGCTGATTCGATGCTGATGCAGGGATCTAGGGCCTCACTAGT--
*****

HDAC6_WT          GGTGAGCTCAGGGAGAGGCTGGGACTGTGGCTTCCTTCTCTTGCCAATTTGTGTCTCCAG
HDAC-6_deltaBUZ  -----GAGGCTGGGACTGTGGCTTCCTTCTCTTGCCCAATTTGTGTCTCCAG
*****

HDAC6_WT          GTAGGAGCATGTGATGAATAAACATATAATGGGGAGATGGGGTCTTCAGCTTACCTAGTT
HDAC-6_deltaBUZ  GTAGGAGCATGTGATGAATAAACATATAATGGGGAGATGGGGTCTTCAGCTTACCTAGTT
*****
    
```

Figure 4.5: Molecular characterization of 293T ΔBUZ edited cells. (A) Western blot analysis was conducted to verify the BUZ domain deletion, the level of acetylated tubulin, and p62 expression, normalized with β Tubulin. (B) HDAC6 wt sequence and HDAC6 ΔBUZ sequence were aligned using BLASTN. In red is circled the STOP codon introduced by CRISPR/Cas9 responsible for the BUZ deletion.

Development of HLA-C KO cell line to study the involvement of the different HLA-C variants in HIV-1 infection outcome

The major histocompatibility complex class I (MHC-I) is composed by a heavy α chain, encoded by the human leukocyte antigen (HLA) class I loci (HLA-A, -B, and -C), non-covalently associated with a light β chain, β_2 microglobulin (β_2m), and a small peptide. MHC-I is crucial for presenting foreign peptides to CD8⁺ T-cells that recognize infected cells, and to modulate the cytolytic function of natural killer cells (NK) (Groothuis and Neefjes 2006). Contrary to HLA-A and HLA-B, HLA-C expression is lower on the cell surface due to its lower binding affinity to the peptide (Snary et al. 1977). The HLA-C instability, compared to HLA-A and -B, is due to reduced HLA-C molecule plasticity that leads to its dissociation from β_2m (Sibilio et al. 2008). Thus, some HLA-C variants are predominantly complexed to β_2m on the cell membrane, while others are mostly present as free-chains, no longer complexed to β_2m . Specifically, HLA-C*06, -*05, -*08, and -*02 more stably bound β_2m , than HLA-C*01, -*03, -*04, and -*07 (Sibilio et al. 2008).

Accordingly, unstable HLA-C allotypes more easily release β_2m remaining as free chains on the cell surface (Parolini et al. 2018; Serena et al. 2017). The HLA-C allotypes differ in the modulation of HIV-1 infectivity due to their differences in their binding stability as heterotrimeric complexes. It is known that HIV-1 exploits HLA-C molecules to escape from the immune system. Indeed, during viral budding from the cell surface, HLA-C molecules are integrated into the newly HIV-1 virions (Cosma et al. 1999). Since some HLA-C alleles display a higher dissociation rate from β_2m than others, the amount of HLA-C free heavy chains on the cell surface, available for interaction with HIV-1 Env, is higher in the presence of unstable HLA-C variants.

Noteworthy, our research group recently reported that HIV-1 viruses produced in the absence of β_2m , which in turn reflects the complete absence of MHC-I complex on the cell surface, resulted less infectious than those produced in wt packaging cells (Serena et al. 2017). Moreover, we also observed that PBMC collected from healthy blood donors with unstable HLA-C variants (HLA-C*01, -*03, -*04, -*07, and -*14) mostly present HLA-C free heavy chains on the cell surface, while

subjects harboring HLA-C stable variants (HLA-C*02, -*05, -*06, -*08, -*12, -*15, and -*16) show a higher amount of HLA-C molecules complexed to β_2m (Parolini et al. 2018). Based on both HLA-C classification in stable and unstable groups (Parolini et al. 2018; Sibilio et al. 2008) and HLA-C phylogenetic evolution (Turner et al. 1998), our research group demonstrated that in the presence of HLA-C unstable variants, HIV-1 virions are more infectious than those produced in the presence of HLA-C stable ones (Parolini et al. 2018). This intriguing observation led us to define stable and unstable HLA-C alleles, as protective and non-protective, respectively, reflecting a faster or slower progression toward AIDS (Parolini et al. 2018).

Furthermore, HIV-1 shows neurovirulence detectable in HIV-1 infected patients (Brew et al. 1995). Very severe complications of HIV-1 infection are classified as HIV-associated neurocognitive disorders (HAND), and the most serious one is the AIDS dementia complex (ADC) (Brew et al. 1995; Saylor et al. 2016). The presence of β_2m in the cerebrospinal fluid (CSF) represents a marker of neuroinflammation. HIV-1 infected patients, who develop HIV-1-related dementia, show a high level of β_2m in the CSF (Alfieri et al. 1992). We recently established that there might be a correlation between the HLA-C binding stability with β_2m and the development of HIV-1 related neurocognitive disorders (Zipeto et al. 2018). Specifically, we found that HIV-1 patients, who develop ADC, show a higher frequency of HLA-C unstable alleles. Patients affected by Alzheimer's and Parkinson's neurodegenerative diseases too might present a high level of β_2m in CSF, and different old studies demonstrated that Alzheimer's patients present a higher frequency of unstable HLA-C *03 and HLA-C*04 alleles (Brew et al. 2005). To study the involvement of HLA-C in the onset of HIV-1-related neurocognitive disorders, blood samples were collected from HIV-1 patients who developed ADC. By performing an HLA-C genotyping analysis, none of ADC patients was found homozygous for stable HLA-C alleles, but they resulted either in heterozygous or homozygous for unstable HLA-C variants (Table 4.2).

Moreover, the distribution of the HLA-C alleles found in HIV-ADC patients was compared to the HLA-C allele frequency in HIV-1 infected patients who did not develop ADC and to the northern Italy population. A significant higher frequency

of unstable HLA-C alleles was detected only in the HIV-1-ADC patients, whereas no differences between stable and unstable HLA-C frequencies were found in the two control groups (Table 4.3).

Our observations suggest that the HLA-C binding stability may correlate with the onset of HIV-1 related cognitive disorders and not with HIV-1 infection status.

Table 4.2: HLA-C genotyping of ADC patients

Patients	HLA-C	Stability
Pt.1	C*03-04	Unstable/Stable
Pt.2	C*04-16	Unstable/Stable
Pt.3	C*04-07	Unstable/Unstable
Pt.4	C*03-07	Unstable/Unstable
Pt.5	C*02-07	Stable/Unstable
Pt.6	C*06-07	Stable/Unstable
Pt.7	C*07-16	Stable/Unstable
Pt.8	C*02-18	Stable/Unstable
Pt.9	C*04-14	Unstable/Unstable
Pt.10	C*07-15	Unstable/Stable
Pt.11	C*04-07	Unstable/Unstable

11 ADC patients were typing for the HLA-C alleles. In red are highlighted the unstable HLA-C variants and in blue the stable variants (Modified from Zipeto et al., 2018).

Table 4.3: HLA-C allele distribution in HIV-1 infected patients with ADC (HIV-ADC).

	HIV-ADC	HIV-no-ADC	Northern Italy
HLA-C UNSTABLE	16 (73%)	16 (50%)	771 (50%)
HLA-C STABLE	6 (27%)	16 (50%)	761 (50%)

p = 0.0293
p = 0.584

The percentage of unstable and stable HLA-C was compared to the distribution in HIV-1 patients who did not develop ADC (HIV-no-ADC) and to the northern Italian population (Guerini et al., 2008, Fisher exact test, $p = 0.029$ (red); $p=0.584$ (grey)) (Modified from Zipeto et al., 2018).

To assess the contribution of each HLA-C variant in HIV-1 infection progression, and their specific binding stability to β_2m , CRISPR/Cas9 was used to produce 293T HLA-C KO packaging cells. To this aim, a specific sgRNA was designed on the exon 2 and 3, common to all HLA-C variants annotated on Ensembl genome browser

(http://www.ensembl.org/Homo_sapiens/Gene/Summary?db=core;g=ENSG00000204525;r=6:31268749-31272130).

The engineered sgRNA(HLA-C)-Cas9 expressing plasmid was transfected into 293T cells and, to obtain a pure HLA-C KO clonal cell line, the transfected cells were selected with puromycin prior to performing single-cell cloning. The HLA-C protein expression was evaluated through western blot and flow cytometry analyses, using as control 293T wt cells (Figure 4.6 A and B).

The HLA-C KO was further confirmed performing a Sanger sequencing, that revealed the presence of 4-nucleotide substitutions and 2-nucleotide insertions (indicated by the red arrows in Figure 4.6 C) responsible for a frameshift and the cosequent premature STOP codon introduction in the exon 2 (circled in red in Figure 4.6 C).

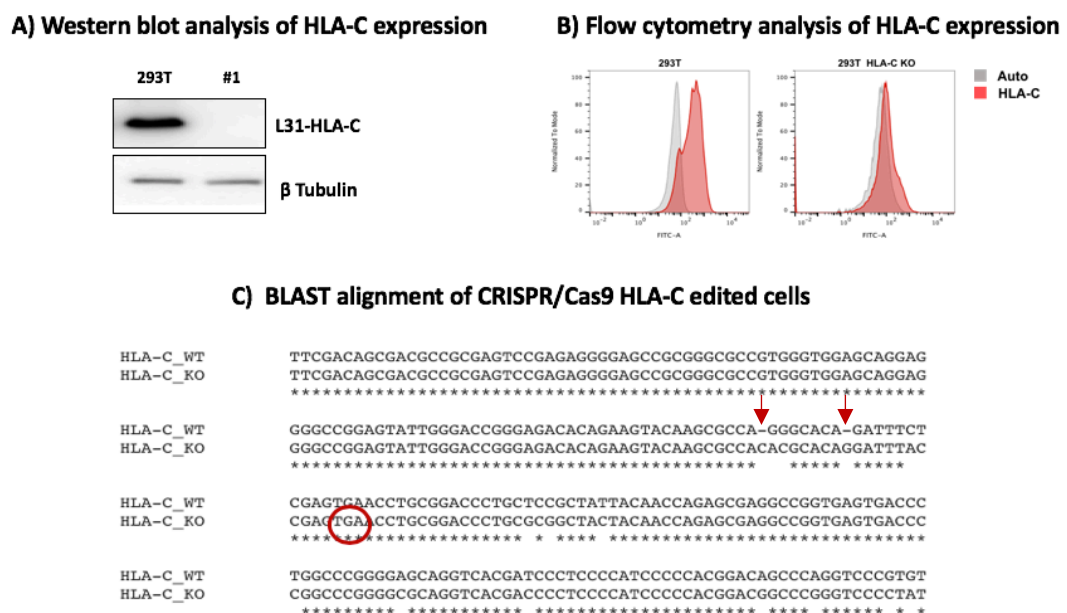


Figure 4.6: HLA-C expression analyses after CRISPR/Cas9 treatment. Western blot and flow cytometry analyses were performed to evaluate the HLA-C expression, normalized with β Tubulin and autofluorescence (panel A and B respectively). (C) Sanger sequencing revealed the introduction of a premature STOP codon, circled in red, in HLA-C KO cells due two 2-nt deletion, highlighted with the red arrows.

To define the contribution of each HLA-C variant in the modulation of HIV-1 infectivity and their specific binding stability to β_2m , 293T HLA-C KO cells were stably transfected to originate new packaging cell lines, each expressing a different specific HLA-C allotype. The HLA-C restoring was analyzed by flow cytometry (Figure 4.7). Flow cytometry analysis confirmed the HLA-C restored expression after stable transfection in 293T HLA-C KO packaging cells (Figure 4.7).

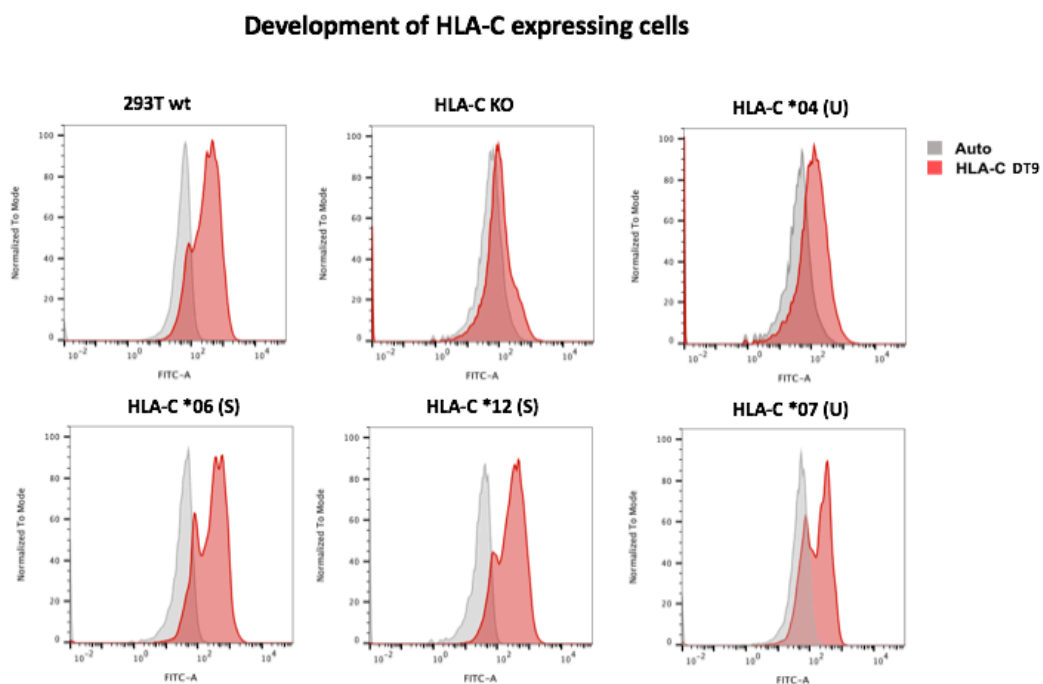


Figure 4.7: Restoring of HLA-C variants. Flow cytometry analysis was performed to detect the HLA-C expression in 293T HLA-C KO cells after HLA-C stable transfection. 293T wt and 293T HLA-C KO cells were used as control. U and S refer to Unstable and Stable, respectively. DT9 antibody was used to detect HLA-C molecules on the cell surface (red). The HLA-C expression was normalized with autofluorescence (grey).

To measure the HLA-C binding stability to β_2m , we set up an acid stripping wash experiment performing a time course, by measuring the increase of HLA-C free chains on the cell surface, which in turn reflected the kinetic dissociation of β_2m . The amount of HLA-C free chains was calculated as the slope of the interpolated curve. Preliminary data were obtained on HLA-C*04, HLA-C*12, and HLA-C*07, using as control 293T wt cells (figure 4.8).

Accordingly to the protective role of HLA-C*12 in HIV-1 infectivity (Chikata et al. 2019), our preliminary results suggest a stronger binding of HLA-C*12 to β_2m (Figure 4.8), suggesting the feasibility of our methodologic approach to stratify the HLA-C variants based on their binding stability.

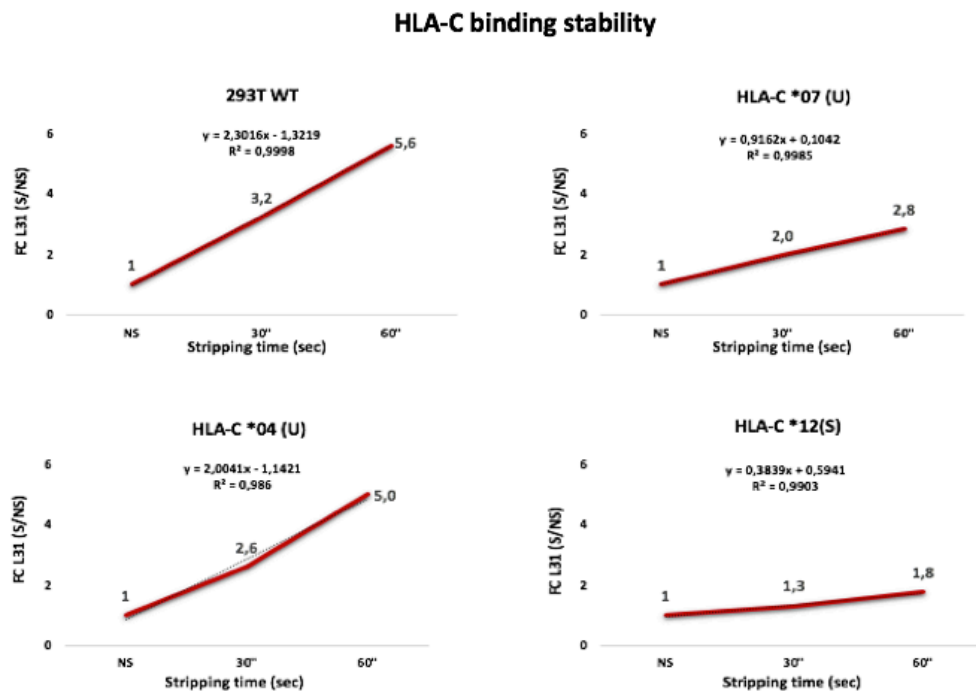


Figure 4.8: Fold change of L31 labeled HLA-C free chains. After stripping wash treatment time course (0, 30, and 60 sec), β_2m detachment from HLA-C molecules was calculated as fold change L31 (Stripped/Not Stripped). U and S refer to Unstable and Stable, respectively.

To correlate the HLA-C binding stability to HIV-1 infectivity, HIV-1 QHO pseudotyped viruses were produced by co-transfecting different amounts of HLA-C expressing plasmid in 293T HLA-C KO packaging cells, to define the right HLA-C concentration for restoring HLA-C expression level close to 293T wt packaging cells. HIV-1 QHO pseudotyped viruses were collected and used to perform a Luciferase gene reporter infectivity assay on TZM-bl cells (Figure 4.9).

The infectivity assay in Figure 4.9 showed that by transiently transfecting 0.125 μg of HLA-C expressing plasmid in 293T HLA-C KO packaging cells, infectivity level comparable to the wt parental cell line was achieved. Interestingly, a strong HIV-1 infectivity reduction was observed in HLA-C overexpression conditions (0.5-1 μg).

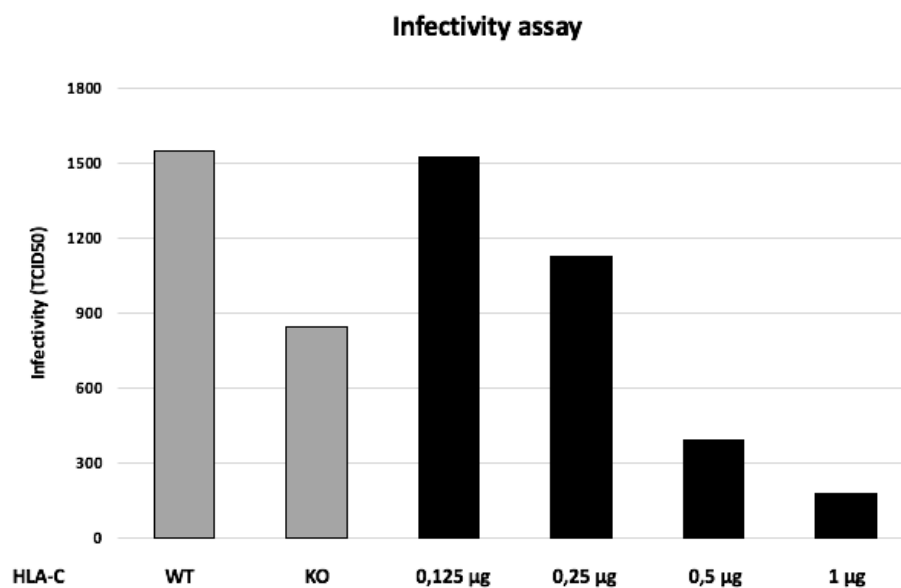


Figure 4.9: Infectivity Luc-assay. QHO pseudotyped viruses were packaged in the presence of increasing amount of HLA-C (black bars), and in 293T wt and HLA-C KO control cells (grey bars). The infectivity values are reported as 50% Tissue Culture Infective Dose (TCID50).

4.1.2 HTLV-1 – host factors interaction

Human T-cell Leukemia virus type-1 (HTLV-1) belongs to the Retroviridae family. HTLV-1 was isolated for the first time in 1980 by Robert Gallo (Poiesz et al. 1980). HTLV-1 infection may cause the onset of two serious diseases: Adult T-cell Leukemia/Lymphoma (ATLL) and Tropical Spastic Paraparesis/HTLV-1 Associated Myelopathy (TSP/HAM). HTLV-1 distribution is restricted to specific endemic regions, such as Japan, South America, Caribbean basin and sub-Saharan Africa, even though HTLV-1 infections have been reported also in Romania, in the Middle East, and in Australo-Malanesia (Gessain and Cassar 2012).

HTLV-1 mainly infects CD4⁺ T-cells (Richardson et al. 1990), but the proviral DNA has been also found in other immune cells (Koyanagi et al. 1993; Macatonia et al. 1992).

The two principal regulatory proteins encoded by the HTLV-1 genome are Tax-1 and the HTLV-1 bZip (HBZ) protein. Tax-1 is the viral long terminal repeat (LTR) transactivator factor, responsible for the CD4⁺ T-cell immortalization. Contrarily, the antisense HBZ viral protein inhibits the Tax-1 transactivation function and is involved in the HTLV-1 persistence (Barbeau, Peloponese, and Mesnard 2013). Tax-1 is mainly responsible for the NF- κ B pathway activation (Fochi et al. 2018; Qu and Xiao 2011), instead, HBZ, together with Tax, deregulates cell growth, apoptosis, immune escape and autophagy (Zhao 2016).

NF- κ B dysregulation represents a crucial step in HTLV-1 pathogenesis. The NF- κ B activation is carried out by both the canonical and the non-canonical pathways. Several signaling molecules activate the NF- κ B canonical pathway, such as TNF- α , LPS, IL-1, and double-stranded RNA (Durand and Baldwin 2017). The main effector of the canonical NF- κ B signaling is the NF- κ B transcription factor, composed by the RelA/p65 dimer, mostly located into the cytoplasm complexed with I κ B α (Bauerle and Baltimore 1988). Under activating stimuli, the I κ B kinase trimeric complex, composed by IKK α , IKK β , and IKK γ , is activated and phosphorylates I κ B α , then polyubiquitinated and degraded via proteasome. The I κ B α degradation release RelA/p65 into the nucleus where it activates the target genes transcription.

The NF- κ B non-canonical signaling activation requires CD40L and BAFF. The TNF-receptor associated factor (TRAF) proteins activate the NF- κ B Inducing Kinase (NIK), responsible for IKK α homodimerization. The activation of IKK α leads to p100 processing, thus activating the p52/RelB NF- κ B non-canonical effector dimer, which then translocates into the nucleus.

The TRAF3 ubiquitin ligase plays a crucial role in controlling NF- κ B activation. Specifically, TRAF3 negatively modulates the NIK expression levels (Gardam et al. 2008), thus acting as an NF- κ B inhibitor factor. It has been reported that TRAF3 is mutated in ATL cells (Kogure and Kataoka 2017).

To study the involvement of TRAF3 in the deregulation of the NF- κ B pathway induced by HLTV Tax-1 antisense protein, CRISPR/Cas9 was employed to generate 293T TRAF3 KO cell line. To obtain TRAF3 KO cells, bioinformatic analysis was conducted to design a specific sgRNA able to target all the TRAF3 splice variants. The sgRNA was selected and cloned in the Cas9 expressing plasmid. After sgRNA(TRAF3)-Cas9 transfection, 293T cells were selected with puromycin and single cell-cloned. The TRAF3 edited cell clones were analyzed by western blot, revealing that TRAF3 expression was abrogated after CRISPR/Cas9 treatment in all the tested clones #2, #3, and #5 (Figure 4.10 A).

The NF- κ B activation was evaluated through an NF- κ B luciferase gene reporter assay (Figure 4.10 B), showing that in the absence of TRAF3, the transfection of the NF- κ B transactivator p65 was not sufficient for a sustained NF- κ B activation. As shown in Figure 4.10 C, in the absence of TRAF3 expression, a constitutive p100 processing was detected, as indicated by the p52 increased expression in TRAF3 KO cells, suggesting that TRAF3 KO cells are characterized by an NF- κ B basal activation.

Our research group reported that Tax-1 interacts with TRAF3 (Diani et al., 2015). To evaluate the contribution of TRAF3/Tax1 interaction in NF- κ B activation, TRAF3 KO cells were co-transfected with Tax1 and NF- κ B-Luc encoding plasmids (Figure 4.11 A). In the absence of TRAF3, Tax1 slightly induced the NF- κ B promoter activation, compared to the stronger NF- κ B activation observed in 293T wt cells (Figure 4.11 A). Furthermore, a reduction of 30% of the NF- κ B inhibitor I κ B α expression was observed in TRAF3 KO cells, compared to 293T wt cells

(Figure 4.11 B). To explore if the NF- κ B basal activation in TRAF3 KO cells correlates with the expression of NF- κ B target genes, the mRNA levels of IL-6, BCL2 and A20 were evaluated. As shown in Figure 4.9 C, a significant increased mRNA expression was detected in TRAF3 deficient cells.

Our results strongly support that the NF- κ B negative regulator TRAF3 is fundamental for an efficient and sustained NF- κ B transactivation mediated by the HTLV Tax1 protein (Fochi et al. 2019).

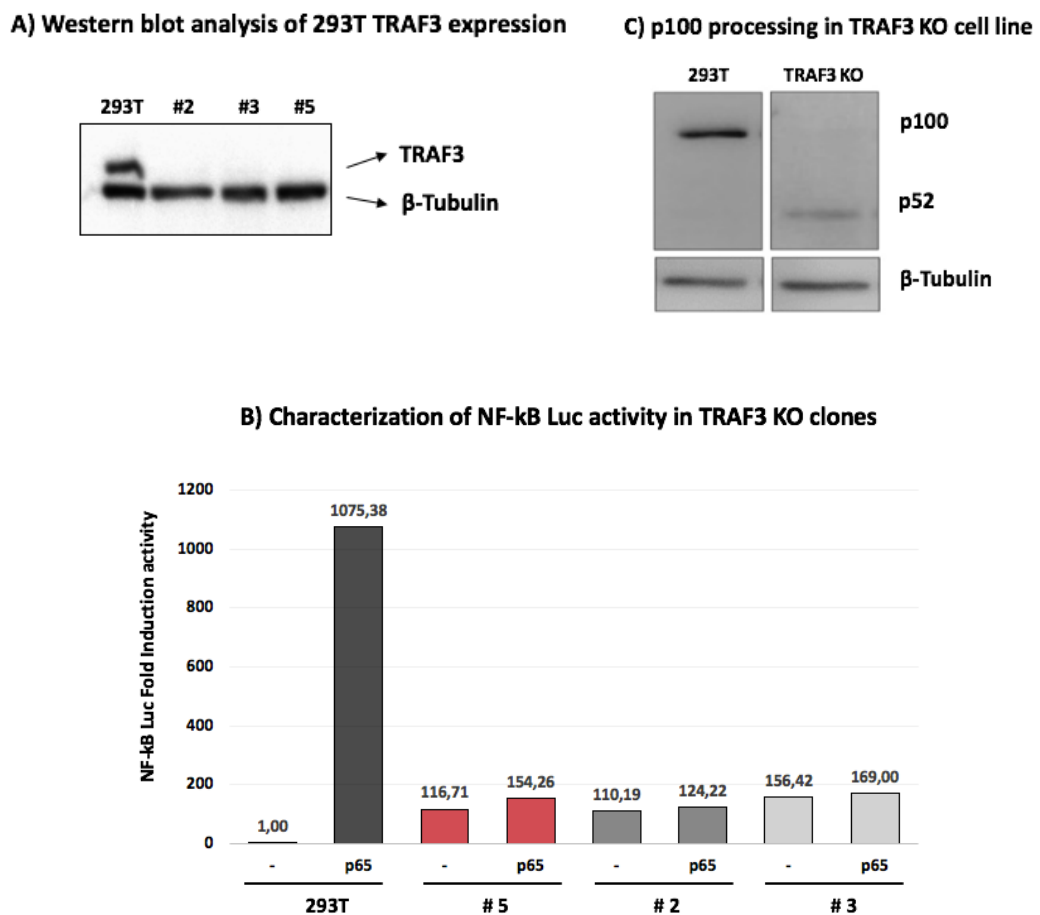


Figure 4.10 Molecular characterization of 293T TRAF3 KO cell lines. (A) Western blot analysis of CRISPR/Cas9 293T TRAF3 KO cells. (B) NF- κ B Luc promoter activation in TRAF3 KO cells. (C) p100 processing in TRAF3 KO cells. TRAF3 expression and p100 processing were normalized with β Tubulin (A and C), NF- κ B promoter activation was normalized with Renilla expressing plasmid (B) (Fochi et al., 2019).

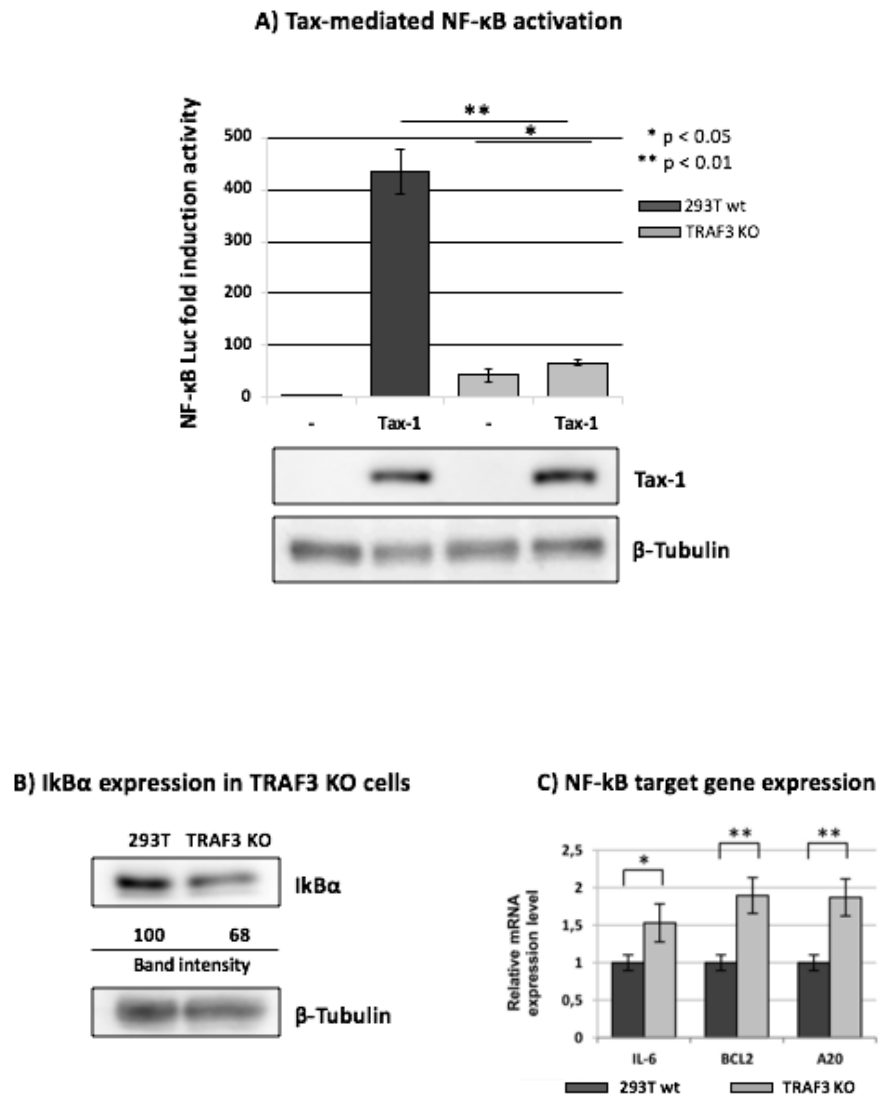


Figure 4.11: NF- κ B activation and its transcription activity. A) Western blot analysis was performed in 293T wt and TRAF3-KO to compare the I κ B α expression level, normalized with β tubulin. B) NF- κ B fold induction activity in 293T wt and TRAF3 KO cells transfected with NF- κ B-Luc and Tax-1 encoding plasmids. C) RNA was extracted from 293T wt and TRAF3 KO cells to analyze the mRNA expression level of NF- κ B target genes, normalized with the mRNA expression of RPLP0 (Fochi et al., 2019).

4.2 CRISPR/Cas9 to study cancer diseases

4.2.1 Development of RUNX2 KO cell line to study its involvement in malignant melanoma

The incidence of Malignant Melanoma (MM) is globally increasing, accounting for 130000 new cases every year (WHO | Skin cancers 2017). The surgical removal of skin lesions allows tumor eradication. However, melanoma cells have a high metastatic potential, due to their stemness characteristics (Quintana et al. 2012). Lung, liver, lymph node, brain, and bone represent the main metastasizing sites. Unfortunately, after metastasis dissemination, there is no effective cure.

The Runt-related transcription factor (RUNX) family includes the transcription factors RUNX1, RUNX2, and RUNX3, sharing the highly conserved Runt-homology DNA binding domain (Blyth et al. 2010). Structurally, starting from the N-terminus, RUNX2 presents the DNA binding RUNT domain, the NLS domain, and both transactivation and inhibitory motifs involved in the regulation of RUNX2 transcriptional activity (Wysokinski, Blasiak, and Pawlowska 2015).

RUNX2 is the master gene for mesenchymal stem cell commitment in osteogenic lineage differentiation (Chen et al. 2014). It has been reported that RUNX2 expression is upregulated in different tumors, such as T-cell lymphoma, acute myeloid leukemia, multiple myeloma, pancreatic, breast, prostate, ovarian epithelial, and lung cancers (Blyth et al. 2006; Valenti 2015), where it plays a pivotal role in tumor progression and metastasis (van der Deen et al. 2012). For instance, in breast cancer, RUNX2 induces metalloproteinases and VEGF expression, which may be related to the first steps driving metastasis (J. Pratap et al. 2005). It has also been reported that, in normal mammary epithelial cell lines, RUNX2 overexpression causes the acquisition of a mesenchymal-like phenotype (Jitesh Pratap et al. 2009). Moreover, in some osteosarcoma cell lines, RUNX2, by controlling PTK2/FAK focal adhesion kinases and TLN1 expressions, interferes with integrins-cytoskeleton connections, thus playing a crucial role in cell mobility (van der Deen et al. 2012). Besides, RUNX2 is also related to the induction of pro-angiogenic factors, such as VEGF and hypoxia-inducible factor 1- α (HIF-1 α).

Specifically, both in normal and hypoxia conditions, RUNX2 stimulates the VEGF transcription in a HIF-1 α -dependent manner (Kwon et al. 2011). RUNX2 is also involved in the sustained activation of MAPK/ERK and PI3K/AKT pathways (Bennett 2008), fundamental in apoptosis escape and in Epithelial-Mesenchymal Transition (EMT) (Cohen-Solal, Boregowda, and Lasfar 2015; Pappalardo et al. 2016). Our research group, through CRISPR/Cas9, developed an A375 Δ RUNT domain melanoma cell line, proving the involvement of the RUNT domain in cell viability, EMT, and cell mobility (Deiana et al. 2018). Cell viability resulted strongly reduced in A375 Δ RUNT melanoma cells, probably due to the inability in activating MYC transcription (Shin et al. 2016), and to the impaired p53 inactivation (Ozaki, Nakagawara, and Nagase 2013). Moreover, SSBP1, which is involved in controlling p53 transcriptional activity and stability, resulted upregulated in A375 Δ RUNT melanoma cells (Deiana et al. 2018). Furthermore, both *in vitro* and *in vivo* analyses confirmed that the RUNX2-RUNT domain is essential in the migration of melanoma cells, mainly ascribed to the downregulation of RMD and STMN1 expression (Deiana et al. 2018).

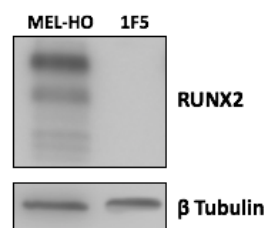
MM represents 60% of death due to skin tumors and, in the last years, the percentage of death has increased, probably due to lifestyle and environmental changes. It results necessary to develop new *in vitro* and *in vivo* models for understanding the molecular mechanisms affecting the behavior of melanoma cells. To fully analyze the oncogenic potential of RUNX2 in MM and its impact in uncontrolled tumor cell growth, apoptosis escape, and tumor cell invasiveness, CRISPR/Cas9 was used to develop a MEL-HO RUNX2 KO melanoma cell line. Two sgRNAs were designed on the exons 2 and 3, to knock out all the 12 RUNX2 splice variants annotated on Ensemble genome browser (http://www.ensembl.org/Homo_sapiens/Gene/Summary?db=core;g=ENSG00000124813;r=6:45328157-45664349).

PX459 2.0 Cas9 expressing plasmid was then engineered with the two selected sgRNAs. After sgRNA(RUNX2)-Cas9 expressing plasmid transfection and antibiotic selection, CRISPR/Cas9 MEL-HO treated cells were single-cell cloned to isolate a pure edited clonal cell line.

To individuate MEL-HO RUNX2 KO cells, western blot analysis was performed, revealing the occurred RUNX2 KO in MEL-HO 1F5 clonal cell line (Figure 4.12 A). To characterized the mutations induced by the Cas9 activity, a Sanger sequencing was performed (Figure 4.12 B), highlighting a deletion of exactly 100 bp, which in turn induces a frameshift leading to the introduction of a premature TGA-STOP codon (highlighted in red in Figure 4.12 B).

The Mel-HO RUNX2 KO cell line will be useful to confirm the oncogenic property of RUNX2 and its involvement in the epithelial-to-mesenchymal transition process.

A) Western blot analysis of MEL-HO RUNX2 expression



B) BLAST alignment of CRISPR/Cas9 RUNX2 edited cells

```

RUNX2_WT      AGACACATCATTTGCAATGAGAATATATTTCTGTTTGTAAAGCCTTTCTGATGTGCCATTAT
RUNX2_KO      AGACACATCATTTGCAATGAGAATATATTTCTGTTTGTAAAGCCTTTCTGATGTGCCATTAT
*****

RUNX2_WT      TGCTGCTGTGTTTCCCTGTTTTATGTAGGTGGTAGCCCTCGGAGAGGTACCAGATGGGACT
RUNX2_KO      TGCTGCTGTGTTTCCCTGTTTTATGTAGGTGGTAGCCCTCG-----
*****

RUNX2_WT      GTGGTTACTGTCATGGCGGGTAACGATGAAAATTATCTGCTGAGCTCCGGAATGCCTCT
RUNX2_KO      -----

RUNX2_WT      GCTGTTATGAAAAACCAAGTAGCAAGGTTCAACGATCTCGAGATTTGTGGGCCGGAGTGGA
RUNX2_KO      -----AGCAAGGTTCAACGATCTGAGATTTGTGGGCCGGAGTGGA
*****

RUNX2_WT      CGAGGTAGG
RUNX2_KO      CGAGGTAGG
*****
    
```

Figure 4.12: Western blot analysis of MEL-HO parental cell line and 1F5 cell line RUNX expression (A). Sanger sequencing showed a 100 bp deletion in the RUNX2 KO clonal cell line, responsible for the introduction of a premature STOP codon (circled in red).

4.2.2 Development of GNA15 KO cell line to study its involvement in pancreatic carcinoma

G-protein coupled receptors (GPCRs) play a crucial role in different physiological processes such as neurotransmission, sensory functions, and immune response. GPCRs are constituted of a heterotrimeric G protein, composed of $G\alpha$ and $G\beta/\gamma$ subunits, and a *hepta*-helix transmembrane receptor. GPCR activation needs the binding of an extracellular agonist, followed by GDP-GTP exchange from the $G\alpha$ subunit, and its dissociation from the $G\beta/\gamma$ dimer. Both $G\alpha$ loaded of GTP and $G\beta/\gamma$ represent the GPCR signaling effectors, influencing downstream signaling such as adenylyl cyclase, Src, phospholipase C, phosphodiesterases and ion channels (Bar-Shavit et al. 2016). The G protein activity ceases upon GTP hydrolysis in GDP, and the $G\alpha$ subunit associates with $G\beta/\gamma$ (O'Hayre et al. 2013). Based on the $G\alpha$ aminoacidic primary sequence, GPCRs are distinguished in four classes: $G\alpha_s$, $G\alpha_{i/o}$, $G\alpha_{q/11}$, and $G\alpha_{12/13}$ (Preininger and Hamm 2004).

GPCRs dysfunction and overexpression are frequently linked to human diseases and cancers (Pierce, Premont, and Lefkowitz 2002), thus representing the target for therapeutic drugs (Ma and Zimmel 2002; Rask-Andersen, Almén, and Schiöth 2011).

The $G\alpha$ subunit GNA15 belongs to $G\alpha_{q/11}$ subclasses but shares with the other $G\alpha_{q/11}$ only 57% of amino acids identity (Hubbard and Hepler 2006). Moreover, contrary to the other $G\alpha_{q/11}$, it is expressed at specific immature stages and it has a promiscuous behavior, as it can associate with different GPCRs (Giannone et al. 2010). Firstly GNA15 expression was found in murine hematopoietic cells (Wilkie et al. 1991), anyway GNA15 expression has been reported also in different epithelia, as well as in the immune system (Giannone et al. 2010).

The specific function of GNA15 is still unknown, mainly due to the high promiscuous activity and the lacking of specific drug inhibitors. Many studies describe its signaling activity taking advantage of GNA15-Q212L, a constitutively active mutant. GNA15-Q212L induces the PKC activation, thus resulting in NF- κ B, STAT3 and MAPK pathways induction (A. M. F. Liu and Wong 2004; Lo and Wong 2006; E. H. T. Wu, Lo, and Wong 2003). GNA15 modulates cell growth,

maturation, viability, neuronal and erythroid differentiation (Ghose, Porzig, and Baltensperger 1999; Heasley et al. 1996). Anyhow, the GNA15 activity characterization is questionable, due to the employment of a constitutive active drug to shed light on its function, mostly due to the decoupling between GNA15 and G β / γ subunits activity, being the GNA15-Q212L drug activity independent from GPCR stimulation.

Pancreatic carcinoma affected patients display an expected 5-year survival rate of 5% (Ducreux et al. 2019), mainly due to the lacking of targeted therapy, late diagnosis, and resistance to chemotherapy and radiation (Rahib et al. 2014).

In a recent work, bioinformatic analysis was conducted to find potential key molecules responsible for the development of pancreatic carcinoma. By analyzing three pancreatic ductal adenocarcinoma (PDAC) with the GEO database (<http://www.ncbi.nlm.nih.gov/geo>), overlapping and differentially expressed genes were found, compared to normal pancreatic tissue. Specifically, 8 candidate genes resulted significantly overexpressed CXCL5, CCL20, NMU, F2R, ANXA1, EDNRA, LPAR6, and GNA15. It is important to note that among these 8 selected genes, five associate with guanine-nucleotide binding protein GNA15, CXCL5, EDNRA, F2R, and LPAR6 (Y. Gu et al. 2019). It has been demonstrated that in pancreatic carcinoma GNA15 promotes the overactivation of different signal pathways, including Ras, Raf, and PI3K (Giovinazzo et al. 2013; Philip et al. 2009). By inducing GNA15 knockdown through RNA interference in carcinoma cell lines, GNA15 was found involved in cell adhesion and in the sensitivity to starvation condition, activating PKD1 signaling involved in the increased mobility, adhesion and survival of tumor cells (Giovinazzo et al. 2013; Waldron et al. 2012). Although many studies have been conducted to reveal the pathomolecular mechanisms involved in the pancreatic carcinogenesis, they still remain unknown, with consequent absence of efficient treatments, and making pancreatic carcinoma one of the main causes of death related to cancer (Y. Gu et al. 2019).

To elucidate the role of GNA15 in the molecular mechanisms leading to pancreatic adenocarcinoma development, CRISPR/Cas9 was used to generate PT45 pancreatic adenocarcinoma GNA15 KO cell line. As reported in Ensemble genome browser, the GNA15 gene transcription produces three splice variants

(https://www.ensembl.org/Homo_sapiens/Gene/Summary?db=core;g=ENSG00000060558;r=19:3136033-3163749). To induce the GNA15 KO, two sgRNAs were designed to direct the Cas9 endonuclease activity on the exon1 and the exon2, common between the three known splice variants. After sgRNA cloning into the Cas9 expressing plasmid and sgRNA-Cas9 plasmid transfection into PT45 cell line, cells were selected with puromycin to enrich the PT45 GNA15 KO cell population. To obtain a clonal cell line not expressing GNA15, a single cell cloning was carried out.

The different PT45 clonal cell lines were tested for PT45 expression through western blot analysis (Figure 4.13 A) and sanger sequencing (Figure 4.13 B).

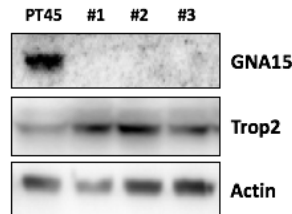
The western blot analysis revealed the absence of GNA15 expression in the three clones analyzed, compared to the control (Figure 4.13 A). The occurred GNA15 KO was further confirmed by Sanger sequencing, showing that Cas9 introduced a single-nucleotide deletion, and thus a frameshift not allowing GNA15 expression (Figure 4.13 B).

One of the main functions of GNA15 is the activation of PKD signaling. After GPCR activation, phospholipase C induces an increase of diacylglycerol (M. S. Kim et al. 2009) that stimulates the PKD autophosphorylation at the C-term Ser910 residue, thus inducing a conformational change that makes PKD able to be phosphorylated by PKC at Ser738/742 (Rybin et al. 2012). Due to the tight link between GNA15 activity and PKD activation, the PKD phosphorylation status was assessed by western blot (Figure 4.13 C).

As expected, the western blot analysis conducted to evaluate the phospho-Ser910/738/742, revealed that the PKD autophosphorylation at Ser910 occurred in the absence of GNA15, instead, the level of phospho-Ser738/742 resulted lower compared to the PT45 control (Figure 4.13 C).

The PKD activation correlates with the lack of GNA15 expression. GNA15 KO cells will be useful to elucidate its involvement in malignant properties, such as cell migration and cancer-related pathways deregulation.

A) Western blot analysis of GNA15 expression



B) BLAST alignment of CRISPR/Cas9 PT45 edited cells

```

GNA15_WT      GCCCGGGGGCGATGCCACCCGGTGCCGACTGAGGCCACCGCACCATGGCCCGCTCGCTGA
GNA15_KO      GCCCGGGGGCGATGCCACCCGGTGCCGACTGAGGCCACCGCACCATGGCCCGCTCGCTGA
*****

GNA15_WT      CCTGGCGCTGCTGCCCTGGTGCCTGAC-GGAGGATGAGAAGCCCGCCGCCGGGTGGAC
GNA15_KO      CCTGGCGCTGCTGCCCTGGTGCCTGACGGGAGGATGAAAGCCCGCCGCCGGGTGGAC
*****

GNA15_WT      CAGGAGATCAACAGGATCCTCTTGGAGCAGAAGAAGCAGGACCGCGGGGAGCTGAAGCTG
GNA15_KO      CAGGAGATCAACAGGATCCTCTTGGAGCAGAAGAAGCAGGACCGCGGGGAGCTGAAGCTG
*****
    
```

C) PKD activation

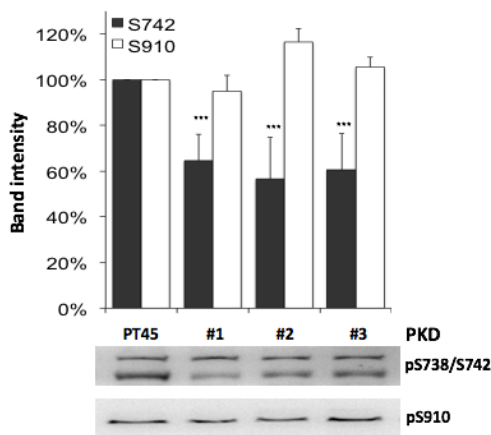


Figure 4.13: Western blot analysis of PT45 parental cell line and #1, #2, and #3 cell lines GNA15 expression (A). Sanger sequencing showed the insertion of a G nucleotide in GNA15 KO clonal cell lines, responsible for the introduction of a premature STOP codon (circled in red, B). Western blot was performed to evaluate the PKD activity in GNA15 KO clonal cell lines, by quantifying the level of phospho-ser738, 732, and 910 (lower panel). The band intensity is reported in the diagram in the upper panel (mean \pm SEM, *** $P < 0.0005$, $n = 10$).

4.2.3 CRISPR/Cas9 to study the involvement of PTPRG in Chronic myeloid leukemia

Chronic myeloid leukemia (CML) is a myeloproliferative malignancy affecting the bone marrow myeloid lineage. CML originates from t(9;22)(q34;q11) reciprocal chromosomal translocation in pluripotent stem cells resulting in a shorter chromosome 22, known as the Philadelphia chromosome, found in more than 90% of CML patients (Salesse and Verfaillie 2002). This translocation leads to the expression of BCR/ABL fusion protein. BCR/ABL is a constitutively active tyrosine kinase (Faderl et al. 1999). BCR/ABL becomes active upon different phosphorylations, among them the most important driving neoplastic transformation is the phosphorylation of Tyr⁸⁹ which occurs in a Src family kinase-dependent manner (Meyn et al. 2006). BCR/ABL interferes with different cell processes, such as cell proliferation, adhesion, cell survival, and differentiation, by activating Jun-kinase, Ras, and PI-3 kinase pathways fundamental in tumor cell transformation (Salesse and Verfaillie 2002). Many efforts have been directed in studying the protein tyrosine phosphatase (PTP) family, comprising 107 members, that act as negative regulators of tyrosine kinases. CML treatment is based on tyrosine kinase inhibitors (TKIs) targeting BCR-ABL, such as imatinib, nilotinib, and dasatinib (Drube et al. 2018).

CML can be distinguished in three phases: chronic, accelerated and blast crisis. The chronic phase shows the acquisition of mutations in leukemia stem cells leading to increased chemokines expression related to cell mobility (Dierks et al. 2008). The accelerated phase is highlighted by the acquisition of resistance to drug treatment, increased blasts or basophils in blood and bone marrow, thrombocytopenia, and splenomegaly (Baccarani et al. 2006). The blast crisis is characterized by the acquisition of other chromosome mutations, besides the Philadelphia chromosome, mainly involving trisomy 8, isochromosome 17q, and trisomy 19 (Campbell et al. 2002). Among the PTP proteins, protein tyrosine phosphatase receptor type γ (PTPRG) belongs to subtype V. Structurally, PTPRG shows an extracellular region, a single transmembrane domain, and two kinase catalytic domains. PTPRG is expressed in leukocytes, hematopoietic precursors, endocrine and epithelial cells

(Mafficini et al. 2007; Vezzalini et al. 2017). PTPRG functions as tumor suppressor and loss of function mutations, as well as promoter methylation, have been detected in renal cell carcinoma, lung carcinoma, breast cancer, and colorectal cancer (Furuta et al. 2006; LaForgia et al. 1991; S. Liu et al. 2004; Z. Wang et al. 2004). Moreover, Della Peruta et al. (2010) reported that in CML cell lines, the downregulation of PTPRG leads to higher clonogenic cell capability, while its overexpression causes the opposite effect and induces BCR/ABL dephosphorylation and its proteasome degradation (Monne et al. 2013; Della Peruta et al. 2010). Of note, it has been demonstrated that PTPRG expression is restored in CML patients treated with TKIs, highlighting its potential prognostic biomarker role (Monne et al. 2013). PTPRG plays a crucial role in CML acting as a potential tumor suppressor by inhibiting the BCR/ABL activity, thus underlying the importance of elucidating its role in counteracting tumor transformation.

To better understand the molecular mechanism by which PTPRG counteracts BCR/ABL oncogenic function, LAMA84 cells were selected since, differently from other CML cell lines, the PTPRG promoter is not methylated and, consequently, the PTPRG protein is expressed (Della Peruta et al. 2010). CRISPR/Cas9 was used to generate the LAMA84 PTPRG KO CML cell line.

Seven splice variants are annotated on the Ensemble genome browser (https://www.ensembl.org/Homo_sapiens/Gene/Summary?db=core;g=ENSG00000144724;r=3:61561569-62297609), thus, to induce the PTPRG KO, a specific sgRNA was designed to target the exon 2, common to all the predicted splicing variants.

LAMA84 cells are a hard-to transfect cell line, thus sgRNA was cloned in the LentiCRISPRv2 Cas9 expressing vector, for conveying the sgRNA-Cas9 complex through lentiviral infection.

The sgRNA(PTPRG)-Cas9 LentiCRISPRv2 expressing vector was co-transfected with the psPAX2 and pVSVg plasmids in 293T packaging cells to produce viral particles. After 48h from transfection, the culture medium, containing the LentiCRISPR-expressing virions, was collected to proceed with the infection of LAMA84. Viral titration was performed to find the right condition for infection. In particular, 5 viral dilutions were used for the infectivity assay: 1:1, 1:100, 1:1000,

and 1:10000. In all the 5 conditions tested a very high cytopathic effect was observed. Anyway, LAMA84 infected with 1:10000 diluted virus showed the highest percentage of survival. Once LAMA84 cells recovered from the infection, they were subjected to puromycin selection to enrich the cell population of infected cells and proceed with single-cell cloning.

Unfortunately, no clone was found, suggesting that for growing, LAMA84 may require the exchanging of growth factors, making the single-cell cloning not feasible. To bypass this issue, LAMA 84 infected and selected cells were single-cell cloned on semisolid matrigel culturing system, thus allowing their physical separation, but permitting cell communication. Very few little cell colonies were detected, but, interestingly, their growth stopped very soon. These surprising observations led us to speculate that LAMA84 cells do not sustain viral infection. To overcome the viral infection, a particular transfection protocol has been thus set up. Specifically, the cells were treated with growth factors inducing their adhesion. LAMA84 adherent cells resulted prone to transfection. The sgRNA was then cloned into the PX459 2.0 Cas9 expressing plasmid and transfected in the LAMA84 adherent cell line. Single-cell cloning is in progress.

4.3 CRISPR/Cas9 to study neurological disorders

4.3.1 Development of PPT1 KO cell line to investigate its involvement in CLN1 disease

Neuronal ceroid lipofuscinoses (NCL) constitute a group of lysosomal storage diseases affecting the brain and retina (Mole, Williams, and Goebel 2012). NCL share clinical characteristics, such as cognitive decline, motor deterioration, and blindness leading to early death (Palmer et al. 2013). Different NCL hallmark genes have been identified so far, and, five of them encode lysosomal proteins (Pezzini et al. 2017). CLN1 identifies a particular type of NCL that, in most cases occurs in childhood (Santavuori, Haltia, and Rapola 1974; Vesa et al. 1995) and, rarely, arises in adulthood (Van Diggelen et al. 2001). Both phenotypes share the reduced activity of Palmitoyl- Protein Thioesterase 1 (PPT1). The hydrolytic lysosomal enzyme PPT1 is normally highly expressed in neuronal cells. It is involved in removing the palmitate residues degrading of S-acylated proteins (Bellizzi et al. 2000; Verkruyse and Hofmann 1996; Vesa et al. 1995). PPT1 has been also found at the synaptic level, where it regulates vesicle trafficking (Aby et al. 2013; S.-J. Kim et al. 2008). Its main function is the control of the palmitoylated state of proteins, thus regulating their shuttling among different neuronal organelles (Fukata and Fukata 2010). Ppt1^{-/-} knockout mice show motor dysfunction, axon degeneration, and brain atrophy with high death of cortical neurons, features of CLN1 disease (Jalanko et al. 2005), due to different altered mechanisms including: cell motility, cell development, membrane trafficking, apoptosis, and deregulation of calcium fluxes and homeostasis in neuronal cells (P. Wang et al. 2011). Proteomic analysis from thalamus derived from Ppt1^{-/-} mice revealed the impairment of mitochondria functions, caused by the dysregulation of cytochrome c complex and ATP synthase (Tikka et al. 2016). In fact, different groups have demonstrated that PPT1 interacts with different components of these enzyme machineries (Lyly et al. 2008; Scifo et al. 2015). Another fundamental characteristic of CLN1 disease is the altered myelination, normally important for impulses propagation. Many myelin components and myelin-associated proteins have been found down-regulated in

CLN1 disease (Tikka et al. 2016). Notably, myelin is enriched in cholesterol, glycosphingolipids, and galactolipids (Chrast et al. 2011) and PPT1 regulates their metabolism, thus it is not surprising that Ppt1^{-/-} mice present defective myelination (Blom et al. 2013).

Nowadays an effective CLN1 treatment is still not available and CLN1 patients are administered just drugs to relieve symptoms (Nita, Mole, and Minassian 2016). It is necessary to clarify the patho-molecular mechanism responsible for the onset of this lethal infantile neurodegeneration, revealing the implication of PPT1 in CLN1 disease.

To investigate the role of PPT1 in the pathogenesis of the infant CLN1 disease, CRISPR/Cas9 was used for developing PPT1 KO SHSY-5Y neuroblastoma cell line.

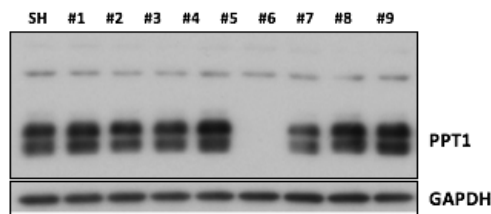
PPT1 transcripts are subjected to canonical and alternative splicing processes, generating 19 splice variants, as reported on Ensemble genome browser (https://www.ensembl.org/Homo_sapiens/Gene/Summary?db=core;g=ENSG00000131238;r=1:40071461-40097727). To induce a complete PPT1 gene KO, a sgRNA was designed to target exons 5, common to all the splicing variants.

The Cas9 expressing plasmids was engineered, thus generating specific sgRNA(PPT1)-Cas9 expressing plasmid, then conveyed within the target cells through nucleofection. The sgRNA(PPT1)-Cas9 treated cells were selected through puromycin and then single-cell cloned.

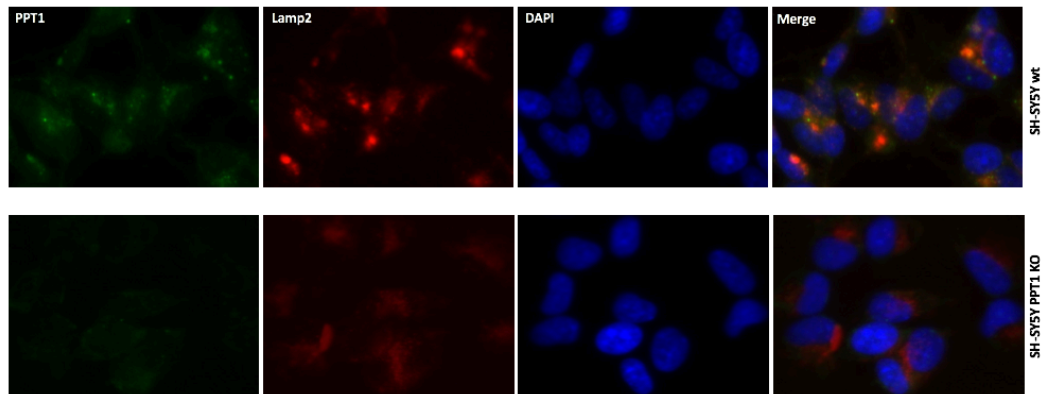
Once obtained CRISPR/Cas9 treated cell clones, the PPT1 expression was analyzed by western blot (Figure 4.14 A) and immunofluorescence (Figure 4.14 B). Western blot analysis revealed that among the tested clones, only the SH-SY5Y #6 clonal cell line did not express PPT1(Figure 4.14A). Sanger sequencing was performed to characterize indel mutations inserted by Cas9 Figure 4.14 C). Western blot analysis showed that the PPT1 KO was achieved in clone #5 compared to SH-SY5Y used as control (referred to as SH in Figure 4.14 A). Immunofluorescence analysis confirmed the lack of the PPT1 protein and lysosomal marker Lamp2 colocalization in SH-SY5Y PPT1 KO cells, compared to the control where merged yellow dots indicated PPT1-Lamp2 colocalization (Figure 4.14 B). To analyze the DNA sequence after CRISPR/Cas9, Sanger sequencing was performed and BLAST

alignment revealed the presence of 37-nucleotide deletion responsible for the introduction of a premature TGA STOP codon (circled in red in Figure 4.14 C), thus explaining the lacking PPT1 expression in the SH-SY5Y PPT1 KO cell line.

A) Western blot analysis of SH-SY5Y PPT1 expression



B) IF analysis of SH-SY5Y PPT1 expression



C) BLAST alignment of CRISPR/Cas9 SH-SY5Y edited cells

```

PPT1_WT      GTGTCAGGCACCTTGCTAAGGATCCTAAATTGCAGCAAGGCTACAATGCTATGGGATTCTC
PPT1_KO      GTGTCAGGCACCTTGCTAAGGATCCTAAATTGCAGCAAGGCTACAATGCTATGGGATTCTC
*****

PPT1_WT      CCAGGGAGGCCAATTTCTGAGGGCAGTGGCTCAGGTTGGGGGACAACATCAGAGATGCC
PPT1_KO      CCAGGGAGGCCAATTTCTGAGGGCAGTGGC-----TCAGAGATGCC
*****

PPT1_WT      TTCACCTCCCATGATCAATCTGATCTC-----AGGTGTTTTGGAC
PPT1_KO      TTCACCTCCCATGATCAATCTGATCTCGGTTTGGGGGACAACATCAAGGTGTTTTGGAC
*****

PPT1_WT      TCCCTCGATGCCAGGAGAGAGCTCTCACATCTGTGACTTCATCCGAAAAAC
PPT1_KO      TCCCTCGATGCCAGGAGAGAGCTCTCACATCTGTGACTTCATCCGAAAAAC
*****
    
```

Figure 4.14: Analyses of PPT1 expression and DNA sequence. (A) Western blot analysis of PPT1 expression after CRISPR/Cas9, normalized with GAPDH. (B) Immunofluorescence (IF) analysis of PPT1 in SH-SY5Y wt cells and in PPT1 KO cells. Lamp2 was used as lysosomal marker. Nuclei were stained with DAPI. (C) Sanger sequencing of SH-SY5Y PPT1 KO cells. The STOP codon introduced by the Cas9 activity is circled in red

4.3.2 CRISPR/Cas9 to study the involvement of GPR3 in Alzheimer's disease

Alzheimer's disease (AD) is an age-related neurodegenerative disorder. The World Health Organization estimates that, in 2019, 50 million people were affected by dementia, and AD contributes to 60-70% of cases. Clinically, AD is characterized by memory loss and behavioral changes. The disease progression leads to damage in structure and function in the hippocampus and cortex (Mota, Ferreira, and Rego 2014). The AD hallmarks include extracellular deposition of amyloid plaques and hyperphosphorylation of the tau protein (L. Ferreira et al. 2012). The typical synaptic dysfunction is mainly due to an over-activity of glutamate receptors, the N-methyl-d-aspartate receptors (NMDARs) that alter Ca²⁺ flux in neurons (Mota, Ferreira, and Rego 2014). Glutamate is an excitatory neurotransmitter and, in the brain, acts on ionotropic receptors allowing fast neuronal communication (Traynelis et al. 2010), and metabotropic receptors that control neurotoxic signals reaching intracellular substrates (Um et al. 2013).

The main feature of Alzheimer disease is the accumulation of amyloid- β (A β) in the brain (Selkoe 2002), generated by sequential cleavages of β -amyloid precursor (APP) by the β - and γ -secretases (Wilquet and Strooper 2004). Evidence showed that in the presence of specific APP mutations, typical of familial AD, its processing is enhanced leading to a higher A β deposition (Haass et al. 1995; Mullan et al. 1992). Different genes involved in the increased A β deposition have been identified, such as the prostaglandin E2 receptor PTGER2 (Pooler et al. 2004) and the serotonin receptor HTR2C (Nitsch et al. 1996). Thathiah et al. (2009), through mass spectrometric, found that G protein-coupled receptor 3 (GPR3) regulates the A β peptide level by modulating the APP cleavage mediated by γ -secretases, without influencing its expression level (Thathiah et al. 2009). GPR3 is an orphan G protein-coupled receptor that activates the G α s subunit that stimulates adenylate cyclase which in turn causes a constitutive increase of cAMP (Oddo et al. 2006; De Strooper 2003). GPR3 is strongly expressed in neurons in the cortex, amygdala, hippocampus, and thalamus, regions strongly involved with the pathogenesis of AD (Heiber et al. 1995). Study conducted on an AD mouse model expressing the AD familial Swedish (Swe) mutation KM670/671NL in the APP peptide, revealed that

the GPR3 expression is fundamental to regulate the assembly of γ -secretases leading to an increase of A β deposition in hippocampus, instead, the complete genetic ablation of GPR3 resulted in reduced deposition of A β (Thathiah et al. 2009). Anyway, GPR3 stimulates the γ -secretases activity in a cAMP-independent manner (Thathiah et al. 2009), thus leading to speculate the involvement of β -arrestins that recently have been shown G-protein functions independent from GPCR signaling activation (Lefkowitz and Shenoy 2005). Interestingly, β -arrestin 2 (β -arr2) is present at high levels in the brain of AD patients. In addition, β arr2^{-/-} mice crossed with AD mice give a progeny with lower A β in cortex and hippocampus (Thathiah et al. 2013). Moreover, GPR3 failed to increase the A β level in β -arr2^{-/-} neurons (Thathiah et al. 2013), suggesting that β -arr2 is required for GPR3-stimulated A β production.

AD is a multifactorial disease and currently, there is no cure. AD patients are treated with drugs that ameliorate AD symptoms. FDA approved the treatment of mild AD with cholinesterase inhibitors (Aricept, Exelon, and Razadyne) for slowing down the loss of acetylcholine in the brain; instead, moderate and severe AD are treated with N-methyl D-aspartate (NMDA) antagonist (memantine and donepezil) to reduce the synaptic dysfunctions. It is important to direct efforts to reveal the molecular mechanisms that lead to the onset of AD for developing new compounds able to block or even prevent the first molecular steps involved in AD pathogenesis (P.-P. Liu et al. 2019).

To investigate the involvement of the orphan GPR3 in the A β production and deposition in Alzheimer's disorder, CRISPR/Cas9 was applied to develop an H4 GPR3 KO neuroglioma cell line. To this aim, the H4 cell line, harboring the Swe mutation KM670/671NL in APP, characteristic of AD, was used.

For obtaining a complete GPR3 KO in the H4 Swe cell line, an Ensemble genome browser analysis revealed that the *GPR3* gene transcription produces a single splice variant

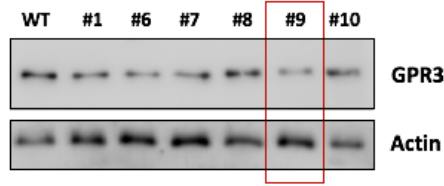
(https://www.ensembl.org/Homo_sapiens/Gene/Summary?db=core;g=ENSG00000181773;r=1:27392622-27395814;t=ENST00000374024). Three specific sgRNAs were designed to knock out GPR3.

Since transfection and nucleofection tests with a GFP expressing plasmid in H4 Swe cell have given poor results, to induce the GPR3 KO, a lentiviral approach was used. Specifically, a sgRNA was cloned in the LentiCRISPRv2 Cas9 expressing vector. LentiCRISPRv2 is a third-generation vector, implying that for viral packaging it is necessary not only to use the sgRNA(GPR3)-LentiCRISPRv2, but also the pVSVg and psPAX2 packaging plasmids, for obtaining infective lentiviral particles (Shalem et al. 2014).

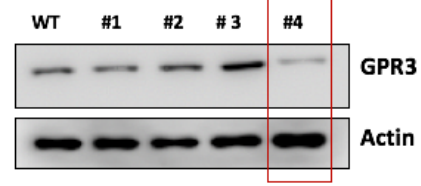
Once engineered the LentiCRISPRv2 transfer vector, 293T packaging cells were co-transfected with sgRNA(GPR3)-LentiCRISPRv2, pVSVg, and psPAX2 for lentiviral production. After 48h from transfection, lentiviral particles were harvested and used for infecting the H4 Swe cell line. To avoid a high cytopathic effect after H4 Swe transduction, different viral titrations were performed. Specifically, H4 Swe cells were infected following 5 conditions. Specifically, the supernatant harvested from 293T packaging cells was diluted 1:1, 1:100, 1:1000, 1:5000, and 1:10000. After 24h from transduction, high cytopathic effect and mortality were observed in all the 5 infection conditions performed. After changing culture medium, the cells recovered, except those infected at the highest viral concentration (1:1 condition) and were subjected to puromycin selection to enrich the cell population of infected H4 Swe cells, before performing single-cell cloning. The H4 Swe clonal cell lines were analyzed through western blot to evaluate the GPR3 expression, finding that all the clones express the CRISPR/Cas9 targeted protein (Figure 4.15 A), compared to H4 Swe parental cell line. However, the H4 Swe #9 clone showed a lower GPR3 expression, thus, according to Dyikanov et al. (2019), it was subjected to another round of LentiCRISPR infection (Dyikanov et al. 2019). The H4 Swe cell clones newly obtained were screened by western blot (Figure 4.15 B), finding that only the clone #4 showed a considerable reduction of GPR3 expression. GPR3 belongs to the Class A family of GPCR together with GPR6 and GPR12. GPR3 share a very high homology percentage with GPR6 and GPR12. In addition GPR3 shows a high percentage of similarity also with cannabinoid receptors (Eggerickx et al. 1995; Morales, Hurst, and Reggio 2017). Noteworthy, GPR6, GPR12, and cannabinoid receptors are highly expressed in brain-derived cell lines (Morales, Isawi, and Reggio 2018; D.-M. Wu et al. 2018).

In this particular circumstance, the presence of false positives cannot be excluded. To deeply assess whether the GPR3 gene sequence was altered by LentiCRISPR/Cas9, GPR3 was analyzed by Sanger sequencing. The BLAST alignment between H4 Swe GPR3 wt gene and H4 Swe CRISPR/Cas9 GPR3 edited gene revealed the presence of a single-nucleotide deletion (indicated with the red arrow in Figure 4.15 C) responsible for the insertion of a premature STOP codon (Figure 4.15 D). To further investigate the efficiency of transduction and integration of lentiviral particles in H4 Swe cells, the #4 clone cell line was grown by adding puromycin to the culture medium. In these growth conditions no cell death was detected, confirming the occurred LentiCRISPR proviral integration within the H4 Swe #4 cell line, responsible for the acquisition of puromycin resistance. H4 Swe GPR3 KO cell line will be fundamental to better understand the pivotal role of the GPR3 protein in A β deposition.

A) H4-SWE GPR3 expression (1st infection)



B) H4-SWE GPR3 expression (2nd infection)



C) Sequence of CRISPR/Cas9 #4 GPR3 edited clone

```

GPR3_WT      GCTGTCTTCTGCATCGGCTCAGCGGAGATGAGCCTGGTGCCTGGTTGGCGTGCCTGGCAATG
GPR3_KO      GCTGTCTTCTGCATCGGCTCAGCGGAGATGAGCCTGGTGCCTGGTTGGCGTGCCTGGCAATG
*****

GPR3_WT      GCCTTTACCGCCAGCATCGGCAGTCTACTGGCCATCACTGTCGACCGCTACCTTTCTCTG
GPR3_KO      GCCTTTACCGCCAGCATCGGCAGTCTACTGGCCATCACTGTCGACCGCTACC-TTCTCTG
*****

GPR3_WT      TACAATGCCCTCACCTACTATTTCAGAGACAACAGTGACACGGACCTATGTGATGCTGGCC
GPR3_KO      TACAATGCCCTCACCTACTATTTCAGAGACAACA(TGA)CACGGACCTATGTGATGCTGGCC
*****

GPR3_WT      TTAGTGTGGGGAGGTGCCCTGGGCCTGGGGCTGCTGCCTGTGCTGGCTGGAAGTGC
GPR3_KO      TTAGTGTGGGGAGGTGCCCTGGGCCTGGGGCTGCTGCCTGTGCTGGCTGGAAGTGC
*****
    
```

D) GPR3 in silico translation of H4 Swe wt and #4

```

H4 Swe wt
Met Met W G A G S P L A W L S A G S G N V N V S S V G P A E G P T G P A A P L P S P K A W D V V L C I S G T
L V S C E N A L V V A I I V G T P A F R A P Met F L L V G S L A V A D L L A G L G L V L H F A A V F C I G S
A E Met S L V L V G V L A Met A F T A S I G S L L A I T V D R Y L S L Y N A L T Y Y S E T T V T R T Y V Met
L A L V W G G A L G L G L L P V L A W N C L D G L T T C G V V Y P L S K N H L V V L A I A F F Met V F G I
Met L Q L Y A Q I C R I V C R H A Q Q I A L Q R H L L P A S H Y V A T R K G I A T L A V V L G A F A A C W L
P F T V Y C L L G D A H S P P L Y T Y L T L L P A T Y N S Met I N P I I Y A F R N Q D V Q K V L W A V C C C
C S S S K I P F R S R S P S D V Stop

#4
Met Met W G A G S P L A W L S A G S G N V N V S S V G P A E G P T G P A A P L P S P K A W D V V L C I S G T
L V S C E N A L V V A I I V G T P A F R A P Met F L L V G S L A V A D L L A G L G L V L H F A A V F C I G S
A E Met S L V L V G V L A Met A F T A S I G S L L A I T V D R Y L L C T Met P S P T I Q R Q Q Stop
    
```

Figure 4.15: Analyses of GPR3 expression. Western blot analysis of GPR3 expression after the first LentiCRISPR transduction (A) and after the second LentiCRISPR transduction (B). (C) Sanger sequencing of H4 Swe #4 cells. The red arrow shows the single nucleotide deletion induced by the Cas9 activity. The premature STOP codon is circled in red. (D) In silico translation of H4 Swe wt and H4 Swe #4 cell lines.

5. DISCUSSION

The CRISPR/Cas9 system represents a milestone for genome manipulation due to its quickness, simplicity, and cost-effectiveness. As for any new emerging revolutionary technique, CRISPR/Cas9 presents several technical limits that need to be investigated before it may be applied to different fields, from plant engineering to gene therapy.

The major CRISPR/Cas9-related issues refer to the karyotype of the target cell line, the appropriate delivery system of sgRNA/Cas9, the analysis of Cas9 off-target cleavages, the screening method to identify edited clones, the characteristic of the targeted gene, as well as ethical issues related to the employment of the CRISPR/Cas9 technology.

5.1 CRISPR/Cas9 targeted cell lines

The genome editing approach needs to take into account the cell karyotype. According to Dyikanov, gene-editing efficiency is considerably reduced in aneuploid cell lines (Dyikanov et al. 2019). In our experience, the development of H4 Swe GPR3 KO cells was particularly difficult. The ATCC web site reports that H4 cells present hypertriploid karyotype with a chromosome number between 63 and 78, reflecting the H4 Swe cells heterogeneity. To induce the GPR3 KO in H4 Swe cells, we used the LentiCRISPR vector. After infection, puromycin selection and single-cell cloning, western blot analysis was performed, finding a CRISPR/Cas9 H4 Swe clone with a significant reduction of GPR3 expression (Figure 4.15 A). To obtain a complete GPR3 KO, a second infection round was carried out and GPR3 expression was further analyzed by western blot (Figure 4.15 B). None of the H4 clones resulted GPR3 KO, but, interestingly, we observed a lower GPR3 expression in the #4 clone, compared to the H4 Swe wt cells used as control. Notably, GPR3 is part of a gene family together with GPR6 and GPR12 and they share more than 60% homology (Eggerickx et al. 1995; Morales, Hurst, and Reggio 2017), thus, we cannot exclude that the anti GPR3 antibody may cross-react with other GPR family members. It is important to consider that the GPR3 expression analysis was verified using a polyclonal antibody, which likely cross-

reacts with other GPR proteins, as indicated in the datasheet. To finally verify the absence of GPR3 in the H4 Swe #4 cells, we will evaluate its expression exploiting the 3B4-G3 monoclonal antibody (Sigma-Aldrich). In line with our speculation, Sanger sequencing was performed for evaluating the DNA mutation introduced by Cas9, and we observed that the H4 Swe #4 clone presented a single nucleotide deletion responsible for the introduction of a premature STOP codon that may not allow the GPR3 protein expression (Figure 4.15 C). Bioinformatic analysis is particularly helpful in the presence of doubtful results. For example, after CRISPR/Cas9 treatment and Sanger sequencing, the ExPASy SIB Bioinformatics Resource Portal (<https://web.expasy.org/translate/>) was used for GPR3 *in silico* translation, confirming the introduction of a premature STOP codon (Figure 4.15 D).

Likewise, after CRISPR/Cas9 treatment to induce the HDAC6 KO, apparent contradictory results were obtained. HDAC6 genomic PCR analysis and Sanger sequencing (Figure 4.3 A and B, respectively) revealed a 74 bp deletion, leading to a frameshift and premature STOP codon. Intriguingly, the western blot analysis revealed the presence of a strongly reduced HDAC6 expression in clone #5 (Figure 4.3 C), which was difficult to explain. In this regard, recently an elegant work by Smits et al. (2019) reported that after the CRISPR/Cas9-induced gene KO, different host mechanisms can be exploited to rescue the expression of the targeted gene. Specifically, translation re-initiation may occur when the sgRNA directs the Cas9 endonuclease activity at 5' terminal portion of the target gene, leading to N-terminal truncated protein expression. CRISPR/Cas9-induced frameshift mutation can also be overcome through the skipping of the indel mutations through alternative splicing. Both translation re-initiation and frameshift skipping allow bypassing the non-sense mediated decay, which in turn enables the protein expression (Smits et al. 2019).

To definitively clarify whether GPR3 and HDAC6 were effectively knocked out, functional analyses need to be performed on the corresponding mRNA.

5.2 CRISPR/Cas9 delivery

A crucial point is the CRISPR/Cas9 delivery method, chosen according to the target cell line (T. K. Kim and Eberwine 2010). As expected, we observed that different cell lines require different CRISPR/Cas9 delivery systems. As a consequence, some cell lines resulted easier to manipulate than others. For example, the development of 293T edited cell lines (Figure 4.1, 4.5 A, 4.6A, and 4.10A) was relatively easy using lipofection protocol. Differently, H4 Swe neuroglioma, SH-SY5Y neuroblastoma, and LAMA chronic myeloid leukemia cell lines were more difficult to transfect. The CRISPR/Cas9 delivery protocol was optimized by performing different transfection tests, conveying a GFP-expressing plasmid through lipofection and nucleofection. The GFP expression was then analyzed by fluorescent microscopy.

In all tested lipofection conditions, SH-SY5Y showed a very low GFP signal, while, the nucleofection gave better results. Thus, the sgRNA(PPT1)-Cas9 expressing plasmid has been shuttled through nucleofection.

Differently, lipofection did not result efficient for the manipulation of H4 Swe and LAMA84 cells, as well as nucleofection. To bypass transfection- and nucleofection-related issues, the LentiCRISPR transduction vector has been employed. LentiCRISPR viral particles have been produced in 293T packaging cells followed by target cell transduction. Opposite results were obtained in the two cell lines. Particularly, concerning cell viability, H4 Swe cells were found to sustain the viral transduction, while the LAMA84 cell line, after LentiCRISPR transduction, presented a very high mortality percentage. Anyway, after LAMA84 recovering the cell cycle arrested, suggesting that, probably, a defense mechanism against lentiviral infection prevented their growth. We can speculate that the low viability and the cell cycle arrest may depend on the induced PTPRG KO and/or the infection. In the attempt to make the LAMA84 cells prone to transfection, they were made adherent, by coating the cell culture vessel and adding three growth factors to the culture medium, for maintaining the cell stemness and their replication capacity. Surprisingly, in this new condition, GFP transfection has shown better results, thus the sgRNA(PTPRG)-Cas9 expressing plasmid will be conveyed through lipofection. However, we cannot exclude that PTPRG is essential for cell

viability. In fact, there is no evidence in the scientific literature about the development of PTPRG KO cell lines or animal models. It has been reported that the RNA interference-induced PTPRG knockdown, correlates with high cell growth in tumor cells (Kostas et al. 2018).

The CRISPR/Cas9 delivery represents an important issue to investigate. Lentiviral shuttling of sgRNA-Cas9 ensures to hit the target sequence, but, exploiting lentiviral constructs, both the Cas9 and the sgRNA continue to be expressed, thus representing an inefficient vehicle method for gene therapy application, mainly for the increased off-target risk (Petris et al. 2017).

Efforts are directed for searching new and suitable convey systems able to increase the Cas9 on-target specificity too. For example, the CRISPR/Cas9 viral vector delivery may lead to undesired Cas9 cleavages. To reduce off-targets, Petris et al. (2017) developed the Lentiviral Self-Limiting Cas9 Enhanced Safety (LentiSLiCES). This approach limits and regulates the Cas9 expression, which in turn reflects the reduction of off-targets, by combining, the on-target sgRNA-Cas9 to a non-active sgRNA able to target the Cas9 coding sequence, thus reducing its expression (Petris et al. 2017).

It has been also reported that using the new CRISPRGold technology (B. Lee et al. 2018; K. Lee et al. 2017), sgRNA-Cas9 can be microinjected within cells difficult to manipulate, such as neurons. CRISPRGold bases its activity on gold nanoparticles coating the DNA donor template and the sgRNA-Cas9 RNP complex (K. Lee et al. 2017).

5.3 Evaluation of Cas9 off-target activity

CRISPR/Cas9 has been engineered to be a highly precise genome editing tool, to introduce a DSB only in the target sequence. However, the Cas9 endonuclease activity may be erroneous, leading to off-target cleavages (Q. Zhang et al. 2018). Obviously, the possibility of Cas9 off-targets must be carefully considered. In fact, unpredicted genome cuts may cause chromosome instability and loss or gain of function gene mutations, with unpredictable cell pathway alterations and important physiological consequences. To specifically direct Cas9 on the on-target sequence, an efficient and specific sgRNA has to be designed. Studies report that Cas9 DNA

cleavage is widely and differently influenced by different sgRNAs (Cong et al. 2013; Mali et al. 2013; Shalem et al. 2014). With respect to off-target effects, it is important to underline that up to five mismatches in the sgRNA-targeted sequence base pairing can be tolerated (Tsai and Joung 2016). Specifically, PAM-distal mismatches do not influence the Cas9 activity, while, PAM-proximal mismatches do not allow the cleavage of the target sequence (Hsu et al. 2013). Certainly, the absence of mismatches helps in preventing off-targets. As mentioned above, the different sgRNA design tools available are useful for off-target prediction.

In our studies, we employed two sgRNA design tools for selecting sgRNAs: MIT guide design resource and Chopchop (<https://zlab.bio/guide-design-resources> and <https://chopchop.cbu.uib.no/>). Both base the sgRNA searching on the presence of the NGG-PAM motif in the sequence of interest, returning a list of predicted sgRNAs. To each sgRNA is associated a score value indicating the efficacy of on-target cutting, thus the sgRNA selection was performed by comparing the sgRNA scores calculated by both MIT and Chopchop. Considering that sgRNA can base-pair with off-target regions, bearing eventual mismatches, BLAST alignment was performed to ensure that each selected sgRNA specifically recognizes the target sequence, avoiding undesired cleavages. Moreover, for an optimal sgRNA selection, in addition to the sgRNA BLAST alignment with the human genome, potential off-target sites have been analyzed by using the CRISPR RGEN tool for each gRNA, as reported in the materials and methods section (Bae, Park, and Kim 2014). Careful analysis of off-targets is particularly important especially when the CRISPR/Cas9 target gene is part of a gene family. For instance, in our experience, to specifically obtain the HLA-C KO (Figure 4.5), bioinformatic analysis was performed to find the percentage of homology with paralogue genes, finding that high identity sequence is shared with the other HLA family members. As reported on Ensemble genome browser, the HLA-C gene sequence shows a homology sequence between 74% and 84% with HLA-B, -F, -G, and -E (https://www.ensembl.org/Homo_sapiens/Gene/Compara_Paralog?db=core;g=ENSG00000204525;r=6:31268749-31272130). Hence, for developing the 293T HLA-C KO cell line, avoiding off-target effects, the sgRNA was designed to target the HLA-C exon 2 sequence not shared with the other HLA genes. It follows that to get

valuable results using CRISPR/Cas9, eventual off-targets must be analyzed, also depending on the target gene family. It is always necessary to check Cas9 off-target cuts, even if they are not detected by bioinformatic analysis. To this aim, after developing 293T HLA-C KO cell line, we performed western blot analysis revealing that HLA-A and HLA-B expression was not affected by CRISPR/Cas9 treatment.

As reported above, our research group developed A375 Δ RUNT melanoma cell line to study its involvement in cancer cell migration and angiogenesis. Since RUNX2 is a member of the RUNX gene family with RUNX1 and RUNX3 (Blyth et al. 2010), whole-genome sequencing was performed to analyze Cas9 off-targets, revealing the absence of undesired Cas9 cleavages.

Off-target cleavages represent one of the most important issues to be addressed for CRISPR/Cas9 application, especially in gene therapy to avoid undesired Cas9 cleavages that may induce important unpredictable consequences.

As shown by Kim et al. (2014), it is possible to convey the Cas9 protein combined to sgRNA as a ribonucleoprotein (RNP) complex into the target cells obtaining an initial high expression of Cas9 followed by a rapid decay, thus reducing off-target cleavages of 10 fold. Moreover, the sgRNA-Cas9 RNP complex, delivered through electroporation, resulted efficient for the genome editing of cell lines recalcitrant to lipofection, such as primary cell line and pluripotent stem cells (S. Kim et al. 2014). Similarly, Dong et al. (2019) reported that, by microinjecting sgRNA-Cas9 RNP into mouse zygotes, the off-target risks are significantly reduced, mainly due to the short half-life of Cas9 (Y. Dong et al. 2019).

Another approach to reducing off-targets is based on the employment of the Cpf1 orthologue AsCas12a, engineered from *Acidaminococcus*. The AsCas12a activity requires a TTTV-PAM motif, where V can be A, G, or C (Gao et al. 2017). Maule et al. (2019) exploited the AsCas12a endonuclease for correcting specific CFTR mutations in human primary cells and in cystic fibrosis-derived organoids, reporting the absence of off-targets, thus underling the value of this approach in preclinical trial phases (Maule et al. 2019).

To reduce uncontrollable Cas9 cleavages, Fu et al. (2014) showed that by truncating the 5'-end of sgRNA up to 17 or 18 nt length, the Cas9 still results working on the on-target sequence, with undetectable off-targets (Fu et al. 2014).

Besides the strategies to reduce the CRISPR off-targets, their detection too represents a challenge in the field of genome editing. For CRISPR/Cas9 gene therapy application it is essential not only to develop an off-target-free CRISPR approach but also to perform a whole genome screening after genome editing.

Although the *in silico* sgRNA design tools may help to avoid undesired DNA cuts, the off-target prediction is based on algorithms predicting off-target cleavages, by checking only on-target closely related sequences (X. H. Zhang et al. 2015).

For individuating off-target events, different tools have been proposed for *in vitro* and *in vivo* off-target detection.

The Breaks Labeling, Enrichment on Streptavidin, and next-generation Sequencing (BLESS) technique allows to flag DSBs into a genome by ligating the 5' DNA blunt end to a biotinylated barcoded linker, which is then sequenced through next generation sequencing (Crosetto et al. 2013; Ran et al. 2015).

Another approach to individuate off-targets is based on the *in vitro* nuclease-digested genome sequencing (digenome-seq). After digestion, different DNA fragments are produced with identical 5'end, thus allowing vertical alignment, making the whole genome sequencing data easier to analyze (D. Kim et al. 2015).

The Circularization for In vitro Reporting of Cleavage Effects by sequencing (CIRCLE-seq) method has been developed by Tsai et al. (2017). It bases on the direct sequencing of Cas9-cleaved genome sequences, by restricting the Cas9 targeted DNA then converted in a circular structure. These circular structures are then linearized and linked to specific adapters for NGS (Tsai et al. 2017).

Recently for *in vivo* off-targets analysis, a technique named Verification of *In Vivo* Off-targets (VIVO) has been described (Akcakaya et al. 2018). Specifically, VIVO relies on a preliminary *in vitro* evaluation of CRISPR/Cas9-induced off-targets by exploiting CIRCLE-seq (Tsai et al. 2017), then confirmed by performing an *in vivo* NGS (Akcakaya et al. 2018).

Although off-targets represent one of the major CRISPR/Cas9 technical limits, different authors reported that they are not so frequent. In this regard, two years

ago, Schaefer et al (2017) showed that mice engineered by CRISPR/Cas9 presented unexpected indel mutations, thus suggesting an important Cas9 off-target activity. Just one year later, this paper was retracted for the lack of appropriate controls that do not allow to associate the presence of these mutations to the CRISPR/Cas9 treatment.

5.4 Screening of CRISPR/Cas9-edited cells

The screening of edited cell lines represents another crucial aspect. Based on the subcellular localization of the CRISPR/Cas9 mutated protein, the proper screening method was chosen. The absence of the intracellular protein encoded by the KO gene, such as ACOT8, TRAF3, RUNX2, GNA15, and PPT1 was evaluated through western blot. Differently, the absence of a cell surface protein, such as HLA-C, was detected not only by western blot but also through flow cytometry (Figure 4.6 B), by directly labeling the surface HLA-C protein. Evenly, the evaluation of restored HLA-C expression was carried out through flow cytometry (Figure 4.7).

The analysis of a gene knock out can be also performed through immunofluorescence (IF). As shown in Figure 4.14 B, the PPT1 KO was further confirmed by IF, taking advantage of its co-localization with the lysosomal marker Lamp2. However, since IF is less sensitive than western blot, we used it as an additional confirmation of PPT1 KO.

When it is possible, it is convenient to evaluate wheatear the expression of the CRISPR/Cas9 edited gene interferes with the regulation of specific pathways. For example, after detecting the absence of the NF-kB negative regulator TRAF3 (Figure 4.10 A), we observed the constitutive NF-kB (p100) processing in p52, reflecting a basal activation of NF-kB (Figure 4.10 C). Interestingly, we also observed that in 293T TRAF3 KO cells, the mRNA expression of NF-kB target genes (IL-6, BCL2, and A20) resulted increased (Figure 4.11 C). Moreover, we reported that in the TRAF3 negative cells, HTLV Tax1 did not induce the strong NF-kB promoter transactivation achieved in 293T wt cells (Figure 4.11 A), underlying that TRAF3 is essential for the NF-kB promoter transactivation mediated by HTLV Tax1 antisense protein (Fochi et al. 2019).

Likewise, after confirming the GNA15 KO through western blot and Sanger sequencing (Figure 4.13 A and B, respectively), we evaluated the PKD phosphorylation, which in turn reflects the GNA15 activity. We observed that, in the absence of GNA15, the level of phospho-Ser738/742 resulted lower compared to the control (Figure 4.13 C).

Western blot screening of CRISPR/Cas9 edited cell lines may be also useful to detect domain deletions. To assess whether our approach designed to delete the HDAC6 BUZ domain (Figure 4.4), western blot analysis has been crucial. In fact, to individuate the CRISPR/Cas9 293T Δ BUZ cell lines, western blot allowed us to identify the edited cells based on the HDAC6 molecular weight (Figure 4.5 A). As above, the functional characterization of HDAC6 edited cells helped us to confirm the BUZ deletion. Indeed, the 293T edited cell lines, characterized by a lower HDAC6 molecular weight presented a higher p62 expression (Figure 4.5 A).

To fully analyze the mutations introduced by CRISPR/Cas9, it is fundamental to sequence the target region. Based on the PAM sequence, it is possible to predict the Cas9 cleavages, that occurs 3 nucleotides upstream the PAM motif (Ran et al. 2013). Although the Cas9 cleavage can be predicted *in silico*, Sanger sequencing revealed that there is not a so tight relation between the cutting site, the PAM sequence, and the indel mutations introduced by NHEJ. For instance, in our experience, the Sanger sequencing performed on CRISPR/Cas9 RUNX2 and PPT1 targeted sequences, showed that the activity of the NHEJ repair mechanism cannot be predicted. Sanger sequencing performed on Mel-HO RUNX2 and SH-SY5Y PPT1 KO cell lines (Figure 4.12 B and 4.14 C, respectively) revealed that different indel mutations were introduced both upstream and downstream to the PAM sequence. It follows that after CRISPR/Cas9, the treated cell population may be composed of a mixture of cells, due to different ways of repairing the DNA damage exerted by the NHEJ process. Furthermore, after the induction of a DSB, rarely the entire gRNA/Cas9 expressing plasmid may be erroneously inserted within the Cas9 targeted region through the host DNA damage repair process itself (Milot et al. 1992).

It is hence necessary to perform single-cell cloning to isolate edited pure clonal cell lines and to sequence the sgRNA-Cas9 targeted region to analyze the introduced mutations.

5.5 Final considerations

Despite ethical concerns, widely discussed in the introduction section, the CRISPR/Cas9 system is radically changing the approach to research. Several lines of evidence show the great impact of CRISPR/Cas9 in increasing the knowledge in basic research, both for improving preliminary data useful for somatic cells editing (Chan et al. 2015) and to create new *in vitro* cell lines and animal models useful for revealing the pathological involvement of specific molecules and for drug testing (Greenfield 2018). An important application of CRISPR/Cas9 concerns also its employment for somatic genome editing, allowing the correction of specific mutations responsible for human diseases, such as monogenic disorders and cancer (Baylis and McLeod 2017; Brokowski and Adli 2019; Reardon 2016).

About the CRISPR/Cas9 employment for correcting human diseases, Choi et al. recently exploited the CRISPR/Cas9 system to engineer chimeric antigen receptor (CAR) T cells (Choi et al. 2019). A previous study showed that glioblastoma affected patients treated with CAR T cells targeting the epidermal growth factor receptor (EGFRvIII), presented a high concentration of CAR T cells within the intracerebral tumor, thus reducing the EGFRvIII expression in tumor cells (O'Rourke et al. 2017), probably due to the programmed cell death ligand 1 (PD-L1) upregulation observed after CAR treatment, likely correlating with CAR T cells function suppression and tumor progression (Choi et al. 2019). By applying CRISPR/Cas9 to CAR T cells, Choi et al. developed CAR T cells deficient for endogenous T cell receptor (TRAC), PD-1, and β_2m , involved in the cell death observed in response to CAR T cell treatment, an increased cell viability was detected in a glioma cell line (Choi et al. 2019). The great potential of CRISPR/Cas9 in CAR T cells engineering was also confirmed in a human glioma mouse model. In fact, after intraventricular infusion of CRISPR/Cas9 edited CAR T cells, a significant prolonged animal survival was observed (Choi et al. 2019).

Significant progress has been made also for the development of new treatment strategies of monogenic disorders, such as sickle cell disease (SCD) and the TDT beta-thalassemia. CRISPR Therapeutics and Vertex Pharmaceuticals engineered SCD and TDT patients' derived hematopoietic stem cells making them able to produce high level of fetal hemoglobin. Briefly, this study was based on the collection of patient's hematopoietic stem cells, engineered with CRISPR/Cas9. The CRISPR/Cas9 edited cells, referred to as CTX001, were then engrafted back. Samarth Kulkarni, Ph.D., CEO of CRISPR Therapeutics, announced the treatment of the first patient affected by beta-thalassemia, through vein infusion of CTX001. Currently, CTX001 is in phase 1 /2 clinical trial to evaluate its safety and efficacy. This CRISPR Therapeutics shocking announcement represents an important milestone for the future of CRISPR/Cas9 in gene therapy.

The CRISPR/Cas9 technique represents a versatile genome engineering tool. In fact, it found application not only for studying and correcting specific gene mutations associated to human pathologies, but also to modify plants (Feng et al. 2013), microorganisms, such as bacteria and viruses (Shipman et al. 2017; Tang et al. 2017), mosquito (S. Dong et al. 2015), and mammals such as pigs and monkeys (Hai et al. 2014; Zuo et al. 2017).

It is becoming increasingly obvious that CRISPR/Cas9 is a breakthrough powerful tool, allowing the development of new engineered cell lines and organisms, but it is exploited also in immunotherapy (Manguso et al. 2017), for organoid development (Drost et al. 2017), and for epigenetic studies (Kuscu et al. 2017).

Important ethical concerns emerged also in non-clinical contexts. For instance, its application for the optimization and implementation of livestock and crops, as well as for gene drive led to a public debate. The World Health Organization reported that about 2 million people suffer from undernourishment. CRISPR/Cas9 may constitute a turning point to increase food nutrients. Worries could arise about the affordability of these products. In addition, CRISPR/Cas9 may be efficiently used for gene-drive, with the purpose to eliminate specific carrier vectors responsible for pathologies, thus opening up new ways to fight deadly human diseases, such as malaria (James et al. 2018) or to avoid plant parasite infestation (Moro et al. 2018). Even if CRISPR/Cas9 may be an important tool for gene drive application,

important aspects need to be considered. Indeed, new genes in a quick and non-Mendelian way inherited could spread in the population with an unknown impact on the ecosystem.

Basic research will play a pivotal role in the CRISPR/Cas9 system improvement and handling, as well as a defined and clear legislature for regulating the employment of the CRISPR/Cas9 technique will be essential.

The CRISPR/Cas9 system is a pioneering genome-editing tool and presents considerable limits that still do not allow its complete safety employment. Once these technical concerns will be overcome and, consequently, a full technique control will be obtained, CRISPR/Cas9 will be definitely a powerful tool for the treatment of different human diseases. There is an urgent need to let people be aware of how this “molecular scissor” works, to avoid uprising, as those observed against the development and employment of genetically modified organisms. In this respect, certainly scientists and media will play a crucial role in promoting a better understanding of the CRISPR/Cas9 technology mechanism and revealing its great potential to the general public.

BIBLIOGRAPHY

- Abudayyeh, Omar O. et al. 2016. "C2c2 Is a Single-Component Programmable RNA-Guided RNA-Targeting CRISPR Effector." *Science* 353(6299).
- Aby, Elizabeth et al. 2013. "Mutations in Palmitoyl-Protein Thioesterase 1 Alter Exocytosis and Endocytosis at Synapses in *Drosophila* Larvae." *Fly* 7(4).
 ———. "Mutations in Palmitoyl-Protein Thioesterase 1 Alter Exocytosis and Endocytosis at Synapses in *Drosophila* Larvae." *Fly* 7(4): 267–79.
<http://www.ncbi.nlm.nih.gov/pubmed/24091420> (December 4, 2019).
- Ahnesorg, Peter, Philippa Smith, and Stephen P. Jackson. 2006. "XLF Interacts with the XRCC4-DNA Ligase IV Complex to Promote DNA Nonhomologous End-Joining." *Cell* 124(2): 301–13.
- Akcakaya, Pinar et al. 2018. "In Vivo CRISPR Editing with No Detectable Genome-Wide off-Target Mutations." *Nature* 561(7723): 416–19.
- Alfieri, R et al. 1992. "Serum Beta 2-Microglobulin Levels and P24 Antigen, Lymphocyte Depletion and Disease Progression in Human Immunodeficiency Virus Infection." *International journal of clinical & laboratory research* 22(1): 48–51.
<http://www.ncbi.nlm.nih.gov/pubmed/1633320> (December 4, 2019).
- Amitai, Gil, and Rotem Sorek. 2016. "CRISPR-Cas Adaptation: Insights into the Mechanism of Action." *Nature Reviews Microbiology* 14(2): 67–76.
- Arold, S et al. 2000. "Characterization and Molecular Basis of the Oligomeric Structure of HIV-1 Nef Protein." *Protein science : a publication of the Protein Society* 9(6): 1137–48.
<http://www.ncbi.nlm.nih.gov/pubmed/10892807> (December 4, 2019).
- Ayoub, Nabieh et al. 2009. "The Carboxyl Terminus of Brca2 Links the Disassembly of Rad51 Complexes to Mitotic Entry." *Current Biology* 19(13): 1075–85.
- Baccarani, Michele et al. 2006. "Evolving Concepts in the Management of Chronic Myeloid Leukemia: Recommendations from an Expert Panel on Behalf of the European LeukemiaNet." *Blood* 108(6): 1809–20.
<http://www.ncbi.nlm.nih.gov/pubmed/16709930> (December 4, 2019).

- Bae, Sangsu, Jeongbin Park, and Jin-Soo Kim. 2014. "Cas-OFFinder: A Fast and Versatile Algorithm That Searches for Potential off-Target Sites of Cas9 RNA-Guided Endonucleases." 30(10): 1473–75.
<http://www.rgenome.net/cas-offinder> (March 26, 2020).
- Baeuerle, Patrick A., and David Baltimore. 1988. "I κ B: A Specific Inhibitor of the NF-KB Transcription Factor." *Science* 242(4878): 540–46.
- Bar-Shavit, Rachel et al. 2016. "G Protein-Coupled Receptors in Cancer." *International Journal of Molecular Sciences* 17(8).
- Barbeau, Benoit, Jean Marie Peloponese, and Jean Miche Mesnard. 2013. "Functional Comparison of Antisense Proteins of HTLV-1 and HTLV-2 in Viral Pathogenesis." *Frontiers in Microbiology* 4(AUG).
- Barrangou, Rodolphe et al. 2007. "CRISPR Provides Acquired Resistance against Viruses in Prokaryotes." *Science* 315(5819): 1709–12.
- Baylis, Françoise, and Marcus McLeod. 2017. "First-in-Human Phase 1 CRISPR Gene Editing Cancer Trials: Are We Ready?" *Current gene therapy* 17(4): 309–19. <http://www.ncbi.nlm.nih.gov/pubmed/29173170> (December 4, 2019).
- Bedi, Atul et al. 1994. "Inhibition of Apoptosis by BCR-ABL in Chronic Myeloid Leukemia." *Blood* 83(8): 2038–44.
- Bellizzi, John J. et al. 2000. "The Crystal Structure of Palmitoyl Protein Thioesterase 1 and the Molecular Basis of Infantile Neuronal Ceroid Lipofuscinosis." *Proceedings of the National Academy of Sciences of the United States of America* 97(9): 4573–78.
- Benichou, S et al. 1994. "Physical Interaction of the HIV-1 Nef Protein with Beta-COP, a Component of Non-Clathrin-Coated Vesicles Essential for Membrane Traffic." *The Journal of biological chemistry* 269(48): 30073–76. <http://www.ncbi.nlm.nih.gov/pubmed/7982906> (December 5, 2019).
- Bennett, Dorothy C. 2008. "How to Make a Melanoma: What Do We Know of the Primary Clonal Events?" *Pigment cell & melanoma research* 21(1): 27–38. <http://www.ncbi.nlm.nih.gov/pubmed/18353141> (December 4, 2019).
- Bentham, Matthew, Sabine Mazaleyrat, and Mark Harris. 2006. "Role of Myristoylation and N-Terminal Basic Residues in Membrane Association of

- the Human Immunodeficiency Virus Type 1 Nef Protein.” *The Journal of general virology* 87(Pt 3): 563–71.
<http://www.ncbi.nlm.nih.gov/pubmed/16476977> (December 4, 2019).
- Berkhout, Ben, and Anthony de Ronde. 2004. “APOBEC3G versus Reverse Transcriptase in the Generation of HIV-1 Drug-Resistance Mutations.” *AIDS (London, England)* 18(13): 1861–63.
<http://www.ncbi.nlm.nih.gov/pubmed/15316354> (December 4, 2019).
- Bertram, Lars et al. 2007. “Systematic Meta-Analyses of Alzheimer Disease Genetic Association Studies: The AlzGene Database.” *Nature Genetics* 39(1): 17–23.
- Bhakta, Mital S et al. 2013. “Highly Active Zinc-Finger Nucleases by Extended Modular Assembly.” *Genome research* 23(3): 530–38.
<http://www.ncbi.nlm.nih.gov/pubmed/23222846> (December 4, 2019).
- Bjørkøy, Geir et al. 2005. “P62/SQSTM1 Forms Protein Aggregates Degraded by Autophagy and Has a Protective Effect on Huntingtin-Induced Cell Death.” *Journal of Cell Biology* 171(4): 603–14.
- Blom, Tea et al. 2013. “Exacerbated Neuronal Ceroid Lipofuscinosis Phenotype in Cln1/5 Double-Knockout Mice.” *Disease models & mechanisms* 6(2): 342–57. <http://www.ncbi.nlm.nih.gov/pubmed/23065637> (December 4, 2019).
- Blyth, Karen et al. 2006. “Runx2 and MYC Collaborate in Lymphoma Development by Suppressing Apoptotic and Growth Arrest Pathways in Vivo.” *Cancer research* 66(4): 2195–2201.
<http://www.ncbi.nlm.nih.gov/pubmed/16489021> (December 4, 2019).
- . 2010. “Runx2 in Normal Tissues and Cancer Cells: A Developing Story.” *Blood cells, molecules & diseases* 45(2): 117–23.
<http://www.ncbi.nlm.nih.gov/pubmed/20580290> (December 4, 2019).
- Brew, B J et al. 2005. “CSF Amyloid Beta42 and Tau Levels Correlate with AIDS Dementia Complex.” *Neurology* 65(9): 1490–92.
<http://www.ncbi.nlm.nih.gov/pubmed/16275845> (December 4, 2019).
- Brew, B J, M Rosenblum, K Cronin, and R W Price. 1995. “AIDS Dementia Complex and HIV-1 Brain Infection: Clinical-Virological Correlations.”

- Annals of neurology* 38(4): 563–70.
<http://www.ncbi.nlm.nih.gov/pubmed/7574452> (December 4, 2019).
- Brightbill, Hans, and Mark S Schlissel. 2009. “The Effects of C-Abl Mutation on Developing B Cell Differentiation and Survival.” *International immunology* 21(5): 575–85. <http://www.ncbi.nlm.nih.gov/pubmed/19299624> (December 4, 2019).
- Brokowski, Carolyn, and Mazhar Adli. 2019. “CRISPR Ethics: Moral Considerations for Applications of a Powerful Tool.” *Journal of molecular biology* 431(1): 88–101. <http://www.ncbi.nlm.nih.gov/pubmed/29885329> (December 4, 2019).
- Brouns, Stan J.J. et al. 2008. “Small CRISPR RNAs Guide Antiviral Defense in Prokaryotes.” *Science* 321(5891): 960–64.
- Burnight, Erin R et al. 2018. “CRISPR-Cas9-Mediated Correction of the 1.02 Kb Common Deletion in CLN3 in Induced Pluripotent Stem Cells from Patients with Batten Disease.” *The CRISPR journal* 1: 75–87.
<http://www.ncbi.nlm.nih.gov/pubmed/31021193> (December 4, 2019).
- Burstein, David et al. 2017. “New CRISPR-Cas Systems from Uncultivated Microbes.” *Nature* 542(7640): 237–41.
- Campbell, Lynda J. et al. 2002. “BCR/ABL Amplification in Chronic Myelocytic Leukemia Blast Crisis Following Imatinib Mesylate Administration.” *Cancer Genetics and Cytogenetics* 139(1): 30–33.
- Chan, Sarah et al. 2015. “Genome Editing Technologies and Human Germline Genetic Modification: The Hinxtion Group Consensus Statement.” *The American journal of bioethics : AJOB* 15(12): 42–47.
- Chandrasegaran, Srinivasan, and Dana Carroll. 2016. “Origins of Programmable Nucleases for Genome Engineering.” *Journal of Molecular Biology* 428(5): 963–89.
- Chen, Haiyan et al. 2014. “Runx2 Regulates Endochondral Ossification through Control of Chondrocyte Proliferation and Differentiation.” *Journal of Bone and Mineral Research* 29(12): 2653–65.
- Chikata, Takayuki et al. 2019. “Identification of Immunodominant HIV-1 Epitopes Presented by HLA-C*12:02, a Protective Allele, Using an

- Immunopeptidomics Approach.” *Journal of Virology* 93(17).
- Chiruvella, Kishore K., Zhuobin Liang, and Thomas E. Wilson. 2013. “Repair of Double-Strand Breaks by End Joining.” *Cold Spring Harbor Perspectives in Biology* 5(5).
- Choi, Bryan D. et al. 2019. “CRISPR-Cas9 Disruption of PD-1 Enhances Activity of Universal EGFRvIII CAR T Cells in a Preclinical Model of Human Glioblastoma.” *Journal for ImmunoTherapy of Cancer* 7(1): 304.
<https://jitc.biomedcentral.com/articles/10.1186/s40425-019-0806-7>
 (December 5, 2019).
- Chrast, Roman, Gesine Saher, Klaus Armin Nave, and Mark H.G. Verheijen. 2011. “Lipid Metabolism in Myelinating Glial Cells: Lessons from Human Inherited Disorders and Mouse Models.” *Journal of Lipid Research* 52(3): 419–34.
- Chu, Van Trung et al. 2015. “Increasing the Efficiency of Homology-Directed Repair for CRISPR-Cas9-Induced Precise Gene Editing in Mammalian Cells.” *Nature Biotechnology* 33(5): 543–48.
- Chylinski, Krzysztof, Anaïs Le Rhun, and Emmanuelle Charpentier. 2013. “The TracrRNA and Cas9 Families of Type II CRISPR-Cas Immunity Systems.” *RNA Biology* 10(5): 726–37.
- Citron, M et al. 1994. “Excessive Production of Amyloid Beta-Protein by Peripheral Cells of Symptomatic and Presymptomatic Patients Carrying the Swedish Familial Alzheimer Disease Mutation.” *Proceedings of the National Academy of Sciences of the United States of America* 91(25): 11993–97.
<http://www.ncbi.nlm.nih.gov/pubmed/7991571> (December 4, 2019).
- Clapham, Paul R., and Áine McKnight. 2002. “Cell Surface Receptors, Virus Entry and Tropism of Primate Lentiviruses.” *Journal of General Virology* 83(8): 1809–29.
- Cohen-Solal, Karine A, Rajeev K Boregowda, and Ahmed Lasfar. 2015. “RUNX2 and the PI3K/AKT Axis Reciprocal Activation as a Driving Force for Tumor Progression.” *Molecular cancer* 14: 137.
<http://www.ncbi.nlm.nih.gov/pubmed/26204939> (December 4, 2019).
- Cohen, G B et al. 2000. “The Human Thioesterase II Protein Binds to a Site on

- HIV-1 Nef Critical for CD4 down-Regulation.” *The Journal of biological chemistry* 275(30): 23097–105.
<http://www.ncbi.nlm.nih.gov/pubmed/10807905> (December 4, 2019).
- Colicelli, John. 2010. “ABL Tyrosine Kinases: Evolution of Function, Regulation, and Specificity.” *Science Signaling* 3(139).
- Cong, Le et al. 2013. “Multiplex Genome Engineering Using CRISPR/Cas Systems.” *Science* 339(6121): 819–23.
- Cosma, A et al. 1999. “Enhanced HIV Infectivity and Changes in GP120 Conformation Associated with Viral Incorporation of Human Leucocyte Antigen Class I Molecules.” *AIDS (London, England)* 13(15): 2033–42.
<http://www.ncbi.nlm.nih.gov/pubmed/10546855> (December 4, 2019).
- Cox, David Benjamin Turitz, Randall Jeffrey Platt, and Feng Zhang. 2015. “Therapeutic Genome Editing: Prospects and Challenges.” *Nature Medicine* 21(2): 121–31.
- Crosetto, Nicola et al. 2013. “Nucleotide-Resolution DNA Double-Strand Break Mapping by next-Generation Sequencing.” *Nature Methods* 10(4): 361–65.
- Cui, X. et al. 2005. “Autophosphorylation of DNA-Dependent Protein Kinase Regulates DNA End Processing and May Also Alter Double-Strand Break Repair Pathway Choice.” *Molecular and Cellular Biology* 25(24): 10842–52.
- van der Deen, Margaretha et al. 2012. “Genomic Promoter Occupancy of Runt-Related Transcription Factor RUNX2 in Osteosarcoma Cells Identifies Genes Involved in Cell Adhesion and Motility.” *The Journal of biological chemistry* 287(7): 4503–17. <http://www.ncbi.nlm.nih.gov/pubmed/22158627> (December 4, 2019).
- Deiana, Michela et al. 2018. “New Insights into the Runt Domain of RUNX2 in Melanoma Cell Proliferation and Migration.” *Cells* 7(11).
<http://www.ncbi.nlm.nih.gov/pubmed/30463392> (December 4, 2019).
- Deltcheva, Elitza et al. 2011. “CRISPR RNA Maturation by Trans-Encoded Small RNA and Host Factor RNase III.” *Nature* 471(7340): 602–7.
- Deng, Dong et al. 2012. “Structural Basis for Sequence-Specific Recognition of DNA by TAL Effectors.” *Science* 335(6069): 720–23.
- Deutsch, Eric et al. 2001. “BCR-ABL down-Regulates the DNA Repair Protein

- DNA-PKcs.” *Blood* 97(7): 2084–90.
- Dever, Daniel P et al. 2019. “CRISPR/Cas9 Genome Engineering in Engraftable Human Brain-Derived Neural Stem Cells.” *iScience* 15: 524–35.
<http://www.ncbi.nlm.nih.gov/pubmed/31132746> (December 4, 2019).
- Dierks, Christine et al. 2008. “Expansion of Bcr-Abl-Positive Leukemic Stem Cells Is Dependent on Hedgehog Pathway Activation.” *Cancer Cell* 14(3): 238–49.
- Van Diggelen, Otto P. et al. 2001. “Adult Neuronal Ceroid Lipofuscinosis with Palmitoyl-Protein Thioesterase Deficiency: First Adult-Onset Patients of a Childhood Disease.” *Annals of Neurology* 50(2): 269–72.
- Dong, Shengzhang et al. 2015. “Heritable CRISPR/Cas9-Mediated Genome Editing in the Yellow Fever Mosquito, *Aedes Aegypti*.” *PloS one* 10(3): e0122353. <http://www.ncbi.nlm.nih.gov/pubmed/25815482> (December 4, 2019).
- Dong, Yan et al. 2019. “Genome-Wide Off-Target Analysis in CRISPR-Cas9 Modified Mice and Their Offspring.” *G3 (Bethesda, Md.)* 9(11): 3645–51.
<http://www.ncbi.nlm.nih.gov/pubmed/31492696> (December 4, 2019).
- Drost, Jarno et al. 2017. “Use of CRISPR-Modified Human Stem Cell Organoids to Study the Origin of Mutational Signatures in Cancer.” *Science* 358(6360): 234–38.
- Drube, Julia et al. 2018. “PTPRG and PTPRC Modulate Nilotinib Response in Chronic Myeloid Leukemia Cells.” *Oncotarget* 9(10): 9442–55.
- Ducreux, Michel et al. 2019. “Systemic Treatment of Pancreatic Cancer Revisited.” *Seminars in Oncology* 46(1): 28–38.
- Durand, J. K., and A. S. Baldwin. 2017. “Targeting IKK and NF- κ B for Therapy.” In *Advances in Protein Chemistry and Structural Biology*, Academic Press Inc., 77–115.
- Dyikanov, Daniyar T. et al. 2019. “Optimization of CRISPR/Cas9 Technology to Knock out Genes of Interest in Aneuploid Cell Lines.” *Tissue Engineering - Part C: Methods* 25(3): 168–75.
- East-Seletsky, Alexandra et al. 2017. “RNA Targeting by Functionally Orthogonal Type VI-A CRISPR-Cas Enzymes.” *Molecular cell* 66(3): 373-

- 383.e3. <http://www.ncbi.nlm.nih.gov/pubmed/28475872> (December 4, 2019).
- Ebina, Hirotaka, Naoko Misawa, Yuka Kanemura, and Yoshio Koyanagi. 2013. “Harnessing the CRISPR/Cas9 System to Disrupt Latent HIV-1 Provirus.” *Scientific Reports* 3.
- Eggerickx, D et al. 1995. “Molecular Cloning of an Orphan G-Protein-Coupled Receptor That Constitutively Activates Adenylate Cyclase.” *The Biochemical journal* 309 (Pt 3): 837–43.
<http://www.ncbi.nlm.nih.gov/pubmed/7639700> (December 4, 2019).
- Elmore, Joshua R. et al. 2016. “Bipartite Recognition of Target RNAs Activates DNA Cleavage by the Type III-B CRISPR–Cas System.” *Genes and Development* 30(4): 447–59.
- Esashi, Fumiko et al. 2007. “Stabilization of RAD51 Nucleoprotein Filaments by the C-Terminal Region of BRCA2.” *Nature Structural and Molecular Biology* 14(6): 468–74.
- Faderl, Stefan et al. 1999. “The Biology of Chronic Myeloid Leukemia.” *New England Journal of Medicine* 341(3): 164–72.
- Fanale-Belasio, Emanuele, Mariangela Raimondo, Barbara Suligo, and Stefano Buttò. 2010. “HIV Virology and Pathogenetic Mechanisms of Infection: A Brief Overview.” *Annali dell’Istituto Superiore di Sanita* 46(1): 5–14.
- Feng, Zhengyan et al. 2013. “Efficient Genome Editing in Plants Using a CRISPR/Cas System.” *Cell Research* 23(10): 1229–32.
- Fochi, Stefania et al. 2018. “HTLV Dereglulation of the NF-KB Pathway: An Update on Tax and Antisense Proteins Role.” *Frontiers in Microbiology* 9(FEB): 285. <http://www.ncbi.nlm.nih.gov/pubmed/29515558> (March 26, 2020).
- . 2019. “TRAF3 Is Required for NF-KB Pathway Activation Mediated by HTLV Tax Proteins.” *Frontiers in microbiology* 10: 1302.
<http://www.ncbi.nlm.nih.gov/pubmed/31244811> (December 5, 2019).
- Friedland, Ari E. et al. 2015. “Characterization of Staphylococcus Aureus Cas9: A Smaller Cas9 for All-in-One Adeno-Associated Virus Delivery and Paired Nickase Applications.” *Genome Biology* 16(1).

- Fu, Yanfang et al. 2013. "High-Frequency off-Target Mutagenesis Induced by CRISPR-Cas Nucleases in Human Cells." *Nature Biotechnology* 31(9): 822–26.
- . 2014. "Improving CRISPR-Cas Nuclease Specificity Using Truncated Guide RNAs." *Nature Biotechnology* 32(3): 279–84.
- Fukata, Yuko, and Masaki Fukata. 2010. "Protein Palmitoylation in Neuronal Development and Synaptic Plasticity." *Nature Reviews Neuroscience* 11(3): 161–75.
- Furuta, Junichi et al. 2006. "Silencing of Peroxiredoxin 2 and Aberrant Methylation of 33 CpG Islands in Putative Promoter Regions in Human Malignant Melanomas." *Cancer Research* 66(12): 6080–86.
- Gao, Linyi et al. 2017. "Engineered Cpf1 Variants with Altered PAM Specificities." *Nature Biotechnology* 35(8): 789–92.
- García-Tuñón, Ignacio et al. 2017. "The CRISPR/Cas9 System Efficiently Reverts the Tumorigenic Ability of BCR/ABL in Vitro and in a Xenograft Model of Chronic Myeloid Leukemia." *Oncotarget* 8(16): 26027–40. <http://www.ncbi.nlm.nih.gov/pubmed/28212528> (December 4, 2019).
- Gardam, Sandra et al. 2008. "TRAF2 and TRAF3 Signal Adapters Act Cooperatively to Control the Maturation and Survival Signals Delivered to B Cells by the BAFF Receptor." *Immunity* 28(3): 391–401. <http://www.ncbi.nlm.nih.gov/pubmed/18313334> (December 4, 2019).
- Garneau, Josiane E. et al. 2010. "The CRISPR/Cas Bacterial Immune System Cleaves Bacteriophage and Plasmid DNA." *Nature* 468(7320): 67–71.
- Gasiunas, Giedrius, Rodolphe Barrangou, Philippe Horvath, and Virginijus Siksnys. 2012. "Cas9-CrRNA Ribonucleoprotein Complex Mediates Specific DNA Cleavage for Adaptive Immunity in Bacteria." *Proceedings of the National Academy of Sciences of the United States of America* 109(39).
- Gee, Peter et al. 2020. "Extracellular Nanovesicles for Packaging of CRISPR-Cas9 Protein and SgRNA to Induce Therapeutic Exon Skipping." *Nature Communications* 11(1).
- Gessain, Antoine, and Olivier Cassar. 2012. "Epidemiological Aspects and World Distribution of HTLV-1 Infection." *Frontiers in microbiology* 3: 388.

- <http://www.ncbi.nlm.nih.gov/pubmed/23162541> (December 4, 2019).
- Ghose, S, H Porzig, and K Baltensperger. 1999. "Induction of Erythroid Differentiation by Altered Galpha16 Activity as Detected by a Reporter Gene Assay in MB-02 Cells." *The Journal of biological chemistry* 274(18): 12848–54. <http://www.ncbi.nlm.nih.gov/pubmed/10212272> (December 4, 2019).
- Giannone, Flavia et al. 2010. "The Puzzling Uniqueness of the Heterotrimeric G15 Protein and Its Potential beyond Hematopoiesis." *Journal of molecular endocrinology* 44(5): 259–69. <http://www.ncbi.nlm.nih.gov/pubmed/20150327> (December 4, 2019).
- Giovinazzo, Francesco et al. 2013. "Ectopic Expression of the Heterotrimeric G15 Protein in Pancreatic Carcinoma and Its Potential in Cancer Signal Transduction." *Cellular signalling* 25(3): 651–59. <http://www.ncbi.nlm.nih.gov/pubmed/23200847> (December 4, 2019).
- Gondim, Marcos Vinicius et al. 2015. "AP-2 Is the Crucial Clathrin Adaptor Protein for CD4 Downmodulation by HIV-1 Nef in Infected Primary CD4 + T Cells ." *Journal of Virology* 89(24): 12518–24.
- Gootenberg, Jonathan S. et al. 2017. "Nucleic Acid Detection with CRISPR-Cas13a/C2c2." *Science* 356(6336): 438–42.
- Greenfield, Andy. 2018. "Carry on Editing." *British Medical Bulletin* 127(1): 23–31. <https://academic.oup.com/bmb/article/127/1/23/5042917> (December 4, 2019).
- Greisman, Harvey A., and Carl O. Pabo. 1997. "A General Strategy for Selecting High-Affinity Zinc Finger Proteins for Diverse DNA Target Sites." *Science* 275(5300): 657–61.
- Groothuis, T., and J. Neefjes. 2006. "The Ins and Outs of Intracellular Peptides and Antigen Presentation by MHC Class I Molecules." *Current Topics in Microbiology and Immunology* 300: 127–48.
- Gu, Jiafeng et al. 2010. "DNA-PKcs Regulates a Single-Stranded DNA Endonuclease Activity of Artemis." *DNA Repair* 9(4): 429–37.
- Gu, Yuan et al. 2019. "Bioinformatic Evidences and Analysis of Putative Biomarkers in Pancreatic Ductal Adenocarcinoma." *Heliyon* 5(8): e02378.

- <http://www.ncbi.nlm.nih.gov/pubmed/31489384> (December 4, 2019).
- Guan, Yuting et al. 2016. “CRISPR/Cas9-Mediated Somatic Correction of a Novel Coagulator Factor IX Gene Mutation Ameliorates Hemophilia in Mouse.” *EMBO molecular medicine* 8(5): 477–88.
- <http://www.ncbi.nlm.nih.gov/pubmed/26964564> (December 4, 2019).
- Guo, Yingying et al. 2014. “Structural Basis for Hijacking CBF- β and CUL5 E3 Ligase Complex by HIV-1 Vif.” *Nature* 505(7482): 229–33.
- <http://www.ncbi.nlm.nih.gov/pubmed/24402281> (December 4, 2019).
- György, Bence et al. 2018. “CRISPR/Cas9 Mediated Disruption of the Swedish APP Allele as a Therapeutic Approach for Early-Onset Alzheimer’s Disease.” *Molecular Therapy - Nucleic Acids* 11: 429–40.
- Haass, Christian et al. 1995. “The Swedish Mutation Causes Early-Onset Alzheimer’s Disease by β -Secretase Cleavage within the Secretory Pathway.” *Nature Medicine* 1(12): 1291–96.
- Hai, Tang et al. 2014. “One-Step Generation of Knockout Pigs by Zygote Injection of CRISPR/Cas System.” *Cell research* 24(3): 372–75.
- <http://www.ncbi.nlm.nih.gov/pubmed/24481528> (December 4, 2019).
- Haltia, Matti. 2003. “The Neuronal Ceroid-Lipofuscinoses.” *Journal of Neuropathology and Experimental Neurology* 62(1): 1–13.
- Haskell, R. E. 2000. “Batten Disease: Evaluation of CLN3 Mutations on Protein Localization and Function.” *Human Molecular Genetics* 9(5): 735–44.
- Heasley, Lynn E. et al. 1996. “Discordant Signal Transduction and Growth Inhibition of Small Cell Lung Carcinomas Induced by Expression of GTPase-Deficient Ga16.” *Journal of Biological Chemistry* 271(1): 349–54.
- Heiber, Michael et al. 1995. “Isolation of Three Novel Human Genes Encoding G Protein-Coupled Receptors.” *DNA and Cell Biology* 14(1): 25–35.
- Henriet, S. et al. 2009. “Tumultuous Relationship between the Human Immunodeficiency Virus Type 1 Viral Infectivity Factor (Vif) and the Human APOBEC-3G and APOBEC-3F Restriction Factors.” *Microbiology and Molecular Biology Reviews* 73(2): 211–32.
- Hsu, Patrick D. et al. 2013. “DNA Targeting Specificity of RNA-Guided Cas9 Nucleases.” *Nature Biotechnology* 31(9): 827–32.

- Hubbard, Katherine B, and John R Hepler. 2006. "Cell Signalling Diversity of the Gqalpha Family of Heterotrimeric G Proteins." *Cellular signalling* 18(2): 135–50. <http://www.ncbi.nlm.nih.gov/pubmed/16182515> (December 4, 2019).
- Hubbert, Charlotte et al. 2002. "HDAC6 Is a Microtubule-Associated Deacetylase." *Nature* 417(6887): 455–58.
- Hwang, Woong Y. et al. 2013. "Efficient Genome Editing in Zebrafish Using a CRISPR-Cas System." *Nature Biotechnology* 31(3): 227–29.
- Ihry, Robert J et al. 2018. "P53 Inhibits CRISPR-Cas9 Engineering in Human Pluripotent Stem Cells." *Nature medicine* 24(7): 939–46. <http://www.ncbi.nlm.nih.gov/pubmed/29892062> (December 4, 2019).
- Ishino, Y. et al. 1987. "Nucleotide Sequence of the Iap Gene, Responsible for Alkaline Phosphatase Isoenzyme Conversion in Escherichia Coli, and Identification of the Gene Product." *Journal of Bacteriology* 169(12): 5429–33.
- Jackson, Aimee L, and Peter S Linsley. 2010. "Recognizing and Avoiding SiRNA Off-Target Effects for Target Identification and Therapeutic Application." *Nature reviews. Drug discovery* 9(1): 57–67. <http://www.ncbi.nlm.nih.gov/pubmed/20043028> (December 4, 2019).
- Jalanko, Anu et al. 2005. "Mice with Ppt1Deltaex4 Mutation Replicate the INCL Phenotype and Show an Inflammation-Associated Loss of Interneurons." *Neurobiology of disease* 18(1): 226–41. <http://www.ncbi.nlm.nih.gov/pubmed/15649713> (December 4, 2019).
- James, Stephanie et al. 2018. "Pathway to Deployment of Gene Drive Mosquitoes as a Potential Biocontrol Tool for Elimination of Malaria in Sub-Saharan Africa: Recommendations of a Scientific Working Group†." *The American journal of tropical medicine and hygiene* 98(6_Suppl): 1–49. <http://www.ncbi.nlm.nih.gov/pubmed/29882508> (December 4, 2019).
- Jarmuz, Adam et al. 2002. "An Anthropoid-Specific Locus of Orphan C to U RNA-Editing Enzymes on Chromosome 22." *Genomics* 79(3): 285–96. <http://www.ncbi.nlm.nih.gov/pubmed/11863358> (December 4, 2019).
- Jiang, Fuguo, and Jennifer A. Doudna. 2017. "CRISPR–Cas9 Structures and

- Mechanisms.” *Annual Review of Biophysics* 46(1): 505–29.
- Jinek, Martin et al. 2012. “A Programmable Dual-RNA-Guided DNA Endonuclease in Adaptive Bacterial Immunity.” *Science* 337(6096): 816–21.
- Johnston, J A et al. 1994. “Increased Beta-Amyloid Release and Levels of Amyloid Precursor Protein (APP) in Fibroblast Cell Lines from Family Members with the Swedish Alzheimer’s Disease APP670/671 Mutation.” *FEBS letters* 354(3): 274–78. <http://www.ncbi.nlm.nih.gov/pubmed/7957938> (December 4, 2019).
- Joung, J K, E I Ramm, and C O Pabo. 2000. “A Bacterial Two-Hybrid Selection System for Studying Protein-DNA and Protein-Protein Interactions.” *Proceedings of the National Academy of Sciences of the United States of America* 97(13): 7382–87. <http://www.ncbi.nlm.nih.gov/pubmed/10852947> (December 4, 2019).
- Kaminski, R. et al. 2016. “Excision of HIV-1 DNA by Gene Editing: A Proof-of-Concept in Vivo Study.” *Gene Therapy* 23(8–9): 690–95.
- Kaminski, Rafal et al. 2016. “Negative Feedback Regulation of HIV-1 by Gene Editing Strategy.” *Scientific reports* 6: 31527. <http://www.ncbi.nlm.nih.gov/pubmed/27528385> (December 4, 2019).
- Karanam, Ketki, Ran Kafri, Alexander Loewer, and Galit Lahav. 2012. “Quantitative Live Cell Imaging Reveals a Gradual Shift between DNA Repair Mechanisms and a Maximal Use of HR in Mid S Phase.” *Molecular Cell* 47(2): 320–29.
- Kato, J. et al. 1993. “Direct Binding of Cyclin D to the Retinoblastoma Gene Product (PRb) and PRb Phosphorylation by the Cyclin D-Dependent Kinase CDK4.” *Genes and Development* 7(3): 331–42.
- Kay, Mark A. 2011. “State-of-the-Art Gene-Based Therapies: The Road Ahead.” *Nature Reviews Genetics* 12(5): 316–28.
- Kim, Daesik et al. 2015. “Digenome-Seq: Genome-Wide Profiling of CRISPR-Cas9 off-Target Effects in Human Cells.” *Nature Methods* 12(3): 237–43.
- Kim, E.-Y. et al. 2010. “Human APOBEC3G-Mediated Editing Can Promote HIV-1 Sequence Diversification and Accelerate Adaptation to Selective Pressure.” *Journal of Virology* 84(19): 10402–5.

- Kim, Min Suk et al. 2009. "Cleavage of Protein Kinase D after Acute Hypoinsulinemia Prevents Excessive Lipoprotein Lipase-Mediated Cardiac Triglyceride Accumulation." *Diabetes* 58(11): 2464–75.
<http://www.ncbi.nlm.nih.gov/pubmed/19875622> (December 4, 2019).
- Kim, Sojung et al. 2014. "Highly Efficient RNA-Guided Genome Editing in Human Cells via Delivery of Purified Cas9 Ribonucleoproteins." *Genome Research* 24(6): 1012–19.
- Kim, Sung-Jo et al. 2008. "Palmitoyl Protein Thioesterase-1 Deficiency Impairs Synaptic Vesicle Recycling at Nerve Terminals, Contributing to Neuropathology in Humans and Mice." *The Journal of clinical investigation* 118(9): 3075–86. <http://www.ncbi.nlm.nih.gov/pubmed/18704195> (December 4, 2019).
- Kim, Tae Kyung, and James H. Eberwine. 2010. "Mammalian Cell Transfection: The Present and the Future." *Analytical and Bioanalytical Chemistry* 397(8): 3173–78.
- Kleinstiver, Benjamin P. et al. 2016. "Genome-Wide Specificities of CRISPR-Cas Cpf1 Nucleases in Human Cells." *Nature Biotechnology* 34(8): 869–74.
- Knott, Gavin J et al. 2017. "Guide-Bound Structures of an RNA-Targeting A-Cleaving CRISPR-Cas13a Enzyme." *Nature structural & molecular biology* 24(10): 825–33. <http://www.ncbi.nlm.nih.gov/pubmed/28892041> (December 4, 2019).
- Kogure, Yasunori, and Keisuke Kataoka. 2017. "Genetic Alterations in Adult T-Cell Leukemia/Lymphoma." *Cancer Science* 108(9): 1719–25.
- Koonin, Eugene V., Kira S. Makarova, and Feng Zhang. 2017. "Diversity, Classification and Evolution of CRISPR-Cas Systems." *Current Opinion in Microbiology* 37: 67–78.
- Kostas, Michal et al. 2018. "Protein Tyrosine Phosphatase Receptor Type G (PTPRG) Controls Fibroblast Growth Factor Receptor (FGFR) 1 Activity and Influences Sensitivity to FGFR Kinase Inhibitors." *Molecular & cellular proteomics : MCP* 17(5): 850–70.
<http://www.ncbi.nlm.nih.gov/pubmed/29371290> (December 4, 2019).
- Koyanagi, Yoshio et al. 1993. "In Vivo Infection of Human T-Cell Leukemia

- Virus Type I in Non-T Cells.” *Virology* 196(1): 25–33.
- Kuscu, Cem et al. 2017. “CRISPR-STOP: Gene Silencing through Base-Editing-Induced Nonsense Mutations.” *Nature methods* 14(7): 710–12.
<http://www.ncbi.nlm.nih.gov/pubmed/28581493> (December 4, 2019).
- Kwon, Tae-Geon et al. 2011. “Physical and Functional Interactions between Runx2 and HIF-1 α Induce Vascular Endothelial Growth Factor Gene Expression.” *Journal of cellular biochemistry* 112(12): 3582–93.
<http://www.ncbi.nlm.nih.gov/pubmed/21793044> (December 4, 2019).
- L. Ferreira, I. et al. 2012. “Multiple Defects in Energy Metabolism in Alzheimers Disease.” *Current Drug Targets* 11(10): 1193–1206.
- LaForgia, S. et al. 1991. “Receptor Protein-Tyrosine Phosphatase γ Is a Candidate Tumor Suppressor Gene at Human Chromosome Region 3p21.” *Proceedings of the National Academy of Sciences of the United States of America* 88(11): 5036–40.
- Lamers, Susanna L. et al. 2012. “HIV-1 Nef in Macrophage-Mediated Disease Pathogenesis.” *International Reviews of Immunology* 31(6): 432–50.
- Lamsoul, I. et al. 2005. “Exclusive Ubiquitination and Sumoylation on Overlapping Lysine Residues Mediate NF- κ B Activation by the Human T-Cell Leukemia Virus Tax Oncoprotein.” *Molecular and Cellular Biology* 25(23): 10391–406.
- Lanphier, Edward et al. 2015. “Don’t Edit the Human Germ Line.” *Nature* 519(7544): 410–11. <http://www.ncbi.nlm.nih.gov/pubmed/25810189> (December 4, 2019).
- Lebbink, Robert Jan et al. 2017. “A Combinational CRISPR/Cas9 Gene-Editing Approach Can Halt HIV Replication and Prevent Viral Escape.” *Scientific reports* 7: 41968. <http://www.ncbi.nlm.nih.gov/pubmed/28176813> (December 4, 2019).
- Lee, Bumwhhee et al. 2018. “Nanoparticle Delivery of CRISPR into the Brain Rescues a Mouse Model of Fragile X Syndrome from Exaggerated Repetitive Behaviours.” *Nature Biomedical Engineering* 2(7): 497–507.
- Lee, Ji Shin et al. 2004. “Reduced PTEN Expression Is Associated with Poor Outcome and Angiogenesis in Invasive Ductal Carcinoma of the Breast.”

- Applied immunohistochemistry & molecular morphology* : AIMM 12(3): 205–10. <http://www.ncbi.nlm.nih.gov/pubmed/15551732> (December 4, 2019).
- Lee, Kunwoo et al. 2017. “Nanoparticle Delivery of Cas9 Ribonucleoprotein and Donor DNA in Vivo Induces Homology-Directed DNA Repair.” *Nature Biomedical Engineering* 1(11): 889–901.
- Lefkowitz, Robert J., and Sudha K. Shenoy. 2005. “Transduction of Receptor Signals by β -Arrestins.” *Science* 308(5721): 512–17.
- Liu, Andrew M F, and Yung H. Wong. 2004. “G16-Mediated Activation of Nuclear Factor KB by the Adenosine A1 Receptor Involves c-Src, Protein Kinase C, and ERK Signaling.” *Journal of Biological Chemistry* 279(51): 53196–204.
- Liu, F., Y. K. Song, and D. Liu. 1999. “Hydrodynamics-Based Transfection in Animals by Systemic Administration of Plasmid DNA.” *Gene Therapy* 6(7): 1258–66.
- Liu, L X et al. 1997. “Binding of HIV-1 Nef to a Novel Thioesterase Enzyme Correlates with Nef-Mediated CD4 down-Regulation.” *The Journal of biological chemistry* 272(21): 13779–85.
<http://www.ncbi.nlm.nih.gov/pubmed/9153233> (December 4, 2019).
- . 2000. “Mutation of a Conserved Residue (D123) Required for Oligomerization of Human Immunodeficiency Virus Type 1 Nef Protein Abolishes Interaction with Human Thioesterase and Results in Impairment of Nef Biological Functions.” *Journal of virology* 74(11): 5310–19.
<http://www.ncbi.nlm.nih.gov/pubmed/10799608> (December 4, 2019).
- Liu, Liang et al. 2017. “Two Distant Catalytic Sites Are Responsible for C2c2 RNase Activities.” *Cell* 168(1–2): 121-134.e12.
- Liu, Pei-Pei, Yi Xie, Xiao-Yan Meng, and Jian-Sheng Kang. 2019. “History and Progress of Hypotheses and Clinical Trials for Alzheimer’s Disease.” *Signal Transduction and Targeted Therapy* 4(1).
- Liu, Suling et al. 2004. “Function Analysis of Estrogenically Regulated Protein Tyrosine Phosphatase γ (PTP γ) in Human Breast Cancer Cell Line MCF-7.” *Oncogene* 23(6): 1256–62.

- Livak, Kenneth J., and Thomas D. Schmittgen. 2001. "Analysis of Relative Gene Expression Data Using Real-Time Quantitative PCR and the 2- $\Delta\Delta$ CT Method." *Methods* 25(4): 402–8.
- Lo, Rico K.H., and Yung H. Wong. 2006. "Transcriptional Activation of C-Fos by Constitutively Active G α 16QL through a STAT1-Dependent Pathway." *Cellular Signalling* 18(12): 2143–53.
- Lovell-Badge, Robin. 2019. "CRISPR Babies: A View from the Centre of the Storm." *Development (Cambridge)* 146(3).
- Lugo, Tracy G., Ann Marie Pendergast, Alexander J. Muller, and Owen N. Witte. 1990. "Tyrosine Kinase Activity and Transformation Potency of Bcr-Abl Oncogene Products." *Science* 247(4946): 1079–82.
- Lyly, Annina et al. 2008. "Deficiency of the INCL Protein Ppt1 Results in Changes in Ectopic F1-ATP Synthase and Altered Cholesterol Metabolism." *Human molecular genetics* 17(10): 1406–17.
<http://www.ncbi.nlm.nih.gov/pubmed/18245779> (December 4, 2019).
- Ma, Philip, and Rodney Zimmel. 2002. "Value of Novelty? Market Indicators." *Nature Reviews Drug Discovery* 1(8): 571–72.
- Macatonia, Steven E., J. K. Cruickshank, Peter Rudge, and Stella C. Knight. 1992. "Dendritic Cells from Patients with Tropical Spastic Paraparesis Are Infected with HTLV-1 and Stimulate Autologous Lymphocyte Proliferation." *AIDS Research and Human Retroviruses* 8(9): 1699–1706.
- Mafficini, Andrea et al. 2007. "Protein Tyrosine Phosphatase Gamma (PTP γ) Is a Novel Leukocyte Marker Highly Expressed by CD34 + Precursors ." *Biomarker Insights* 2: 117727190700200.
- Maggio, Ignazio et al. 2014. "Adenoviral Vector Delivery of RNA-Guided CRISPR/Cas9 Nuclease Complexes Induces Targeted Mutagenesis in a Diverse Array of Human Cells." *Scientific reports* 4: 5105.
<http://www.ncbi.nlm.nih.gov/pubmed/24870050> (December 4, 2019).
- Makarova, Kira S. et al. 2006. "A Putative RNA-Interference-Based Immune System in Prokaryotes: Computational Analysis of the Predicted Enzymatic Machinery, Functional Analogies with Eukaryotic RNAi, and Hypothetical Mechanisms of Action." *Biology Direct* 1.

- . 2011. “Evolution and Classification of the CRISPR-Cas Systems.” *Nature Reviews Microbiology* 9(6): 467–77.
- Mali, Prashant et al. 2013. “RNA-Guided Human Genome Engineering via Cas9.” *Science* 339(6121): 823–26.
- Mangeot, Philippe E. et al. 2019. “Genome Editing in Primary Cells and in Vivo Using Viral-Derived Nanoblades Loaded with Cas9-SgRNA Ribonucleoproteins.” *Nature Communications* 10(1).
- Manguso, Robert T. et al. 2017. “In Vivo CRISPR Screening Identifies Ptpn2 as a Cancer Immunotherapy Target.” *Nature* 547(7664): 413–18.
- Marin, Mariana, Kristine M. Rose, Susan L. Kozak, and David Kabat. 2003. “HIV-1 Vif Protein Binds the Editing Enzyme APOBEC3G and Induces Its Degradation.” *Nature Medicine* 9(11): 1398–1403.
- Maruyama, Takeshi et al. 2015. “Increasing the Efficiency of Precise Genome Editing with CRISPR-Cas9 by Inhibition of Nonhomologous End Joining.” *Nature Biotechnology* 33(5): 538–42.
- Mateos-Gomez, Pedro A et al. 2017. “The Helicase Domain of Pol θ Counteracts RPA to Promote Alt-NHEJ.” *Nature structural & molecular biology* 24(12): 1116–23. <http://www.ncbi.nlm.nih.gov/pubmed/29058711> (December 4, 2019).
- Maule, Giulia et al. 2019. “Allele Specific Repair of Splicing Mutations in Cystic Fibrosis through AsCas12a Genome Editing.” *Nature Communications* 10(1).
- Mbisa, J. L. et al. 2007. “Human Immunodeficiency Virus Type 1 CDNAs Produced in the Presence of APOBEC3G Exhibit Defects in Plus-Strand DNA Transfer and Integration.” *Journal of Virology* 81(13): 7099–7110.
- Mbisa, J. L., W. Bu, and V. K. Pathak. 2010. “APOBEC3F and APOBEC3G Inhibit HIV-1 DNA Integration by Different Mechanisms.” *Journal of Virology* 84(10): 5250–59.
- Meek, K. et al. 2007. “Trans Autophosphorylation at DNA-Dependent Protein Kinase’s Two Major Autophosphorylation Site Clusters Facilitates End Processing but Not End Joining.” *Molecular and Cellular Biology* 27(10): 3881–90.

- Meyn, Malcolm A et al. 2006. "Src Family Kinases Phosphorylate the Bcr-Abl SH3-SH2 Region and Modulate Bcr-Abl Transforming Activity." *The Journal of biological chemistry* 281(41): 30907–16.
<http://www.ncbi.nlm.nih.gov/pubmed/16912036> (December 4, 2019).
- Miller, Jason B. et al. 2017. "Non-Viral CRISPR/Cas Gene Editing In Vitro and In Vivo Enabled by Synthetic Nanoparticle Co-Delivery of Cas9 mRNA and SgRNA." *Angewandte Chemie - International Edition* 56(4): 1059–63.
- Milot, E. et al. 1992. "Chromosomal Illegitimate Recombination in Mammalian Cells Is Associated with Intrinsically Bent DNA Elements." *The EMBO Journal* 11(13): 5063–70. <http://doi.wiley.com/10.1002/j.1460-2075.1992.tb05613.x> (December 5, 2019).
- Mojica, F. J.M., G. Juez, and F. Rodriguez-Valera. 1993. "Transcription at Different Salinities of *Haloflex* Mediterranean Sequences Adjacent to Partially Modified PstI Sites." *Molecular Microbiology* 9(3): 613–21.
- Mole, Sara, Ruth Williams, and Hans Goebel, eds. 2012. 1 *The Neuronal Ceroid Lipofuscinoses (Batten Disease)*. Oxford University Press.
<http://oxfordmedicine.com/view/10.1093/med/9780199590018.001.0001/med-9780199590018> (December 4, 2019).
- Monne, Maria et al. 2013. "Ptpyg and BCR/ABL1 Expression In CML Patients At Diagnosis and Upon TKI Treatment: Preliminary Results." *Blood* 122(21): 5163–5163.
- Moore, M, A Klug, and Y Choo. 2001. "Improved DNA Binding Specificity from Polyzinc Finger Peptides by Using Strings of Two-Finger Units." *Proceedings of the National Academy of Sciences of the United States of America* 98(4): 1437–41. <http://www.ncbi.nlm.nih.gov/pubmed/11171969> (December 4, 2019).
- Morales, Paula, Dow P. Hurst, and Patricia H. Reggio. 2017. "Methods for the Development of In Silico GPCR Models." In *Methods in Enzymology*, Academic Press Inc., 405–48.
- Morales, Paula, Israa Isawi, and Patricia H Reggio. 2018. "Towards a Better Understanding of the Cannabinoid-Related Orphan Receptors GPR3, GPR6, and GPR12." *Drug metabolism reviews* 50(1): 74–93.

- <http://www.ncbi.nlm.nih.gov/pubmed/29390908> (December 4, 2019).
- Moro, Dorian et al. 2018. "Identifying Knowledge Gaps for Gene Drive Research to Control Invasive Animal Species: The next CRISPR Step." *Global Ecology and Conservation* 13.
- Moses, Colette et al. 2019. "Activating PTEN Tumor Suppressor Expression with the CRISPR/DCas9 System." *Molecular therapy. Nucleic acids* 14: 287–300. <http://www.ncbi.nlm.nih.gov/pubmed/30654190> (December 4, 2019).
- Mota, Sandra I, Ildete L Ferreira, and A Cristina Rego. 2014. "Dysfunctional Synapse in Alzheimer's Disease - A Focus on NMDA Receptors." *Neuropharmacology* 76 Pt A: 16–26. <http://www.ncbi.nlm.nih.gov/pubmed/23973316> (December 4, 2019).
- Mullan, M et al. 1992. "A Pathogenic Mutation for Probable Alzheimer's Disease in the APP Gene at the N-Terminus of Beta-Amyloid." *Nature genetics* 1(5): 345–47. <http://www.ncbi.nlm.nih.gov/pubmed/1302033> (December 4, 2019).
- Mulvihill, John J et al. 2017. "Ethical Issues of CRISPR Technology and Gene Editing through the Lens of Solidarity." *British medical bulletin* 122(1): 17–29. <http://www.ncbi.nlm.nih.gov/pubmed/28334154> (December 4, 2019).
- Naldini, Luigi et al. 1996. "In Vivo Gene Delivery and Stable Transduction of Nondividing Cells by a Lentiviral Vector." *Science* 272(5259): 263–67.
- Newman, Edmund N.C. et al. 2005. "Antiviral Function of APOBEC3G Can Be Dissociated from Cytidine Deaminase Activity." *Current Biology* 15(2): 166–70.
- Niewolik, Doris et al. 2006. "DNA-PKcs Dependence of Artemis Endonucleolytic Activity, Differences between Hairpins and 5' or 3' Overhangs." *Journal of Biological Chemistry* 281(45): 33900–909.
- Nishimasu, Hiroshi et al. 2014. "Crystal Structure of Cas9 in Complex with Guide RNA and Target DNA." *Cell* 156(5): 935–49.
- Nita, Dragos A., Sara E. Mole, and Berge A. Minassian. 2016. "Neuronal Ceroid Lipofuscinoses." *Epileptic Disorders* 18: S73–88.
- Nitsch, R M, M Deng, J H Growdon, and R J Wurtman. 1996. "Serotonin 5-HT2a and 5-HT2c Receptors Stimulate Amyloid Precursor Protein Ectodomain Secretion." *The Journal of biological chemistry* 271(8): 4188–94.

- <http://www.ncbi.nlm.nih.gov/pubmed/8626761> (December 4, 2019).
- O'Hayre, Morgan et al. 2013. "The Emerging Mutational Landscape of G Proteins and G-Protein-Coupled Receptors in Cancer." *Nature reviews. Cancer* 13(6): 412–24. <http://www.ncbi.nlm.nih.gov/pubmed/23640210> (December 4, 2019).
- O'Rourke, Donald M. et al. 2017. "A Single Dose of Peripherally Infused EGFRvIII-Directed CAR T Cells Mediates Antigen Loss and Induces Adaptive Resistance in Patients with Recurrent Glioblastoma." *Science Translational Medicine* 9(399).
- Oddo, Salvatore et al. 2006. "Reduction of Soluble A β and Tau, but Not Soluble A β Alone, Ameliorates Cognitive Decline in Transgenic Mice with Plaques and Tangles." *Journal of Biological Chemistry* 281(51): 39413–23.
- Ouyang, Hui et al. 2012. "Protein Aggregates Are Recruited to Aggresome by Histone Deacetylase 6 via Unanchored Ubiquitin C Termini." *The Journal of biological chemistry* 287(4): 2317–27.
<http://www.ncbi.nlm.nih.gov/pubmed/22069321> (December 4, 2019).
- Ozaki, Toshinori, Akira Nakagawara, and Hiroki Nagase. 2013. "[A Novel Role of RUNX2 in the Regulation of P53-Dependent DNA Damage Response]." *Seikagaku. The Journal of Japanese Biochemical Society* 85(11): 1002–7.
<http://www.ncbi.nlm.nih.gov/pubmed/24364254> (December 4, 2019).
- Pai, Ming-Tao et al. 2007. "Solution Structure of the Ubp-M BUZ Domain, a Highly Specific Protein Module That Recognizes the C-Terminal Tail of Free Ubiquitin." *Journal of molecular biology* 370(2): 290–302.
<http://www.ncbi.nlm.nih.gov/pubmed/17512543> (December 4, 2019).
- Palazzo, Alexander, Brian Ackerman, and Gregg G. Gundersen. 2003. "Tubulin Acetylation and Cell Motility." *Nature* 421(6920): 230.
- Palmer, David N., Lucy A. Barry, Jaana Tyynelä, and Jonathan D. Cooper. 2013. "NCL Disease Mechanisms." *Biochimica et Biophysica Acta - Molecular Basis of Disease* 1832(11): 1882–93.
- Pankiv, Serhiy et al. 2007. "P62/SQSTM1 Binds Directly to Atg8/LC3 to Facilitate Degradation of Ubiquitinated Protein Aggregates by Autophagy." *The Journal of biological chemistry* 282(33): 24131–45.

- <http://www.ncbi.nlm.nih.gov/pubmed/17580304> (December 4, 2019).
- Pappalardo, Francesco et al. 2016. “Computational Modeling of PI3K/AKT and MAPK Signaling Pathways in Melanoma Cancer.” *PloS one* 11(3): e0152104. <http://www.ncbi.nlm.nih.gov/pubmed/27015094> (December 4, 2019).
- Paquet, Dominik et al. 2016. “Efficient Introduction of Specific Homozygous and Heterozygous Mutations Using CRISPR/Cas9.” *Nature* 533(7601): 125–29.
- Parolini, Francesca et al. 2018. “Stability and Expression Levels of HLA-C on the Cell Membrane Modulate HIV-1 Infectivity.” *Journal of virology* 92(1). <http://www.ncbi.nlm.nih.gov/pubmed/29070683> (December 4, 2019).
- Pavletich, Nikola P., and Carl O. Pabo. 1991. “Zinc Finger-DNA Recognition: Crystal Structure of a Zif268-DNA Complex at 2.1 Å.” *Science* 252(5007): 809–17.
- Peng, Bo, and Marjorie Robert-Guroff. 2001. “Deletion of N-Terminal Myristoylation Site of HIV Nef Abrogates Both MHC-1 and CD4 down-Regulation.” *Immunology Letters* 78(3): 195–200.
- Della Peruta, Marco et al. 2010. “Protein Tyrosine Phosphatase Receptor Type γ Is a Functional Tumor Suppressor Gene Specifically Downregulated in Chronic Myeloid Leukemia.” *Cancer Research* 70(21): 8896–8906.
- Petris, Gianluca et al. 2017. “Hit and Go CAS9 Delivered through a Lentiviral Based Self-Limiting Circuit.” *Nature Communications* 8.
- Pezzini, Francesco et al. 2017. “The Networks of Genes Encoding Palmitoylated Proteins in Axonal and Synaptic Compartments Are Affected in PPT1 Overexpressing Neuronal-Like Cells.” *Frontiers in molecular neuroscience* 10: 266. <http://www.ncbi.nlm.nih.gov/pubmed/28878621> (December 4, 2019).
- Philip, Philip A et al. 2009. “Consensus Report of the National Cancer Institute Clinical Trials Planning Meeting on Pancreas Cancer Treatment.” *Journal of clinical oncology : official journal of the American Society of Clinical Oncology* 27(33): 5660–69. <http://www.ncbi.nlm.nih.gov/pubmed/19858397> (December 4, 2019).
- Pierce, Kristen L., Richard T. Premont, and Robert J. Lefkowitz. 2002. “Seven-

- Transmembrane Receptors.” *Nature Reviews Molecular Cell Biology* 3(9): 639–50.
- Piperno, G., M. LeDizet, and X. J. Chang. 1987. “Microtubules Containing Acetylated Alpha-Tubulin in Mammalian Cells in Culture.” *The Journal of cell biology* 104(2): 289–302.
- Poiesz, B. J. et al. 1980. “Detection and Isolation of Type C Retrovirus Particles from Fresh and Cultured Lymphocytes of a Patient with Cutaneous T-Cell Lymphoma.” *Proceedings of the National Academy of Sciences of the United States of America* 77(12 II): 7415–19.
- Pooler, Amy M, Anibal A Arjona, Robert K Lee, and Richard J Wurtman. 2004. “Prostaglandin E2 Regulates Amyloid Precursor Protein Expression via the EP2 Receptor in Cultured Rat Microglia.” *Neuroscience letters* 362(2): 127–30. <http://www.ncbi.nlm.nih.gov/pubmed/15193769> (December 4, 2019).
- Pratap, J. et al. 2005. “The Runx2 Osteogenic Transcription Factor Regulates Matrix Metalloproteinase 9 in Bone Metastatic Cancer Cells and Controls Cell Invasion.” *Molecular and Cellular Biology* 25(19): 8581–91.
- Pratap, Jitesh et al. 2009. “Ectopic Runx2 Expression in Mammary Epithelial Cells Disrupts Formation of Normal Acini Structure: Implications for Breast Cancer Progression.” *Cancer research* 69(17): 6807–14. <http://www.ncbi.nlm.nih.gov/pubmed/19690135> (December 4, 2019).
- Preininger, Anita M., and Heidi E. Hamm. 2004. “G Protein Signaling: Insights from New Structures.” *Science’s STKE : signal transduction knowledge environment* 2004(218).
- Qu, Zhaoxia, and Gutian Xiao. 2011. “Human T-Cell Lymphotropic Virus: A Model of NF-KB-Associated Tumorigenesis.” *Viruses* 3(6): 714–49. <http://www.ncbi.nlm.nih.gov/pubmed/21743832> (December 4, 2019).
- Quintana, Elsa et al. 2012. “Human Melanoma Metastasis in NSG Mice Correlates with Clinical Outcome in Patients.” *Science translational medicine* 4(159): 159ra149. <http://www.ncbi.nlm.nih.gov/pubmed/23136044> (December 4, 2019).
- Rahib, Lola et al. 2014. “Projecting Cancer Incidence and Deaths to 2030: The Unexpected Burden of Thyroid, Liver, and Pancreas Cancers in the United

- States.” *Cancer Research* 74(11): 2913–21.
- Ramalingam, Sivaprakash et al. 2013. “Generation and Genetic Engineering of Human Induced Pluripotent Stem Cells Using Designed Zinc Finger Nucleases.” *Stem cells and development* 22(4): 595–610.
<http://www.ncbi.nlm.nih.gov/pubmed/22931452> (December 4, 2019).
- Ramalingam, Sivaprakash, Narayana Annaluru, Karthikeyan Kandavelou, and Srinivasan Chandrasegaran. 2014. “TALEN-Mediated Generation and Genetic Correction of Disease-Specific Human Induced Pluripotent Stem Cells.” *Current Gene Therapy* 14(6): 461–72.
- Ran, F. Ann et al. 2013. “Genome Engineering Using the CRISPR-Cas9 System.” *Nature Protocols* 8(11): 2281–2308.
- . 2015. “In Vivo Genome Editing Using *Staphylococcus Aureus* Cas9.” *Nature* 520(7546): 186–91.
- Rask-Andersen, Mathias, Markus Sällman Almén, and Helgi B. Schiöth. 2011. “Trends in the Exploitation of Novel Drug Targets.” *Nature Reviews Drug Discovery* 10(8): 579–90.
- Raveux, Aurélien, Sandrine Vandormael-Pournin, and Michel Cohen-Tannoudji. 2017. “Optimization of the Production of Knock-in Alleles by CRISPR/Cas9 Microinjection into the Mouse Zygote.” *Scientific reports* 7: 42661.
<http://www.ncbi.nlm.nih.gov/pubmed/28209967> (December 4, 2019).
- Reardon, Sara. 2016. “First CRISPR Clinical Trial Gets Green Light from US Panel.” *Nature*.
- Richardson, J H et al. 1990. JOURNAL OF VIROLOGY *In Vivo Cellular Tropism of Human T-Cell Leukemia Virus Type 1*. <http://jvi.asm.org/> (December 4, 2019).
- Rogakou, Emmy P. et al. 1998. “DNA Double-Stranded Breaks Induce Histone H2AX Phosphorylation on Serine 139.” *Journal of Biological Chemistry* 273(10): 5858–68.
- Rybin, Vitaliy O et al. 2012. “Regulatory Domain Determinants That Control PKD1 Activity.” *The Journal of biological chemistry* 287(27): 22609–15.
<http://www.ncbi.nlm.nih.gov/pubmed/22582392> (December 4, 2019).
- Salesse, Stephanie, and Catherine M. Verfaillie. 2002. “BCR/ABL: From

- Molecular Mechanisms of Leukemia Induction to Treatment of Chronic Myelogenous Leukemia.” *Oncogene* 21(56 REV. ISS. 7): 8547–59.
- Santavuori, Pirkko, Matti Haltia, and Juhani Rapola. 1974. “Infantile Type of So-called Neuronal Ceroid-lipofuscinosis.” *Developmental Medicine & Child Neurology* 16(5): 644–53.
- Saylor, Deanna et al. 2016. “HIV-Associated Neurocognitive Disorder - Pathogenesis and Prospects for Treatment.” *Nature Reviews Neurology* 12(4): 234–48.
- Schumann, Kathrin et al. 2015. “Generation of Knock-in Primary Human T Cells Using Cas9 Ribonucleoproteins.” *Proceedings of the National Academy of Sciences of the United States of America* 112(33): 10437–42.
- Scifo, Enzo et al. 2015. “Quantitative Analysis of PPT1 Interactome in Human Neuroblastoma Cells.” *Data in brief* 4: 207–16.
<http://www.ncbi.nlm.nih.gov/pubmed/26217791> (December 4, 2019).
- Selkoe, Dennis J. 2002. “Alzheimer’s Disease Is a Synaptic Failure.” *Science* 298(5594): 789–91.
- Serena, Michela et al. 2016. “Molecular Characterization of HIV-1 Nef and ACOT8 Interaction: Insights from in Silico Structural Predictions and in Vitro Functional Assays.” *Scientific reports* 6: 22319.
<http://www.ncbi.nlm.nih.gov/pubmed/26927806> (December 4, 2019).
- . 2017. “HIV-1 Env Associates with HLA-C Free-Chains at the Cell Membrane Modulating Viral Infectivity.” *Scientific Reports* 7.
- Serrador, Juan M. et al. 2004. “HDAC6 Deacetylase Activity Links the Tubulin Cytoskeleton with Immune Synapse Organization.” *Immunity* 20(4): 417–28.
- Shalem, Ophir et al. 2014. “Genome-Scale CRISPR-Cas9 Knockout Screening in Human Cells.” *Science* 343(6166): 84–87.
- Sharma, Gaurav, Gurvinder Kaur, and Narinder Mehra. 2011. “Genetic Correlates Influencing Immunopathogenesis of HIV Infection.” *The Indian journal of medical research* 134(6): 749–68.
<http://www.ncbi.nlm.nih.gov/pubmed/22310811> (December 4, 2019).
- Shearer, Robert F, and Darren N Saunders. 2015. “Experimental Design for Stable Genetic Manipulation in Mammalian Cell Lines: Lentivirus and

- Alternatives.” *Genes to cells : devoted to molecular & cellular mechanisms* 20(1): 1–10. <http://www.ncbi.nlm.nih.gov/pubmed/25307957> (December 4, 2019).
- Shin, Min Hwa et al. 2016. “A RUNX2-Mediated Epigenetic Regulation of the Survival of P53 Defective Cancer Cells.” *PLoS genetics* 12(2): e1005884. <http://www.ncbi.nlm.nih.gov/pubmed/26925584> (December 4, 2019).
- Shipman, Seth L., Jeff Nivala, Jeffrey D. Macklis, and George M. Church. 2017. “CRISPR-Cas Encoding of a Digital Movie into the Genomes of a Population of Living Bacteria.” *Nature* 547(7663): 345–49.
- Shmakov, Sergey et al. 2015. “Discovery and Functional Characterization of Diverse Class 2 CRISPR-Cas Systems.” *Molecular Cell* 60(3): 385–97.
- . 2017. “Diversity and Evolution of Class 2 CRISPR-Cas Systems.” *Nature Reviews Microbiology* 15(3): 169–82.
- Shrivastav, Meena, Leyma P. De Haro, and Jac A. Nickoloff. 2008. “Regulation of DNA Double-Strand Break Repair Pathway Choice.” *Cell Research* 18(1): 134–47.
- Sibilio, Leonardo et al. 2008. “A Single Bottleneck in HLA-C Assembly.” *The Journal of biological chemistry* 283(3): 1267–74. <http://www.ncbi.nlm.nih.gov/pubmed/17956861> (December 4, 2019).
- Singleton, B. K. et al. 1999. “The C Terminus of Ku80 Activates the DNA-Dependent Protein Kinase Catalytic Subunit.” *Molecular and Cellular Biology* 19(5): 3267–77.
- Smith, J et al. 2000. “Requirements for Double-Strand Cleavage by Chimeric Restriction Enzymes with Zinc Finger DNA-Recognition Domains.” *Nucleic acids research* 28(17): 3361–69. <http://www.ncbi.nlm.nih.gov/pubmed/10954606> (December 4, 2019).
- Smits, Arne H. et al. 2019. “Biological Plasticity Rescues Target Activity in CRISPR Knock Outs.” *Nature Methods* 16(11): 1087–93.
- Snary, D., C. J. Barnstable, W. F. Bodmer, and M. J. Crumpton. 1977. “Molecular Structure of Human Histocompatibility Antigens: The HLA-C Series.” *European Journal of Immunology* 7(8): 580–85.
- De Strooper, Bart. 2003. “Aph-1, Pen-2, and Nicastrin with Presenilin Generate

- an Active γ -Secretase Complex.” *Neuron* 38(1): 9–12.
- Swarts, Daan C, John van der Oost, and Martin Jinek. 2017. “Structural Basis for Guide RNA Processing and Seed-Dependent DNA Targeting by CRISPR-Cas12a.” *Molecular cell* 66(2): 221-233.e4.
<http://www.ncbi.nlm.nih.gov/pubmed/28431230> (December 4, 2019).
- Tang, Yan-Dong et al. 2017. “CRISPR/Cas9-Mediated Multiple Single Guide RNAs Potently Abrogate Pseudorabies Virus Replication.” *Archives of virology* 162(12): 3881–86. <http://www.ncbi.nlm.nih.gov/pubmed/28900740> (December 4, 2019).
- Thathiah, Amantha et al. 2009. “The Orphan G Protein-Coupled Receptor 3 Modulates Amyloid-Beta Peptide Generation in Neurons.” *Science (New York, N.Y.)* 323(5916): 946–51.
<http://www.ncbi.nlm.nih.gov/pubmed/19213921> (December 4, 2019).
- . 2013. “ β -Arrestin 2 Regulates A β Generation and γ -Secretase Activity in Alzheimer’s Disease.” *Nature medicine* 19(1): 43–49.
<http://www.ncbi.nlm.nih.gov/pubmed/23202293> (December 4, 2019).
- Tikka, Saara et al. 2016. “Proteomic Profiling in the Brain of CLN1 Disease Model Reveals Affected Functional Modules.” *Neuromolecular medicine* 18(1): 109–33. <http://www.ncbi.nlm.nih.gov/pubmed/26707855> (December 4, 2019).
- Traynelis, Stephen F. et al. 2010. “Glutamate Receptor Ion Channels: Structure, Regulation, and Function.” *Pharmacological Reviews* 62(3): 405–96.
- Tsai, Shengdar Q. et al. 2017. “CIRCLE-Seq Supplementary Protocol.” *Nature Methods* 14(6): 607–14.
- Tsai, Shengdar Q., and J. Keith Joung. 2016. “Defining and Improving the Genome-Wide Specificities of CRISPR-Cas9 Nucleases.” *Nature Reviews Genetics* 17(5): 300–312.
- Tsao, H, X Zhang, E Benoit, and F G Haluska. 1998. “Identification of PTEN/MMAC1 Alterations in Uncultured Melanomas and Melanoma Cell Lines.” *Oncogene* 16(26): 3397–3402.
<http://www.ncbi.nlm.nih.gov/pubmed/9692547> (December 4, 2019).
- Turner, S et al. 1998. “Sequence-Based Typing Provides a New Look at HLA-C

- Diversity.” *Journal of immunology (Baltimore, Md. : 1950)* 161(3): 1406–13.
<http://www.ncbi.nlm.nih.gov/pubmed/9686604> (December 4, 2019).
- Ueda, Shuhei et al. 2016. “Anti-HIV-1 Potency of the CRISPR/Cas9 System Insufficient to Fully Inhibit Viral Replication.” *Microbiology and Immunology* 60(7): 483–96.
- Um, Ji Won et al. 2013. “Metabotropic Glutamate Receptor 5 Is a Coreceptor for Alzheimer A β Oligomer Bound to Cellular Prion Protein.” *Neuron* 79(5): 887–902.
- “UNAIDS Data 2018 | UNAIDS.”
<https://www.unaids.org/en/resources/documents/2018/unaids-data-2018>
 (December 4, 2019).
- Valenti, Maria Teresa. 2015. “Mesenchymal Stem Cells: A New Diagnostic Tool?” *World Journal of Stem Cells* 7(5): 789.
- Valera, María Soledad et al. 2015. “The HDAC6/APOBEC3G Complex Regulates HIV-1 Infectiveness by Inducing Vif Autophagic Degradation.” *Retrovirology* 12(1).
- Verkruyse, Linda A., and Sandra L. Hofmann. 1996. “Lysosomal Targeting of Palmitoyl-Protein Thioesterase.” *Journal of Biological Chemistry* 271(26): 15831–36.
- Vesa, Jouni et al. 1995. “Mutations in the Palmitoyl Protein Thioesterase Gene Causing Infantile Neuronal Ceroid Lipofuscinosis.” *Nature* 376(6541): 584–87.
- Vezzalini, Marzia et al. 2017. “A New Monoclonal Antibody Detects Downregulation of Protein Tyrosine Phosphatase Receptor Type γ in Chronic Myeloid Leukemia Patients.” *Journal of hematology & oncology* 10(1): 129. <http://www.ncbi.nlm.nih.gov/pubmed/28637510> (December 4, 2019).
- Wah, David A., Jurate Bitinaite, Ira Schildkraut, and Aneel K. Aggarwal. 1998. “Structure of FokI Has Implications for DNA Cleavage.” *Proceedings of the National Academy of Sciences of the United States of America* 95(18): 10564–69.
- Waldron, Richard T et al. 2012. “Differential PKC-Dependent and -Independent

- PKD Activation by G Protein α Subunits of the Gq Family: Selective Stimulation of PKD Ser⁷⁴⁸ Autophosphorylation by G α q.” *Cellular signalling* 24(4): 914–21. <http://www.ncbi.nlm.nih.gov/pubmed/22227248> (December 4, 2019).
- Wang, Gang, Na Zhao, Ben Berkhout, and Atze T Das. 2016. “CRISPR-Cas9 Can Inhibit HIV-1 Replication but NHEJ Repair Facilitates Virus Escape.” *Molecular therapy : the journal of the American Society of Gene Therapy* 24(3): 522–26. <http://www.ncbi.nlm.nih.gov/pubmed/26796669> (December 4, 2019).
- Wang, Peirong et al. 2011. “A Two-Dimensional Protein Fragmentation-Proteomic Study of Neuronal Ceroid Lipofuscinoses: Identification and Characterization of Differentially Expressed Proteins.” *Journal of chromatography. B, Analytical technologies in the biomedical and life sciences* 879(5–6): 304–16. <http://www.ncbi.nlm.nih.gov/pubmed/21242110> (December 4, 2019).
- Wang, Weiming et al. 2014. “CCR5 Gene Disruption via Lentiviral Vectors Expressing Cas9 and Single Guided RNA Renders Cells Resistant to HIV-1 Infection.” *PloS one* 9(12): e115987. <http://www.ncbi.nlm.nih.gov/pubmed/25541967> (December 4, 2019).
- Wang, Zhenghe et al. 2004. “Mutational Analysis of the Tyrosine Phosphatome in Colorectal Cancers.” *Science* 304(5674): 1164–66.
- Watanabe, H et al. 1997. “A Novel Acyl-CoA Thioesterase Enhances Its Enzymatic Activity by Direct Binding with HIV Nef.” *Biochemical and biophysical research communications* 238(1): 234–39. <http://www.ncbi.nlm.nih.gov/pubmed/9299485> (December 4, 2019).
- “WHO | Skin Cancers.” 2017. *WHO*.
- Wilkie, Thomas M. et al. 1991. “Characterization of G-Protein α Subunits in the Gq Class: Expression in Murine Tissues and in Stromal and Hematopoietic Cell Lines.” *Proceedings of the National Academy of Sciences of the United States of America* 88(22): 10049–53.
- Wilquet, Valérie, and Bart De Strooper. 2004. “Amyloid-Beta Precursor Protein Processing in Neurodegeneration.” *Current Opinion in Neurobiology* 14(5):

582–88.

- Wu, Dong-Mei et al. 2018. “MircoRNA-1275 Promotes Proliferation, Invasion and Migration of Glioma Cells via SERPINE1.” *Journal of cellular and molecular medicine* 22(10): 4963–74.
<http://www.ncbi.nlm.nih.gov/pubmed/30024092> (December 4, 2019).
- Wu, Eddy H T, Rico K H Lo, and Yung H Wong. 2003. “Regulation of STAT3 Activity by G16-Coupled Receptors.” *Biochemical and biophysical research communications* 303(3): 920–25.
<http://www.ncbi.nlm.nih.gov/pubmed/12670499> (December 4, 2019).
- Wu, Zhijian, Hongyan Yang, and Peter Colosi. 2010. “Effect of Genome Size on AAV Vector Packaging.” *Molecular therapy : the journal of the American Society of Gene Therapy* 18(1): 80–86.
<http://www.ncbi.nlm.nih.gov/pubmed/19904234> (December 4, 2019).
- Wysokinski, Daniel, Janusz Blasiak, and Elzbieta Pawlowska. 2015. “Role of RUNX2 in Breast Carcinogenesis.” *International Journal of Molecular Sciences* 16(9): 20969–93.
- Xu, Lei et al. 2019. “CRISPR-Edited Stem Cells in a Patient with HIV and Acute Lymphocytic Leukemia.” *New England Journal of Medicine* 381(13): 1240–47. <http://www.nejm.org/doi/10.1056/NEJMoa1817426> (December 5, 2019).
- Xue, Wen et al. 2014. “CRISPR-Mediated Direct Mutation of Cancer Genes in the Mouse Liver.” *Nature* 514(7522): 380–84.
- Yamano, Takashi et al. 2016. “Crystal Structure of Cpf1 in Complex with Guide RNA and Target DNA.” *Cell* 165(4): 949–62.
- Yang, Diane et al. 2016. “Enrichment of G2/M Cell Cycle Phase in Hipsocs Supplementary.” *Scientific Reports* 6: 21264.
<http://www.ncbi.nlm.nih.gov/pubmed/26887909> (December 4, 2019).
- Yang, Hui et al. 2013. “One-Step Generation of Mice Carrying Reporter and Conditional Alleles by CRISPR/Cas-Mediated Genome Engineering.” *Cell* 154(6): 1370–79. <http://www.ncbi.nlm.nih.gov/pubmed/23992847> (December 4, 2019).
- Yang, Meijia et al. 2017. “Targeted Disruption of V600E-Mutant BRAF Gene by CRISPR-Cpf1.” *Molecular therapy. Nucleic acids* 8: 450–58.

- <http://www.ncbi.nlm.nih.gov/pubmed/28918044> (December 4, 2019).
- Yin, Chaoran et al. 2017. "In Vivo Excision of HIV-1 Provirus by SaCas9 and Multiplex Single-Guide RNAs in Animal Models." *Molecular therapy : the journal of the American Society of Gene Therapy* 25(5): 1168–86.
<http://www.ncbi.nlm.nih.gov/pubmed/28366764> (December 4, 2019).
- Zelensky, Alex N et al. 2017. "Inactivation of Pol θ and C-NHEJ Eliminates off-Target Integration of Exogenous DNA." *Nature communications* 8(1): 66.
<http://www.ncbi.nlm.nih.gov/pubmed/28687761> (December 4, 2019).
- Zetsche, Bernd et al. 2015. "Cpf1 Is a Single RNA-Guided Endonuclease of a Class 2 CRISPR-Cas System." *Cell* 163(3): 759–71.
- Zetsche, Bernd, Sara E Volz, and Feng Zhang. 2015. "A Split-Cas9 Architecture for Inducible Genome Editing and Transcription Modulation." *Nature biotechnology* 33(2): 139–42.
<http://www.ncbi.nlm.nih.gov/pubmed/25643054> (December 4, 2019).
- Zhang, Qiang et al. 2018. "Potential High-Frequency off-Target Mutagenesis Induced by CRISPR/Cas9 in Arabidopsis and Its Prevention." *Plant Molecular Biology* 96(4–5): 445–56.
- Zhang, Xiao Hui et al. 2015. "Off-Target Effects in CRISPR/Cas9-Mediated Genome Engineering." *Molecular Therapy - Nucleic Acids* 4(11): e264.
- Zhang, Yu et al. 2017. "CRISPR-Cpf1 Correction of Muscular Dystrophy Mutations in Human Cardiomyocytes and Mice." *Science advances* 3(4): e1602814. <http://www.ncbi.nlm.nih.gov/pubmed/28439558> (December 4, 2019).
- Zhao, Tiejun. 2016. "The Role of HBZ in HTLV-1-Induced Oncogenesis." *Viruses* 8(2).
- Zhu, Weijun et al. 2015. "The CRISPR/Cas9 System Inactivates Latent HIV-1 Proviral DNA." *Retrovirology* 12(1).
- Zipeto, Donato et al. 2018. "HIV-1-Associated Neurocognitive Disorders: Is HLA-C Binding Stability to B2-Microglobulin a Missing Piece of the Pathogenetic Puzzle?" *Frontiers in neurology* 9: 791.
<http://www.ncbi.nlm.nih.gov/pubmed/30298049> (December 4, 2019).
- Zuo, Erwei et al. 2017. "One-Step Generation of Complete Gene Knockout Mice

and Monkeys by CRISPR/Cas9-Mediated Gene Editing with Multiple SgRNAs.” *Cell research* 27(7): 933–45.

<http://www.ncbi.nlm.nih.gov/pubmed/28585534> (December 4, 2019).

ACKNOWLEDGEMENTS

First of all, I would like to thank my mentor Prof. Donato Zipeto who welcomed me in his lab, following me during my Ph.D., giving me precious advice, and encouraged me to face new challenges.

I also thank my co-tutor Prof. Maria Grazia Romanelli, who always helped me to tackle the difficulties encountered during my Ph.D.

I thank Prof. Agustin Valenzuela-Fernandez, from the University of La Laguna, who hosted me in his lab for my Ph.D. mobility program and all his group.

I thank all our collaborators, without whom all this would not have been possible: Dr. Maria Teresa Valenti (University of Verona) and Dr. Giulio Innamorati (University of Verona) that allowed me to develop edited melanoma and adenopancreatic cell lines, Prof. Mario Buffelli (University of Verona) and Prof. Claudio Sorio (University of Verona) that let me generate AD and CML engineered cell models, Prof. Alessandro Simonati and his collaborator Dr. Francesco Pezzini (University of Verona) who allowed me to develop CLN manipulated cells.

Last but not least, I thank Massimiliano who always supported me and all my family that has always spurred me to move forward.

I would also like to thank those who are no longer with me and those who, instead, entered my life during this journey.

ATTACHMENTS



IHV2019
INSTITUTE OF
HUMAN VIROLOGY

**Progress In HIV/AIDS:
Challenges In 2020**

Poster Abstracts

CONTENTS
EVENTS SCHEDULE
SPEAKER INDEX
ABSTRACT INDEX
POSTER INDEX

PA-104

A Meta-Analysis of Neurometabolite Changes Associated with HIV Infection

Lydia Chelala, Erin O'Connor, Peter Barker and Thomas Zeffiro, Laboratory of Translational Neuroradiology, University of Maryland Medical Center, Baltimore, MD

Introduction: HIV infection can adversely affect performance in cognitive and motor domains, possibly related to early involvement of basal ganglia nuclei or their axonal connections. Numerous studies have used magnetic resonance spectroscopy (MRS) to measure HIV effects on basal ganglia metabolite levels. While many have reported changes in N-acetyl aspartate (NAA), Choline (Cho), Myo-inositol (MI), and Creatine (Cr) following HIV infection, quantitative inconsistencies observed across studies are substantial. To investigate the potential clinical utility of using MRS in measuring HIV disease effects, we evaluated the consistency and temporal stability of serostatus effects on brain metabolic measures, including NAA, Cho, MI, and Cr.

Methods: The meta-analysis sample included cross-sectional studies between 1993 – 2019 reporting HIV infection effects on cortical and subcortical metabolites. Because structural and functional changes have been repeatedly reported in the basal ganglia, NAA/Cr (21 papers), Cho/Cr (21 papers) and MI/Cr (17 papers) ratios were a focus of the analysis. Random effects meta-analysis using inverse variance weighting and bias corrected Cohen's d standardized mean differences (SMD) was used to estimate individual study SMDs and study heterogeneity. Meta-regression was used to examine effects of study publication year and data acquisition techniques.

Results: Meta-analysis revealed basal ganglia SMDs related to serostatus of -0.088 (NS) for NAA/Cr, 0.31 (p<0.01) for Cho/Cr and 0.63 (p<0.01) for MI/Cr. Similar, but somewhat stronger effects, were observed in gray and white matter. Nevertheless, estimates of between study heterogeneity suggested that the majority of the observed variance was between studies. Many studies pooled participants with varying durations of treatment, disease duration and comorbidities. Image acquisition methods changed with time.

Conclusions: While published studies of HIV effects on brain metabolites exhibit substantial variations that may result from measurement technique variations or changes in HIV treatment practice over the study period, quantitative metabolic measures showing decreased NAA/Cr, increased Cho/Cr and increased MI/Cr are consistent and can reliably detect the effects of HIV infection during treatment, serving as practical biomarkers.

PB-101

Involvement of HLA-C binding stability to β2-microglobulin in HIV-1 infection

Simona Mutascio, PhD student, University of Verona; **Francesca Parolini, PhD,** University of Verona; **Chiara Stefani, PhD student,** University of Verona; **Stefania Fochi, PhD,** University of Verona; **Donato Zipeto, MSc,** University of Verona; **Maria Grazia Romanelli, MSc,** University of Verona

MHC-I is a heterotrimeric complex composed by HLA/β2-microglobulin/peptide. HLA-C binding to β2-microglobulin is weaker compared to HLA-A and -B. The HLA-C gene encodes different allotypes classified in stable and unstable clusters based on their binding stability to β2-microglobulin. Unstable HLA-C molecules release more β2-microglobulin than stable variants. The ratio of complete heterotrimers and HLA-C free chains at the cell surface is involved in controlling HIV-1 infection. We recently reported that HIV-1 Env associates with HLA-C during viral budding, increasing viral infectivity and spreading.

We aimed to address how the binding stability of different HLA-C allotypes to β2-microglobulin influences HIV-1 infectivity. We showed that HIV-1 virions produced in PBMCs with unstable HLA-C variants are more infectious than those produced in PBMCs with stable ones. To deeply investigate the role of each HLA-C variant in HIV-1 infection modulation, 293T HLA-C-/- packaging cells were developed using CRISPR/Cas9. The different HLA-C alleles were then restored, developing cell lines expressing specific HLA-C allotypes. To analyse the binding stability to β2-microglobulin of each HLA-C variant, an acid wash treatment will be performed to assign a binding stability score ranking. Moreover, to investigate how HLA-C variants modulate HIV-1 infectivity, the homozygous HLA-C cells will be employed to produce HIV-1 pseudotyped viruses to evaluate their infectivity through a luciferase infectivity assay.

This study will allow us to stratify the HLA-C alleles according to their binding stability to β2-microglobulin. Furthermore, these analyses will be fundamental to clarify the relationship among HLA-C allotypes binding stability and HIV-1 infection progression.



Simona Mutascio received a Master of Science in Cellular and Molecular Biology in 2015 at the University of Rome Tor Vergata, Italy. In 2016 she started her Ph.D in Applied Life and Health Sciences at the University of Verona, Italy, in the molecular biology laboratory directed by Prof. Donato Zipeto. Her Ph.D. thesis project is focused on the development of new cell models using CRISPR/Cas9, to study the modulation of HIV-1 infectivity.

IHV , 4 – 5 October, 2019 Baltimore (USA)

Progress in HIV/AIDS: challenges in 2020

ABSTRACT BOOK



SESSION 8 - INFECTION & IMMUNITY AND VACCINOLOGY

OC 46 HIV-1 and HLA-C relationship: a matter of stability

D. Zipeto¹, S. Mutascio¹, C. Stefani¹, M. Serena¹, F. Parolini¹, S. Fochi¹, M.G. Romanelli¹, D. Gibellini²

¹Department of Neuroscience, Biomedicine and Movement Sciences and ²Department of Diagnostics and Public Health, School of Medicine, University of Verona, Italy

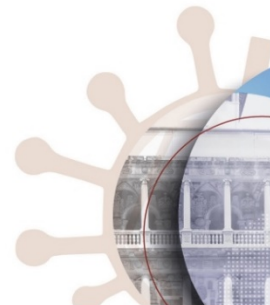
HLA-C requires β 2-microglobulin (β 2m) for proper folding and cell surface expression. The HLA-C gene is highly polymorphic, encoding different allotypes classified in stable and unstable clusters, based on their binding stability to β 2m. Unstable HLA-C molecules release more β 2m than stable variants, generating more HLA-C free chains on the cell surface. HLA-C plays an important role in modulating HIV-1 infection. It has been reported that a higher HLA-C expression is associated with better HIV-1 infection control, while its lower expression leads to a rapid progression toward AIDS. Highly and lowly expressed HLA-C alleles have been defined as protective and non-protective, respectively, in relation to HIV-1 disease progression.

Differently, in our previous studies, we reported that HIV-1 virions lacking HLA-C have reduced infectivity and increased susceptibility to neutralizing antibodies. The reasons behind this apparent contradiction were explained by our recent findings showing that HIV-1 Env interacts with HLA-C free-chains, after their dissociation from β 2m, and that protective HLA-C alleles bind β 2m more efficiently ("stable" variants), compared to non-protective alleles presenting more free chains on the cell surface ("unstable" variants). It is known that patients affected by AIDS Dementia Complex (ADC), a very severe neurological condition of HIV-1 infection, present high level of β 2m in the cerebrospinal fluid.

We propose that the outcome of HIV-1 infection might be driven both by HLA-C surface expression levels and by HLA-C/ β 2m binding stability. According to this model, the expression of unstable variants leads to a higher β 2m shedding and to a reduction of immunocompetent HLA-C complexes expressed on the cell surface. Consequently, the increase of HLA-C free chains raises viral infectivity contributing to a rapid progression toward AIDS. This model was supported by our recent findings showing that unstable HLA-C variants are more frequently associated with the development of ADC in HIV-1 infected patients.

To further investigate the contribution of HLA-C variants in HIV-1 infection, we used CRISPR/Cas9 to develop an HLA-C KO human cell line. The different HLA-C alleles have been then restored by transfection, generating cell lines expressing each a specific HLA-C allotype. To assign a binding stability score to each HLA-C variant, an acid wash treatment will be performed to study the kinetic of β 2m detachment. Furthermore, to evaluate the HIV-1 infectivity modulation, each HLA-C expressing cell line will be employed to produce HIV-1 pseudotyped viruses to be tested in infectivity assays.

This study will allow us to stratify HLA-C alleles according to their binding stability to β 2m and to clarify the relationship between HLA-C allotypes binding stability, HIV-1 infection progression and HIV-1 related neurocognitive disorders onset.



10 – 12 September, 2019 Padua (Italy).

SIV Italian Society for Virology Congress

replicated in both cell types. Further, an HCV-specific protease inhibitor, telaprevir, inhibited infection in both cell types. Emergence of unique HCV variants and release of HCV RNA-reactive particles with biophysical properties different from virions in plasma inoculants suggested that distinct viral particles were assembled. These results are consistent with our previous demonstration of HCV replication in CD4⁺ and CD8⁺ T cells in patients with chronic hepatitis C and asymptomatic (occult) infection. Infection of T cells, which are central to the adaptive antiviral responses, can directly affect HCV clearance, favor virus persistence and influence progression to chronic hepatitis.

Biography

Dr. Thomas Michalak is the Honorary and University Research Professor at Memorial University (MUN), St. John's, Canada. He is a former Professor of Molecular Virology and Medicine (Hepatology) and the Senior Canada Research Chair in Viral Hepatitis/ Immunology at the Faculty of Medicine, MUN. He is a fellow of the Canadian Academy of Health Sciences and the American Association for the Study of Liver Diseases, and recipient of the Queen Elizabeth II Diamond Jubilee Medal for contributions to medical science. He has widely published on immunopathogenesis of liver diseases and lymphotropism of hepatitis B and C viruses. He significantly contributed to discovery and characterization of asymptomatic (occult) HBV and HCV infections.

HLA-C and HIV-1: A Matter of Stability

Donato Zipeto^{1*}, Simona Mutascio¹, Chiara Stefani¹, Michela Serena¹, Francesca Parolini¹, Stefania Fochi¹, Davide Gibellini² and Maria Grazia Romanelli¹

¹Department of Neuroscience, Biomedicine and Movement Sciences, University of Verona, Italy

²Department of Diagnostics and Public Health, School of Medicine, University of Verona, Italy

Abstract

HLA-C requires β 2-microglobulin (β 2m) for proper folding and cell surface expression. However, this association is quite weak, thus generating HLA-C free chains. HLA-C plays an important role in modulating HIV-1 infection. It has been reported that a higher HLA-C expression is associated with better HIV-1 infection control, while its lower expression leads to a rapid progression toward AIDS. Highly and lowly expressed HLA-C alleles have been defined as protective and non-protective, respectively, in relation to HIV disease progression. Differently, in our previous studies, we reported that HIV-1 virions lacking HLA-C have reduced infectivity and increased susceptibility to neutralizing antibodies. The reasons behind this apparent contradiction were explained by our recent findings showing that HIV-1 Env interacts with HLA-C free-chains, following their dissociation from β 2m, and that protective HLA-C alleles bind β 2m more efficiently ("stable" variants), compared to non-protective alleles that present more free chains on the cell surface ("unstable" variants).

We propose that the outcome of HIV-1 infection might be driven both by HLA-C surface expression levels and by HLA-C/ β 2m binding stability. According to this model, the expression of unstable variants leads to a higher β 2m shedding and to a reduction of immunocompetent HLA-C complexes expressed on the cell surface. Consequently, the increase of HLA-C free chains raises viral infectivity contributing to a rapid progression toward AIDS. This model was supported by our recent findings showing that unstable HLA-C variants are more frequently associated with development of AIDS dementia complex in HIV-1 infected patients.

Biography

Dr. Donato Zipeto is a Molecular Biologist working at the University of Verona (Italy) since 2002, where he teaches Molecular Biology, Zoonosis and Emerging Viruses, Basics in Virology and Gene Therapy. He graduated in Biology in 1989 at the University of Pavia (Italy), and worked previously as Research Fellow in the Center for AIDS Research, Stanford University Medical Center (USA) and in the Viral Immunology Unit, Pasteur Institute, Paris (France). He studies the interactions between host and viruses, in particular HCMV, HTLV and HIV.

Antibody Repertoire Sequencing of Cancer Patients Reveals Potent and Broadly Applicable Anti-Tumor Antibodies

Alexander Scholz
Atreca, Inc., CA, USA

Abstract

Cancer patients, that respond to checkpoint inhibitor therapy, are thought to mount an active immune response against their

1-3 July, 2019 San Francisco (California, USA)

International Conference on Immunity and Immunochemistry

Poster presentation + Flash presentation

P.21

TRAF3 involvement in the NF- κ B pathway deregulation mediated by HTLV-1 Tax protein

Simona Mutascio, S. Fochi, P. Lorenzi, M. Galasso, D. Zipeto, M.G. Romanelli
Dept of Neurosciences, Biomedicine and Movement Sciences, Univ. of Verona, Verona, Italy

The retrovirus human T-lymphotropic virus type 1 (HTLV-1) is the causative agent of adult T-cell leukemia (ATL). The viral genome encodes two main regulatory proteins involved in the cell transformation, Tax and HTLV-1 basic zipper protein (HBZ). Tax is crucial for CD4⁺ T-cell transformation by constitutively activating both the classical and alternative NF- κ B pathways that play a primary role in inflammation, cell survival and cancer. HBZ is essential for viral persistence and T-cell proliferation contributing to ATL development. HTLV-2 is genetically related to HTLV-1 and is not associated with ATL. Comparative studies of Tax-1 and HBZ and HTLV-2 homologous regulatory proteins, Tax-2 and APH-2, are useful to understand the HTLVs pathobiology. The aim of this study is to investigate the role of TRAF3 in the deregulation NF- κ B activation mediated by Tax and HBZ. TNF-receptor associated factor 3 (TRAF3) is a negative regulator of the alternative NF- κ B pathway that we have previously demonstrated to interact with Tax. To analyze the contribution of TRAF3 in the Tax-induced deregulation of NF- κ B, we generated TRAF3^{-/-} cell line using the CRISPR/Cas9 technique. By co-immunoprecipitation and confocal microscopy analyses, we showed that TRAF3 interacts with Tax and APH-2 in the cytoplasm. Performing luciferase assay, we found that TRAF3^{-/-} cells show activation of the NF- κ B promoter. Western blot analyses revealed that the processing of p100 is detected in the absence of TRAF3, indicating the activation of the alternative NF- κ B pathway. Furthermore, analyzing the localization of the transcription factor p65, we found that p65 is more represented in the nucleus of TRAF3^{-/-} cells, than in the parental line. Moreover, the results indicate that the activation of the NF- κ B promoter mediated by Tax-1 is dramatically reduced in the absence of TRAF3. Further analyses will be performed to study the effects of the antisense HBZ and APH-2 proteins on NF- κ B promoter activity in TRAF3^{-/-} cells.

SIBBM 2018 • 20-22 June 2018 • Rome, Italy

20-22 June, 2018 Rome (Italy)

SIBBM 2018

Monday 24 July
Tuesday 25 July Poster Exhibition
Wednesday 26 July
Late Breaker Abstracts
Author Index

production were significantly augmented in HESN compared to HC. Interestingly, IL-21 upregulation correlated with a significantly increased expression of miR29a, b, c and reduced susceptibility to in vitro HIV-1 infection in HESN alone.
Conclusions: The IL-21-miR-29 axis is upregulated by HIV infection in HESN; this axis could play an important role in the natural resistance to HIV-infection seen in HESN. Approaches that exogenously increase IL-21 production or prompt pre-existing cellular IL-21 reservoir could confine the magnitude of the early HIV-1-infection.

TUPEA0156

Immune signatures linked with HIV-1 neutralization breadth

C. Kadelka^{1,2}, T. Liechti¹, H. Ebner¹, P. Ruser¹, R. Kouyou², H. Günthard², A. Trkola¹, The Swiss HIV Cohort Study
¹University of Zurich, Institute of Medical Virology, Zurich, Switzerland, ²University Hospital Zurich, Division of Infectious Diseases and Hospital Epidemiology, Zurich, Switzerland
Presenting author email: kadelka.claus@virology.uzh.ch

Background: The factors that drive broadly neutralizing antibodies (bnAbs) development in natural infection are still poorly understood. In the Swiss 4.5K Screen, a systematic survey of bnAb activity in 4,484 HIV-1 infected individuals (Ruser, Kouyou Nat Med 2016), we identified 239 bnAb inducers, and showed that viral load, infection length, viral diversity, and black ethnicity were positively and independently associated with bnAb development. We recently found several HIV-1 antibody binding profiles predictive of neutralization breadth (Kadelka CROI 2017). Here, we compare the parameters associated with binding activity with those associated with bnAb activity, and report on improved predictors of neutralization breadth.

Methods: Using an in-house established Luminex bead assay, we probed 4,283 plasma samples included in the Swiss 4.5K Screen for binding antibodies of IgG subclasses 1, 2 and 3 against 13 HIV-1 proteins and peptides encompassing Gag (p17, p24) and Env. Multivariable regression models were used to detect associations. Predictive power was measured using the area under the ROC-curve (AUC).

Results: Viral load differentially steered responses to HIV-1 antigens affecting both the magnitude of the response and the IgG subclass diversification; high viral load was linked with low binding titers of IgG1 p17&p24, and IgG3 gp41 (each $p < 10^{-9}$), but also with high binding titers of IgG1 gp41 ($p < 10^{-7}$) and IgG2 gp120 ($p = 0.01-10^{-10}$). Viral diversity was positively associated with gp120 responses, particularly strongly with IgG1 BG505 trimer ($p < 10^{-7}$). Interestingly, diversity had no influence on Gag and gp41, both of which have lower genetic variability than gp120. Infection length was in contrast linked with high IgG1 binding titers across diverse antigens highlighting that breadth development requires time. Independent from viral subtype, black ethnicity was associated with high IgG1 BG505 trimer responses ($p < 10^{-2}$) and IgG1 BG505 trimer responses were most predictive of neutralization breadth (AUC=0.85). Advanced prediction models based on multiple binding responses and patient characteristics provided even better bnAb prediction.

Conclusions: Previously identified independent drivers of bnAb activity proved to be associated with distinctive HIV-1 binding antibody immune signatures. Importantly, binding antibody responses to the BG505 trimer reliably predict neutralization breadth, providing a valuable assessment tool of forthcoming vaccine efficacy trials.

TUPEA0157

Preservation of lymphopoietic potential and virus suppressive capacity by CD8+ T cells in HIV-2-infected controllers

M. Angin¹, G. Wong^{2,3}, L. Papagno⁴, P. Versmissen⁵, A. David¹, C. Bayard², B. Charmeteau-De Muylder^{4,5}, A. Besseghir⁶, R. Thiebaut⁶, F. Boufassa⁷, G. Pancino⁸, D. Sauce⁹, O. Lambotte⁶, F. Brun-Vézinet⁸, S. Matheron¹⁰, S.L. Rowland-Jones³, R. Cheyner^{4,5}, A. Saez-Cirion¹, V. Appay¹, ANRS CO5 IMMUNOVR-2 Study Group

¹Institut Pasteur, Unité HIV Inflammation et Persistance, Paris, France, ²Sorbonne Universités, UPMC Université Paris 06, DHU FAST, CR7, Centre d'Immunologie et des Maladies Infectieuses (CIMI-Paris), INSERM U 1135, Paris, France, ³Nuffield Department of Medicine, Oxford, United Kingdom, ⁴INSERM U 1016, Institut Cochin, Equipe 'Cytokines and Viral Infections', Paris, France, ⁵CNRS UMR 8104, Université Paris Descartes, Sorbonne Paris Cité, Paris, France, ⁶CMG de l'INSERM U 1219, VIH, Hépatites Virales et Comorbidités: Épidémiologie Clinique et Santé Publique, Bordeaux, France, ⁷INSERM U 1018, Centre de Recherche en Épidémiologie et Santé des Populations, Université Paris Sud, Le Kremlin Bicêtre, France, ⁸INSERM UMR 1184, Immunologie des Maladies Virales et Autoimmunes (IMVA), Assistance Publique-Hôpitaux de Paris, Service de Médecine Interne, Hôpitaux Universitaires, Université Paris Sud, Le Kremlin Bicêtre, France, ⁹AP-HP, Laboratoire de Virologie, Hôpital Bichat, Paris, France, ¹⁰INSERM UMR 1137, Infections, Antimicrobiens, Modélisation, Evolution (IAME), Université Paris Diderot, Sorbonne Paris Cité, AP-HP, Service des Maladies Infectieuses et Tropicales, Hôpital Bichat, Paris, France
Presenting author email: mangin@pasteur.fr

Background: Compared with HIV-1, HIV-2 infection is characterized by a larger proportion of slow or non-progressors. A better understanding of HIV-2 pathogenesis should open new therapeutic avenues to establish control of HIV-1 replication in infected patients.

Methods: In this study, we performed a fine characterization of HIV-2-specific CD8+ T cells in HIV-2 infected controllers from the French ANRS CO5 HIV-2 cohort, taking in consideration CD8+T-cell production capacity, the phenotype of HIV-2 tetramer positive cells and HIV-2 suppressive capacity.

Results: HIV-2 controllers display a robust capacity to support long-term renewal of the CD8+ T-cell compartment by preserving immune resources, including hematopoietic progenitors and thymic activity, which could contribute to the long-term maintenance of the CD8+ T cell response and the avoidance of premature immune aging. Our data support the presence of HIV-2 Gag-specific CD8+ T cells that display an early memory differentiation phenotype and robust effector potential in HIV-2 controllers. We show for the first time to our knowledge that HIV-2 controllers possess also CD8+ T cells that show an unusually strong capacity to suppress HIV-2 infection in autologous CD4+ T cells ex vivo. The HIV-2 suppressive capacity of CD8+ T cells correlated with patient CD4+ T cell counts, supporting a role of these cells to limit disease progression.

Conclusions: Our data suggest that the effective and durable control in HIV-2 infected individuals probably participates in a virtuous circle, during which controlled viral replication permits the preservation of immune functions, including potent HIV-2-specific CD8+ T cells, thus preventing HIV-2 disease progression.

TUPEA0158

HLA-C expression levels and binding stability to β_2m modulate HIV-1 infectivity

F. Parolini¹, P. Biswas², M. Serena³, F. Sironi², S. Mutascio¹, V. Muraro⁴, E. Guizzardi⁵, M. Malnati², A. Beretta², M.G. Romanelli¹, D. Zepeto¹
¹Università degli Studi di Verona, Neurosciences, Biomedicine and Movement Sciences, Verona, Italy, ²IRCCS Ospedale San Raffaele, Milan, Italy, ³University of Oxford, Oxford, United Kingdom, ⁴Service of Transfusion Medicine, AOUI Verona, Verona, Italy
Presenting author email: francesca.parolini@univr.it

Background: HLA-C expression levels lead to different HIV-1 infection outcomes. A higher expression is associated with a better activation of cytotoxic T lymphocytes (CTLs) and thus a better HIV-1 infection control. Vice versa, a lower HLA-C expression leads to a rapid progression toward AIDS. Thus, HLA-C highly and lowly expressed alleles are defined as protective and non-protective, respectively. Furthermore, different HLA-C alleles have different binding stabilities to β_2m microglobulin (β_2m). Interestingly, HLA-C protective alleles are also those that bind β_2m more efficiently, while the non-protective variants present more free chains (not bound to β_2m) on the cell surface. It is also known that virions lacking HLA-C have reduced infectivity and increased susceptibility to neutralizing antibodies.

Methods: The A3.01 cell line and its HIV-1-infected counterpart ACH-2 were used as an in vitro infection model. 293T β_2m negative cells, generated using CRISPR/Cas9 system, were utilized to produce HIV-1 pseudoviruses. PBMC from healthy blood donors, harboring both protective or non-protective alleles, were exploited to

characterize the proportion between HLA-C associated to β_2m and HLA-C presents as free chains on the cell surface. In addition, PBMC from the same donors were tested for their ability to support HIV-1 infection *in vitro*.

Results: HLA-C free chains, specifically more represented on the surface of infected cells, are responsible for the increase of virions' infectivity. We observed that HIV-1 Env-pseudotyped viruses produced in β_2m negative cells, thus lacking HLA-C on their envelope, are less infectious than those produced in the presence of β_2m .

In PBMC we found that protective HLA-C variants are more stably bound to β_2m than non-protective ones and that HIV-1, *in vitro*, infects more efficiently PBMC harboring non-protective, weakly bound to β_2m , HLA-C alleles.

Conclusions: We propose that the outcome of HIV-1 infection might be driven both by the HLA-C surface expression levels and by the HLA-C/ β_2m binding stability. According to this model, the expression of non-protective HLA-C alleles, which bind weakly β_2m , leads to a reduction of immunocompetent complexes expressed on the cell surface and to an increase of HLA-C free chains that raises viral infectivity, both leading to a rapid progression toward AIDS.

TUPEA0159

HIV-specific CD8+ T cells from natural HIV-1 controllers have a distinct signature associated with enhanced metabolic plasticity and antiviral function. ANRS CO21 CODEX

M. Angin¹, S. Volant², C. Lecroux³, M.-A. Dillies³, F. Boufassa⁴, M. Müller-Trutwin¹, O. Lambotte⁵, A. Sáez-Cirión¹, ANRS CO21 CODEX Study Group
¹Institut Pasteur, ²Unité HIV Inflammation et Persistance, Paris, France, ³Institut Pasteur, ⁴Bioinformatics and Biostatistics Hub - C3BI, USR 3756 IP CNRS, Paris, France, ⁵INS, Le Kremlin Bicêtre, France, ⁶INSERM U 1018, Centre de Recherche en Épidémiologie et Santé des Populations, Université Paris Sud, Le Kremlin Bicêtre, France, ⁷INSERM UMR 1184, Immunologie des Maladies Virales et Autoimmunes (IMVA), Assistance Publique-Hôpitaux de Paris, Service de Médecine Interne, Hôpitaux Universitaires, Université Paris Sud, Le Kremlin Bicêtre, France
 Presenting author email: mathieu.angin@pasteur.fr

Background: HIV-controllers (HC) are a rare group of infected patients who can control the virus below the limit of detection without antiretroviral therapy. This control is usually associated with a strong capacity of HIV-specific CD8 T cells to eliminate infected autologous CD4 T cells *ex vivo*. This capacity seems to be related to inherent characteristics of CD8 T cells but the mechanisms are still not well understood. We made the hypothesis that such enhanced antiviral capacity could be engrained in the transcription profile of HIV-specific memory CD8 T cells from controllers.

Methods: To define a transcriptional signature associated with control of infection, and take into account cellular heterogeneity, single HIV-specific central memory CD8 T cells from HC and antiretroviral treated individuals were flow-sorted. Single cell gene expression was then measured by real time PCR. Statistical analyses were performed to identify markers that are differentially expressed between the two groups and to identify clusters of cells sharing common characteristics. Intracellular cytokine staining was used to assess HIV-specific CD8 T cells responses under metabolic stress conditions.

Results: Single cell profiling showed that HIV-specific memory CD8 T cells from HC and non-controllers have distinct transcriptional signatures. When compared with non-controllers, HC upregulated genes linked to effector function and survival. In contrast non-controllers upregulated genes associated with proliferation and exhaustion. These profiles were associated with higher expression of genes promoting glycolysis in non-controllers and a different balance of the mTORC1/mTORC2 pathways in HC and non-controllers. Functional analyses showed that HIV-specific CD8 T cells from HC were partially dependent on glucose and mitochondrial activity, while cells from non-controllers were exclusively dependent on glucose.

Conclusions: Overall our results suggest that poor functionality of HIV-specific CD8 T cells from non-controllers could be related to their dependence on glycolysis as primary energy source. In contrast cells from HC appear to diversify their metabolic resources. Our data highlight the inherent singularity of HIV-specific CD8 T cells from HC and hint to a metabolic profile compatible with better cell survival and potential to develop anti-HIV effector function under metabolic stress conditions. HIV-specific CD8 T cells metabolism appears to be paramount for control of infection.

TUPEA0160

Functionality of tissue-resident SIV-specific CD8⁺ T cells

C.E.C. Starke, J.M. Brenchley
 National Institutes of Health, NIAID, Bethesda, United States
 Presenting author email: carlyelizabeth.starke@nih.gov

Background: Simian immunodeficiency virus (SIV)-specific CD8⁺ T lymphocytes can reduce SIV replication, slowing disease progression. However, SIV-specific CD8⁺ T cells are incapable of reducing viral replication to low levels for the lifespan of most SIV-infected rhesus macaques (RM) and the majority of animals progress to simian AIDS. Recent studies demonstrated that SIV persists in lymphoid follicles. In a small group of elite controller Asian macaques, SIV replication is spontaneously controlled.

This phenomenon is suggested to be attributed to the unique ability of some CD8⁺ T cells to penetrate into lymphoid follicles and reduce SIV infection of CD4⁺ follicular helper T (T_H) cells.

Methods: To determine whether there are signatures of tissue-resident SIV-specific CD8⁺ T cells associated with increased virologic control, we analyzed molecular and immunological characteristics of SIV-epitope specific CD8⁺ T cells in lymphoid and gastrointestinal tract tissues of 12 SIVmac239, SIVsmE543, or SIVsmE660 infected RM. Seven macaques with viral load less than 10,000 copies/mL were considered to be controllers while the remaining 5 were noncontrollers. MHC-I tetramers loaded with SIV epitopes were used to identify SIV-specific CD8⁺ T cells and flow cytometric and gene chip analyses were used to unravel phenotypic and functional qualities.

Results: While we found no differences in the magnitude of SIV-specific T cell responses based upon their ability to control viral replication, RM who controlled viral replication to low levels exhibited increased CXCR5 expression in lymphoid tissues compared to RM with higher viral loads and frequencies of CXCR5⁺ SIV-specific CD8⁺ T cells negatively correlated with plasma RNA viral load and viral DNA within T_H cells. Additionally, frequencies and phenotypes of SIV-specific CD8⁺ T cells were closely associated with those found in the gastrointestinal tract.

Conclusions: Our data suggest that inherent functionality and particular trafficking of SIV-specific CD8⁺ T cells are important for virologic control. Additionally, these results demonstrate that analysis of lymphoid tissues may be reflective of T cell responses within the gastrointestinal tract. These results will help to better understand the mechanisms that underlie SIV disease progression and the role of SIV-specific CD8⁺ T cells in SIV pathogenesis, which may lead to rational vaccine development.

TUPEA0161

NK cell capacity to accumulate in lymph node follicles is associated with SIV control

N. Huet^{1,2}, P. Rasle^{1,2}, B. Jacquelin¹, T. Garcia¹, M. Plouquin¹, R.K. Reeves³, N. Derreudre-Boquet¹, M. Müller-Trutwin^{1,2}
¹Institut Pasteur, ²HIPER, Paris, France, ³Vaccine Research Institute, Creteil, France, ⁴Center for Virology and Vaccine Research, BIDMC, Boston, United States, ⁵CEA, IDMIT, Fontenay aux Roses, France
 Presenting author email: nicolas.huet@pasteur.fr

Background: During cART, HIV persists in lymph nodes (LN), in particular in B-cell follicles. LN follicles also represent a niche for HIV to hide from most CD8⁺ T cells in HIV/SIV controllers. In this study, we explored mechanisms that allow control of viral replication within follicles using a natural host of SIV model, the African Green monkey (AGM), which has an uncommon capacity to efficiently control SIV replication in LN.

Methods: Six AGM and six cynomolgus macaques were infected respectively with SIV_{agm} sab₂₀₀₉ and SIV_{mac}239 and followed for 6 months. Blood, peripheral LN and rectal biopsies were collected at regular intervals before, during acute and during chronic infection. Viremia as well as cell-associated viral RNA and DNA were quantified. Confocal microscopy was used to determine viral RNA distribution, changes in NK cell localization and cytokine expression. NK cell phenotypes and IL-15⁺ cells were analysed by flow cytometry. Functional assays for evaluating NK cell suppressive activity were performed.

Results: We confirmed that AGM show a strong control of viral replication in LNs, in particular in follicles. Surprisingly, SIV_{agm} infection induced the accumulation of high numbers of NK cells within follicles, associated with a high frequency (25%) of CXCR5⁺ NK cells in secondary lymphoid organs not observed in gut. Follicles during SIV_{agm} infection were a large source of IL-15 suggesting a contribution in NK cell survival and/or differentiation. We observed an increase of differentiated NK cells in AGM LNs at the end of the acute phase when the virus starts to be controlled. CXCR5⁺ NK cells from LN displayed a cytotoxic phenotype. We also observed a strong capacity of LN AGM NK cells to degranulate. In contrast, intestinal NK cells were rare in AGM in contrast to MAC and did not show an increased degranulation during infection.

Monday 24 July
Tuesday 25 July Poster Exhibition
Wednesday 26 July
Late Breaker Abstracts
Author Index

Poster presentation

P.28

Host-virus interactions: HTLV antisense regulatory proteins play a role in the dysregulation of NF- κ B pathway

Stefania Fochi, S. Mutascio, F. Parolini, D. Zipeto, M.G. Romanelli
Dept of Neurosciences, Biomedicine and Movement Sciences, University of Verona, Verona, Italy

Human T-cell leukemia virus type 1 (HTLV-1) is the causative agent of adult T-cell leukemia (ATL), an aggressive form of T-cell malignancy with no cure. The HTLV-1 oncoprotein Tax plays a key role in CD4+ T-cell transformation, mainly through constitutive activation of both the canonical and the alternative NF- κ B pathways. The HTLV-1 basic zipper protein (HBZ), encoded by the antisense viral genome strand, plays an essential role in the oncogenic process in concert with Tax, mediating T-cell proliferation. Unlike HTLV-1, the genetically related retrovirus HTLV-2 is not associated with ATL diseases. Functional comparisons between HTLV-1 regulatory proteins, Tax-1 and HBZ, and the HTLV-2 homologs, Tax-2 and APH-2, may highlight different mechanisms of their oncogenic potential. The aim of this study is to investigate how the antisense proteins HBZ and APH-2 impaired the NF- κ B pathway activation. We found that both HBZ and APH-2 antagonized the NF- κ B promoter activity mediated by Tax, but not in the same extent. Analyzing the intracellular distribution of the antisense proteins, we found that APH-2 is retained in cytoplasm complexes, whereas HBZ is mainly distributed into the nucleus. We observed that in presence of APH-2 and Tax-2, the degradation of the I κ B- α inhibitor was reduced. Moreover, we found that unlike HBZ, APH-2 formed complexes with an upstream inhibitor of the alternative NF- κ B pathway, the TNF receptor-associated factor 3, TRAF3. We generated a TRAF3 knock-out cell line applying the CRISPR/Cas9-mediated genome editing. By luciferase assays, we showed that TRAF3 is not required for Tax mediated NF κ B promoter activation. Analyses are in progress to test the inhibitory effect of the antisense HBZ and APH-2 proteins on NF- κ B promoter activity in absence of TRAF3. The results of this study may contribute to clarify the effect of the alternative NF- κ B viral deregulation pathway in the expression of proinflammatory genes.

SIBBM 2017 • 14-16 June 2017 • Milan, Italy

14-16 June, 2017 Milan (Italy)

SIBBM 2017

Poster presentation

P.68

CRISPR/Cas9 to study virus-host interactions

Francesca Parolini, S. Mulascio, M. Serena, S. Fochi, M.G. Romanelli, D. Zipeto
 Dept of Neurosciences, Biomedicine and Movement Sciences, University of Verona, Verona, Italy

The new CRISPR/Cas9 technique enables the editing of specific DNA sequences of any given genome. It has found many applications in virology, allowing, among others, the viral DNA excision from latently infected cells and the generation of useful knock out cell lines.

Using the CRISPR/Cas9 system we originated β_2 microglobulin (β_2m), human thioesterase 8 (ACOT8) and histone deacetylase 6 (HDAC6) negative cells, to study their role in HIV-1 infection. We evaluated the editing efficiency by the T7 endonuclease I assay, western blot and flow cytometry analyses.

The β_2m is crucial for the HLA molecules membrane translocation. HLA-C interacts with HIV-1 Env on the cell membrane increasing viral infectivity (Zipeto & Beretta, *Retrovirology* 2012). We targeted the β_2m gene in 293T, HeLa-Lai (expressing HIV-1 Env), TZM-bl (HeLa cells susceptible to HIV-1 infection) and parental HeLa cells. We showed in 293T cells that β_2m absence abrogates HLA-C surface expression, even in the presence of HIV-1 proteins expression. We confirmed the observation in β_2m negative HeLa-Lai cells. Moreover, by comparing HIV-1 infectivity in β_2m positive/negative TZM-bl cells, we observed that virions produced in β_2m negative 293T cells are significantly less infectious than those produced in parental cells.

We reported that ACOT8 interacts with HIV-1 Nef preventing its degradation (Serena et al, *Scientific Reports* 2016). We observed in TZM-bl cells that ACOT8 absence did not affect HIV-1 infectivity. The ACOT8 role in HIV-1 production and infectivity is being tested using 293T ACOT8 negative cells.

HDAC6 is an important regulator of membrane dynamics involved in HIV-1 infection. We inactivated the HDAC6 gene in 293T cells to evaluate its influence on HIV-1 infectivity and syncytia formation and analyses are in progress.

In conclusion, the CRISPR/Cas9 genome edited cell lines are powerful tools to study the molecular interaction required for HIV efficient infection.

SIBBM 2017 • 14-16 June 2017 • Milan, Italy

14-16 June, 2017 Milan (Italy)

SIBBM 2017

IS06 CRISPR/Cas9 mediated knock-out of RUNX2 in melanoma cells

Valenti MT¹, Zipeto D², Deiana M¹, Serena M², Parolini F², Cheri S¹, Gandini A³, Mina M⁴, Mutascio S², Viser A¹, Dalle Carbonare L¹.

¹Department of Medicine, Internal Medicine, section D, University of Verona

²Dep. of Neurosciences, Biomedicine and Movement Sciences, - University of Verona

³Department of Surgery, Dentistry, Paediatrics and Gynaecology

⁴Department of Medicine, Medical Oncology Section, University of Verona.

Incidence of MM has increased considerably as a consequence of lifestyle and environmental changes. The mortality rate for MM is very high as it is highly invasive and also genetically resistant to chemotherapeutic treatments. It has been reported that mutation rate and gene modulation in melanoma are higher than in other solid malignancies. In addition, transcription factors by acting on gene expression can affect cellular processes. In particular a higher expression of RUNX2 in melanoma than in normal melanocytes has been shown.

RUNX2 is overexpressed in several tumor tissues, including pancreatic cancer , breast cancer, ovarian epithelial cancer , prostate cancer , lung cancer and osteosarcoma.

As no direct RUNX2 inhibitor is available and experiments performed with RNA interference were scarcely reproducible we applied CRISPR/Cas 9 technology to knockout the RUNT domain of RUNX2 in melanoma cell line.

CRISPR/Cas 9 tecnologia was able to delete, partially, the RUNT domain. The deleted clone showed a reduced proliferation, reduced EMT features and reduced migration ability, suggesting the involvement of RUNT in different pathways of MM. In addition, the deleted clone showed a reduction of genes involved in migration ability and an increased expression of SSBP1 gene suggesting RUNT as oncotarget in MM.

8 – 9 June 2017 Catanzaro (Italy)

AICC congress ‘The future of cancer therapy: the genome editing era’

P09 A CRISPR/Cas9 based approach to study the implication of HTLV regulatory proteins in the NF- κ B modulation

Fochi S, Mutascio S, Parolini F, Zipeto D, Romanelli MG

Department of Neurosciences, Biomedicine and Movement Sciences, University of Verona

Human T-cell leukemia virus type 1 (HTLV-1) infects approximately 20 million people worldwide and 5% of them may develop adult T-cell leukemia (ATL), a fatal T-cell malignancy with no effective treatment currently available. The homologous HTLV-2 does not cause ATL, but is associated with milder neurologic disorders. Both viruses encode a potent viral oncoprotein, termed Tax, which deregulates several cellular pathways, including NF- κ B. In addition to Tax, the HTLV-1 proviral genome encodes from the antisense strand, a basic leucine zipper factor, HBZ, which plays an essential role in the oncogenic process leading to ATL. Comparative studies of the functional activity of Tax-1 and HBZ, and the HTLV-2 homologous, Tax-2 and APH-2 (HTLV-2 antisense protein), may provide clues to explain the dissimilar pathobiology of HTLVs. Herein, we compared the effect of the viral regulatory proteins HBZ and APH-2 on Tax-modulated NF- κ B cell signaling. Our data demonstrated that APH-2 suppressed, more efficiently than HBZ, the Tax-dependent NF- κ B activation. By confocal microscopy, we observed that, differently from HBZ, the APH-2 protein is recruited into cytoplasmic structures where co-localized with Tax. The co-expression of APH-2 and Tax impaired the degradation of the NF- κ B inhibitor I κ B- α , restraining the transcriptional factor p65 into the cytoplasm. APH-2, but not HBZ, was present in complex containing the TRAF3 protein, an upstream inhibitor of the alternative NF- κ B pathway. Applying the CRISPR/Cas9 technique, we generated TRAF3 knock-out cell lines. Several TRAF3^{-/-} clones were selected and NF- κ B promoter activity was analyzed by luciferase assays. The results showed that, in absence of induction, the NF- κ B promoter is slightly activated, in the TRAF3^{-/-} cell line compared to the parental cell line. The absence of TRAF3 adaptor factor did not inhibit the Tax-mediated NF- κ B activation. Ongoing studies using TRAF3^{-/-} clones will allow to clarify the effect of the HTLV antisense protein on the alternative NF- κ B pathway activation.

8 – 9 June 2017 Catanzaro (Italy)

AICC congress ‘The future of cancer therapy: the genome editing era’

P17 CRISPR/Cas9 for the Study of the Interactions between Viruses and Host

Parolini E, Mutascio S, Serena M, Fochi S, Romanelli MG, Zipeto D

Department of Neurosciences, Biomedicine and Movement Sciences, University of Verona

The CRISPR/Cas9 system has many applications in virology: it has been used to achieve viral DNA inactivation from latently infected cells, allowing viral eradication, or to inactivate specific proteins involved in virus-host cell interaction. Herein we applied the CRISPR/Cas9 technique to generate knock-out cell lines useful for the study of cellular determinants critical for HIV-1 infection. As a preliminary screening, the editing efficiency was evaluated by T7 endonuclease I assay, and then confirmed by western blot and flow cytometry analyses. We targeted β 2microglobulin (β 2m), human thioesterase 8 (ACOT8) and histone deacetylase 6 (HDAC6) genes. β 2microglobulin is required for the membrane translocation of HLA molecules where HLA-C interacts with HIV-1 Env and modulates viral infectivity (Zipeto & Beretta, *Retrovirology* 2012). We edited β 2m in 293T, HeLa-Lai (expressing HIV-1 Env), TZM-bl (CD4 and CCR5 expressing HeLa, highly sensitive to HIV-1 infection) and parental HeLa cells. We showed in 293T cells that HIV-1 proteins transfection did not translocate HLA-C at the cell surface in absence of β 2m. We obtained similar result in β 2m negative HeLa-Lai cells, showing that HIV-1 Env interacts with HLA-C at the plasma membrane after its surface translocation. Besides, we demonstrated that HIV-1 pseudoviruses produced in β 2m negative 293T cells were significantly less infectious than those produced in parental ones (Serena et al., *Scientific Reports*, 2017). ACOT8 thioesterase interacts with HIV-1 Nef protein preventing its degradation (Serena et al, *Scientific Reports* 2016). To better understand the role of ACOT8 in HIV-1 infectivity, we developed ACOT8 knock out 293T and TZM-bl cell lines. We observed in TZM-bl cells, susceptible to HIV-1 infection, that ACOT8 absence did not affect the infectivity. The role of ACOT8 in pseudoviruses production is being tested using 293T edited cells. HDAC6 is an important regulator of membrane dynamics involved in HIV-1 infection (Valenzuela-Fernandez et al, *Molecular biology of the cell*, 2005). We inactivated the HDAC6 gene in 293T cells. These cells will be used to test the HIV-1 infectivity and syncytia formation. In conclusion, the CRISPR/Cas9 system represents a new, powerful tool in basic and applied research in virology.

8 – 9 June 2017 Catanzaro (Italy)

AICC congress 'The future of cancer therapy: the genome editing era'

P09 A CRISPR/Cas9 based approach to study the implication of HTLV regulatory proteins in the NF- κ B modulation


Fochi S, Mutascio S, Parolini F, Zipeto D, Romanelli MG

Department of Neurosciences, Biomedicine and Movement Sciences, University of Verona

Human T-cell leukemia virus type 1 (HTLV-1) infects approximately 20 million people worldwide and 5% of them may develop adult T-cell leukemia (ATL), a fatal T-cell malignancy with no effective treatment currently available. The homologous HTLV-2 does not cause ATL, but is associated with milder neurologic disorders. Both viruses encode a potent viral oncoprotein, termed Tax, which deregulates several cellular pathways, including NF- κ B. In addition to Tax, the HTLV-1 proviral genome encodes from the antisense strand, a basic leucine zipper factor, HBZ, which plays an essential role in the oncogenic process leading to ATL. Comparative studies of the functional activity of Tax-1 and HBZ, and the HTLV-2 homologous, Tax-2 and APH-2 (HTLV-2 antisense protein), may provide clues to explain the dissimilar pathobiology of HTLVs. Herein, we compared the effect of the viral regulatory proteins HBZ and APH-2 on Tax-modulated NF- κ B cell signaling. Our data demonstrated that APH-2 suppressed, more efficiently than HBZ, the Tax-dependent NF- κ B activation. By confocal microscopy, we observed that, differently from HBZ, the APH-2 protein is recruited into cytoplasmic structures where co-localized with Tax. The co-expression of APH-2 and Tax impaired the degradation of the NF- κ B inhibitor I κ B- α , restraining the transcriptional factor p65 into the cytoplasm. APH-2, but not HBZ, was present in complex containing the TRAF3 protein, an upstream inhibitor of the alternative NF- κ B pathway. Applying the CRISPR/Cas9 technique, we generated TRAF3 knock-out cell lines. Several TRAF3^{-/-} clones were selected and NF- κ B promoter activity was analyzed by luciferase assays. The results showed that, in absence of induction, the NF- κ B promoter is slightly activated, in the TRAF3^{-/-} cell line compared to the parental cell line. The absence of TRAF3 adaptor factor did not inhibit the Tax-mediated NF- κ B activation. Ongoing studies using TRAF3^{-/-} clones will allow to clarify the effect of the HTLV antisense protein on the alternative NF- κ B pathway activation.

8 – 9 June 2017 Catanzaro (Italy)


AICC congress ‘The future of cancer therapy: the genome editing era’



Involvement of HLA-C binding stability to β_2 microglobulin in HIV-1 infection

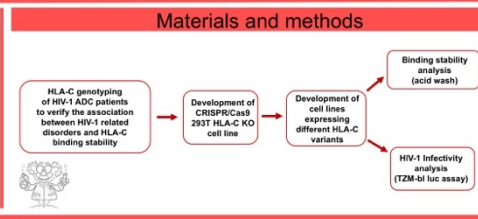
Simona Mutascio, Francesca Parolini, Chiara Stefani, Stefania Fochi, Maria Grazia Romanelli, Donato Zipeto
University of Verona

simona.mutascio@univr.it



Introduction

HLA-C heavy chain is part of the MHC-I complex together with β_2 microglobulin and an antigenic peptide. Upon HIV-1 infection, the viral protein Nef induces the internalization of HLA-A and -B^[1] whereas HLA-C, when it is present on the cell surface as a free chain, can associate with HIV-1, increasing its infectivity^[2]. The different HLA-C variants can be grouped as stable and unstable based on the binding stability to β_2 microglobulin^[3]. We reported that HIV-1 virions produced in the presence of unstable HLA-C allotypes are more infectious than those produced in the presence of stable variants, suggesting that the presence of HLA-C free chains is involved in the modulation of HIV-1 infectivity^[4]. Of note, unstable HLA-C variants release β_2 microglobulin leading to its accumulation, characteristic of patients with AIDS Dementia Complex (ADC)^[5]. We recently reported that patients who developed ADC present HLA-C unstable variants, suggesting a potential role of HLA-C in HIV-1 infection outcome^[6].



Results

1. HLA-C binding stability impacts on HIV-1 related cognitive disorders

Unstable HLA-C variants are associated with the production of more infectious virions. We recently reported that HIV-1 infected patients who developed HIV-related neurological disorders present unstable HLA-C alleles. Particularly, we found that 73% of HIV-ADC patients present unstable HLA-C alleles and 27% present stable variants, compared to HIV-no-ADC patients and to the Northern Italian population (Figure 1). None among HIV-1 ADC patients harbour homozygous stable HLA-C variants.

HLA-C	HIV-ADC	HIV-no-ADC	Northern Italy
HLA-C UNSTABLE	34 (73%)	36 (50%)	773 (50%)
HLA-C STABLE	13 (27%)	36 (50%)	761 (50%)

$p < 0.001$

HIV-ADC	HLA-C	Stability
PL 1	C*08:04	Unstable/Unstable
PL 2	C*08:01	Unstable/Unstable
PL 3	C*08:07	Unstable/Unstable
PL 4	C*08:07	Unstable/Unstable
PL 5	C*08:07	Stable/Unstable
PL 6	C*08:07	Stable/Unstable
PL 7	C*08:36	Stable/Unstable
PL 8	C*08:38	Stable/Unstable
PL 9	C*08:34	Unstable/Unstable
PL 10	C*08:35	Unstable/Unstable
PL 11	C*08:07	Unstable/Unstable

Figure 1. 27 HIV-1 infected patients have been divided into two groups: 11 with AIDS Dementia Complex (HIV-ADC) and 16 without ADC, HIV-no-ADC, left table. The right table reports the HLA-C genotype analysis of HIV-ADC patients.

4. Dissociation rate of the different HLA-C variants from β_2 microglobulin

To study the binding stability to β_2 microglobulin of HLA-C*07, HLA-C*04, and HLA-C*12, an acid wash time course was performed (Figure 4 and 5). A higher curve slope indicates a lower HLA-C binding stability.

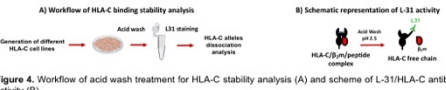
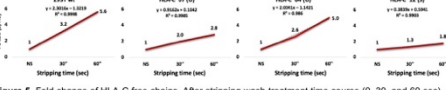



Figure 5. Fold change of HLA-C free chains. After stripping wash treatment time course (0, 30, and 60 sec), β_2 m detachment from HLA-C molecules was calculated as fold change L31 (S/N). U and S refer to Unstable and Stable, respectively.

2. CRISPR/Cas9 to develop HLA-C KO packaging cell line

To study the contribution of each HLA-C variant, 293T HLA-C KO packaging cells were developed using CRISPR/Cas9. After CRISPR/Cas9, the HLA-C expression was evaluated by western blot and flow cytometry analyses (Figure 2 A and B, respectively).

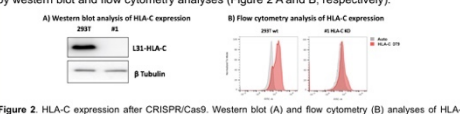


Figure 2. HLA-C expression after CRISPR/Cas9. Western blot (A) and flow cytometry (B) analyses of HLA-C expression of #1 HLA-C KO clone. The HLA-C expression was normalized using β Tubulin (A) and autofluorescence (B).

5. HLA-C expression levels and HIV-1 infectivity

To correlate the HLA-C binding stability to HIV-1 infectivity, HIV-1 pseudotyped viruses will be produced in the presence of different HLA-C variants. Preliminary data suggest that it is possible to restore HLA-C expression levels close to wt cells by transfecting 0.125 μ g of HLA-C expressing plasmid in HLA-C KO cells (Figure 6).

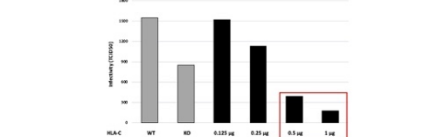


Figure 6. Infectivity Luc-assay. HIV-1 pseudotyped viruses were packaged in the presence of increasing amount of HLA-C (black bars), and in 293T wt and HLA-C KO control cells (grey bars).

3. Development of HLA-C expressing cell lines

According to Guerini et al^[6], the more frequent HLA-C variants in the Italian population were restored in 293T HLA-C KO cells (Figure 3).

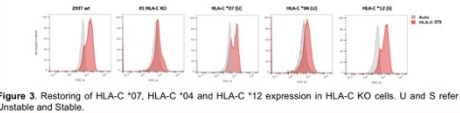


Figure 3. Restoring of HLA-C*07, HLA-C*04 and HLA-C*12 expression in HLA-C KO cells. U and S refer to Unstable and Stable.

Interestingly, we observed that in the presence of HLA-C overexpression, a lower infectivity was detected (highlighted in the red box, Figure 6). Since only 10% of HLA-C is complexed to β_2 m and reaches the plasma membrane, we will investigate whether intracellular HLA-C interacts with HIV-1 Env, interfering with its translocation on the cell surface, which in turn might result in a lower infectivity of HIV-1 virions.

Discussion


The analysis of the dissociation rate of each stable and unstable HLA-C variant from β_2 microglobulin will be mandatory to elucidate the molecular mechanism explaining the key steps of HIV-1 infection and the development of HIV-1 related diseases.

Take Home Message

The presence of HLA-C unstable variants may represent a predictor factor for HIV-1 infection progression and to develop personalized therapies.

References

[1] Apps et al., Cell Host Microbe, 2016, [2] Sibilo et al., J Biol Chem, 2008, [3] Serena et al., Sci. Rep, 2017, [4] Parolini et al., J Virol., 2017, [5] Brew et al., AIDS, 1996, [6] Zipeto et al., Front Neurol., 2018, [7] Chikata et al., J Virol., 2019, [8] Guerini et al., Transpl Immunol., 2008.



CRISPR/Cas9 to generate a new cell model to study the HLA-C binding stability in HIV-1 infection and in cognitive disorders

Mutascio S., Stefani C., Fochi S., Romanelli M.G., Zipeto D.

Simona Mutascio

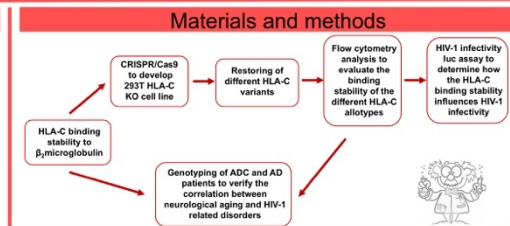
Graduate School for Health and Life Sciences
Ph.D. Program in Applied Life and Health Sciences
Cycle XXXII

Tutor Prof. Donato Zipeto, Maria Grazia Romanelli

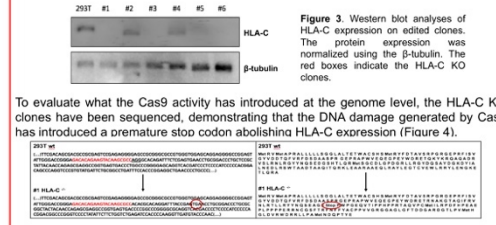
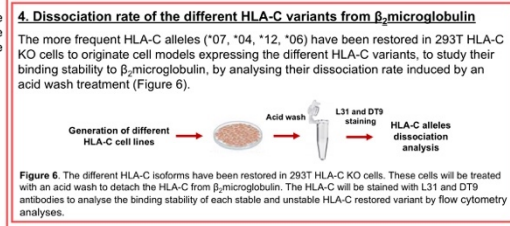
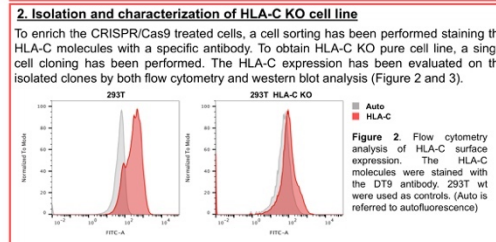
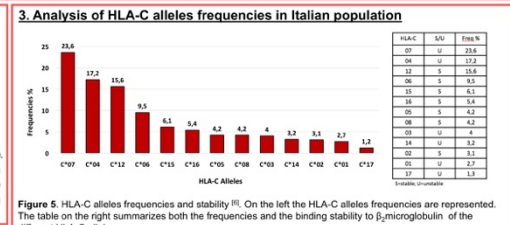
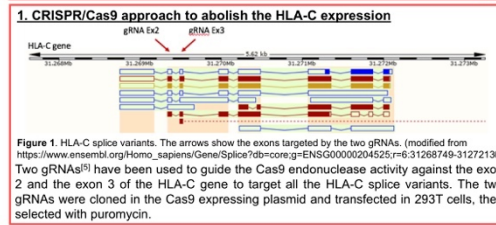
simona.mutascio@univr.it

Introduction

HLA-C is part of MHC-I complex together with β_2 microglobulin and the peptide. Upon HIV-1 infection, the viral protein Nef induces the internalization of HLA-A and -B¹ whereas HLA-C, when it is present on the cell surface as a free chain, can associate with HIV-1, increasing its infectivity. The different HLA-C variants can be grouped in stable and unstable clusters based on the binding stability to β_2 microglobulin^[2]. We reported that virions produced in the presence of unstable HLA-C allotypes are more infectious than those produced in the presence of stable variants, suggesting that the presence of HLA-C free chains is involved in the modulation of HIV-1 infectivity^[3]. Of note, unstable HLA-C variants release β_2 microglobulin leading to its accumulation, characteristic of patients with AIDS Dementia Complex (ADC) and with Alzheimer Disease (AD). We have recently reported that patients who develop ADC present HLA-C unstable variants^[4].



Results



5. Correlation between HLA-C binding stability, HIV-1 infection and AD

Unstable HLA-C variants can be considered as non-protective alleles, since in their presence more infectious HIV-1 virions are produced. Moreover, we have recently reported that HIV-1 infected patients who develop HIV-related neurological disorders present unstable HLA-C alleles. Particularly, we found that the 73% of HIV-ADC patients present unstable HLA-C alleles and the 27% present stable variants, compared to HIV-no-ADC and to Northern Italian population (Figure 7).

	HIV-ADC	HIV-no-ADC	Northern Italy
HLA-C UNSTABLE	16 (73%)	16 (59%)	771 (50%)
HLA-C STABLE	6 (27%)	16 (59%)	761 (50%)

Figure 7. 27 HIV-1 infected patients have been divided in two groups: 11 with AIDS Dementia Complex, referred as HIV-ADC, and 16 without ADC, referred as HIV-no-ADC.


To evaluate what the Cas9 activity has introduced at the genome level, the HLA-C KO clones have been sequenced, demonstrating that the DNA damage generated by Cas9 has introduced a premature stop codon abolishing HLA-C expression (Figure 4).

Figure 4. The left panel shows the genome sequences of the gRNA targeted exon both in 293T wt cells and in 293T HLA-C KO selected clone. In red is highlighted the gRNA sequence and in bold is represented the premature stop codon introduced by the Cas9 activity. The right panel shows the translated sequences of both the 293T wt and 293T HLA-C KO cells. In red is indicated the premature stop codon.

There is a link between HIV-1 cognitive disorders and aging related cognitive disorders, probably due to the release of β_2 microglobulin that leads to amyloid β deposition.

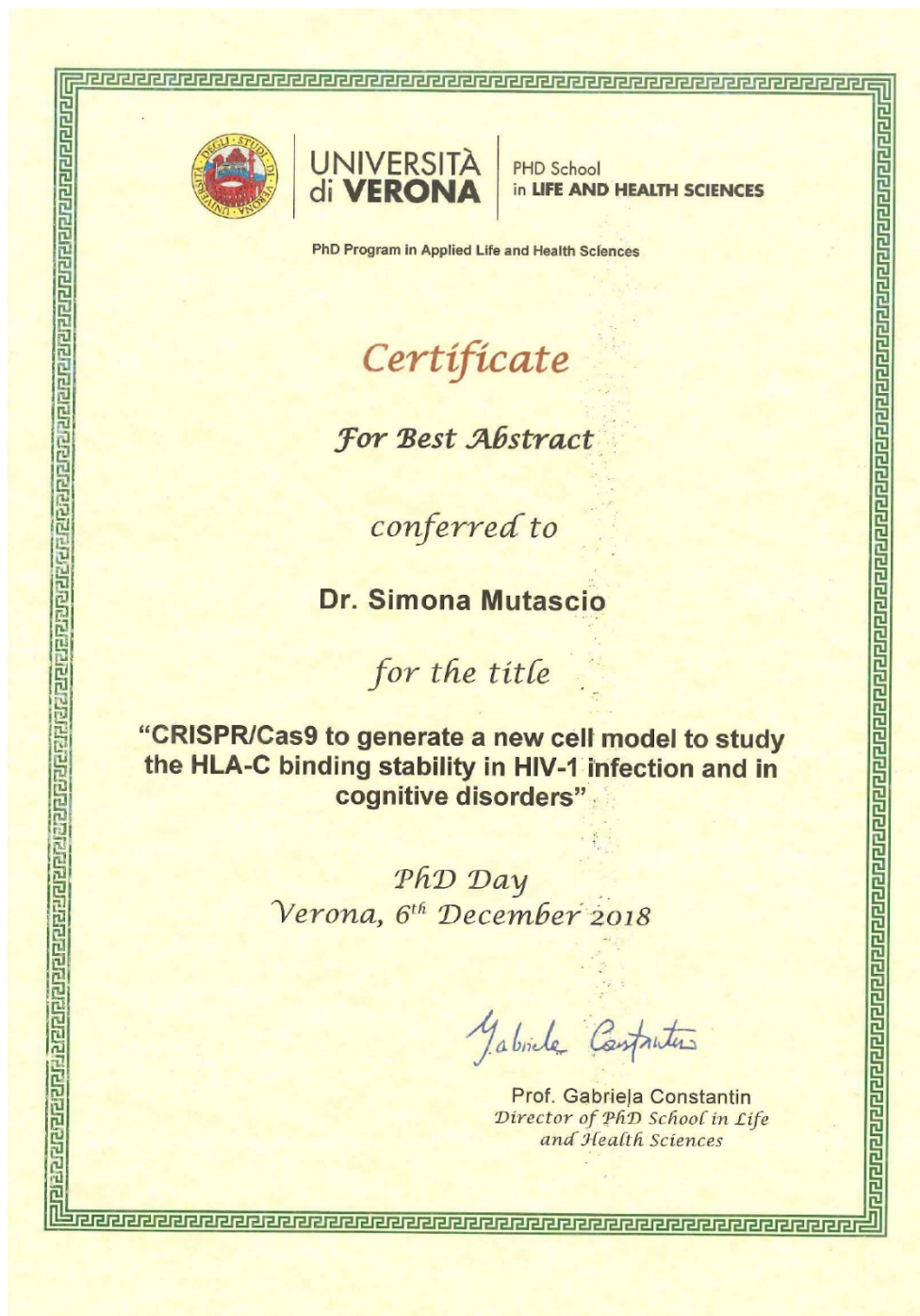
References

- [1] Apps et al., Cell Host Microbe, 2016
- [2] Sibillo et al., J Biol Chem., 2008
- [3] Parolini et al., J Virol., 2017
- [4] Zipeto et al., Front Neurol., 2018
- [5] Hong et al., J Immunother., 2017
- [6] Guerin et al., Transp Immunol., 2008


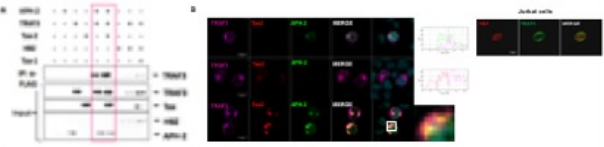
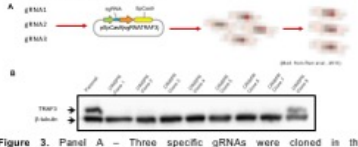
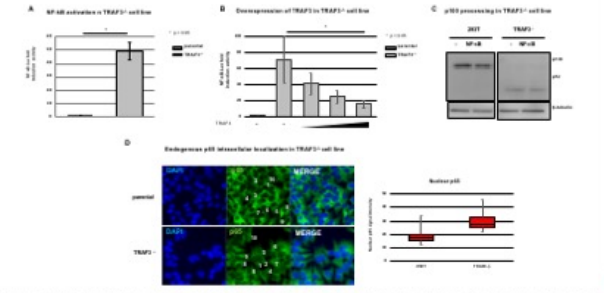
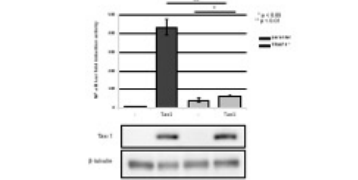




Take Home Message

The presence of HLA-C unstable variants may represent a predictor factor for HIV-1 infection progression and for HIV-1 and aging cognitive disorders to develop personalised therapies.



Ph.D. Day, 6 December, 2018 Verona (Italy)

TRAF3 involvement in the NF-κB pathway deregulation mediated by HTLV-1 Tax protein	
	
Simona Mutascio, Stefania Fochi, Pamela Lorenzi, Marilisa Galasso, Donato Zipeto, Maria Grazia Romanelli Dep. of Neurosciences, Biomedicine and Movement Sciences, University of Verona, Verona, Italy simona.mutascio@univr.it	
BACKGROUND The retrovirus human T-lymphotropic virus type 1 (HTLV-1) is the causative agent of adult T-cell leukemia (ATL). The viral genome encodes two main regulatory proteins Tax and HTLV-1 basic zipper protein (HBZ). Tax is crucial for CD4+ T-cell transformation by maintaining constitutive activation of both the canonical and non canonical NF- κ B pathways that play a primary role in inflammation, cell survival and cancer [1]. HBZ is essential for viral persistence and T-cell proliferation contributing to ATL development. HTLV-2 is genetically related to HTLV-1 and is not associated with ATL. Comparative studies of Tax-1 and HBZ and HTLV-2 homologous regulatory proteins, Tax-2 and APH-2, are useful to understand the HTLVs pathobiology.	MATERIALS AND METHODS Cell culture and transfection: 293T and Jurkat cells were transfected with plasmids expressing the retroviral regulatory proteins. Immunofluorescence microscopy: The intracellular distribution of host and viral proteins was detected by fluorescent dye-labeled antibodies using confocal microscopy. Reporter gene assay: The luciferase expression was measured in triplicate to analyze NF- κ B promoter activity in the presence of viral and host factors, transfecting cells with pNF- κ B-Luc recombinant vector. Immunoprecipitation and western blot: viral and cellular protein complexes were immunoprecipitated using specific antibodies and magnetic beads, from lysed transfected cells. Immunocomplexes were analyzed by western blot and the presence of specific proteins was detected using enhanced chemiluminescence reagent. CRISPR/Cas9: gRNAs were cloned into the pSpCas9(sgRNA) plasmid and transfected into 293T cells to produce clones negative for TRAF3 [2].
AIM OF THE STUDY	
TNF-receptor associated factor 3 (TRAF3) is a negative regulator of the non canonical NF- κ B pathway that interacts with the viral regulatory protein Tax [3]. The aim of this study is to investigate the role of TRAF3 in the deregulation of NF- κ B activation mediated by Tax and HBZ.	
RESULTS	
1. TRAF3 interacts with Tax-2 and APH-2 The negative NF- κ B regulator TRAF3 forms complexes with Tax-2 and APH-2 more efficiently than with Tax-1 and HBZ (Fig. 2A). TRAF3, Tax-2 and APH-2 co-localize in the cytoplasm (Fig. 2B), differently from Tax-1 and HBZ.	2. Development of TRAF3 KO cell line Specific gRNAs were cloned into a Cas9 expressing plasmid (pSpCas9(sgRNA)) to produce TRAF3 negative cell lines (Fig. 3A and 3B).
3. Activation of NF-κB pathway in the absence of TRAF3 TRAF3 ^{-/-} cells, transfected with pNF- κ B-Luc, show a basal activation of the NF- κ B promoter (Fig. 4A), which is reduced by reintroducing TRAF3 (Fig. 4B). Moreover, the processing of p100 is detected in the absence of TRAF3 (Fig. 4C), indicating the activation of the alternative NF- κ B pathway. Furthermore, the transcription factor p65 is more represented in the nucleus of TRAF3 ^{-/-} cells than in the parental line, as shown by confocal microscopy analyses in Fig 4D.	4. Tax-1 activity on NF-κB is reduced in TRAF3^{-/-} line The activation of the NF- κ B promoter mediated by Tax-1 is strongly reduced (p<0.01) in the TRAF3 ^{-/-} cells, compared to the parental cell line (Fig. 4).
 <p>Figure 2. Panel A - Co-immunoprecipitation results of complexes containing TRAF3 and the HTLV regulatory proteins. Lysates were immunoprecipitated with anti-Flag antibody and analyzed by western blot. Panel B - Confocal microscopy analysis of TRAF3 intracellular distribution in the presence of APH-2 and Tax-2 or HBZ and Tax-1. Jurkat cells were transfected with VSV, APH-2 and His-Tax-2 or with Flag-HBZ and His-Tax-1 plasmids, fixed, stained with appropriate antibodies and with DAPI to detect the nucleus.</p>	 <p>Figure 3. Panel A - Three specific gRNAs were cloned in the pSpCas9(sgRNA) plasmid to induce the TRAF3 KO. 293T cells were transfected with the pSpCas9(sgRNA)-TRAF3 plasmid and a single cell cloning was performed. Panel B - Western blot analysis on the clones obtained after CRISPR/Cas9 treatment using a specific antibody against TRAF3 were performed to detect its expression.</p>
 <p>Figure 4. Panel A and B - Analysis of basal NF-κB promoter activity in TRAF3^{-/-} cells (Panel A), after restoring TRAF3 in the TRAF3^{-/-} cells (Panel B). Panel C - Western blot analysis of p100 processing in TRAF3^{-/-} cell line. Parental and TRAF3^{-/-} cells stained with appropriate antibody to detect p65 and with DAPI to detect the nucleus.</p>	 <p>Figure 4. Analysis of the NF-κB promoter mediated by Tax-1 in TRAF3^{-/-} cell line. Tax-1 expressing vector was co-transfected with NF-κB promoter-Luc. The transfection efficiency was evaluated by western blot to detect the presence of Tax-1 and it was normalized to renilla luciferase activity. * p<0.05, ** p<0.01.</p>
CONCLUSIONS	
An aberrant NF- κ B signaling has been identified in many types of cancer, including lymphoma. Our results reveal the importance of the interaction between the TRAF3 and the oncoprotein Tax-1 in the modulation of the NF- κ B pathway. Tax-1 induces the activation of NF- κ B signaling, but its action is dramatically reduced in the absence of the upstream negative regulator TRAF3. The study contributes to clarify the effect of the alternative NF- κ B viral deregulation pathway. Further analyses will be performed to study the effects of the antisense HBZ and APH-2 proteins on the NF- κ B promoter activity in TRAF3 ^{-/-} cells.	
REFERENCES	
[1] Fochi S, Mutascio S, Bertazzoni U, Zipeto D, Romanelli MG. HTLV Deregulation of the NF- κ B Pathway: An Update on Tax and Antisense Proteins Role. <i>Front Microbiol.</i> 2018; 9:285. [2] Ran FA, Hsu PD, Wright J, Agarwala V, Scott DA, Zhang F. Genome engineering using the CRISPR-Cas9 system. <i>Nat Protoc.</i> 2013; 8(11):2281-2308. [3] Diari E, Avessani F, Bergamo E, Oranowski G, Bertazzoni U, Romanelli MG. HTLV-1 Tax protein recruitment into IKK ϵ and TBK1 kinase complexes enhances IFN- λ expression. <i>Virology.</i> 2015; 476:92-99.	
SIBBM 2018 • Frontiers in Molecular Biology Società Italiana di Biofisica e Biologia Molecolare  	

20-22 June, 2018 Rome (Italy)

SIBBM 2018

HLA-C expression levels and binding stability to β_2m are involved in HIV-1 infectivity

Parolini E.^{1*}, Biswas P.², Serena M.,¹ Sironi R.,² Mutascio S.,¹ Muraro V.,³ Guizzardi E.,³ Malnati M.,² Beretta A.,² Romanelli M. G.,¹ Zipeto D.¹

¹ Dep. of Neuroscience, Biomedicine and Movement Sciences, University of Verona, Strada le Grazie 8, Verona, Italy
² Division of Immunology, Transplantation and Infectious Diseases IRCCS Ospedale San Raffaele, Via Olgettina 60, Milan, Italy
³ Service of Transfusion Medicine, AOUI Verona, Piazzale A. Stefani 1, Verona, Italy

* francesca.parolini@univr.it

Background

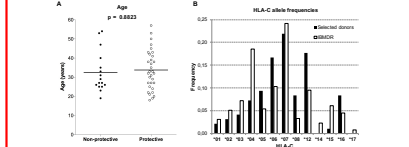
Recent studies have correlated HLA-C expression levels to different HIV-1 infection outcomes. A higher HLA-C expression leads to a better antigen presentation to cytotoxic T lymphocytes (CTLs) and thus to a better HIV-1 infection control. Instead, a lower expression of HLA-C is associated to a rapid progression toward AIDS (Kulkarni et al, 2011; Apps et al, 2013). The highly expressed HLA-C alleles bind more stably the β_2m than the lowly expressed ones (Sbilio et al, 2008). HIV-1 virions lacking HLA-C on their surface have a reduced infectivity and an increased susceptibility to neutralizing antibodies (Matucci et al, 2008; Zipeto et al, 2012). Our group recently reported that HIV-1 Env selectively binds to HLA-C free chains (Serena et al, 2017). The protective role of a higher expression level of HLA-C on the cell membrane appears to be in contrast with the increased infectivity of HIV-1 when HLA-C is incorporated into the virion. This study explains this apparent contradiction shedding light on the association between the HIV-1 protein Env and HLA-C, focusing on the HLA-C/ β_2m /peptide heterotrimer stability.

Methods

PBMC donors registered at the Italian Bone Marrow Donor Register (IBMDR) AOUI Verona, were typed for HLA-A*, -B* and -C*. Donors were selected to have both protective or non-protective HLA-C alleles and not to have HLA-B alleles cross-reactive with the antibodies used (L31 and DT9). Only about 10% of the typed donors satisfied these requirements. HLA-C trimeric complexes and HLA-C free chains present on PBMC membranes were tested by cytofluorimetric analysis, and HLA-C and β_2m expression by western blot. PBMC were also infected with HIV-1 RS and X4 tropic isolates to test their susceptibility to viral infection.

Results

No significant differences neither for sex nor for age (χ^2 test, t-test, respectively) were observed between the HLA-C variants of protective and non-protective groups. Differences in HLA-C frequencies observed in the selected population compared to the whole IBMDR afferent donors were observed, most likely due to the exclusion of donors harbouring cross-reactive HLA-B alleles which are in linkage disequilibrium with specific HLA-C alleles (Figure 1).



The HLA-C surface expression of PBMC was evaluated by cytofluorimetric analyses using two different antibodies, DT9 and L31, specific for the HLA-C/ β_2m /peptide trimeric complex and HLA-C free chains, respectively. Cells were analysed before and after an Acid Wash that dissociates the vast majority of HLA-C trimers. The expression of both HLA-C free chains and trimers is generally slightly higher in the protective group compared with the non-protective one, although the differences were not statistically significant (Figure 2 A, B, D and E). The L31 fluorescence fold change was calculated as the ratio between the L31 RFI after and before the Acid Wash. This value was significantly higher in the protective group, indicating that the HLA-C/ β_2m /peptide binding stability is higher in this group (Wilcoxon test). The DT9 fluorescence fold change, calculated as the ratio before and after the Acid Wash, was slightly lower in the protective group, suggesting that a higher proportion of trimeric complexes was present on the cell surface after the Acid Wash (Figure 2 C and F).

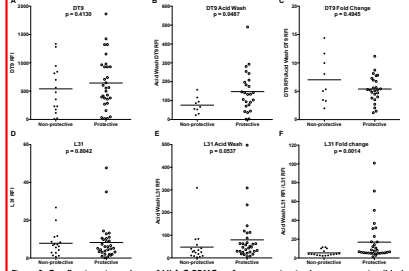


Figure 2. Cytofluorimetric analyses of HLA-C PBMC surface expression in the non-protective (black dots) and protective (white dots) groups. Expression of HLA-C trimeric complexes (A and B), and HLA-C free chains (D and E), are evaluated previously and after the Acid Wash treatment. Finally, the Fluorescence Fold Changes are reported (C and F).

The L31 fluorescence fold change was analysed in a controlled cellular model, the 721.221-CD4 cells. These cell line presents a deletion of the MHC-I locus. After transfection with different HLA-C variants the fluorescence fold change was measured (Figure 3). 721.221-CD4 cells expressing HLA-C*06, a protective HLA-C allele, presented a higher L31 fold change than the 721.221-CD4 cells expressing HLA-C*07, a non-protective HLA-C allele (two-way ANOVA). The use of this cellular model excludes any other genetic or immunological component, which can interfere with the experiments, as might occur in PBMC.

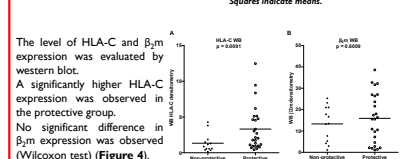


Figure 3. L31 fold change in HLA-C*07 (black dots) and HLA-C*06 (white dots) 221 expressing cells. The experiment was repeated 4 times. Lines connect same-day experiments. Squares indicate means.

The level of HLA-C and β_2m expression was evaluated by western blot. A significantly higher HLA-C expression was observed in the protective group. No significant difference in β_2m expression was observed (Wilcoxon test) (Figure 4).

PBMC with protective and non-protective HLA-C variants were coupled and analysed in parallel in the same experiment. PBMC were infected with HIV-1, supernatants were normalized for p24 content and used to infect TZM-bl cells, to minimise the variability of the target of infection. Two HIV-1 isolates were tested: Bal (RS-tropic) and IIB (X4-tropic) (Figure 5). The infectivity of Bal virions was significantly higher (three-way ANOVA) when they were grown in PBMC carrying non-protective HLA-C alleles (Figure 5 A). According to this observation, a virion budding from PBMC carrying non-protective alleles might be more infectious because a higher proportion of HLA-C free chains is available to interact with HIV-1 Env, determining an increase of infectivity and a lower susceptibility to neutralizing antibodies. No difference in infectivity was observed when using the IIB, X4-tropic isolate (Figure 5 B). The correlation between protective/non-protective HLA-C alleles and viral load was observed during the asymptomatic set-point period of infection, characterized by the predominance of RS-tropic variants. Our data are in agreement with these findings, since the effect of non-protective HLA-C alleles in enhancing viral infectivity is observed with an RS-tropic virus, but not with an X4-tropic one.

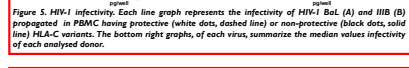


Figure 5. HIV-1 infectivity. Each line graph represents the infectivity of HIV-1 Bal (A) and IIB (B) propagated in PBMC having protective (white dots, dashed line) or non-protective (black dots, solid line) HLA-C variants. The bottom right graphs, of each virus, summarize the median values infectivity of each analysed donor.

Conclusions

We propose that the outcome of HIV-1 infection might depend not only on the amount of surface expressed HLA-C, but also on its stability as trimeric complex. According to this model, individuals with lowly expressed HLA-C alleles and unstable binding to β_2m /peptide (non-protective) might have a worse immunologic control of HIV-1 infection, as well as an intrinsically lower ability to counteract viral replication. On the contrary, individuals with highly expressed HLA-C alleles and stable binding to β_2m /peptide (protective) might have a better immunologic control of HIV-1 infection (Figure 6).

Host-virus interactions: HTLV antisense regulatory proteins play a role in the dysregulation of NF- κ B pathway.

Stefania Fochi, Simona Mutascio, Francesca Parolini, Donato Zipeto, Maria Grazia Romanelli
 Dep. of Neurosciences, Biomedicine and Movement Sciences, University of Verona, Verona, Italy
 stefania.fochi@univr.it

BACKGROUND	MATERIALS AND METHODS
<p>Human T-cell leukemia virus type 1 (HTLV-1) infection is associated with adult T-cell leukemia (ATL), an aggressive malignancy with no cure. The HTLV-1 oncoprotein Tax plays a key role in CD4+ T-cell transformation, mainly through constitutive activation of the NF-κB pathway (Fig.1) [1]. The HTLV-1 basic leucine zipper protein (HBZ), encoded by the antisense viral genome strand, plays an essential role in the oncogenic process in concert with Tax, mediating T-cell proliferation [2]. Unlike HTLV-1, the genetically related retrovirus HTLV-2 is not associated with ATL diseases. Functional comparisons between HTLV-1 and HTLV-2 regulatory proteins, may highlight different mechanisms of their oncogenic potential.</p> <p style="text-align: center; font-size: small;">Figure 1 – Tax mediates the activation of the NF-κB pathway</p>	<p>Cell culture and transfection: 293T, HeLa and Jurkat cell lines were transfected with plasmids expressing the retroviral regulatory proteins.</p> <p>Immunofluorescence microscopy: the intracellular distribution of host and viral proteins was detected by fluorescent dye-labeled antibodies using confocal microscopy.</p> <p>Reporter gene assay: the luciferase expression was measured in triplicate to study NF-κB promoter activity in presence of viral and host factors, using pNF-κB-Luc recombinant vector.</p> <p>Immunoprecipitation and western blot: viral and cellular protein complexes were immunoprecipitated using specific antibodies and magnetic beads, by lysed transfected cells. Complexes were analyzed by western blot and the presence of specific proteins was detected using enhanced chemiluminescence reagent.</p> <p>CRISPR/Cas9: gRNAs were designed and transfected with Cas9 plasmid into 293T to produce clones negative for TRAF3.</p>
AIM OF THE STUDY	
<p>Functional comparison between HTLV-1 and HTLV-2 regulatory proteins may highlight the contribution of viral proteins to oncogenesis. HTLV represents a useful model to study the molecular mechanisms of several cellular processes, including critical steps on HTLV-mediated oncogenesis. The study aims to investigate the role of the HTLV regulatory retroviral proteins in the deregulation of NF-κB cell signaling pathway mediated by their interaction with host factors.</p>	
RESULTS	
<p>1. Inhibition of Tax-mediated NF-κB activation by HBZ and APH-2</p> <p>HBZ and APH-2 differ in the suppression of the NF-κB promoter activation mediated by Tax less efficiently than APH-2 (Fig. 2).</p> <p style="text-align: center; font-size: small;">Figure 2. Effect of HBZ and APH-2 expression on NF-κB activation induced by Tax proteins. HBZ or APH-2 expressing vectors were co-transfected with NF-κB promoter-Luc alone or in the presence of increasing amounts of Tax-1 (panel A) or Tax-2 (panel B). The transfection efficiency was normalized to renilla luciferase activity. *p<0.05, **p<0.005.</p>	<p>4. p65 nuclear translocation is impaired in presence of APH-2</p> <p>In presence of APH-2 and Tax-2, the transcriptional factor p65 is restrained in the cytoplasm (Fig. 5A). The NF-κB inhibitor IκB accumulates in presence of APH-2 and Tax-2 (Fig. 5B).</p> <p style="text-align: center; font-size: small;">Figure 5. Panel A – p65 nuclear translocation in presence of APH-2 and Tax-2. Jurkat cells were transfected with VSV-APH-2 (green signal), His-Tax-2 (red signal), fixed, stained with specific antibodies (endogenous p65 magenta signal), and with DAPI to detect the nucleus, finally analyzed by confocal microscopy. Panel B – Endogenous IκB expression in presence of APH-2 and Tax-2. Lysates were analyzed by western blot with specific antibodies.</p>
<p>2. HBZ and APH-2 differ in their cellular distribution in presence of Tax proteins</p> <p>Tax-1 and HBZ do not co-localize in transfected cells (Fig. 3A), whereas APH-2 is recruited in punctuated cytoplasmic structures in presence of Tax-2 (Fig. 3B).</p> <p style="text-align: center; font-size: small;">Figure 3. Confocal microscopy analysis of HBZ and APH-2 intracellular distribution in presence of Tax. HeLa cells were transfected with HBZ-Flag (panel A, red signal), Tax-1 (panel A, green signal) or APH-2-GFP (panel B, green signal), Tax-2 (panel B, red signal), fixed, stained with specific antibodies, and with DAPI to detect the nucleus.</p>	<p>5. TRAF3 interacts with APH-2 and Tax-2</p> <p>The upstream negative NF-κB regulator TRAF3 forms complexes with Tax-2 and APH-2 more efficiently than with Tax-1 and HBZ (Fig. 6A). TRAF3, Tax-2 and APH-2 co-localize in cytoplasmic structures (Fig. 6B).</p> <p style="text-align: center; font-size: small;">Figure 6. Panel A – Co-immunoprecipitation results of complexes containing TRAF3 and the HTLV regulatory proteins. Lysates were immunoprecipitated with anti-Flag antibody and analyzed by western blot. Panel B – Confocal microscopy analysis of TRAF3 intracellular distribution in presence of APH-2 and Tax-2. Jurkat cells were transfected with VSV-APH-2 (green signal) or His-Tax-2 (red signal) plasmids, fixed, stained with appropriate antibodies and with DAPI to detect the nucleus.</p>
<p>3. APH-2 is recruited in Tax-2-cytoplasmic complexes that contain cellular factors involved in the classical NF-κB pathway</p> <p>APH-2 is partially recruited in complexes with Tax-2 and the adaptor protein TAB2 (Fig. 4A).</p> <p style="text-align: center; font-size: small;">Figure 4. TAB2 and NEMO intracellular localization in presence of APH-2 and Tax-2. Jurkat cells were transfected with Flag TAB2 (magenta signal – panel A), VSV-APH-2 (green signal), His-Tax-2 (red signal), fixed, stained with specific antibodies (endogenous NEMO magenta signal – panel B), and with DAPI to detect the nucleus, finally analyzed by confocal microscopy.</p>	<p>6. NF-κB activity in TRAF3^{-/-} cell lines</p> <ul style="list-style-type: none"> The CRISPR/Cas9 system was applied to produce TRAF3 negative cell lines, clones 1-7 (Fig. 7A). In absence of specific NF-κB induction, the NF-κB promoter is slightly activated in the TRAF3^{-/-} cell line compared to the parental ones (Fig. 7B). <p style="text-align: center; font-size: small;">Figure 7. Panel A – Clones negative for TRAF3. The knockout of TRAF3 was verified by western blot analysis. Panel B – Analysis of the NF-κB promoter activity in TRAF3^{-/-} cell line. NF-κB promoter-Luc alone was transfected in TRAF3^{-/-} cell line and its activity is compared to the control.</p>
<p>7. Tax-mediated NF-κB activation is impaired in absence of TRAF3</p> <ul style="list-style-type: none"> Tax-mediated NF-κB activation is reduced in TRAF3^{-/-} cell line (Fig. 8A). Western blot analyses show Tax-1 processing in TRAF3^{-/-} cell line (Fig. 8B). <p style="text-align: center; font-size: small;">Figure 8. Panel A – Analysis of the NF-κB promoter activity mediated by Tax-1 in TRAF3^{-/-} cell line. Tax-1 expressing vector was co-transfected with NF-κB promoter-Luc. The transfection efficiency was normalized to renilla luciferase activity. *p<0.05. Panel B – Western blot analysis of Tax expression in TRAF3^{-/-} cell line.</p>	<p style="text-align: center; background-color: red; color: white; padding: 5px;">CONCLUSIONS</p> <p>The NF-κB pathway plays an essential role in inflammation and an aberrant NF-κB signaling has been identified in many types of cancer initiation and progression, including in lymphoma. Our results demonstrated that the HTLV retroviral proteins differ in their interaction with host factors involved in the NF-κB activation. In particular, APH-2, differently to HBZ, is recruited in Tax-2-cytoplasmic structure and inhibits the NF-κB activation preventing the nuclear translocation of the transcriptional factor p65. Moreover, the absence of the upstream negative regulator TRAF3 impaired the transactivation of the NF-κB promoter mediated by the oncoprotein Tax. Ongoing studies using TRAF3^{-/-} clones will allow to clarify the effect of the HTLV antisense protein on the alternative NF-κB pathway activation. This study will contribute to clarify the effect of the alternative NF-κB viral deregulation pathway in the expression of proinflammatory genes.</p>
REFERENCES	
<p>[1] Romanelli MG, Diari E, Bergamo E, Casoli C, Ciminale V, Bex F, Bertazzoni U. Highlights on distinctive structural and functional properties of HTLV Tax proteins. <i>Front. Microbiol.</i> 2013; 4:271</p> <p>[2] Zhou T. The role of HBZ in HTLV-1-induced oncogenesis. <i>Viruses.</i> Feb; 8(2): 34.</p>	

SIBBM 2017
 Firenze in Microbiologia
 Società Italiana di Microbiologia e Biologia Molecolare
 from Single Cells to 3D Cell Culture

14-16 June, 2017 Milan (Italy)

SIBBM 2017



CRISPR/Cas9 to study virus-host interactions

Parolini F., Mutascio S., Serena M., Fochi S., Romanelli M. G., Zipeto D.

Department of Neurosciences, Biomedicine and Movement Sciences, University of Verona

Introduction

The CRISPR/Cas9 system is a powerful tool for genome editing¹. Recently, this technique has found many applications in different fields, including virology. In the present work, using CRISPR/Cas9 we generated different knock out cell lines that we used to study the host/viral proteins interaction. We studied the β_2m involvement in modulating HIV-1 infectivity by generating HEK 293T, HeLa, HeLa-Lai and T2M-bl negative cells. Furthermore, to investigate the ACOT8 role in HIV-1 infection, ACOT8 negative T2M-bl and 293T cells were originated. Finally, to determine the HDAC6 role in *syncytia* formation during HIV-1 infection, we developed HDAC6 negative 293T cells, which will be employed to study the role of HDAC6.

Materials and methods

Selected gRNA sequences, designed on the first exon of the target gene, were cloned into the PX459 V2.0 plasmid (Addgene) expressing Cas9. HEK 293T, HeLa, HeLa-Lai (expressing HIV-1-Lai Env) and T2M-bl (highly sensitive to HIV infection) cells were co-transfected with different gRNAs plasmids, to obtain the desired β_2m , ACOT8 and HDAC6 knock-out. Following selection and expansion, cells were tested by PCR analysis. Edited cells were obtained by cell sorting or single cell cloning. The gene inactivation was verified by western blot or cytofluorimetric analysis. β_2m and ACOT8 negative HEK 293T and T2M-bl cells were used to test HIV-1 infectivity.³

β_2m -microglobulin CRISPR/Cas9

Results

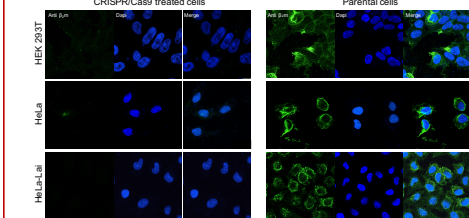


Figure 1. Immunofluorescence analysis. β_2m surface expression was evaluated in HEK 293T, HeLa and HeLa-Lai cells transfected with Cas9 and β_2m gRNA#13² expressing plasmids. Parental cells were used as positive control.

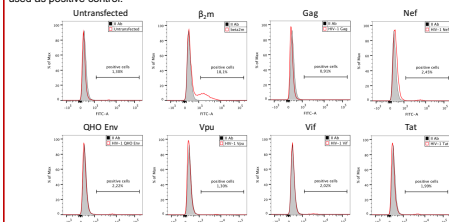


Figure 2. Cytofluorimetric analysis of HLA-C surface expression in β_2m negative cells. After transfection with plasmids encoding different HIV-1 proteins, HLA-C surface expression of HEK 293T β_2m negative cells were evaluated. Cells transfected with β_2m were used as positive control.

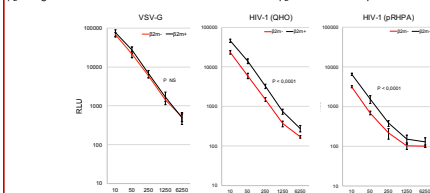


Figure 3. HIV-1 infectivity assay. QH0 and pRHPA Env HIV-1 viruses produced in HEK 293T β_2m positive cells (black line) were more infectious than those produced in β_2m negative ones (red line). An unrelated virus (VSV-G) was used as control³.

Discussion

Since it is known that HIV-1 Env protein interacts with HLA-C increasing viral infectivity we generated β_2m negative cell lines to investigate β_2m role in HIV-1 infection. We demonstrated that HLA-C molecules strictly require β_2m to reach the plasma membrane, where they can interact with HIV-1 Env. Besides, we showed that viruses produced in β_2m negative cells were significantly less infectious than β_2m positive ones⁴.

ACOT8 CRISPR/Cas9

Results

```

GGTTACTAGGGCACTCCGGGAAGTCAGTCTCTGTATGTCCTCCGCTCTCCCGAGGG
GGTGTTCAGGGCTCTGACGATTAACATGATGTCCTCCCGCAGGCCCAAGATGGGAGCT
GTGTGGATGGGGGATCCCTGCGGACCTCTGCGGCTCTGCTGATGAGGAGCTCTGATCC
GAGCCGCTGACGAGGATCTTTCAG
    
```

Figure 4. gRNAs designed on the first exon of ACOT8 gene. In red are highlighted PAM sequences. Cas9 targets sites are indicated by arrows.

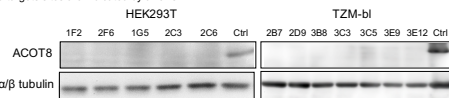


Figure 5. Western blot analysis of ACOT8 expression. Single clones of HEK 293T and T2M-bl treated with the CRISPR/Cas9 system were analysed by western blot for ACOT8 protein expression.

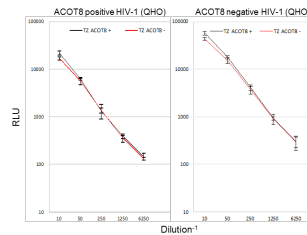


Figure 6. HIV-1 infectivity assay. HIV-1 Env pseudotyped viruses produced in HEK 293T ACOT8 positive cells (black line) showed a similar infectivity than those produced in ACOT8 negative cells (red line).³

Discussion

Since ACOT8 thioesterase interacts with HIV-1 Nef protein preventing its degradation⁴, we investigated its involvement in HIV-1 infectivity, developing ACOT8 knock out HEK 293T and T2M-bl cell lines. We observed in T2M-bl cells, susceptible to HIV-1 infection, that ACOT8 absence did not affect the HIV-1 infectivity. The role of ACOT8 in HIV-1 production is being tested using 293T edited cells.

HDAC6 CRISPR/Cas9

Results

```

AAGCGAAATATTAAGGAGGAGCCGTTCCCGCTCTATCCCAATCTAGCGAGGTA
AAGAAGAAAGGCAAAATGAAGAGCTCGCCCAAGCAATGGAAGAAAGACCTAATCTGT
GGACTGCAAGGGATG
    
```



Figure 7. HDAC6 PCR analysis of HEK 293T cells treated with the CRISPR/Cas9 system. (Left panel) the target sequences of the two used gRNAs. In red: PAM sequences. (Right panel) PCR analysis after selection reveals the presence of insertion/deletion mutants in HEK 293T treated with CRISPR/Cas9 system.

Discussion

HDAC6 is an important regulator of membrane dynamics involved in HIV-1 infection⁵. To inactivate the HDAC6 gene in HEK 293T cells we designed two gRNAs to obtain the deletion between the two guides. These cells will be used to test the role of HDAC6 in HIV-1 infectivity and syncytia formation.

References

- ¹ Prashant Mali et al. *Science*, 15, 339, 2013
- ² Pankaj K. Mandal et al. *Cell Press*, 15, 643, 2014
- ³ Ming Li et al. *J. Virol.*, 79, 10108, 2005
- ⁴ Serena et al. *Scientific Report*, 7, 40037, 2017
- ⁵ Valenzuela-Fernandez et al. *Molecular biology of the cell*, 16(11): 5445-545, 2005

Conclusions

The CRISPR/Cas9 system is a very useful tool to generate specific gene knock out cell lines which can be exploited to study cell host/virus interactions. We use this approach to investigate the role of cellular proteins β_2m , ACOT8 and HDAC6 important to support HIV-1 infection.

14-16 June, 2017 Milan (Italy)

SIBBM 2017

CRISPR/Cas9 for the study of the interactions between viruses and host
Parolini F., Mutascio S., Serena M., Fochi S., Romanelli M. G., Zipeto D.
 Department of Neurosciences, Biomedicine and Movement Sciences, University of Verona

Introduction
 The CRISPR/Cas9 system, exploiting a short RNA-guided specific endonuclease (Cas9), permits the genome editing¹. In the last few years this technique has found applications in different fields, including virology. In the present work through the CRISPR/Cas9 system we generated different knock out cell lines helpful in studying the host/viral proteins interaction. We studied the role of β_2m in modulating HIV-1 infectivity by generating HEK 293T, HeLa, HeLa-Lai and T2M-bl negative cells. Furthermore, ACOT8 negative T2M-bl and 293T cells were originated to investigate the ACOT8 role in HIV-1 infection. Finally, we obtained HDAC6 negative 293T cells, which will be employed to shed light on the HDAC6 importance in determining the syncytia formation during HIV-1 infection.

Materials and methods
 Selected gRNA sequences, designed on the first exon of the target gene, were cloned into the PX459 V2.0 plasmid (Addgene) expressing Cas9. HEK 293T, HeLa, HeLa-Lai (expressing HIV-1-Lai Env) and T2M-bl (CD4 and CCR5 expressing HeLa, highly sensitive to HIV infection) cells were co-transfected with different gRNAs plasmids, to obtain the desired knock-out: β_2m , ACOT8 and HDAC6. Following puromycin selection and expansion, cells were tested for heteroduplex presence through T7 assay. Edited cells were obtained through cell sorting or single cell cloning. The gene inactivation was verified by western blot or cytofluorimetric analysis. β_2m and ACOT8 negative HEK 293T and T2M-bl cells were used to test their effect in HIV-1 infectivity, through the generation of Env pseudotyped viruses and neutralization assay³.

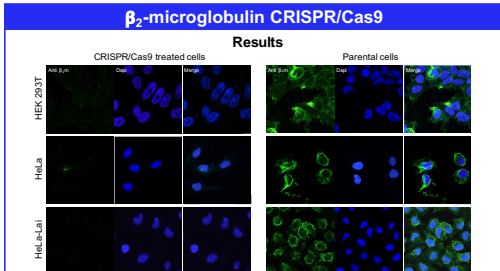


Figure 1. Immunofluorescence analysis. β_2m surface expression was tested in HEK 293T, HeLa and HeLa-Lai transfected with Cas9 and β_2m gRNA#13* expressing plasmids. Parental cells were used as controls.

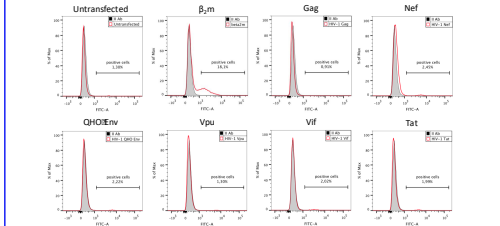


Figure 2. HLA-C surface expression in β_2m negative cells. After transfection with plasmids encoding different HIV-1 proteins, HEK 293T β_2m negative cells were surface labeled with the L31 antibody. As positive control cells were transfected with β_2m .

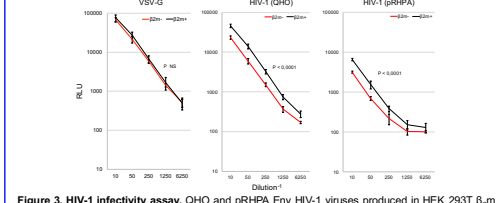


Figure 3. HIV-1 infectivity assay. QH and pRHPA Env HIV-1 viruses produced in HEK 293T β_2m positive cells (black line) are more infectious than those produced in β_2m negative ones (red line). An unrelated virus (VSV-G) was used as control³.

Discussion
 Since it is known that HIV-1 Env protein interacts with HLA-C increasing viral infectivity we generated β_2m negative cell lines to deeply investigate HLA-C role in HIV-1 infection. First of all we demonstrated that HLA-C molecules strictly require β_2m for reaching the plasma membrane, where they can interact with HIV-1 Env. Besides, we showed that β_2m negative HIV-1 pseudoviruses were significantly less infectious than β_2m positive ones⁴.

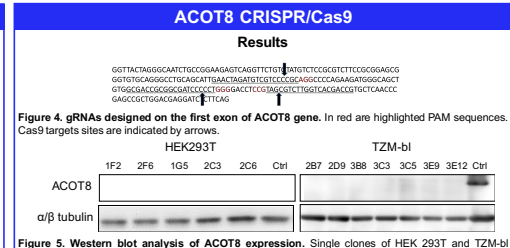


Figure 5. Western blot analysis of ACOT8 expression. Single clones of HEK 293T and T2M-bl treated with the CRISPR/Cas9 system were analysed by western blot for ACOT protein expression.

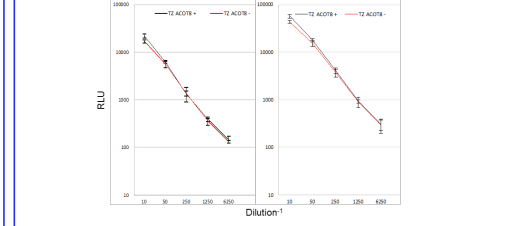


Figure 6. HIV-1 infectivity assay. HIV-1 Env pseudotyped viruses produced in expressing/non-expressing ACOT8 HEK 293T cells were used to infect T2M-bl expressing ACOT8 cells (black line) and T2M-bl ACOT8 negative cells (red line)³.

Discussion
 Since ACOT8 thioesterase interacts with HIV-1 Nef protein preventing its degradation⁵, we investigated its role in HIV-1 infectivity, developing ACOT8 knock out HEK 293T and T2M-bl cell lines. We observed in T2M-bl cells, susceptible to HIV-1 infection, that ACOT8 absence did not affect the infectivity. The role of ACOT8 in pseudoviruses production is being tested using 293T edited cells.

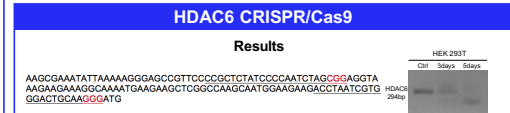


Figure 7. HDAC6 PCR analysis of HEK 293T cells treated with CRISPR/Cas9 system. A. Target sequences of the two used gRNAs. In red: PAM sequences B. PCR analysis after puromycin selection reveals the presence of insertion/deletion mutants in HEK 293T treated with CRISPR/Cas9 system.

Discussion
 HDAC6 is an important regulator of membrane dynamics involved in HIV-1 infection⁵. We inactivated the HDAC6 gene in HEK 293T cells. These cells will be used to test the HIV-1 infectivity and syncytia formation.

References
¹ Prashant Mali et al, Science, 15, 339, 2013
² Pankaj K. Mandal et al, Cell Press, 15, 643, 2014
³ Ming Li et al, J. Virol, 79, 10108, 2005
⁴ Serena et al, Scientific Report, 7, 40037, 2017
⁵ Valenzuela-Fernandez et al, Molecular biology of the cell, 16(11): 5445-545, 2005


Take home message
 CRISPR/Cas9 system provides a high specificity of genomic editing. It has already found many potential applications to human diseases, including viral associated disorders. Our results highlighted the efficacy of CRISPR/Cas9 based application to study the host factors involved in HIV-1 infection.

8 – 9 June 2017 Catanzaro (Italy)

AICC congress ‘The future of cancer therapy: the genome editing era’

CRISPR/Cas9 system and its application against human retroviruses

Mutascio S., Parolini F., Fochi S., Romanelli M.G., Zipeto D.
 Simona Mutascio
 Graduate School for Health and Life Sciences
 Ph.D. Program in Applied Life and Health Sciences
 Cycle XXXII
 Tutor Prof. Donato Zipeto, Maria Grazia Romanelli simona.mutascio@univr.it




Introduction

The CRISPR/Cas9 system, exploiting a short RNA-guided specific endonuclease (Cas9), allows the genome editing⁽¹⁾. In the last few years this technique has found applications in different fields, including virology. In the present work through the CRISPR/Cas9 system we generated different knock out cell lines helpful in studying infectivity of retroviruses. The aim of this study is to develop knock out cells useful to study HIV-1 infectivity and the host /HTLV proteins interaction. Specifically, we studied the role of β_2m in modulating HIV-1 infectivity by generating Hek-293T and T2M-bl β_2m negative cells. Furthermore, HDAC6 negative Hek-293T cells were generated, to better understand the role of HDAC6 protein upon HIV-1 infection in modulating HIV-1 spreading and membrane dynamics. HTLV-1 induces a constitutive activation of NF- κ B signalling⁽²⁾. To define the contribution of the interaction between a negative regulator of NF- κ B pathway, TRAF3, and HTLV regulatory proteins, we developed TRAF3 KO cells.

Materials and Methods

CRISPR/Cas9 and survivor assays
 To obtain β_2m , HDAC6 and TRAF3 knock-out, specific gRNAs were cloned into the PX459 V2.0 plasmid expressing Cas9 endonuclease and transfected in Hek-293T and T2M-bl cells. The transfected cells were selected by puromycin. The KO cells were obtained performing a single cell cloning or a cell sorting.



The gene inactivation was verified by western blot, PCR or flow cytometry.

Luciferase assay
 The NF- κ B promoter activity was analysed by luciferase in triplicate.

Results

1 Generation of β_2m KO cell line applying CRISPR/Cas9 system
 β_2m with the HLA-A, -B or C take part to MHC class I complex formation⁽³⁾. To obtain T2M-bl β_2m negative cells, CRISPR/Cas9 has been applied and the KO cells were selected through cell sorting.

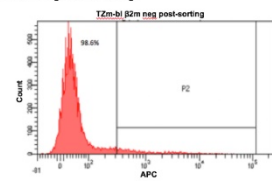


Figure 1. Cytofluorimetric analysis of β_2m surface expression.

2 Generation of HDAC6 KO cell lines applying CRISPR/Cas9 system
 HDAC6 is a cytoplasm enzyme essential for tubulin acetylation⁽⁴⁾. To generate Hek-293T HDAC6 KO cells, CRISPR/cas9 system has been performed, inducing a specific 74 bp deletion in the exon 2 of HDAC6 gene.

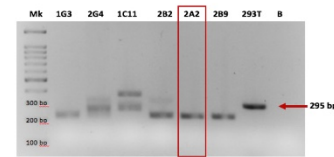


Figure 2. PCR analysis of obtained clones after gRNAs/Cas9 transfection. The arrow shows the HDAC6 product length derived from Hek-293T parental cell line (295 bp). The red box highlights the selected clone for further analyses.

3 Generation of TRAF3 KO cell lines applying CRISPR/Cas9 system
 TRAF3 is a negative modulator of non canonical NF- κ B signalling⁽⁵⁾. TRAF3 KO cells were obtained through CRISPR/Cas9 (fig 4).

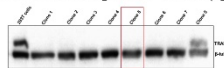


Figure 4. Western blot analyses of TRAF3 expression of edited clones. The protein expression was normalized using the β -tubulin. The red box indicates the selected clone. By luciferase assay the NF- κ B promoter activity was evaluated (fig. 5). NF- κ B promoter is activated in TRAF3 KO cells (panel A). This basal activation is abolished restoring TRAF3 in the edited cells (panel B).

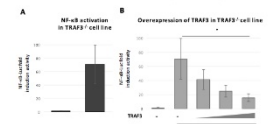


Figure 5 NF- κ B promoter activity analyzed by luciferase assay in TRAF3^{-/-} cells.

2A2 clone was selected for Sanger sequencing. The sequencing analysis confirmed the occurred 74 bp deletion (fig. 3)

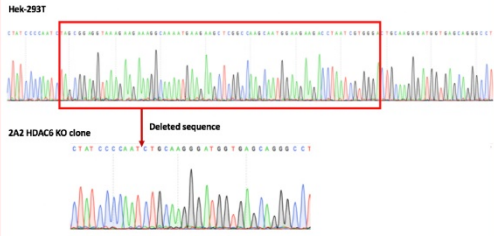


Figure 3. Sanger sequencing of 2A2 HDAC6 KO selected clone. The sequence profile reveals a 74 bp deletion indicated in the red box .

Discussion

The new promising powerful tool CRISPR/Cas9 has been applied to develop three specific cell models, to deeply investigate virus-host interactions in HIV and HTLV viral models.

- T2M-bl β_2m negative cells that will be employed to discriminate the role of β_2m in HIV-1 infectivity;
- Hek-293T HDAC6 KO cells that will be useful to characterize its role in membrane dynamics and syncytia formation upon HIV-1 infection;
- Hek-293T TRAF3 KO cells that will be essential to highlight the importance of host/viral proteins interaction in the regulation of NF- κ B pathway.

References

- 1 Ran et al., Nat Protoc., 2013
- 2 Romanelli et al., Front Microbiol., 2013
- 3 Serena et al., Scientific Report, 7, 40037, 2017
- 4 Valenzuela-Fernandez et al, Molecular biology of the cell, 2005
- 5 Sun et al., Cell Research, 2011

Take Home Message

Since the CRISPR/Cas9 is a specific genome editing technique, it has found applications to counteract human retroviruses to investigate viruses infectivity and the contribution of specific host factors in cell signaling pathways regulation.



HTLV Deregulation of the NF- κ B Pathway: An Update on Tax and Antisense Proteins Role

Stefania Fochi, Simona Mutascio, Umberto Bertazzoni, Donato Zipeto and Maria G. Romanelli*

Department of Neurosciences, Biomedicine and Movement Sciences, University of Verona, Verona, Italy

OPEN ACCESS

Edited by:

Hirofumi Akari,
Primate Research Institute, Japan

Reviewed by:

Jun-ichirou Yasunaga,
Kyoto University, Japan
Antonio C. R. Vallinoto,
Institute of Biological Sciences of
Federal University of Pará, Brazil

*Correspondence:

Maria G. Romanelli
mariagrazia.romanelli@univr.it

Specialty section:

This article was submitted to
Virology,
a section of the journal
Frontiers in Microbiology

Received: 18 December 2017

Accepted: 07 February 2018

Published: 21 February 2018

Citation:

Fochi S, Mutascio S, Bertazzoni U,
Zipeto D and Romanelli MG (2018)
HTLV Deregulation of the NF- κ B
Pathway: An Update on Tax and
Antisense Proteins Role.
Front. Microbiol. 9:285.
doi: 10.3389/fmicb.2018.00285

Human T-cell lymphotropic virus type 1 (HTLV-1) is the causative agent of adult T-cell leukemia (ATL), an aggressive CD4⁺/CD25⁺ T-cell malignancy and of a severe neurodegenerative disease, HTLV-1 associated myelopathy/tropical spastic paraparesis (HAM/TSP). The chronic activation or deregulation of the canonical and non-canonical nuclear factor kappa B (NF- κ B) pathways play a crucial role in tumorigenesis. The HTLV-1 Tax-1 oncoprotein is a potent activator of the NF- κ B transcription factors and the NF- κ B response is required for promoting the development of HTLV-1 transformed cell lines. The homologous retrovirus HTLV-2, which also expresses a Tax-2 transforming protein, is not associated with ATL. In this review, we provide an updated synopsis of the role of Tax-1 in the deregulation of the NF- κ B pathway, highlighting the differences with the homologous Tax-2. Special emphasis is directed toward the understanding of the molecular mechanisms involved in NF- κ B activation resulting from Tax interaction with host factors affecting several cellular processes, such as cell cycle, apoptosis, senescence, cell proliferation, autophagy, and post-translational modifications. We also discuss the current knowledge on the role of the antisense viral protein HBZ in down-regulating the NF- κ B activation induced by Tax, and its implication in cellular senescence. In addition, we review the recent studies on the mechanism of HBZ-mediated inhibition of NF- κ B activity as compared to that exerted by the HTLV-2 antisense protein, APH-2. Finally, we discuss recent advances aimed at understanding the role exerted in the development of ATL by the perturbation of NF- κ B pathway by viral regulatory proteins.

Keywords: HTLV, NF- κ B, Tax, HBZ, APH-2, adult T-cell leukemia, cell proliferation, apoptosis

INTRODUCTION

Human T-cell lymphotropic/leukemia virus type 1 (HTLV-1) is the etiological agent of adult T-cell leukemia (ATL), a malignancy of CD4⁺/CD25⁺ T cells and of a chronic inflammatory disease called HTLV-1 associated myelopathy/tropical spastic paraparesis (HAM/TSP) (Poesz et al., 1980; Hinuma et al., 1981; Gessain et al., 1985; Gallo et al., 2017). It is estimated that at least 20 million people worldwide are infected with HTLV-1 (Gessain and Cassar, 2012; Willems et al., 2017) and approximately 5% of HTLV-1 carriers develop ATL after a latency of 20–50 years from infection (Zhang et al., 2017). HTLV-1 provirus encodes, among others, a regulatory protein, Tax and an accessory antisense strand product HTLV-1 bZip protein (HBZ), which are pivotal factors in

HTLV-1 pathogenesis (Yasuma et al., 2016). Tax is a transcriptional activator of the viral long terminal repeat (LTR) with the capability to unsettle several cellular signal transduction pathways. HBZ is an inhibitor of 5' LTR Tax-1 transactivation and is required for viral persistence (Barbeau et al., 2013). HBZ is a potent viral oncoprotein which plays an important role in deregulating several cellular processes in concerted action with Tax, affecting cell proliferation, apoptosis, autophagy, and immune escape (Zhao, 2016). Both these viral regulatory proteins promote T-cell proliferation. However, the exact mechanism underlying their role in inducing cell proliferation is still not clearly understood. The genetically related HTLV type 2 virus, although its association with ATL has not been established, encodes a homolog Tax-2 regulatory protein that induces T-cell proliferation *in vitro* and an antisense protein, named antisense protein HTLV-2 (APH-2) that, unlike HBZ, is dispensable for HTLV-2 infection and persistence (Yin et al., 2012). Their structural properties are shown in **Figures 1A,B**. Comparative studies between HTLV-1 and HTLV-2 have contributed to highlight differences in the virus-host interaction that may have key roles in tumorigenesis (Higuchi and Fujii, 2009; Bertazzoni et al., 2011; Romanelli et al., 2013).

Persistent activation of NF- κ B by Tax is a key event for the T-cell transformation and development of ATL (Qu and Xiao, 2011; Zhang et al., 2017). Accumulating evidence indicates that the HTLVs have evolved specific strategies mediated by Tax and antisense proteins to deregulate NF- κ B signaling pathways. While HBZ is consistently expressed in all ATL cells, Tax is not expressed in approximately 60% of them, even though the HTLV-1 proviral genome is integrated and NF- κ B is constitutively activated (Zhao, 2016). This suggests that additional factors contribute to sustain the persistent activation of NF- κ B, in the absence of Tax, in ATL cells (Matsuoka and Jeang, 2007). The alteration of the NF- κ B signaling pathway could also be involved in the inflammatory state observed in HAM/TSP (Peloponese et al., 2006). An interesting aspect of Tax and HBZ functions is their opposite effect on the regulation of cellular signaling pathways (Zhao and Matsuoka, 2012; Ma et al., 2016) as further discussed here.

In this review, we summarize the recent advances in understanding the molecular mechanisms involved in NF- κ B deregulation, mediated by Tax and antisense proteins, through the interaction with host factors and their roles in cell survival and proliferation.

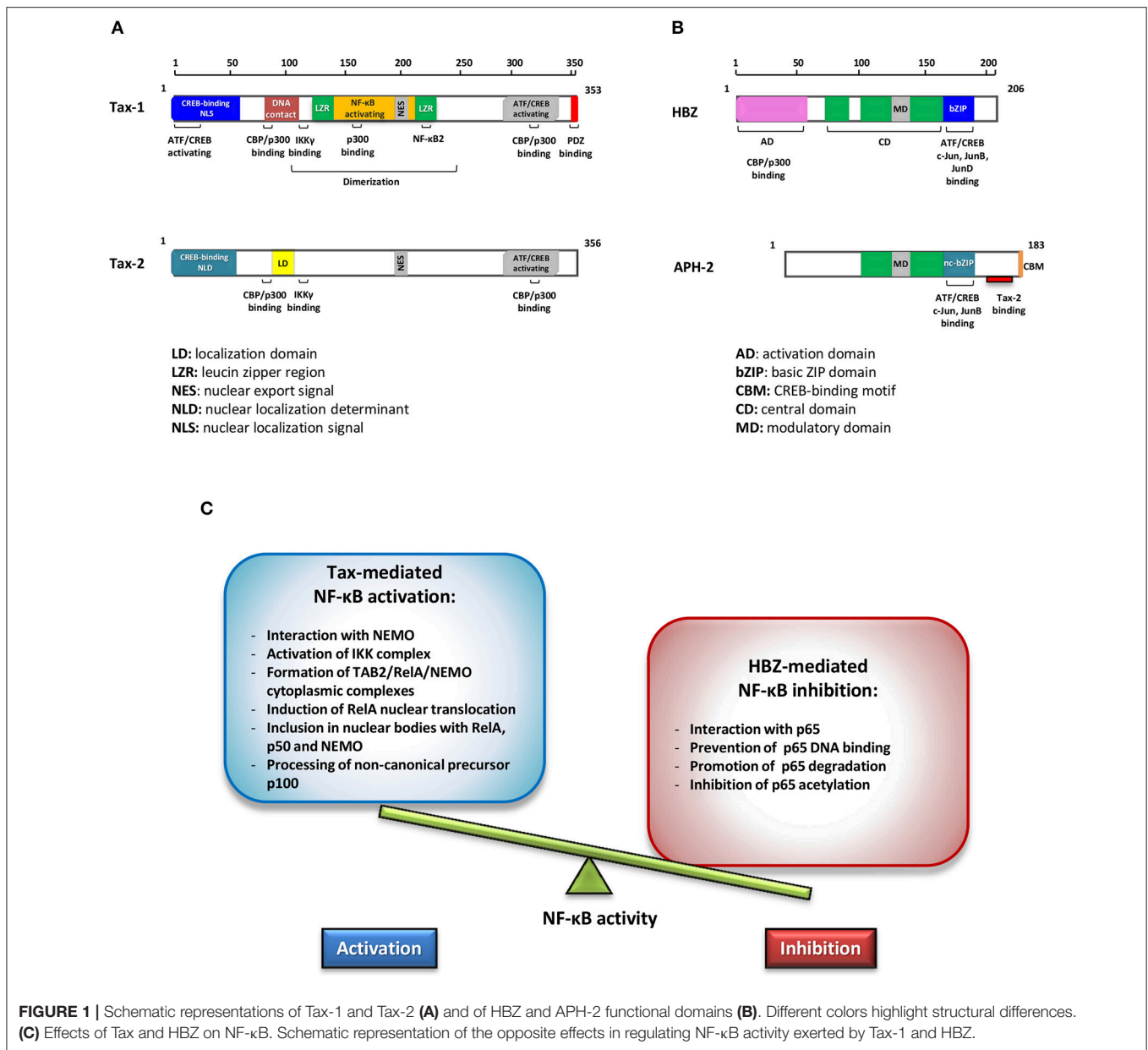
TAX-MEDIATED NF- κ B ACTIVATION

Two distinct pathways lead to NF- κ B activation, known as the canonical and the non-canonical pathways that involve different upstream, intermediate, and effector factors. A common step of both pathways is the activation of a complex that contains a serine-specific I κ B kinase (IKK) composed by two catalytic kinase subunits, IKK α and IKK β , and the regulatory non-enzymatic scaffold protein NEMO (known as IKK γ). In the canonical pathway, adaptor proteins (TRAFs) are recruited to the cytoplasmic domain of the cell membrane tumor necrosis

factor receptor (TNF-R) and activate the IKK complex thus inducing the phosphorylation of I κ B inhibitor and the seclusion of NF- κ B precursors within the cytoplasm (Sun, 2017). This phenomenon leads to I κ B degradation and nuclear translocation of the p50/RelA transcriptional effectors. At variance with the canonical pathway, the non-canonical one involves an IKK complex that does not contain NEMO, but two IKK α subunits. The NF- κ B-inducing kinase (NIK) activates the IKK complex, leading to p100 processing and the final release in the nucleus of p52/RelB active heterodimer (Durand and Baldwin, 2017).

Based on the study of the molecular mechanisms of NF- κ B activation driven by Tax-1, two relevant aspects emerged: the recruitment of Tax in cellular protein complexes (Bertazzoni et al., 2011; Qu and Xiao, 2011) and their post-translational modifications (Lavorgna and Harhaj, 2014). Studies comparing Tax-1 and Tax-2 have highlighted relevant differences in their activation of the NF- κ B pathway as a result of protein interaction: both proteins activate the classical pathway, but only Tax-1 activates the non-canonical one; Tax-1, unlike Tax-2, triggers the activation of the non-canonical pathway recruiting NEMO and IKK α to p100, promoting the processing of p100 to p52 (Xiao et al., 2001; Higuchi et al., 2007; Shoji et al., 2009); both Tax proteins interact with TAB2 and NEMO/IKK γ stimulating the translocation of the p50/RelA heterodimers into the nucleus, but only Tax-1 interacts with TRAF6, an E3 ligase that triggers the ubiquitination and activation of the downstream NF- κ B signaling cascade (Avesani et al., 2010; Journo et al., 2013). Furthermore, only Tax-1 interacts with the p52/p100 and RelB factors of the non-canonical pathway, inducing the expression of OX40L, a T-cell co-stimulatory molecule of the tumor necrosis factor family implicated in the adaptive immunity (Motai et al., 2016).

We have recently shown that Tax-1 and Tax-2 form complexes with two homologous non-canonical I κ B kinases, IKK ϵ and TBK1, which are not component of IKK complexes, but are implicated in the activation of NF- κ B, STAT3 and induction of IFN α (Shen and Hahn, 2011; Diani et al., 2015). An additional study demonstrating the presence of Tax and TBK1 in lipid raft microdomains along with canonical I κ B supports the role of Tax-1 as a promoter of the molecular crosstalk between the canonical IKKs and additional signaling pathways involved in cell survival and proliferation (Zhang et al., 2016). Interestingly, it has also been reported that Tax-1 forms complexes with the ubiquitin-conjugating enzyme Ubc13, NEMO, Tax1 binding protein1 (TAX1BP) and NRP/Optineurin in the membrane lipid rafts microdomain. In these complexes, the cell adhesion molecule 1 (CADM1) acts as a molecular scaffold recruiting Tax-1 (Pujari et al., 2015). This interaction contributes to the activation of the IKK complex and the inactivation of the NF- κ B negative regulator A20 enzyme, thus maintaining a persistent NF- κ B activation. An additional consequence of the Tax reorganization of the component of the lipid raft is the deregulation of autophagy. Tax-1, in fact, participates to the connection of the IKK complex to the autophagy molecular complexes by interacting directly with Beclin1 and PI3KC3 and contributing to the assembly of autophagosomes (Ren et al., 2012, 2015; Chen et al., 2015). Tax-1 induction of NF- κ B also increases the expression of inhibitors of apoptosis, such as the anti-apoptotic



c-Flip gene, and of genes involved in cell cycle progression, including cyclin D2, cyclin E, E2F1, CDK2, CDK4, and CDK6 (Wang et al., 2014; Bangham and Matsuoka, 2017; Karimi et al., 2017).

It has been recently reported that Tax-activation of NF-κB can be suppressed by host factors. Among them, the transcriptional regulator of the major histocompatibility complex class II (CIITA) impairs the nuclear translocation of RelA and directly interacts with Tax-1/RelA in nuclear bodies, preventing Tax-1 mediated activation of NF-κB-responsive promoters (Forlani et al., 2013, 2016). In addition, the apoptotic regulator Bcl-3 has been demonstrated to inhibit RelA nuclear translocation and its DNA binding activity, resulting in a downregulation of Tax-induced NF-κB activation (Wang et al., 2013). The decrease

in Tax-NF-κB activation could also be due to Tax proteasomal degradation induced by host factor interaction (Lavorgna and Harhaj, 2014). Tax-1 interaction with the molecular chaperone HSP90 was shown to protect Tax from proteasomal degradation (Gao and Harhaj, 2013), whereas the interaction with PDLIM2 (PDZ-LIM domain-containing protein) within the nuclear matrix induces its polyubiquitination-mediated proteasomal degradation (Yan et al., 2009; Fu et al., 2010). Furthermore, two tumor suppressor genes, MDFIC and MDFE, have been recently identified as Tax-1 interactors that alter its subcellular distribution and stability, reducing Tax-dependent activation of NF-κB (Kusano et al., 2015).

The second major mechanism required for Tax-1 and Tax-2 NF-κB activation is the process of post-translational

modification, which includes ubiquitination, SUMOylation and phosphorylation. It is well established that Tax phosphorylation is required for its nuclear translocation and stabilization in the nuclear bodies containing RelA (Bex et al., 1999; Turci et al., 2006). The requirements of ubiquitination and SUMOylation are more complex to define. Both the E2 enzyme Ubc13 and the E3 Ring Finger Protein 8 (RNF8) promote Tax K63-linked polyubiquitination and are essential for the activation of the IKK complex (Shembade et al., 2007; Ho et al., 2015). Other proteins, including E3 ubiquitin ligases, TRAF2, 5, or 6, can potentiate Tax polyubiquitination (Yu et al., 2008). SUMOylated Tax has been demonstrated to bind p300, RelA and NEMO in nuclear bodies (Nasr et al., 2006). In addition, SUMOylation of Tax may be involved in the regulation of Tax stability and NF- κ B pathway activation (Kfoury et al., 2011). We have described that SUMOylation and ubiquitination influence Tax proteins intracellular localization, as well as the interaction with NF- κ B factors and their transactivating activity (Turci et al., 2012). However, the role of Tax SUMOylation in NF- κ B activation remains controversial, given that Tax-induced IKK activation has been shown to correlate with the level of Tax ubiquitination, but not with Tax SUMOylation (Bonnet et al., 2012; Pène et al., 2014). A recent study suggests that Tax itself may function as an ubiquitin E3 ligase that, in association with the ubiquitin-conjugating enzyme E2, catalyzes the assembly of mixed polyUb chains (Wang et al., 2016). However, a more recent study does not attribute to Tax an E3 ligase activity, while suggesting that multivalent interactions between NEMO proteins and Ub-chains can lead to the formation of a macromolecular Taxisome and consequently to the activation of the IKK complex (Shibata et al., 2017).

An additional mechanism that operates within the cells to maintain the NF- κ B activation induced by Tax-1 is the positive feedback loop derived by NF- κ B target genes. A recent report describes that the over-expression of the early growth response protein 1 (EGR1) induced by Tax-1 activation of NF- κ B, results in the stabilization of EGR1 by direct interaction with Tax and nuclear translocation of p65, enhancing NF- κ B activation (Huang et al., 2017). A similar positive loop is fostered by the overexpression of the interleukin receptor IL-17RB. Tax-1 promotes the expression of IL-17RB by NF- κ B activation and establishes an IL-17RB-NF- κ B feed-forward autocrine loop that maintains persistent NF- κ B activation (Lavorgna et al., 2014).

TAX AND HBZ INTERPLAY ON NF- κ B DEREGULATION

HBZ can promote viral latency by antagonizing many of the activities mediated by Tax. HBZ inhibits the activation of the HTLV-1 5' LTR preventing the formation of the Tax transactivation complex (Gaudray et al., 2002; Clerc et al., 2008). The activation of the classical NF- κ B pathway by Tax is inhibited selectively by HBZ expression (Zhao et al., 2009; Wurm et al., 2012). This inhibition is connected to the following properties of HBZ as shown in **Figure 1C**: (a) the interaction with p65; (b) the inhibition of p65 DNA binding; (c) the enhanced degradation

of p65 through PDLIM2 E3 ubiquitin ligase; (d) the reduction of p65 acetylation. All these processes result in the reduction of the expression of several NF- κ B target genes. A typical example is the *cyclin D1* promoter gene, an essential regulator of the G1/S phase transition of the cell cycle that is overexpressed by Tax-mediated NF- κ B activation, while it is downregulated by HBZ interaction with p65 (Ma et al., 2017).

The HBZ inhibition of NF- κ B has been proposed to be a critical step in the oligoclonal expansion of HTLV-1-infected cells by downregulating the senescence process (Giam and Semmes, 2016). NF- κ B hyper-activation induced by Tax leads to the over-expression of the cyclin-dependent kinase inhibitors, p21 and p27, thus promoting an arrest of cell proliferation that triggers senescence. The proposed model envisages that in HTLV-1 infected cells, in which the p21/p27 functions is impaired, the HBZ downregulation of NF- κ B may contrast the senescence induced by Tax hence promoting the expansion of the infected cells (Kuo and Giam, 2006; Zhang et al., 2009; Zhi et al., 2011).

In contrast to HBZ, the HTLV-2 homolog protein APH-2 is dispensable for HTLV infection and persistence and does not promote T-cell proliferation *in vitro* (Yin et al., 2012; Barbeau et al., 2013). In addition, APH-2 expression correlates with the proviral load in HTLV-2 infected subjects and, contrary to HBZ, does not promote lymphocytosis (Saito et al., 2009; Douceron et al., 2012). Of note, HBZ and APH-2 also diverge in the interaction with Tax, since HBZ does not bind Tax-1, whereas Tax-2 interacts with APH-2 (Marban et al., 2012). A recent study has shown that despite HBZ and APH-2 interact with p65/RelA and repress its transactivation activity in transfected cells, they diverge in the induction of p65 degradation since this is not detected in the presence of APH-2 (Panfil et al., 2016). This different effect suggests that the two proteins may adopt different mechanisms to interfere with NF- κ B activation. The differences between regulatory proteins of HTLV-1 and HTLV-2 in deregulating NF- κ B are outlined in **Table 1**.

ROLE OF TAX AND HBZ IN ATL DEVELOPMENT

The opposite functions of Tax and HBZ in the regulation of signaling pathways and their effects in survival and proliferation appear as relevant steps during HTLV-1 cellular transformation and tumorigenesis (Giam and Semmes, 2016; Bangham and Matsuoka, 2017; Zhang et al., 2017). The absence of Tax expression in the late stages of the infection is linked to *tax* gene mutations and DNA methylation of the 5' LTR provirus (Furukawa et al., 2001; Koiwa et al., 2002). On the opposite, the 3' LTR negative strand remains intact and non-methylated, allowing HBZ to be systematically expressed in ATL cells (Taniguchi et al., 2005; Miyazaki et al., 2007). Unlike HBZ, Tax-1 is highly immunogenic and its inactivation may represent a fundamental strategy to evade the host immune system, a critical step in ATL development (Kogure and Kataoka, 2017). HBZ, like Tax-1, deregulates cell proliferation by targeting key factors implicated in cell survival. HBZ, in fact, binds to ATF3/p53 complexes and inhibits the p53 expression induced by ATF3, thus

TABLE 1 | Comparative effects of HTLV regulatory proteins on NF- κ B pathways.

	Tax-1	Tax-2	References
Canonical NF- κ B transactivation	+	+	Sun et al., 1994
Non-canonical NF- κ B transactivation	+	–	Higuchi et al., 2007
NF- κ B transactivation (lipid raft translocation of IKK)	+	–	Huang et al., 2009
Interaction with p100/p52	+	–	Shoji et al., 2009
Interaction with p65	+	+	Zhao et al., 2009; Panfil et al., 2016
	HBZ	APH-2	References
Canonical NF- κ B inhibition	+	+	Zhao et al., 2009; Panfil et al., 2016
Non-canonical NF- κ B inhibition	–	nd	Zhao et al., 2009
Interaction with p65	+	+	Zhao et al., 2009; Panfil et al., 2016
Inhibition of Tax-mediated transactivation of NF- κ B	+	nd	Zhao et al., 2009
Binding to Tax	–	+	Marban et al., 2012
Inhibition of p65 DNA binding capacity	+	nd	Zhao et al., 2009
p65 degradation	+	–	Panfil et al., 2016
Inhibition of p65 acetylation	+	nd	Wurm et al., 2012

nd, Not determined.

promoting ATL cells proliferation (Hagiya et al., 2011). HBZ also induces the expression of the anti-apoptotic genes *BCL2* and *Flip*, interacting with C/EBP α and deregulating the C/EBP signaling (Zhao et al., 2013). Both Tax-1 and HBZ are involved in the inhibition of the tumor suppressor p53. In particular, Tax inhibits p53 activity through the p65 subunit of NF- κ B or by sequestering p300/CBP from p53 (Ariumi et al., 2000; Karimi et al., 2017). Recent studies revealed that HBZ, by binding p300/CBP, inhibits p53 acetylation and decreases the p53 activity (Wright et al., 2016).

The selectivity of HBZ in inhibiting the classical NF- κ B pathway opens an interesting area of investigation on the role of the non-canonical NF- κ B pathway in tumorigenesis. During ATL development, HBZ might downmodulate the classical NF- κ B pathway more efficiently when Tax expression is silenced, leading to predominant activation of the alternative pathway (Zhao et al., 2009). It has also been demonstrated that freshly isolated ATL cells display high expression levels of NIK, persistent phosphorylation of I κ B α , aberrant processing of p52, and nuclear translocation of p50, p52, and RelB, despite the absence of Tax-1 expression (Chan and Greene, 2012).

Genetic and epigenetic alterations, including miRNAs expression profile, have been intensively investigated in the genome of ATL patients (Yeung et al., 2008; Bellon et al., 2009; Yamagishi and Watanabe, 2012; Watanabe, 2017). It has been proposed that the genomic instability may derive from Tax inhibition of DNA double-strand break repair and induction of micronuclei formation. ATL cells are characterized by frequent gain-of-function alterations of genes involved in the T-cell receptor/NF- κ B signaling pathway, such as PLCG1,

PKCB, and CARD11 or loss-of-function mutations in upstream factors, such as TRAF3 (Cook et al., 2017; Kogure and Kataoka, 2017). Mutations or intragenic deletions of these genes result in NF- κ B induction in the absence of Tax-1. A progressive epigenetic downregulation of *miR-31* has been demonstrated in ATL (Fujikawa et al., 2016). Of note, miR-31 negatively regulates the expression of NIK and miR-31 loss in ATL triggers the persistent activation of NF- κ B, inducing apoptosis resistance and contributing to the abnormal proliferation of cancer cells (Yamagishi et al., 2012). In addition, Fujikawa et al. (2016) showed that Tax-mediated NF- κ B activation induces the over-expression of the histone-lysine methyltransferase, EZH2, leading to host epigenetic machinery deregulation. It has been proposed that EZH2 may contribute to NF- κ B activation through miR-31 silencing and consequently NIK induction, in a positive feedback loop (Sasaki et al., 2011; Fujikawa et al., 2016). Genetic mutations have been also suggested to cause IL-17RB overexpression which triggers classical NF- κ B activation by an autocrine-loop in a subset of Tax-negative ATL cell lines (Lavorgna et al., 2014).

CONCLUSIONS AND PERSPECTIVES

HTLV-1 appears to benefit from the antagonistic functions of Tax and HBZ in the deregulation of cellular signaling pathways, resulting in the loss of control of many biological processes such as proliferation and survival of HTLV-1-infected cells. The interplay between Tax and HBZ on NF- κ B regulation has a prominent role in viral persistence in ATL cells, thus contributing to leukemic transformation. The intensive studies conducted in recent years aimed at understanding the effect of Tax constitutive activation and HBZ inhibition of NF- κ B have contributed to further elucidate the molecular mechanism of NF- κ B activation. However, several open questions about its functional role in ATL development still need to be addressed: the exact role of the persistent NF- κ B activation in ATL cells; the contribution to tumorigenesis of the alternative pathway activation; the role of the different mechanisms that are adopted by HBZ and APH-2 to interfere with NF- κ B activation; the dynamic organization of lipid raft complexes in HTLV-1 infected cell. It is hoped that the application of the CRISPR/Cas9 genome editing new technique will offer a useful tool to investigate the requirement of specific interactions of Tax and HBZ with cell factors that activate the mechanisms driving to tumorigenesis.

AUTHOR CONTRIBUTIONS

SF, SM, and MR wrote the review. SF, SM, UB, DZ, and MR participated in the conception and design of the review. All authors read and approved the final manuscript.

FUNDING

This study was supported by grants from University of Verona (FFO 2016 Romanelli) and University of Verona-Veneto Institute of Oncology. Joint Project 2016 grant (Romanelli).

REFERENCES

- Ariumi, Y., Kaida, A., Lin, J. Y., Hirota, M., Masui, O., Yamaoka, S., et al. (2000). HTLV-1 Tax oncoprotein represses the p53-mediated trans-activation function through coactivator CBP sequestration. *Oncogene* 19, 1491–1499. doi: 10.1038/sj.onc.1203450
- Avesani, F., Romanelli, M. G., Turci, M., Di Gennaro, G., Sampaio, C., Bidoia, C., et al. (2010). Association of HTLV Tax proteins with TAK1-binding protein 2 and RelA in calreticulin-containing cytoplasmic structures participates in Tax-mediated NF- κ B activation. *Virology* 408, 39–48. doi: 10.1016/j.virol.2010.08.023
- Bangham, C. R. M., and Matsuoka, M. (2017). Human T-cell leukaemia virus type 1: parasitism and pathogenesis. *Philos. Trans. R. Soc. Lond. B Biol. Sci.* 372:20160272. doi: 10.1098/rstb.2016.0272
- Barbeau, B., Peloponese, J. M., and Mesnard, J. M. (2013). Functional comparison of antisense proteins of HTLV-1 and HTLV-2 in viral pathogenesis. *Front. Microbiol.* 4:226. doi: 10.3389/fmicb.2013.00226
- Bellon, M., Lepelletier, Y., Hermine, O., and Nicot, C. (2009). Deregulation of microRNA involved in hematopoiesis and the immune response in HTLV-I adult T-cell leukemia. *Blood* 113, 4914–4917. doi: 10.1182/blood-2008-11-189845
- Bertazzoni, U., Turci, M., Avesani, F., Di Gennaro, G., Bidoia, C., and Romanelli, M. G. (2011). Intracellular localization and cellular factors interaction of HTLV-1 and HTLV-2 tax proteins: similarities and functional differences. *Viruses* 3, 541–560. doi: 10.3390/v3050541
- Bex, F., Murphy, K., Wattiez, R., Burny, A., and Gaynor, R. B. (1999). Phosphorylation of the human T-cell leukemia virus type 1 transactivator tax on adjacent serine residues is critical for tax activation. *J. Virol.* 73, 738–745.
- Bonnet, A., Randrianarison-huetz, V., Nzounza, P., Nedelec, M., Chazal, M., Waast, L., et al. (2012). Low nuclear body formation and tax SUMOylation do not prevent NF-kappaB promoter activation. *Retrovirology* 9:77. doi: 10.1186/1742-4690-9-77
- Chan, J. K., and Greene, W. C. (2012). Dynamic roles for NF- κ B in HTLV-I and HIV-1 retroviral pathogenesis. *Immunol. Rev.* 246, 286–310. doi: 10.1111/j.1600-065X.2012.01094.x
- Chen, L., Liu, D., Zhang, Y., Zhang, H., and Cheng, H. (2015). The autophagy molecule Beclin 1 maintains persistent activity of NF- κ B and Stat3 in HTLV-1-transformed T lymphocytes. *Biochem. Biophys. Res. Commun.* 465, 739–745. doi: 10.1016/j.bbrc.2015.08.070
- Clerc, I., Polakowski, N., André-Arpin, C., Cook, P., Barbeau, B., Mesnard, J. M., et al. (2008). An interaction between the human T cell leukemia virus type 1 basic leucine zipper factor (HBZ) and the KIX domain of p300/CBP contributes to the down-regulation of Tax-dependent viral transcription by HBZ. *J. Biol. Chem.* 283, 23903–23913. doi: 10.1074/jbc.M803116200
- Cook, L., Melamed, A., Yaguchi, H., and Bangham, C. R. (2017). The impact of HTLV-1 on the cellular genome. *Curr. Opin. Virol.* 26, 125–131. doi: 10.1016/j.coviro.2017.07.013
- Diani, E., Avesani, F., Bergamo, E., Cremonese, G., Bertazzoni, U., and Romanelli, M. G. (2015). HTLV-1 Tax protein recruitment into IKK ϵ and TBK1 kinase complexes enhances IFN-I expression. *Virology* 476, 92–99. doi: 10.1016/j.virol.2014.12.005
- Douceron, E., Kaidarova, Z., Miyazato, P., Matsuoka, M., Murphy, E. L., and Mahieux, R. (2012). HTLV-2 APH-2 expression is correlated with proviral load but APH-2 does not promote lymphocytosis. *J. Infect. Dis.* 205, 82–86. doi: 10.1093/infdis/jir708
- Durand, J. K., and Baldwin, A. S. (2017). Targeting IKK and NF- κ B for therapy. *Adv. Protein Chem. Struct. Biol.* 107, 77–115. doi: 10.1016/bs.apcsb.2016.11.006
- Forlani, G., Abdallah, R., Accolla, R. S., and Tosi, G. (2013). The MHC-II transactivator CIITA, a restriction factor against oncogenic HTLV-1 and HTLV-2 retroviruses: similarities and differences in the inhibition of Tax-1 and Tax-2 viral transactivators. *Front. Microbiol.* 4:234. doi: 10.3389/fmicb.2013.00234
- Forlani, G., Abdallah, R., Accolla, R. S., and Tosi, G. (2016). The major histocompatibility complex class II transactivator CIITA inhibits the persistent activation of NF- κ B by the human T cell lymphotropic virus type 1 Tax-1 oncoprotein. *J. Virol.* 90, 3708–3721. doi: 10.1128/JVI.03000-15
- Fu, J., Yan, P., Li, S., Qu, Z., and Xiao, G. (2010). Molecular determinants of PDLIM2 in suppressing HTLV-I Tax-mediated tumorigenesis. *Oncogene* 29, 6499–6507. doi: 10.1038/ncr.2010.374
- Fujikawa, D., Nakagawa, S., Hori, M., Kurokawa, N., Soejima, A., Nakano, K., et al. (2016). Polycomb-dependent epigenetic landscape in adult T-cell leukemia. *Blood* 127, 1790–1802. doi: 10.1182/blood-2015-08-662593
- Furukawa, Y., Kubota, R., Tara, M., Izumo, S., and Osame, M. (2001). Existence of escape mutant in HTLV-I tax during the development of adult T-cell leukemia. *Blood* 97, 987–993. doi: 10.1182/blood.V97.4.987
- Gallo, R. G., Willems, L., and Tagaya, Y. (2017). Time to go back to the original name. *Front. Microbiol.* 2017, 8:1800. doi: 10.3389/fmicb.2017.01800
- Gao, L., and Harhaj, E. W. (2013). HSP90 protects the human T-cell leukemia virus type 1 (HTLV-1) tax oncoprotein from proteasomal degradation to support NF- κ B activation and HTLV-1 replication. *J. Virol.* 87, 13640–13654. doi: 10.1128/JVI.02006-13
- Gaudray, G., Gachon, F., Basbous, J., Biard-Piechaczyk, M., Devaux, C., and Mesnard, J. M. (2002). The complementary strand of the human T-cell leukemia virus type 1 RNA genome encodes a bZIP transcription factor that down-regulates viral transcription. *J. Virol.* 76, 12813–12822. doi: 10.1128/JVI.76.24.12813-12822.2002
- Gessain, A., Barin, F., Vernant, J. C., Gout, O., Maurs, L., Calender, A., et al. (1985). Antibodies to human T-lymphotropic virus type-I in patients with tropical spastic paraparesis. *Lancet* 2, 407–410. doi: 10.1016/S0140-6736(85)92734-5
- Gessain, A., and Cassar, O. (2012). Epidemiological aspects and world distribution of HTLV-1 infection. *Front. Microbiol.* 3:388. doi: 10.3389/fmicb.2012.00388
- Giam, C. Z., and Semmes, O. J. (2016). HTLV-1 infection and adult T-cell leukemia/lymphoma—a tale of two proteins: Tax and HBZ. *Viruses* 8:E161. doi: 10.3390/v8060161
- Hagiya, K., Yasunaga, J. I., Satou, Y., Ohshima, K., and Matsuoka, M. (2011). ATF3, an HTLV-1 bZip factor binding protein, promotes proliferation of adult T-cell leukemia cells. *Retrovirology* 8:19. doi: 10.1186/1742-4690-8-19
- Higuchi, M., and Fujii, M. (2009). Distinct functions of HTLV-1 Tax1 from HTLV-2 Tax2 contribute key roles to viral pathogenesis. *Retrovirology* 6:117. doi: 10.1186/1742-4690-6-117
- Higuchi, M., Tsubata, C., Kondo, R., Yoshida, S., Takahashi, M., Oie, M., et al. (2007). Cooperation of NF-kappaB2/p100 activation and the PDZ domain binding motif signal in human T-cell leukemia virus type 1 (HTLV-1) Tax1 but not HTLV-2 Tax2 is crucial for interleukin-2-independent growth transformation of a T-cell line. *J. Virol.* 81, 11900–11907. doi: 10.1128/JVI.00532-07
- Hinuma, Y., Nagata, K., Hanaoka, M., Nakai, M., Matsumoto, T., Kinoshita, K. I., et al. (1981). Adult T-cell leukemia: antigen in an ATL cell line and detection of antibodies to the antigen in human sera. *Proc. Natl. Acad. Sci. U.S.A.* 78, 6476–6480. doi: 10.1073/pnas.78.10.6476
- Ho, Y. K., Zhi, H., Bowlin, T., Dorjbal, B., Philip, S., Zahoor, M. A., et al. (2015). HTLV-1 Tax stimulates ubiquitin E3 ligase, ring finger protein 8, to assemble lysine 63-linked polyubiquitin chains for TAK1 and IKK activation. *PLoS Pathog.* 11, 1–19. doi: 10.1371/journal.ppat.1005102
- Huang, J., Ren, T., Guan, H., Jiang, Y., and Cheng, H. (2009). HTLV-1 Tax is a critical lipid raft modulator that hijacks IkkappaB kinases to the microdomains for persistent activation of NF-kappaB. *J. Biol. Chem.* 284, 6208–6217. doi: 10.1074/jbc.M806390200
- Huang, Q., Niu, Z., Han, J., Liu, X., Lv, Z., Yuan, L., et al. (2017). HTLV-1 Tax upregulates early growth response protein 1 through nuclear factor- κ B signaling. *Oncotarget* 8, 51123–51133. doi: 10.18632/oncotarget.17699
- Journo, C., Bonnet, A., Favre-Bonvin, A., Turpin, J., Vainer, J., Côté, E., et al. (2013). Human T cell leukemia virus type 2 tax-mediated NF- κ B activation involves a mechanism independent of Tax conjugation to ubiquitin and SUMO. *J. Virol.* 87, 1123–1136. doi: 10.1128/JVI.01792-12
- Karimi, M., Mohammadi, H., Hemmatzadeh, M., Mohammadi, A., Rafatpanah, H., and Baradaran, B. (2017). Role of the HTLV-1 viral factors in the induction of apoptosis. *Biomed. Pharmacother.* 85, 334–347. doi: 10.1016/j.biopha.2016.11.034
- Kfoury, Y., Setterblad, N., El-Sabban, M., Dassouki, Z., El Hajj, H., et al. (2011). Tax ubiquitylation and SUMOylation control the dynamic shuttling of Tax and NEMO between Ubc9 nuclear bodies and the centrosome. *Blood* 117, 190–199. doi: 10.1182/blood-2010-05-285742
- Kogure, Y., and Kataoka, K. (2017). Genetic alterations in adult T-cell leukemia/lymphoma. *Cancer Sci.* 108, 1719–1725. doi: 10.1111/cas.13303

- Koiwa, T., Hamano-Usami, A., Ishida, T., Okayama, A., Yamaguchi, K., Kamiyama, S., et al. (2002). 5'-long terminal repeat-selective CpG methylation of latent human T-cell leukemia virus type 1 provirus *in vitro* and *in vivo*. *J. Virol.* 76, 9389–9397. doi: 10.1128/JVI.76.18.9389-9397.2002
- Kuo, Y. L., and Giam, C. Z. (2006). Activation of the anaphase promoting complex by HTLV-1 tax leads to senescence. *EMBO J.* 25, 1741–1752. doi: 10.1038/sj.emboj.7601054
- Kusano, S., Yoshimitsu, M., Hachiman, M., and Ikeda, M. (2015). I-mfa domain proteins specifically interact with HTLV-1 Tax and repress its transactivating functions. *Virology* 486, 219–227. doi: 10.1016/j.virol.2015.09.020
- Lavorgna, A., and Harhaj, E. W. (2014). Regulation of HTLV-1 tax stability, cellular trafficking and NF- κ B activation by the ubiquitin-proteasome pathway. *Viruses* 6, 3925–3943. doi: 10.3390/v6103925
- Lavorgna, A., Matsuoka, M., and Harhaj, E. W. (2014). A critical role for IL-17RB signaling in HTLV-1 tax-induced NF- κ B activation and T-cell transformation. *PLoS Pathog.* 10:e1004418. doi: 10.1371/journal.ppat.1004418
- Ma, G., Yasunaga, J., and Matsuoka, M. (2016). Multifaceted functions and roles of HBZ in HTLV-1 pathogenesis. *Retrovirology* 13:16. doi: 10.1186/s12977-016-0249-x
- Ma, Y., Zhang, B., Wang, D., Qian, L., Song, X., Wang, X., et al. (2017). HTLV-1 basic leucine zipper factor downregulates cyclin D1 expression via interactions with NF- κ B. *Int. J. Mol. Med.* 764–770. doi: 10.3892/ijmm.2017.2868
- Marban, C., McCabe, A., Bukong, T. N., Hall, W. W., and Sheehy, N. (2012). Interplay between the HTLV-2 Tax and APH-2 proteins in the regulation of the AP-1 pathway. *Retrovirology* 9:98. doi: 10.1186/1742-4690-9-98
- Matsuoka, M., and Jeang, K. T. (2007). Human T-cell leukaemia virus type 1 (HTLV-1) infectivity and cellular transformation. *Nat. Rev. Cancer* 7, 270–280. doi: 10.1038/nrc2111
- Miyazaki, M., Yasunaga, J. I., Taniguchi, Y., Tamiya, S., Nakahata, T., and Matsuoka, M. (2007). Preferential selection of human T-cell leukemia virus type 1 provirus lacking the 5' long terminal repeat during oncogenesis. *J. Virol.* 81, 5714–5723. doi: 10.1128/JVI.02511-06
- Motai, Y., Takahashi, M., Takachi, T., Higuchi, M., Hara, T., Mizuguchi, M., et al. (2016). Human T-cell leukemia virus type 1 (HTLV-1) Tax1 oncoprotein but not HTLV-2 Tax2 induces the expression of OX40 ligand by interacting with p52/p100 and RelB. *Virus Genes* 52, 4–13. doi: 10.1007/s11262-015-1277-7
- Nasr, R., Chiari, E., El-sabbah, M., Mahieux, R., Kfoury, Y., Abdulhay, M., et al. (2006). Tax ubiquitylation and sumoylation control critical cytoplasmic and nuclear steps of NF- κ B activation Tax ubiquitylation and sumoylation control critical cytoplasmic and nuclear steps of NF- κ B activation. *Blood* 107, 4021–4029. doi: 10.1182/blood-2005-09-3572
- Panfili, A. R., Dissinger, N. J., Howard, C. M., Murphy, B. M., Landes, K., Fernandez, S. A., et al. (2016). Functional comparison of HBZ and the related APH-2 protein provides insight into human T-cell leukemia virus type 1 pathogenesis. *J. Virol.* 90, 3760–3772. doi: 10.1128/JVI.03113-15
- Peloponese, J. M., Yeung, M. L., and Jeang, K. T. (2006). Modulation of nuclear factor-kappaB by human T cell leukemia virus type 1 Tax protein: implications for oncogenesis and inflammation. *Immunol. Res.* 34, 1–12. doi: 10.1385/IR:34:1:1
- Pène, S., Waast, L., Bonnet, A., Bénéit, L., and Pique, C. (2014). A non-SUMOylated tax protein is still functional for NF- κ B pathway activation. *J. Virol.* 88, 10655–10661. doi: 10.1128/JVI.01827-14
- Poesz, B. J., Ruscetti, F. W., Gazdar, A. F., Bunn, P. A., Minna, J. D., and Gallo, R. C. (1980). Detection and isolation of type C retrovirus particles from fresh and cultured lymphocytes of a patient with cutaneous T-cell lymphoma. *Proc. Nat. Acad. Sci. U.S.A.* 77, 7415–7419. doi: 10.1073/pnas.77.12.7415
- Pujari, R., Hunte, R., Thomas, R., van der Weyden, L., Rauch, D., Ratner, L., et al. (2015). Human T-cell leukemia virus type 1 (HTLV-1) tax requires CADM1/TSLC1 for inactivation of the NF- κ B inhibitor A20 and constitutive NF- κ B signaling. *PLoS Pathog.* 11:e1004721. doi: 10.1371/journal.ppat.1004721
- Qu, Z., and Xiao, G. (2011). Human T-cell lymphotropic virus: a model of NF- κ B-associated tumorigenesis. *Viruses* 3, 714–749. doi: 10.3390/v3060714
- Ren, T., Dong, W., Takahashi, Y., Xiang, D., Yuan, Y., Liu, X., et al. (2012). HTLV-2 tax immortalizes human CD4+ memory T lymphocytes by oncogenic activation and dysregulation of autophagy. *J. Biol. Chem.* 287, 34683–34693. doi: 10.1074/jbc.M112.377143
- Ren, T., Takahashi, Y., Liu, X., Loughran, T. P., Sun, S. C., Wang, H. G., et al. (2015). HTLV-1 Tax deregulates autophagy by recruiting autophagic molecules into lipid raft microdomains. *Oncogene* 34, 334–345. doi: 10.1038/nc.2013.552
- Romanelli, M. G., Diani, E., Bergamo, E., Casoli, C., Ciminale, V., Bex, F., et al. (2013). Highlights on distinctive structural and functional properties of HTLV Tax proteins. *Front. Microbiol.* 4:271. doi: 10.3389/fmicb.2013.00271
- Saito, M., Matsuzaki, T., Satou, Y., Yasunaga, J. I., Saito, K., Arimura, K., et al. (2009). *In vivo* expression of the HBZ gene of HTLV-1 correlates with proviral load, inflammatory markers and disease severity in HTLV-1 associated myelopathy/tropical spastic paraparesis (HAM/TSP). *Retrovirology* 6:19. doi: 10.1186/1742-4690-6-19
- Sasaki, D., Imaizumi, Y., Hasegawa, H., Osaka, A., Tsukasaki, K., Choi, Y. L., et al. (2011). Overexpression of enhancer of zeste homolog 2 with trimethylation of lysine 27 on histone H3 in adult T-cell leukemia/lymphoma as a target for epigenetic therapy. *Haematologica* 96, 712–719. doi: 10.3324/haematol.2010.028605
- Shembade, N., Harhaj, N. S., Yamamoto, M., Akira, S., and Harhaj, E. W. (2007). The human T-cell leukemia virus type 1 Tax oncoprotein requires the ubiquitin-conjugating enzyme Ubc13 for NF- κ B activation. *J. Virol.* 81, 13735–13742. doi: 10.1128/JVI.01790-07
- Shen, R. R., and Hahn, W. C. (2011). Emerging roles for the non-canonical IKKs in cancer. *Oncogene* 30, 631–641. doi: 10.1038/nc.2010.493
- Shibata, Y., Tokunaga, F., Goto, E., Komatsu, G., Gohda, J., Saeki, Y., et al. (2017). HTLV-1 Tax induces formation of the active macromolecular IKK complex by generating Lys63- and Met1-linked hybrid polyubiquitin Chains. *PLoS Pathog.* 13, 1–25. doi: 10.1371/journal.ppat.1006162
- Shoji, T., Higuchi, M., Kondo, R., Takahashi, M., Oie, M., Tanaka, Y., et al. (2009). Identification of a novel motif responsible for the distinctive transforming activity of human T-cell leukemia virus (HTLV) type 1 Tax1 protein from HTLV-2 Tax2. *Retrovirology* 6:83. doi: 10.1186/1742-4690-6-83
- Sun, S. C. (2017). The non-canonical NF- κ B pathway in immunity and inflammation. *Nat. Rev. Immunol.* 17, 545–558. doi: 10.1038/nri.2017.52
- Sun, S. C., Elwood, J., Béraud, C., and Greene, W. C. (1994). Human T-cell leukemia virus type I Tax activation of NF- κ B/Rel involves phosphorylation and degradation of I kappa B alpha and RelA (p65)-mediated induction of the c-rel gene. *Mol. Cell. Biol.* 14, 7377–7384. doi: 10.1128/MCB.14.11.7377
- Taniguchi, Y., Nosaka, K., Yasunaga, J., Maeda, M., Mueller, N., Okayama, A., et al. (2005). Silencing of human T-cell leukemia virus type I gene transcription by epigenetic mechanisms. *Retrovirology* 2:64. doi: 10.1186/1742-4690-2-64
- Turci, M., Lodewick, J., Di Gennaro, G., Rinaldi, A. S., Marin, O., Diani, E., et al. (2012). Ubiquitination and sumoylation of the HTLV-2 Tax-2B protein regulate its NF- κ B activity: a comparative study with the HTLV-1 Tax-1 protein. *Retrovirology* 9:102. doi: 10.1186/1742-4690-9-102
- Turci, M., Romanelli, M. G., Lorenzi, P., Righi, P., and Bertazzoni, U. (2006). Localization of human T-cell lymphotropic virus type II Tax protein is dependent upon a nuclear localization determinant in the N-terminal region. *Gene* 365, 119–124. doi: 10.1016/j.gene.2005.09.043
- Wang, C., Long, W., Peng, C., Hu, L., Zhang, Q., Wu, A., et al. (2016). HTLV-1 Tax functions as a ubiquitin E3 ligase for direct IKK activation via synthesis of mixed-linkage polyubiquitin Chains. *PLoS Pathog.* 12, 1–25. doi: 10.1371/journal.ppat.1005584
- Wang, J., Li, J., Huang, Y., Song, X., Niu, Z., Gao, Z., et al. (2013). Bcl-3 suppresses Tax-induced NF- κ B activation through p65 nuclear translocation blockage in HTLV-1-infected cells. *Int. J. Oncol.* 42, 269–276. doi: 10.3892/ijo.2012.1685
- Wang, W., Zhou, J., Shi, J., Zhang, Y., Liu, S., Liu, Y., et al. (2014). Human T-cell leukemia virus type 1 Tax-deregulated autophagy pathway and c-FLIP expression contribute to resistance against death receptor-mediated apoptosis. *J. Virol.* 88, 2786–2798. doi: 10.1128/JVI.03025-13
- Watanabe, T. (2017). Adult T-cell leukemia: molecular basis for clonal expansion and transformation of HTLV-1-infected T cells. *Blood* 129, 1071–1081. doi: 10.1182/blood-2016-09-692574
- Willems, L., Hasegawa, H., Accolla, R., Bangham, C., Bazarbachi, A., Bertazzoni, U., et al. (2017). Reducing the global burden of HTLV-1 infection: an agenda for research and action. *Antiviral Res.* 137, 41–48. doi: 10.1016/j.antiviral.2016.10.015
- Wright, D. G., Marchal, C., Hoang, K., Ankney, J. A., Nguyen, S. T., Rushing, A. W., et al. (2016). Human T-cell leukemia virus type-1-encoded protein HBZ

- represses p53 function by inhibiting the acetyltransferase activity of p300/CBP and HBO1. *Oncotarget* 7, 1687–1706. doi: 10.18632/oncotarget.6424
- Wurm, T., Wright, D. G., Polakowski, N., Mesnard, J. M., and Lemasson, I. (2012). The HTLV-1-encoded protein HBZ directly inhibits the acetyl transferase activity of p300/CBP. *Nucleic Acids Res.* 40, 5910–5925. doi: 10.1093/nar/gks244
- Xiao, G., Cvijic, M. E., Fong, A., Harhaj, E. W., Uhlik, M. T., Waterfield, M., et al. (2001). Retroviral oncoprotein Tax induces processing of NF-kappaB2/p100 in T cells: evidence for the involvement of IKKalpha. *EMBO J.* 20, 6805–6815. doi: 10.1016/j.emboj.20.23.6805
- Yamagishi, M., Nakano, K., Miyake, A., Yamochi, T., Kagami, Y., Tsutsumi, A., et al. (2012). Polycomb-mediated loss of miR-31 activates NIK-dependent NF- κ B pathway in adult T cell leukemia and other cancers. *Cancer Cell* 21, 121–135. doi: 10.1016/j.ccr.2011.12.015
- Yamagishi, M., and Watanabe, T. (2012). Molecular hallmarks of adult T cell leukemia. *Front. Microbiol.* 3:334. doi: 10.3389/fmicb.2012.00334
- Yan, P., Fu, J., Qu, Z., Li, S., Tanaka, T., Grusby, M. J., et al. (2009). PDLIM2 suppresses human T-cell leukemia virus type I Tax-mediated tumorigenesis by targeting Tax into the nuclear matrix for proteasomal degradation. *Blood* 113, 4370–4380. doi: 10.1182/blood-2008-10-185660
- Yasuma, K., Yasunaga, J. I., Takemoto, K., Sugata, K., Mitobe, Y., Takenouchi, N., et al. (2016). HTLV-1 bZIP factor impairs anti-viral immunity by inducing co-inhibitory molecule, T cell immunoglobulin and ITIM domain (TIGIT). *PLoS Pathog.* 12, 1–22. doi: 10.1371/journal.ppat.1005372
- Yeung, M. L., Yasunaga, J., Bennasser, Y., Dusetti, N., Harris, D., Ahmad, N., et al. (2008). Roles for microRNAs, miR-93 and miR-130b, and tumor protein 53-induced nuclear protein 1 tumor suppressor in cell growth dysregulation by human T-cell lymphotropic virus 1. *Cancer Res.* 68, 8976–8985. doi: 10.1158/0008-5472.CAN-08-0769
- Yin, H., Kannian, P., Dissinger, N., Haines, R., Niewiesk, S., and Green, P. L. (2012). Human T-cell leukemia virus type 2 antisense viral protein 2 is dispensable for *in vitro* immortalization but functions to repress early virus replication *in vivo*. *J. Virol.* 86, 8412–8421. doi: 10.1128/JVI.00717-12
- Yu, Q., Minoda, Y., Yoshida, R., Yoshida, H., Iha, H., Kobayashi, T., et al. (2008). HTLV-1 Tax-mediated TAK1 activation involves TAB2 adapter protein. *Biochem. Biophys. Res. Commun.* 365, 189–194. doi: 10.1016/j.bbrc.2007.10.172
- Zhang, H., Chen, L., Cai, S. H., and Cheng, H. (2016). Identification of TBK1 and IKK ϵ , the non-canonical I κ B kinases, as crucial pro-survival factors in HTLV-1-transformed T lymphocytes. *Leuk. Res.* 46, 37–44. doi: 10.1016/j.leukres.2016.04.012
- Zhang, L. L., Wei, J., Wang, L., Huang, S., and Chen, J. L. (2017). Human T-cell lymphotropic virus type 1 and its oncogenesis. *Acta Pharmacol. Sin.* 38, 1093–1103. doi: 10.1038/aps.2017.17
- Zhang, L., Zhi, H., Liu, M., Kuo, Y. L., and Giam, C. Z. (2009). Induction of p21(CIP1/WAF1) expression by human T-lymphotropic virus type 1 Tax requires transcriptional activation and mRNA stabilization. *Retrovirology* 6:35. doi: 10.1186/1742-4690-6-35
- Zhao, T. (2016). The role of HBZ in HTLV-1-induced oncogenesis. *Viruses* 8, 1–12. doi: 10.3390/v8020034
- Zhao, T., Coutts, A., Xu, L., Yu, J., Ohshima, K., and Matsuoka, M. (2013). HTLV-1 bZIP factor supports proliferation of adult T cell leukemia cells through suppression of C/EBP α signaling. *Retrovirology* 10:159. doi: 10.1186/1742-4690-10-159
- Zhao, T., and Matsuoka, M. (2012). HBZ and its roles in HTLV-1 oncogenesis. *Front. Microbiol.* 3:247. doi: 10.3389/fmicb.2012.00247
- Zhao, T., Yasunaga, J., Satou, Y., Nakao, M., Takahashi, M., Fujii, M., et al. (2009). Human T-cell leukemia virus type 1 bZIP factor selectively suppresses the classical pathway of NF-kappaB. *Blood* 113, 2755–2764. doi: 10.1182/blood-2008-06-161729
- Zhi, H., Yang, L., Kuo, Y. L., Ho, Y. K., Shih, H. M., and Giam, C. Z. (2011). NF- κ B hyper-activation by HTLV-1 tax induces cellular senescence, but can be alleviated by the viral anti-sense protein HBZ. *PLoS Pathog.* 7, 1–12. doi: 10.1371/journal.ppat.1002025

Conflict of Interest Statement: The authors declare that the research was conducted in the absence of any commercial or financial relationships that could be construed as a potential conflict of interest.

The reviewer JY and handling Editor declared their shared affiliation.

Copyright © 2018 Fochi, Mutascio, Bertazzoni, Zipeto and Romanelli. This is an open-access article distributed under the terms of the Creative Commons Attribution License (CC BY). The use, distribution or reproduction in other forums is permitted, provided the original author(s) and the copyright owner are credited and that the original publication in this journal is cited, in accordance with accepted academic practice. No use, distribution or reproduction is permitted which does not comply with these terms.



HIV-1-Associated Neurocognitive Disorders: Is HLA-C Binding Stability to β_2 -Microglobulin a Missing Piece of the Pathogenetic Puzzle?

Donato Zipeto^{1*}, Michela Serena¹, Simona Mutascio¹, Francesca Parolini¹, Erica Diani², Elisabetta Guizzardi³, Valentina Muraro³, Emanuela Lattuada⁴, Sebastiano Rizzardo⁴, Marina Malena⁵, Massimiliano Lanzafame⁴, Giovanni Malerba¹, Maria Grazia Romanelli¹, Stefano Tamburin¹ and Davide Gibellini²

OPEN ACCESS

Edited by:

Avindra Nath,
National Institute of Neurological
Disorders and Stroke (NINDS),
United States

Reviewed by:

Dianne T. Langford,
Lewis Katz School of Medicine,
Temple University, United States
Olimpia Meucci,
College of Medicine, Drexel University,
United States

*Correspondence:

Donato Zipeto
donato.zipeto@univr.it

Specialty section:

This article was submitted to
Neuroinfectious Diseases,
a section of the journal
Frontiers in Neurology

Received: 20 June 2018

Accepted: 03 September 2018

Published: 21 September 2018

Citation:

Zipeto D, Serena M, Mutascio S,
Parolini F, Diani E, Guizzardi E,
Muraro V, Lattuada E, Rizzardo S,
Malena M, Lanzafame M, Malerba G,
Romanelli MG, Tamburin S and
Gibellini D (2018) HIV-1-Associated
Neurocognitive Disorders: Is HLA-C
Binding Stability to β_2 -Microglobulin a
Missing Piece of the Pathogenetic
Puzzle? *Front. Neurol.* 9:791.
doi: 10.3389/fneur.2018.00791

¹ Department of Neurosciences, Biomedicine and Movement Sciences, University of Verona, Verona, Italy, ² Department of Diagnostics and Public Health, University of Verona, Verona, Italy, ³ Service of Transfusion Medicine, AOUI, Verona, Italy, ⁴ U.O.C. Infectious Diseases, AOUI, Verona, Italy, ⁵ U.O.S. Infectious Diseases, AULSS 9 Scaligera, Verona, Italy

AIDS dementia complex (ADC) and HIV-associated neurocognitive disorders (HAND) are complications of HIV-1 infection. Viral infections are risk factors for the development of neurodegenerative disorders. Aging is associated with low-grade inflammation in the brain, i.e., the inflammaging. The molecular mechanisms linking immunosenescence, inflammaging and the pathogenesis of neurodegenerative disorders, such as Alzheimer's disease (AD) and Parkinson's disease, are largely unknown. ADC and HAND share some pathological features with AD and may offer some hints on the relationship between viral infections, neuroinflammation, and neurodegeneration. β_2 -microglobulin (β_2m) is an important pro-aging factor that interferes with neurogenesis and worsens cognitive functions. Several studies published in the 80–90s reported high levels of β_2m in the cerebrospinal fluid of patients with ADC. High levels of β_2m have also been detected in AD. Inflammatory diseases in elderly people are associated with polymorphisms of the MHC-I locus encoding HLA molecules that, by associating with β_2m , contribute to cellular immunity. We recently reported that HLA-C, no longer associated with β_2m , is incorporated into HIV-1 virions, determining an increase in viral infectivity. We also documented the presence of HLA-C variants more or less stably linked to β_2m . These observations led us to hypothesize that some variants of HLA-C, in the presence of viral infections, could determine a greater release and accumulation of β_2m , which in turn, may be involved in triggering and/or sustaining neuroinflammation. ADC is the most severe form of HAND. To explore the role of HLA-C in ADC pathogenesis, we analyzed the frequency of HLA-C variants with unstable binding to β_2m in a group of patients with ADC. We found a higher frequency of unstable HLA-C alleles in ADC patients, and none of them was harboring stable HLA-C alleles in homozygosis. Our data suggest that the role of HLA-C variants in ADC/HAND pathogenesis deserves further studies. If

confirmed in a larger number of samples, this finding may have practical implication for a personalized medicine approach and for developing new therapies to prevent HAND. The exploration of HLA-C variants as risk factors for AD and other neurodegenerative disorders may be a promising field of study.

Keywords: HIV, AIDS, HLA, AIDS dementia complex (ADC), HIV-associated neurocognitive disorders (HAND), β_2 -microglobulin (β_2m)

INTRODUCTION

Neurovirulence is detectable in patients infected with human immunodeficiency virus type 1 (HIV-1) both in the early (i.e., acute infection) and the later stages of the disease. During the acute infection, 25–50% of HIV-1 patients show neurological symptoms within 3–6 weeks after infection whereas central nervous system (CNS) complications appear, to a variable extent, during the course of HIV-1 infection (1). In early studies on HIV-1 neurovirulence, the neurological syndromes were well described, and the most severe CNS form was defined as AIDS dementia complex (ADC) (2).

The cerebral complications of HIV-1 infection, which include disturbances of cognitive, behavioral, motor and autonomic functions, still represent an issue in everyday practice (3). The old concept of ADC (2, 4), a condition not commonly encountered today in Western countries because of the wide use of combination antiretroviral treatment (cART), has been replaced by the wider term HIV-associated neurocognitive disorders (HAND) (3, 5). HAND encompasses cognitive syndromes caused by HIV-1 itself, as opposed to opportunistic infections, and includes HIV-1-associated asymptomatic neurocognitive impairment (ANI), HIV-1-associated mild neurocognitive disorder (MND), and HIV-1-associated dementia (HAD) (5), the latter conditions corresponding to ADC.

HAD represents the most severe form of the spectrum of HIV-related CNS syndromes. Risk factors for HAD were reported by several studies and they include nadir CD4 count, increasing age, substance abuse, anemia, viral co-infection and viral clade subtypes (6, 7). Before the introduction of cART, the prevalence of dementia showed an annual incidence of 7% among subjects in the later stages of infection (4). Following cART introduction, HAD cases dramatically decreased, as newly diagnosed moderate to severe dementia changed from 6.6% in 1989 to 1% in 2000 (8).

The pathogenesis of CNS damage by HIV-1 is multifactorial and mediated by direct and indirect mechanisms (9). The early detection of acute meningoencephalitis in several patients indicates a rapid involvement of the brain (10). HIV-1 enters the CNS either via infected monocytes and lymphocytes or through choroid plexus infection (11, 12). The impairment of the blood-brain barrier is associated with inflammation by cytokine-driven mechanisms. In the brain, HIV-1 mainly replicates in macrophage/microglial cells thus determining the onset of chronic local inflammation. The pathological hallmark of HIV-1 infection in the brain is represented by multinucleated giant cells, which are formed by cellular syncytia of HIV-1 infected macrophages (2, 13). In addition, HIV-1 infection of astrocytes

was detected in patients with HIV-1 associated encephalopathy (14). It is noteworthy that astrocyte activation and increased glial fibrillary acidic protein expression do not represent a specific response to HIV-1 infection, but are associated with other neurological conditions, such as neurodegenerative diseases (15, 16).

The persistent HIV-1 infection in the macrophages and microglia causes the releases of the phospholipid ligand PAF, glutamate, arachidonic acid, quinolinic acid, nitric oxide, and several pro-inflammatory cytokines including IL-1 β , IL-6, TNF α , and TRAIL: all these factors are involved in neural damage (12, 17–23).

Persistent CNS inflammation and chronic immune activation play an important role in the pathogenesis of neurological diseases (24) where inflammatory mediators, such as neopterin, quinolinic acid, monocyte chemoattractant protein 1 and β_2 -microglobulin (β_2m) were found to be increased (25). Importantly, these markers are also elevated in the CSF from patients with HAD suggesting that increased immune activation is related to more severe damage.

Most likely, the complexity of the pathogenetic model is not related to a one-dimensional and direct pathogenetic event, but rather to multi-dimensional and complex immunopathological processes that are governed by viral as well as by host factors (3).

β_2 -Microglobulin, HLA-C Variants and HIV Infection

Several old studies reported abnormally high β_2m levels in sera of HIV-1 infected patients with high p24 concentrations and a reduced number of lymphocytes (26–28). High levels of β_2m were also detected in the cerebrospinal fluid (CSF) of HIV-1 infected patients with ADC (29–32). HIV-infected individuals without dementia showed a consistent correlation between β_2m levels in plasma and CSF. Contrarily in patients with dementia, CSF β_2m level was found to be increased independently from that in plasma β_2m levels, indicating intrathecal β_2m production, which was proposed to be used as a marker for HIV-1 dementia (25). This association between β_2m high levels and HIV-1 infection has never been fully explained and clarified.

β_2m is associated with HLA proteins (A, B, or C) and a small peptide forming the major histocompatibility complex type I (MHC-I), which plays an important role in the activation and modulation of cellular immunity. The interaction between β_2m and HLA in the MHC-I complex stabilizes the structure of β_2m (33).

The immune complex made by HLA-C, β_2m , and peptide expressed on the cell surface tends to dissociate and to generate

a pool of free-chains molecules devoid of β_2m . This higher HLA-C instability, compared to HLA-A and -B, is caused by the presence of a specific amino acid sequence in the groove that binds the peptide (34), which reduces its plasticity and increases its instability (35).

The binding stability of different HLA-C variants and β_2m was documented through the analysis of the relationship between free and β_2m associated HLA-C molecules (35). Recently, differences in specific HLA-C domains were reported to influence the peptide binding stability (36), supporting the hypothesis of the existence of HLA-C variants with a higher or a lower binding stability to β_2m .

We previously reported that HLA-C is incorporated on HIV-1 virions increasing their infectivity (37–39), that the expression of HIV-1 Env on the cell membrane promotes the formation of HLA-C molecules as free-chain, no longer bound to β_2m (40) and that HLA-C variants bind more or less strongly to β_2m . We showed that some HLA-C variants may be predominantly associated with β_2m on the cell membrane, while other ones are predominant as free-chains, dissociated from β_2m (41). In the same study, we reported that some unstable HLA-C variants, such as C*03 or C*07, are also the ones previously described to have a low expression level, while some stable variants such as C*02, C*06, C*12, or C*16, are highly transcribed and expressed (41). HLA-C expression has been associated with a different ability to control HIV-1 infection, with high HLA-C expression levels associated to a better control of HIV-1 infection, and low HLA-C expression levels associated with poor HIV-1 control and rapid progression to AIDS (42–44).

β_2m -Microglobulin: A Possible Pathogenetic Role in HAND and Neurodegeneration

β_2m is one of the main markers of immune activation and inflammation in CSF in HAND (25, 45, 46).

In the CNS, β_2m is involved in the regulation of brain development and plasticity of synapses (47–49). High levels of β_2m are potentially neurotoxic, and β_2m reduction has a protective effect in animal models of dementia (50). β_2m has also been reported to be a pro-aging factor impairing cognitive functions (51).

β_2m is responsible for “dialysis-related amyloidosis,” a clinical condition that is caused by β_2m accumulation as insoluble protein aggregate (52) in joints, bones, and muscles (53). Studies on fatal hereditary systemic amyloidosis identified a natural variant of β_2m which shows a dramatic decrease in thermodynamic stability and a remarkable increase in aggregation propensity (54, 55).

Of interest, high CSF levels of β_2m were detected in neurodegenerative conditions, such as Alzheimer’s disease (AD) and Parkinson’s disease (PD) (56–59), which are caused by protein misfolding and abnormal aggregation (60), but the potential pathogenetic significance of this finding is still unclear.

Symptomatic similarities between HAND/ADC and AD have been documented (61). It has been shown that the Apo- $\epsilon 4$ haplotype, a known risk factor for AD, enhances the infectivity

of HIV-1 (62) and that HIV-infected patients harboring the Apo- $\epsilon 4$ allele have excess dementia and peripheral neuropathy (63). ApoE has been found to stabilize and enhance the deposition of β_2m amyloid fibrils (62, 64–67). In addition, the pathogenesis and clearance of the amyloid- β peptide ($A\beta$), the pathological hallmark feature of AD, may be influenced by HIV-1 infection. Enhanced amyloidosis has been reported in patients with HAND (68). Neurofibrillary tangles containing hyperphosphorylated tau protein are a pathological hallmark of AD. A significantly higher concentration of tau has been reported in brain tissues of HAD patients (68–71). The loss of neuroprotective functions of microglial cells has been suggested to contribute to the development of AD. A similar phenomenon is observed in HIV-infected patients since the virus can infect microglial cells, and loss of neuroprotection might trigger neurodegenerative process, leading to HAD (72).

After the report of patients with AD pathology and HIV-1 infection, the hypothesis that HIV-1 could create conditions ripe for AD development, and that a link between the two diseases does exist, has been considered (73). The view that ADC and AD share some pathogenetic pathways may pave the way for future studies comparing the commonalities between the two conditions.

Inflammaging, Viral Infections, and Neurodegenerative Diseases

The term “inflammaging” characterizes a widely accepted paradigm that aging is accompanied by a low-grade chronic up-regulation of pro-inflammatory responses (74). Inflammaging is supposed to interact with processing and production of $A\beta$ and to be important in the prodromal phase of AD (75). Chronic viral infections may contribute to inflammaging. Infections caused by cytomegalovirus (CMV) (76), herpes simplex (HSV) I (77–79), human herpes virus 6 (80), varicella zoster, Epstein-Barr, influenza, arboviruses, rabies and polyoma viruses, coxsackie and other enteroviruses, echoviruses (81, 82) have all been suspected to be associated with increased risk of developing CNS and neurodegenerative diseases, such as AD (83) and PD (84). β_2m is involved in several viral infections, such as CMV, HSV, coxsackieviruses, echoviruses, and others (81, 82, 85–88). CMV has the ability to remove β_2m from MHC-I molecules when it binds to cells it will infect (86–88), and to express an MHC-I homolog that binds and sequesters β_2m (89). A very recent study reports that cell-free particles from the respiratory syncytial virus (RSV) and HSV type 1 may catalyze amyloid aggregation in the extracellular environment, suggesting a new connection between viral infections and neurodegenerative diseases (90).

We thus hypothesized that some HLA-C variants which more easily dissociate from β_2m will have a higher proportion of free heavy chains, increasing HIV-1 infectivity and promoting β_2m release, which in turn may contribute to chronic inflammation and may be involved in the pathogenesis of HAND. Similar phenomena may also contribute to the pathogenesis of neurodegenerative conditions such as AD and PD, potentially triggered by other infectious agents.

MATERIALS AND METHODS

Participants

With the introduction of cART for HIV-1, patients developing ADC have become rare; as a consequence, we were able to collect only a very limited number of subjects. From a database of almost 1100 HIV-infected subjects followed since 1985 by the Infectious Diseases Outpatient Clinic, Azienda Ospedaliera Universitaria Integrata Verona, we retrospectively selected patients who had an unequivocal diagnosis of ADC. Among these, only 11 were still available for blood sample collection and DNA extraction and analysis. We analyzed HLA-C variants in 11 HIV-1 infected individuals with ADC/HAD (HIV-ADC group), which was diagnosed using standardized brain imaging and neuropsychological criteria (91, 92).

This study was carried out in accordance with the recommendations of the Declaration of Helsinki. The protocol was approved by the Institutional Review Board of the University of Verona. All the patients, or their tutors in case of severe dementia, gave written informed consent to participate in the study.

The baseline characteristics of the patients (9 men, 2 women) are shown in **Table 1**. The patients had a median age of 50 years (interquartile range, IQR 39–58); all of them were naive to antiretroviral treatment. CD4+ T lymphocyte count and HIV RNA load were determined at ADC diagnosis. The median CD4+ T lymphocytes nadir was 50 cells/mm³ (IQR 26–157), while the median plasmatic zenith HIV-RNA viral load was 71350 copies/mL (IQR 22300–141000). A lumbar puncture was performed in 9 patients at the time when ADC was diagnosed, with a median CSF HIV-RNA viral load of 204000 copies/mL (IQR 70085–511500). The diagnosis of ADC was made using, in addition to CSF HIV-RNA viral load, brain MRI, minimal state examination (MMSE), and full neuropsychological evaluation. The most common findings observed on brain MRI were symmetric periventricular and deep white matter T2 hyperintensity and widespread cerebral atrophy. MMSE was <25 in all ADC patients. A full neuropsychological evaluation was performed in 4 patients and showed mild-to-moderate dementia. The severity of dementia in the remaining 7 patients made full neuropsychological testing difficult.

We collected a control group of 16 HIV-infected patients (14 men, 2 women; median age: 46.5 years, IQR 35.5–51) with no neurocognitive disorders and MMSE \geq 25 (HIV-no-ADC group), whose baseline characteristics are reported in **Table 2**. Gender and age did not significantly differ between patients and control groups.

Patients were classified according to the CDC 1993 classification system, whereby HIV infection was divided into three clinical categories (i.e., A, B and C). Category A included the patients with asymptomatic acute (primary) infection or persistent generalized lymphadenopathy. Category C included the patients with AIDS-indicator conditions. The symptomatic patients, who could not be classified in categories A or C, were included in B one. HIV positive patients were further sub-grouped according to the absolute lymphocyte T CD4+ count (i.e., 1: >500 cells/ μ L; 2: 200–499 cells/ μ L; 3:

<200 cells/ μ L) (93). According to the CDC 1993 classification, HIV-related neurological complications were described as HIV-related encephalopathy and associated to category C. Hence, HIV positive patients with ADC were classified in category C, as was the case for our 11 HIV-ADC patients (**Table 1**).

HLA-C Typing

HLA-C alleles were classified as unstable (HLA-C*01, *03, *04, *07, *14, *17, *18) or stable (C*02, *05, *06, *08, *12, *15, *16) according to previous phylogenetic, structural and densitometry findings (35, 36, 41, 94).

HLA-C typing was carried out at the HLA laboratory of tissue typing, Azienda Ospedaliera Universitaria Integrata (AOUI) of Verona. The laboratory is accredited by the European Federation of Immunogenetics (EFI) since 1999.

DNA was prepared from whole blood using the QIAamp DNA Blood Kit (Qiagen) and HLA-C phototyping was performed by PCR-SSP using the commercial kit “HLA-C SSP kit” BioRad, followed by gel electrophoresis for the detection of positive bands and the interpretation of the data (95).

Data Analysis

We compared HLA-C alleles (stable/unstable) and genotypes distribution between the ADC group and the population of northern Italy, low-resolution typing (96). Guerini and coworkers (2008) described HLA-C allele frequencies in a large Italian population cohort showing a consistent picture of their distribution in Italy. These data can be currently used as reference population for clinical and anthropological studies. Similarly, we compared the HIV-no-ADC group with the same reference population. Finally, we compared the two HIV-infected groups, i.e., HIV-ADC vs. HIV-no-ADC.

The significance of the association between groups of categorical data (stable and unstable alleles) was examined using 2×2 contingency tables and the Fisher's exact test, while quantitative data were examined using the Mann Whitney U test. The Fisher's exact test is conservative but guarantees type I error control for small sample sizes.

Genetic associations were conducted using a 2×2 contingency table of 2N case-control by allele counts, where N is the number of individuals tested. The strength of association was reported as Odds Ratio (OR) with a 95% confidence interval (CI).

When the statistical significance was tested under the hypothesis of a specific direction of association (i.e., unstable alleles are positively associated with ADC), a one-tailed test was employed. A two-tailed test was instead used when the association was explored without any expectation about the direction of the association between the tested variables. An association was deemed to be statistically significant by setting a significant level of 5%, that is all tests showing a nominal *p*-value < 0.05 were considered to be statistically significant. Given the exploratory nature of this study, no correction for multiple testing was employed.

TABLE 1 | Baseline characteristics of HIV-1 infected patients with AIDS dementia complex (HIV-ADC group).

No.	Age range	Infection route	CDC CLASS '93	CD4+ T lymphocyte plasma nadir (cells/ μ L, % of lymphocytes)	HIV RNA load zenith (copies/ml)	HIV RNA CSF at ADC diagnosis (copies/ml)	HLA-C alleles	HLA-C stability
1	46-50	BISEX	C3	111 (7.3%)	52100	204000	03/04	U/U
2	56-60	IDU	C3	50 (4%)	16250	72320	04/16	U/S
3	56-60	BISEX	C3	26 (1%)	205000	>500000	04/07	U/U
4	31-35	BISEX	C3	157 (7%)	22300	67850	03/07	U/U
5	36-40	BISEX	C3	47 (8%)	62300	187000	02/07	S/U
6	36-40	HETERO	C3	4 (1%)	98000	230000	06/07	S/U
7	36-40	HETERO	C2	286 (17.5%)	11853	3066	07/16	U/S
8	61-65	HETERO	C3	18 (9%)	267851	NA	02/18	S/U
9	56-60	IDU	C2	468 (40%)	NA	NA	04/14	U/U
10	51-55	HOMO	C3	41 (3%)	80400	523000	07/15	U/S
11	46-50	HOMO	C3	56 (4%)	141000	6000000	04/07	U/U

BISEX, bisexual; IDU, injection drug user; HETERO, heterosexual; HOMO, homosexual; NA, not available; U, unstable HLA-C allele; S, stable HLA-C allele.

TABLE 2 | Baseline characteristics of the control group of HIV-infected patients without AIDS dementia complex (HIV-no-ADC group).

No.	Age range	Infection route	CDC CLASS '93	CD4+ T lymphocyte plasma nadir (cells/ μ L, % of lymphocyte)	HIV RNA load zenith (copies/ml)	HLA-C alleles	HLA-C stability
1	41-45	HETERO	A1	362 (14.1%)	4380	01/07	U/U
2	31-35	HOMO	A2	304 (15%)	200000	03/07	U/U
3	21-25	HOMO	B3	601 (39%)	> 10000000	04/12	U/S
4	51-55	BISEX	A2	302 (18.2%)	32000	07/12	U/S
5	51-55	IDU	A1	328 (20%)	21000	04/12	U/S
6	31-35	HOMO	C2	268 (14%)	1328	07/12	U/S
7	56-60	HETERO	A1	221 (17%)	253061	06/12	S/S
8	36-40	HOMO	A3	60 (7.1%)	191463	07/12	U/S
9	61-65	BISEX	A1	713 (17%)	481000	04/15	U/S
10	31-35	BISEX	A3	120 (7.4%)	200000	06/07	S/U
11	46-50	HOMO	A2	300 (18.8%)	86000	06/12	S/S
12	46-50	BISEX	A2	214 (20.2%)	16900	02/12	S/S
13	46-50	HOMO	A1	294 (22%)	75200	04/07	U/U
14	56-60	HOMO	A2	302 (28%)	30400	02/16	S/S
15	36-40	HOMO	A2	391 (14%)	52900	14/15	U/S
16	46-50	HOMO	A2	330 (20%)	72000	04/07	U/U

BISEX, bisexual; IDU, injection drug user; HETERO, heterosexual; HOMO, homosexual; U, unstable HLA-C allele; S, stable HLA-C allele.

RESULTS

All 11 HIV-ADC subjects carried unstable HLA-C alleles in homozygosis (U/U, $n = 5$) or in heterozygosis (U/S, $n = 6$), but none of them was carrying stable alleles in homozygosis (S/S; **Table 1**).

Among the 16 HIV-no-ADC subjects, four carried unstable HLA-C alleles in homozygosis (U/U), 4 stable alleles in homozygosis (S/S) and eight were heterozygotes (U/S; **Table 2**).

The HLA-C stable/unstable allele distribution was different between the HIV-ADC group (stable 27%, unstable 73%) and the northern Italy population [stable 50%, unstable 50%; Fisher exact test, $p = 0.029$; OR 2.630 [CI: 1.112- ∞]; **Table 3**].

No differences in alleles distribution were observed when the HIV-no-ADC group (stable 50%, unstable 50%) was compared with the northern Italy population [Fisher exact test, $p = 0.584$; OR 0.098 [CI: 0.514- ∞]; **Table 3**].

We also compared the HIV-ADC group with the HIV-no-ADC group, showing a slight difference in stable/unstable HLA-C alleles distribution [Fisher's exact test, $p = 0.082$; OR 2.618 [CI: 0.870- ∞]; **Table 3**]. The two groups differed neither for sex (Fisher's exact test, $p = 1.000$) nor for age (Mann Whitney U test, $p = 0.312$).

The two HIV-infected groups did not differ for HIV RNA zenith level (Mann Whitney U test, $p = 0.896$), while they were different for CD4+ T lymphocyte nadir (Mann Whitney U test, $p = 0.001$). The lower CD4 count in HIV-infected patients

TABLE 3 | HLA-C alleles distribution (stable, unstable) in HIV-infected patients with ADC (HIV-ADC), HIV-infected patients without ADC (HIV-no-ADC), and in northern Italy (96).

	HIV-ADC	HIV-no-ADC	Northern Italy
HLA-C unstable	16	16	771
HLA-C stable	6	16	761

TABLE 4 | HLA-C allele 12 distribution in HIV-infected patients with ADC (HIV-ADC), HIV-infected patients without ADC (HIV-no-ADC), and in northern Italy (96).

	HIV-ADC	HIV-no-ADC	Northern Italy
HLA-C*12	0	8	261
HLA-C Others	22	24	1271

with ADC is the consequence of the longer duration of HIV-1 infection with worsening immunodeficiency, which was frequent in the pre-cART times.

Finally, we analyzed the distribution of the different HLA-C alleles between the 3 groups.

We found interesting differences on HLA-C subtypes, in that HLA-C*12 appeared to be absent in the HIV-ADC group (0%) when compared either with the reference northern Italy population (17%, $p = 0.038$) and with the HIV-no-ADC group (25%, $p = 0.016$; **Table 4**). No difference was observed for the distribution of HLA-C*12 between the HIV-no-ADC group and the northern Italy population ($p = 0.237$; **Table 4**).

DISCUSSION

Our results, despite being very preliminary, and derived from a small sample of patients, may have some implications for better understanding HAND/ADC pathogenesis and eventually improve the treatment of this condition.

ADC was common in patients with HIV-1 infection during disease progression in the pre-cART era (97). The introduction of cART regimens tackled the onset of ADC in these patients and reduced the likelihood and severity of HAND, indicating that the treatment of HIV-1 infection is essential to reduce neurological damage (98). At variance, the prevalence of less severe HAND syndromes is 46% of HIV-1-infected people and is expected to increase in the next years (99). Why HAND prevalence did not significantly decrease after the introduction of cART (100) is poorly understood (3).

To answer this question, we hypothesized that the development of HAND could be associated with the expression of specific unstable variants of HLA-C and the subsequent CNS release and deposition of free β_2m , which has been reported to be neurotoxic and to deteriorate cognitive functions (50, 51). To this aim, from a large database of nearly 1100 HIV-infected subjects, we retrospectively selected patients who had an unequivocal diagnosis of ADC, the most severe form of HAND. Only 11

among them were still available for sample collection, DNA extraction, and analysis.

Our findings showed a higher frequency of unstable HLA-C alleles in HIV-1 infected patients who developed ADC in comparison to northern Italy general population. This finding argues in favor of a possible involvement of β_2m in triggering and/or sustaining the development of neurologic complications of AIDS. In contrast, the HIV-infected population without ADC showed the same distribution than the general population of northern Italy, thus excluding the hypothesis that the higher frequency of unstable HLA-C alleles is associated with a higher susceptibility to HIV-1 infection. The present data raise the question whether patients expressing unstable HLA-C alleles in the control group did not develop ADC. We speculate that unstable alleles might predispose to ADC pathogenesis, but other viral and host factors (e.g., time of infection, HIV subtypes, immunological response) could contribute to the development of HAND/ADC. Moreover, the degree of stability vary across different alleles, and exploring single HLA-C variants may help better stratify the risk of ADC/HAND.

We observed an unexpected lower frequency of HLA-C*12, a stable HLA-C variant, in HIV-ADC subjects. Recent studies reported a protective role of HLA-C*12 in HIV-1 infection (101, 102). It would be tempting to speculate that the presence of HLA-C*12 might have some kind of protective effect on the risk of developing ADC in HIV-infected individuals. A study on a higher number of cases, allowing the analysis of the effect of single HLA-C alleles on the risk of developing neurological diseases in HIV-1 patients is definitely needed, to confirm this very preliminary but also very tempting observation.

HIV-1 neurovirulence could contribute to the dissociation of β_2m from HLA-C molecules, as a consequence of the association of HIV-1 Env with unstable HLA-C variants (40). A three amino acid position in HIV-1 gp120 glycoprotein was recently reported to be associated with HAND (99).

The treatment of HAND is still an issue in the era of cART (103, 104), as the improvement of neurocognitive symptoms to cART is variable (105), mild neurocognitive impairment is found in some patients, and factors predicting a response in single patients are unknown. Indeed, several studies demonstrated that cART is not effective on HAND in all HIV-1 positive patients (106, 107).

It would be reasonable to use antiretroviral drugs with high CNS penetration/effectiveness score, such as darunavir, abacavir or raltegravir (108, 109), to reduce the risk of HAND. However, some antiretroviral drugs are potentially neurotoxic: they may increase the production of A β protein by neurons and reduce its microglial phagocytosis, leading to the deposition of amyloid plaques in the CNS (68, 110). If our hypothesis is confirmed by further studies, an antiretroviral therapy with CNS-targeted drugs might be considered for patients with unstable HLA-C variants, paying attention to the possible side effects of some of them.

Effective cART suppresses HIV-1 replication and increases the immune system activity, thus determining a beneficial effect on the CNS through the reduction of HIV viral load, viral neurotoxic proteins production, and neuroinflammation.

However, neuroinflammation may still be active as microglial activation in specific brain areas, including the hippocampus and temporal cortex, whereas in pre-cART era these changes were more common in the basal ganglia (111). Chronic inflammation and other immune mechanisms triggered by viral infection, rather than direct HIV-1 involvement, may thus play a key role in HAND pathogenesis.

ADC is rare nowadays due to the cART, and, despite our efforts, we were not able to recruit a larger ADC sample. We are fully aware that our data are preliminary and should be considered with caution. However, they are appealing and may pave the way for recruiting a larger population of patients through a multicenter study. If confirmed in larger populations of patients, these findings would suggest that HIV-infected patients carrying specific unstable variants of HLA-C should undergo strict monitoring of neuropsychological and neurological symptoms to promptly recognize early HAND stages. Moreover, CSF β_2m levels might be explored as a molecular biomarker to recognize early HAND stages, given the absence of specific tests for this condition (112).

The observation we reported may be a starting point to explore whether some HLA-C variants are associated with higher risk of CNS viral infection, neuroinflammation and neurodegenerative disorders (113, 114). HLA-C*07, which is one of the most unstable variants (36), was found to be associated with AD (115). Similarly, very old studies associated HLA-C*03, another unstable HLA-C variant, to higher AD risk (116–118).

There are many features in common between HAND/ADC and AD, including clinical features that overlap between the two conditions (61). A β peptide biogenesis and clearance may be influenced by HIV-1 infection (119). Increased A β amyloid has been reported in up to 72% of HIV-1 patients with HAND (68), but also in 38% of those without HIV-1 but no cognitive symptoms (73, 119). We may speculate that shared pathogenetic mechanisms in response to neurotropic viral infections (e.g., herpesviridae) may contribute to A β amyloid deposition in AD patients without HIV-1 and that neuroinflammation due to β_2m release in patients with unstable HLA-C alleles may accelerate this phenomenon.

The large number of HIV-infected patients under cART with a long-life expectancy due to a nearly complete control of viral load raises concern about their risk of cognitive dysfunction in the presence of cardiovascular risk factors (e.g., smoking, hypertension, diabetes, hypercholesterolemia) (120) that are known to increase also the risk of AD (121). The presence of unstable HLA-C variants might be explored as a possible predictor for worse cognitive performance at older age in HIV-infected patients with cardiovascular risk factors.

CONCLUSIONS

Our very preliminary data suggests that HIV-1 infected individuals carrying unstable HLA-C allelic variants may

be at higher risk of CNS complications. Specifically, we observed that alleles encoding unstable HLA-C variants were more frequent in HIV-1 infected patients who developed ADC, the most severe HAND subtype. The identification of specific variants of HLA-C as risk factors for HAND can provide a contribution both in the field of personalized medicine and for the development of new therapies, aimed at preventing and/or reducing neurocognitive damage in AIDS patients.

Given the potential commonalities between HIV-induced aging, neurocognitive decline and AD that represent a promising future hot research topic (73), our findings might be helpful for better understanding the pathogenesis, and for identifying disease-modifying therapeutic strategies to be offered to patients at higher risk of neurodegenerative disorders at presymptomatic disease stages.

AUTHOR CONTRIBUTIONS

DZ conceived, designed supervised, and coordinated the study, conducted data analysis and took care of drafting and writing the manuscript. MS, SM, FP, and ED were involved in samples collection, extraction, and analysis. EG and VM conducted HLA-C typing. SR, EL, MM, and ML contributed to patients selection, clinical data collection, and manuscript writing. GM conducted genetic and statistical analysis. MGR helped to coordinate the study and assisting in manuscript preparation. ST and DG contributed to planning the study, to the analysis and collection of neurologic and virologic data and to manuscript drafting and writing.

FUNDING

This research received no specific grant from any funding agency in the public, commercial, or not-for-profit sector. Since the cancelation of the AIDS National program, it has been very difficult to pursue basic research in the field of HIV/AIDS in Italy. As a consequence, this study was conducted with leftover nonperishable materials and reagents from previous grants (Europrise Network of Excellence, Life Science Programme, European Commission), and limited funding support from the Department of Neurosciences, Biomedicine and Movement Sciences, University of Verona, through the FUR 2016.

ACKNOWLEDGMENTS

SM and FP participated in this study as the fulfillment of their Ph.D. degree. We thank Dr. G. Gandini, Service of Transfusion Medicine AOUI Verona, and Prof. M. Tinazzi, University of Verona, for supporting and encouraging this study. We thank Dr. A. Beretta for the stimulating discussions on the topic of the interaction between HLA-C, HIV-1 infection, and neurological diseases.

REFERENCES

- Nathanson N, Cook DG, Kolson DL, Gonzalez-Scarano F. Pathogenesis of HIV encephalopathy. *Ann N Y Acad Sci.* (1994) 724:87–106. doi: 10.1111/j.1749-6632.1994.tb38898.x
- Navia BA, Jordan BD, Price RW. The AIDS dementia complex: I. *Clini Featur Ann Neurol.* (1986) 19:517–24. doi: 10.1002/ana.410190602
- Eggers C, Arendt G, Hahn K, Husstedt IW, Maschke M, Neuen-Jacob E, et al. HIV-1-associated neurocognitive disorder: epidemiology, pathogenesis, diagnosis, and treatment. *J Neurol.* (2017) 264:1715–27. doi: 10.1007/s00415-017-8503-2
- Mcarthur JC, Hoover DR, Bacellar H, Miller EN, Cohen BA, Becker JT, et al. Dementia in AIDS patients: incidence and risk factors. Multicenter AIDS Cohort Study. *Neurology* (1993) 43:2245–52. doi: 10.1212/WNL.43.1.2245
- Antinori A, Arendt G, Becker JT, Brew BJ, Byrd DA, Cherner M, et al. Updated research nosology for HIV-associated neurocognitive disorders. *Neurology* (2007) 69:1789–99. doi: 10.1212/01.WNL.0000287431.88658.8b
- Valcour V, Yee P, Williams AE, Shiramizu B, Watters M, Selnes O, et al. Lowest ever CD4 lymphocyte count (CD4 nadir) as a predictor of current cognitive and neurological status in human immunodeficiency virus type 1 infection—The Hawaii Aging with HIV Cohort. *J Neurovirol.* (2006) 12:387–91. doi: 10.1080/13550280600915339
- Jayadev S, Garden GA. Host and viral factors influencing the pathogenesis of HIV-associated neurocognitive disorders. *J Neuroimmune Pharmacol.* (2009) 4:175–89. doi: 10.1007/s11481-009-9154-6
- Mcarthur JC. HIV dementia: an evolving disease. *J Neuroimmunol.* (2004) 157:3–10. doi: 10.1016/j.jneuroim.2004.08.042
- Nath A. Eradication of human immunodeficiency virus from brain reservoirs. *J Neurovirol.* (2015) 21:227–34. doi: 10.1007/s13365-014-0291-1
- Gendelman HE, Lipton SA, Tardieu M, Bukrinsky MI, Nottet HS. The neuropathogenesis of HIV-1 infection. *J Leukoc Biol.* (1994) 56:389–98. doi: 10.1002/jlb.56.3.389
- Fujimura RK, Bockstahler LE, Goodkin K, Werner T, Brack-Werner R, Shapshak P. Neuropathology and virology of hiv associated dementia. *Rev Med Virol.* (1996) 6, 141–50. doi: 10.1002/(SICI)1099-1654(199609)6:3<141::AID-RMV141>3.0.CO;2-1
- Kaul M, Zheng J, Okamoto S, Gendelman HE, Lipton SA. HIV-1 infection and AIDS: consequences for the central nervous system. *Cell Death Differ.* (2005) 12(Suppl. 1):878–92. doi: 10.1038/sj.cdd.4401623
- Mattson MP, Haughey NJ, Nath A. Cell death in HIV dementia. *Cell Death Differ.* (2005) 12 (Suppl. 1):893–904. doi: 10.1038/sj.cdd.4401577
- Ranki A, Nyberg M, Ovod V, Haltia M, Elovaara I, Raininko R, et al. Abundant expression of HIV Nef and Rev proteins in brain astrocytes in vivo is associated with dementia. *AIDS* (1995) 9:1001–8. doi: 10.1097/00002030-199509000-00004
- Zhou BY, Liu Y, Kim B, Xiao Y, He JJ. Astrocyte activation and dysfunction and neuron death by HIV-1 Tat expression in astrocytes. *Mol Cell Neurosci.* (2004) 27:296–305. doi: 10.1016/j.mcn.2004.07.003
- Vanzani MC, Iacono RE, Caccuri RL, Troncoso AR, Berria MI. Regional differences in astrocyte activation in HIV-associated dementia. *Medicina* (2006) 66:108–12.
- Brenneman DE, Westbrook GL, Fitzgerald SP, Ennist DL, Elkins KL, Ruff MR, et al. Neuronal cell killing by the envelope protein of HIV and its prevention by vasoactive intestinal peptide. *Nature* (1988) 335:639–42. doi: 10.1038/335639a0
- Kaiser PK, Offermann JT, Lipton SA. Neuronal injury due to HIV-1 envelope protein is blocked by anti-gp120 antibodies but not by anti-CD4 antibodies. *Neurology* (1990) 40:1757–61. doi: 10.1212/WNL.40.1.1757
- Gelbard HA, Dzenko KA, Diloreto D, Del Cerro C, Del Cerro M, Epstein LG. Neurotoxic effects of tumor necrosis factor alpha in primary human neuronal cultures are mediated by activation of the glutamate AMPA receptor subtype: implications for AIDS neuropathogenesis. *Dev Neurosci.* (1993) 15:417–22. doi: 10.1159/00011367
- Nottet HS, Jett M, Flanagan CR, Zhai QH, Persidsky Y, Rizzino A, et al. A regulatory role for astrocytes in HIV-1 encephalitis. An overexpression of eicosanoids, platelet-activating factor, and tumor necrosis factor-alpha by activated HIV-1-infected monocytes is attenuated by primary human astrocytes. *J Immunol.* (1995) 154:3567–3581.
- Adamson DC, Wildemann B, Sasaki M, Glass JD, McArthur JC, Christov VI, et al. Immunologic NO synthase: elevation in severe AIDS dementia and induction by HIV-1 gp41. *Science* (1996) 274:1917–21. doi: 10.1126/science.274.5294.1917
- Kerr SJ, Armati PJ, Pemberton LA, Smythe G, Tattam B, Brew BJ. Kynurenine pathway inhibition reduces neurotoxicity of HIV-1-infected macrophages. *Neurology* (1997) 49:1671–81. doi: 10.1212/WNL.49.6.1671
- Miura Y, Misawa N, Kawano Y, Okada H, Inagaki Y, Yamamoto N, et al. Tumor necrosis factor-related apoptosis-inducing ligand induces neuronal death in a murine model of HIV central nervous system infection. *Proc Natl Acad Sci USA.* (2003) 100:2777–82. doi: 10.1073/pnas.2628048100
- Manji H, Jager HR, Winston A. HIV, dementia and antiretroviral drugs: 30 years of an epidemic. *J Neurol Neurosurg Psychiatr.* (2013) 84:1126–37. doi: 10.1136/jnnp-2012-304022
- Enting RH, Foudraire NA, Lange JM, Jurriaans S, Van Der Poll T, Weverling GJ, et al. Cerebrospinal fluid beta2-microglobulin, monocyte chemoattractant protein-1, and soluble tumour necrosis factor alpha receptors before and after treatment with lamivudine plus zidovudine or stavudine. *J Neuroimmunol.* (2000) 102:216–21. doi: 10.1016/S0165-5728(99)00219-2
- Mulder JW, Krijnen P, Coutinho RA, Bakker M, Goudsmit J, Lange JM. Serum beta 2-microglobulin levels in asymptomatic HIV-1-infected subjects during long-term zidovudine treatment. *Genitourin Med.* (1991) 67:188–93. doi: 10.1136/sti.67.3.188
- Alfieri R, Chirianni A, Mancino T, Remondelli P, Russo P, Liuzzi G, et al. Serum beta 2-microglobulin levels and p24 antigen, lymphocyte depletion and disease progression in human immunodeficiency virus infection. *Int J Clin Lab Res.* (1992) 22:48–51. doi: 10.1007/BF02591394
- Boffa J. Beta-2 microglobulin as a marker for HIV infection. *J Insur Med.* (1994) 26:14–5.
- Bhalla RB, Safai B, Pahwa S, Schwartz MK. Beta 2-microglobulin as a prognostic marker for development of AIDS. *Clin Chem.* (1985) 31:1411–2.
- Brew BJ, Bhalla RB, Fleisher M, Paul M, Khan A, Schwartz MK, et al. Cerebrospinal fluid beta 2 microglobulin in patients infected with human immunodeficiency virus. *Neurology* (1989) 39:830–4. doi: 10.1212/WNL.39.6.830
- Sonnerborg AB, Von Stedingk LV, Hansson LO, Strannegard OO. Elevated neopterin and beta 2-microglobulin levels in blood and cerebrospinal fluid occur early in HIV-1 infection. *AIDS* (1989) 3:277–83. doi: 10.1097/00002030-198905000-00005
- Mcarthur JC, Nance-Sproson TE, Griffin DE, Hoover D, Selnes OA, Miller EN, et al. The diagnostic utility of elevation in cerebrospinal fluid beta 2-microglobulin in HIV-1 dementia. Multicenter AIDS cohort study. *Neurology* (1992) 42:1707–12. doi: 10.1212/WNL.42.9.1707
- Halabelian L, Ricagno S, Giorgetti S, Santambrogio C, Barbiroli A, Pellegrino S, et al. Class I major histocompatibility complex, the trojan horse for secretion of amyloidogenic beta2-microglobulin. *J Biol Chem.* (2014) 289:3318–27. doi: 10.1074/jbc.M113.524157
- Zemmour J, Parham P. Distinctive polymorphism at the HLA-C locus: implications for the expression of HLA-C. *J Exp Med.* (1992) 176:937–50. doi: 10.1084/jem.176.4.937
- Sibilio L, Martayan A, Setini A, Lo Monaco E, Tremante E, Butler RH, et al. A single bottleneck in HLA-C assembly. *J Biol Chem.* (2008) 283:1267–74. doi: 10.1074/jbc.M708068200
- Kaur G, Gras S, Mobbs JI, Vivian JP, Cortes A, Barber T, et al. Structural and regulatory diversity shape HLA-C protein expression levels. *Nat Commun.* (2017) 8:15924. doi: 10.1038/ncomms15924
- Matucci A, Rossolillo P, Baroni M, Siccardi AG, Beretta A, Zipeto D. HLA-C increases HIV-1 infectivity and is associated with gp120. *Retrovirology* (2008) 5:68. doi: 10.1186/1742-4690-5-68
- Baroni M, Matucci A, Scarlatti G, Soprana E, Rossolillo P, Lopalco L, et al. HLA-C is necessary for optimal human immunodeficiency virus type 1 infection of human peripheral blood CD4 lymphocytes. *J Gen Virol.* (2010) 91:235–41. doi: 10.1099/vir.0.015230-0

39. Zipeto D, Beretta A. HLA-C and HIV-1: Friends or Foes? *Retrovirology* (2012) 9:39. doi: 10.1186/1742-4690-9-39
40. Serena M, Parolini F, Biswas P, Sironi F, Blanco Miranda A, Zoratti E, et al. HIV-1 Env associates with HLA-C free-chains at the cell membrane modulating viral infectivity. *Sci Rep.* (2017) 7:40037. doi: 10.1038/sre p40037
41. Parolini F, Biswas P, Serena M, Sironi F, Muraro V, Guizzardi E, et al. Stability and expression levels of HLA-C on the cell membrane modulate HIV-1 infectivity. *J Virol.* (2018) 92:e01711–01717. doi: 10.1128/JVI.01 711-17
42. Kulkarni S, Savan R, Qi Y, Gao X, Yuki Y, Bass SE, et al. Differential microRNA regulation of HLA-C expression and its association with HIV control. *Nature* (2011) 472:495–8. doi: 10.1038/nature09914
43. Apps R, Qi Y, Carlson JM, Chen H, Gao X, Thomas R, et al. Influence of HLA-C expression level on HIV control. *Science* (2013) 340:87–91. doi: 10.1126/science.1232685
44. Kulkarni S, Qi Y, O'huigin C, Pereyra F, Ramsuran V, McLaren P, et al. Genetic interplay between HLA-C and MIR148A in HIV control and Crohn disease. *Proc Natl Acad Sci USA.* (2013) 110:20705–10. doi: 10.1073/pnas.13122 37110
45. Brew BJ, Bhalla RB, Paul M, Sidtis JJ, Keilp JJ, Sadler AE, et al. Cerebrospinal fluid beta 2-microglobulin in patients with AIDS dementia complex: an expanded series including response to zidovudine treatment. *AIDS* (1992) 6:461–5. doi: 10.1097/00002030-199205000- 00004
46. Brew BJ, Dunbar N, Pemberton L, Kaldor J. Predictive markers of AIDS dementia complex: CD4 cell count and cerebrospinal fluid concentrations of beta 2-microglobulin and neopterin. *J Infect Dis.* (1996) 174:294–8. doi: 10.1093/infdis/174.2.294
47. Huh GS, Boulanger LM, Du H, Riquelme PA, Brotz TM, Shatz CJ. Functional requirement for class I MHC in CNS development and plasticity. *Science* (2000) 290:2155–9. doi: 10.1126/science.290.5499.2155
48. Shatz CJ. MHC class I: an unexpected role in neuronal plasticity. *Neuron* (2009) 64:40–5. doi: 10.1016/j.neuron.2009.09.044
49. Lee H, Brott BK, Kirkby LA, Adelson JD, Cheng S, Feller MB, et al. Synapse elimination and learning rules co-regulated by MHC class I H2-Db. *Nature* (2014) 509:195–200. doi: 10.1038/nature13154
50. Giorgetti S, Raimondi S, Cassinelli S, Bucciantini M, Stefani M, Gregorini G, et al. Beta2-Microglobulin is potentially neurotoxic, but the blood brain barrier is likely to protect the brain from its toxicity. *Nephrol Dial Transplant.* (2009) 24:1176–81. doi: 10.1093/ndt/gfn623
51. Smith LK, He Y, Park JS, Bieri G, Sneathlidge CE, Lin K, et al. Beta2-microglobulin is a systemic pro-aging factor that impairs cognitive function and neurogenesis. *Nat Med.* (2015) 21:932–7. doi: 10.1038/nm.3898
52. Natalello A, Relini A, Penco A, Halabelian L, Bolognesi M, Doglia SM, et al. Wild type beta-2 microglobulin and DE loop mutants display a common fibrillar architecture. *PLoS ONE* (2015) 10:e0122449. doi: 10.1371/journal.pone.0122449
53. Gejyo F, Yamada T, Odani S, Nakagawa Y, Arakawa M, Kunitomo T, et al. A new form of amyloid protein associated with chronic hemodialysis was identified as beta 2-microglobulin. *Biochem Biophys Res Commun.* (1985) 129:701–6. doi: 10.1016/0006-291X(85)91948-5
54. Mangione PP, Esposito G, Relini A, Raimondi S, Porcari R, Giorgetti S, et al. Structure, folding dynamics, and amyloidogenesis of D76N beta2-microglobulin: roles of shear flow, hydrophobic surfaces, and alpha-crystallin. *J Biol Chem.* (2013) 288:30917–30. doi: 10.1074/jbc.M113.498857
55. Le Marchand T, De Rosa M, Salvi N, Sala BM, Andreas LB, Barbet-Massin E, et al. Conformational dynamics in crystals reveal the molecular bases for D76N beta-2 microglobulin aggregation propensity. *Nat Commun.* (2018) 9:1658. doi: 10.1038/s41467-018-04078-y
56. Carrette O, Demalte I, Scherl A, Yalkinoglu O, Corthals G, Burkhard P, et al. A panel of cerebrospinal fluid potential biomarkers for the diagnosis of Alzheimer's disease. *Proteomics* (2003) 3:1486–94. doi: 10.1002/pmic.200300470
57. Hunot S, Hirsch EC. Neuroinflammatory processes in Parkinson's disease. *Ann Neurol.* (2003) 53(Suppl. 3):S49–58. discussion: S58–60. doi: 10.1002/ana.10481
58. Zhang J, Goodlett DR, Montine TJ. Proteomic biomarker discovery in cerebrospinal fluid for neurodegenerative diseases. *J Alzheimers Dis.* (2005) 8:377–86. doi: 10.3233/JAD-2005-8407
59. Svatonova J, Borecka K, Adam P, Lanska V. Beta2-microglobulin as a diagnostic marker in cerebrospinal fluid: a follow-up study. *Dis Mark.* (2014) 2014:495402. doi: 10.1155/2014/495402
60. Merlini G, Bellotti V. Molecular mechanisms of amyloidosis. *N Engl J Med.* (2003) 349:583–96. doi: 10.1056/NEJMra023144
61. Kuhlmann I, Minihane AM, Huebbe P, Nebel A, Rimbach G. Apolipoprotein E genotype and hepatitis C, HIV and herpes simplex disease risk: a literature review. *Lipids Health Dis.* (2010) 9:8. doi: 10.1186/1476-511X-9-8
62. Burt TD, Agan BK, Marconi VC, He W, Kulkarni H, Mold JE, et al. Apolipoprotein (apo) E4 enhances HIV-1 cell entry in vitro, and the APOE epsilon4/epsilon4 genotype accelerates HIV disease progression. *Proc Natl Acad Sci USA.* (2008) 105:8718–23. doi: 10.1073/pnas.0803526105
63. Corder EH, Robertson K, Lannfelt L, Bogdanovic N, Eggertsen G, Wilkins J, et al. HIV-infected subjects with the E4 allele for APOE have excess dementia and peripheral neuropathy. *Nat Med.* (1998) 4:1182–4. doi: 10.1038/2677
64. Yamaguchi I, Hasegawa K, Takahashi N, Gejyo F, Naiki H. Apolipoprotein E inhibits the depolymerization of beta 2-microglobulin-related amyloid fibrils at a neutral pH. *Biochemistry* (2001) 40:8499–507. doi: 10.1021/bi0027128
65. Naiki H, Yamamoto S, Hasegawa K, Yamaguchi I, Goto Y, Gejyo F. Molecular interactions in the formation and deposition of beta2-microglobulin-related amyloid fibrils. *Amyloid* (2005) 12:15–25. doi: 10.1080/13506120500032352
66. Yamamoto S, Hasegawa K, Yamaguchi I, Goto Y, Gejyo F, Naiki H. Kinetic analysis of the polymerization and depolymerization of beta(2)-microglobulin-related amyloid fibrils *in vitro*. *Biochim Biophys Acta* (2005) 1753:34–43. doi: 10.1016/j.bbapap.2005.07.007
67. Myers SL, Jones S, Jahn TR, Morten IJ, Tennent GA, Hewitt EW, et al. A systematic study of the effect of physiological factors on beta2-microglobulin amyloid formation at neutral pH. *Biochemistry* (2006) 45:2311–21. doi: 10.1021/bi052434i
68. Xu J, Ikezu T. The comorbidity of HIV-associated neurocognitive disorders and Alzheimer's disease: a foreseeable medical challenge in post-HAART era. *J Neuroimmune Pharmacol.* (2009) 4:200–12. doi: 10.1007/s11481-008-9136-0
69. Andersson L, Blennow K, Fuchs D, Svennerholm B, Gisslen M. Increased cerebrospinal fluid protein tau concentration in neuro-AIDS. *J Neurol Sci.* (1999) 171:92–6. doi: 10.1016/S0022-510X(99)00253-1
70. Brew BJ, Pemberton L, Blennow K, Wallin A, Hagberg L. CSF amyloid beta42 and tau levels correlate with AIDS dementia complex. *Neurology* (2005) 65:1490–2. doi: 10.1212/01.wnl.0000183293.95787.b7
71. Anthony IC, Ramage SN, Carnie FW, Simmonds P, Bell JE. Accelerated Tau deposition in the brains of individuals infected with human immunodeficiency virus-1 before and after the advent of highly active anti-retroviral therapy. *Acta Neuropathol.* (2006) 111:529–38. doi: 10.1007/s00401-006-0037-0
72. Streit WJ, Xue QS. Alzheimer's disease, neuroprotection, and CNS immunosenescence. *Front Pharmacol.* (2012) 3:138. doi: 10.3389/fphar.2012.00138
73. Chakradhar S. A tale of two diseases: aging HIV patients inspire a closer look at Alzheimer's disease. *Nat Med.* (2018) 24:376–7. doi: 10.1038/nm0418-376
74. Franceschi C, Campisi J. Chronic inflammation (inflammaging) and its potential contribution to age-associated diseases. *J Gerontol A Biol Sci Med Sci.* (2014) 69(Suppl. 1):S4–9. doi: 10.1093/gerona/glu057
75. Giunta B, Fernandez F, Nikolic WV, Obregon D, Rrapo E, Town T, et al. Inflammaging as a prodrome to Alzheimer's disease. *J Neuroinflammation* (2008) 5:51. doi: 10.1186/1742-2094-5-51
76. Barnes LL, Capuano AW, Aiello AE, Turner AD, Yolken RH, Torrey EF, et al. Cytomegalovirus infection and risk of Alzheimer disease in older black and white individuals. *J Infect Dis.* (2015) 211:230–7. doi: 10.1093/infdis/jiu437
77. Itzhaki RF, Cosby SL, Wozniak MA. Herpes simplex virus type 1 and Alzheimer's disease: the autophagy connection. *J Neurovirol.* (2008) 14:1–4. doi: 10.1080/13550280701802543
78. Itzhaki RF, Wozniak MA. Herpes simplex virus type 1 in Alzheimer's disease: the enemy within. *J Alzheimers Dis.* (2008) 13:393–405. doi: 10.3233/JAD-2008-13405

79. Itzhaki RF, Wozniak MA. Alzheimer's disease-like changes in herpes simplex virus type 1 infected cells: the case for antiviral therapy. *Rejuvenation Res.* (2008) 11:319–20. doi: 10.1089/rej.2008.0673
80. Westman G, Blomberg J, Yun Z, Lannfelt L, Ingelsson M, Eriksson BM. Decreased HHV-6 IgG in Alzheimer's Disease. *Front Neurol.* (2017) 8:40. doi: 10.3389/fneur.2017.00040
81. Ward T, Powell RM, Pipkin PA, Evans DJ, Minor PD, Almond JW. Role for beta2-microglobulin in echovirus infection of rhabdomyosarcoma cells. *J Virol.* (1998) 72:5360–5.
82. Triantafilou M, Triantafilou K, Wilson KM, Takada Y, Fernandez N, Stanway G. Involvement of beta2-microglobulin and integrin alphavbeta3 molecules in the coxsackievirus A9 infectious cycle. *J Gen Virol.* (1999) 80:2591–600. doi: 10.1099/0022-1317-80-10-2591
83. Itzhaki RF, Lathé R, Balin BJ, Ball MJ, Bearer EL, Braak H, et al. Microbes and Alzheimer's disease. *J Alzheimers Dis.* (2016) 51:979–84. doi: 10.3233/JAD-160152
84. Jang H, Boltz DA, Webster RG, Smeyne RJ. Viral parkinsonism. *Biochim Biophys Acta* (2009) 1792:714–21. doi: 10.1016/j.bbdis.2008.08.001
85. Cooper EH, Forbes MA, Hambling MH. Serum beta 2-microglobulin and C reactive protein concentrations in viral infections. *J Clin Pathol.* (1984) 37:1140–3. doi: 10.1136/jcp.37.10.1140
86. Grundy JE, Mckeating JA, Ward PJ, Sanderson AR, Griffiths PD. Beta 2 microglobulin enhances the infectivity of cytomegalovirus and when bound to the virus enables class I HLA molecules to be used as a virus receptor. *J Gen Virol.* (1987) 68:793–803. doi: 10.1099/0022-1317-68-3-793
87. Mckeating JA, Griffiths PD, Grundy JE. Cytomegalovirus in urine specimens has host beta 2 microglobulin bound to the viral envelope: a mechanism of evading the host immune response? *J Gen Virol.* (1987) 68 (Pt 3):785–92.
88. Stannard LM. Beta 2 microglobulin binds to the tegument of cytomegalovirus: an immunogold study. *J Gen Virol.* (1989) 70:2179–84. doi: 10.1099/0022-1317-70-8-2179
89. Browne H, Smith G, Beck S, Minson T. A complex between the MHC class I homologue encoded by human cytomegalovirus and beta 2 microglobulin. *Nature* (1990) 347:770–2. doi: 10.1038/347770a0
90. Ezzat K, Pernemalm M, Palsson S, Roberts TC, Jarver P, Dondalska A, et al. The viral protein Corona directs viral pathogenesis and amyloid aggregation. *bioRxiv [Preprint]* (2018). doi: 10.1101/246785
91. Heaton RK, Cysique LA, Jin H, Shi C, Yu X, Letendre S, et al. Neurobehavioral effects of human immunodeficiency virus infection among former plasma donors in rural China. *J Neurovirol.* (2008) 14:536–49. doi: 10.1080/13550280802378880
92. Thames AD, Streiff V, Patel SM, Panos SE, Castellon SA, Hinkin CH. The role of HIV infection, cognition, and depression in risky decision-making. *J Neuropsychiatry Clin Neurosci.* (2012) 24:340–8. doi: 10.1176/appi.neuropsych.11110340
93. MMWR Recommendations and Report 1993 revised classification system for HIV infection and expanded surveillance case definition for AIDS among adolescents and adults. *MMWR Recommend Rep.* (1992) 41:1–19.
94. Turner S, Ellexson ME, Hickman HD, Sidebottom DA, Fernandez-Vina M, Confer DL, et al. Sequence-based typing provides a new look at HLA-C diversity. *J Immunol.* (1998) 161:1406–13.
95. Bunce M, O'Neill CM, Barnardo MC, Krausa P, Browning MJ, Morris PJ, et al. Phototyping: comprehensive DNA typing for HLA-A, B, C, DRB1, DRB3, DRB4, DRB5 & DQB1 by PCR with 144 primer mixes utilizing sequence-specific primers (PCR-SSP). *Tissue Antigens* (1995) 46:355–67. doi: 10.1111/j.1399-0039.1995.tb03127.x
96. Guerini FR, Fusco C, Mazzi B, Favoino B, Nocera G, Agliardi C, et al. HLA-Cw allele frequencies in northern and southern Italy. *Transpl Immunol.* (2008) 18:286–9. doi: 10.1016/j.trim.2007.08.003
97. Ghafouri M, Amini S, Khalili K, Sawaya BE. HIV-1 associated dementia: symptoms and causes. *Retrovirology* (2006) 3:28. doi: 10.1186/1742-4690-3-28
98. Ances BM, Clifford DB. HIV-associated neurocognitive disorders and the impact of combination antiretroviral therapies. *Curr Neurol Neurosci Rep.* (2008) 8:455–61. doi: 10.1007/s11910-008-0073-3
99. Ogishi M, Yotsuyanagi H. Prediction of HIV-associated neurocognitive disorder (HAND) from three genetic features of envelope gp120 glycoprotein. *Retrovirology* (2018) 15:12. doi: 10.1186/s12977-018-0401-x
100. Saylor D, Dickens AM, Sacktor N, Haughey N, Slusher B, Pletnikov M, et al. HIV-associated neurocognitive disorder—pathogenesis and prospects for treatment. *Nat Rev Neurol.* (2016) 12:234–48. doi: 10.1038/nrneuro.2016.27
101. Lin Z, Kuroki K, Kuse N, Sun X, Akahoshi T, Qi Y, et al. HIV-1 Control by NK Cells via Reduced Interaction between KIR2DL2 and HLA-C(*)12:02/C(*)14:03. *Cell Rep.* (2016) 17:2210–20. doi: 10.1016/j.celrep.2016.10.075
102. Chikata T, Tran GV, Murakoshi H, Akahoshi T, Qi Y, Naranbhai V, et al. HLA class I-mediated HIV-1 control in vietnamese infected with HIV-1 subtype A/E. *J Virol.* (2018) 92:e01749–17. doi: 10.1128/JVI.01749-17
103. McArthur JC, Brew BJ. HIV-associated neurocognitive disorders: is there a hidden epidemic? *AIDS* (2010) 24:1367–70. doi: 10.1097/QAD.0b013e3283391d56
104. Sanford R, Fellows LK, Ances BM, Collins DL. Association of brain structure changes and cognitive function with combination antiretroviral therapy in HIV-positive individuals. *JAMA Neurol.* (2018) 75:72–9. doi: 10.1001/jamaneurol.2017.3036
105. Cysique LA, Vaida F, Letendre S, Gibson S, Cherner M, Woods SP, et al. Dynamics of cognitive change in impaired HIV-positive patients initiating antiretroviral therapy. *Neurology* (2009) 73:342–8. doi: 10.1212/WNL.0b013e3181ab2b3b
106. Sacktor N, McDermott MP, Marder K, Schifitto G, Selnes OA, McArthur JC, et al. HIV-associated cognitive impairment before and after the advent of combination therapy. *J Neurovirol.* (2002) 8:136–42. doi: 10.1080/13550280290049615
107. Heaton RK, Clifford DB, Franklin DR Jr, Woods SP, Ake C, Vaida F, et al. HIV-associated neurocognitive disorders persist in the era of potent antiretroviral therapy: charter study. *Neurology* (2010) 75:2087–96. doi: 10.1212/WNL.0b013e318200d727
108. Hammond ER, Crum RM, Treisman GJ, Mehta SH, Marra CM, Clifford DB, et al. The cerebrospinal fluid HIV risk score for assessing central nervous system activity in persons with HIV. *Am J Epidemiol.* (2014) 180:297–307. doi: 10.1093/aje/kwu098
109. Calcagno A, Barco A, Trunfio M, Bonora S. CNS-targeted antiretroviral strategies: when are they needed and what to choose. *Curr HIV/AIDS Rep.* 15:84–91. (2018). doi: 10.1007/s11904-018-0375-2
110. Giunta B, Ehrhart J, Obregon DE, Lam L, Le L, Jin J, et al. Antiretroviral medications disrupt microglial phagocytosis of beta-amyloid and increase its production by neurons: implications for HIV-associated neurocognitive disorders. *Mol Brain* (2011) 4:23. doi: 10.1186/1756-6606-4-23
111. Langford D, Marquie-Beck J, De Almeida S, Lazzaretto D, Letendre S, Grant I, et al. Relationship of antiretroviral treatment to postmortem brain tissue viral load in human immunodeficiency virus-infected patients. *J Neurovirol.* (2006) 12:100–7. doi: 10.1080/13550280600713932
112. Price RW, Epstein LG, Becker JT, Cinque P, Gisslen M, Pulliam L, et al. Biomarkers of HIV-1 CNS infection and injury. *Neurology* (2007) 69:1781–8. doi: 10.1212/01.wnl.0000278457.55877.eb
113. De Chiara G, Marcocci ME, Sgarbanti R, Civitelli L, Ripoli C, Piacentini R, et al. Infectious agents and neurodegeneration. *Mol Neurobiol.* (2012) 46:614–38. doi: 10.1007/s12035-012-8320-7
114. Wyss-Coray T, Rogers J. Inflammation in Alzheimer disease—a brief review of the basic science and clinical literature. *Cold Spring Harb Perspect Med.* (2012) 2:a006346. doi: 10.1101/cshperspect.a006346
115. Lehmann DJ, Barnardo MC, Fuggle S, Quiroga I, Sutherland A, Warden DR, et al. Replication of the association of HLA-B7 with Alzheimer's disease: a role for homozygosity? *J Neuroinflammation* (2006) 3:33. doi: 10.1186/1742-2094-3-33
116. Henschke PJ, Bell DA, Cape RD. Alzheimer's disease and HLA. *Tissue Antigens* (1978) 12:132–5. doi: 10.1111/j.1399-0039.1978.tb01308.x
117. Renvoize EB, Hambling MH, Pepper MD, Rajah SM. Possible association of Alzheimer's disease with HLA-BW15 and cytomegalovirus infection. *Lancet* (1979) 1:1238. doi: 10.1016/S0140-6736(79)91914-7
118. Walford RL. Immunology and aging Philip Levine Award. *Am J Clin Pathol.* (1980) 74:247–53. doi: 10.1093/ajcp/74.3.247

119. Achim CL, Adame A, Dumaop W, Everall IP, Masliah E, Neurobehavioral Research C. Increased accumulation of intraneuronal amyloid beta in HIV-infected patients. *J Neuroimmune Pharmacol.* (2009) 4:190–9. doi: 10.1007/s11481-009-9152-8
120. Ciccarelli N, Grima P, Fabbiani M, Baldonero E, Borghetti A, Milanini B, et al. Baseline CD4(+) T-cell count and cardiovascular risk factors predict the evolution of cognitive performance during 2-year follow-up in HIV-infected patients. *Antivir Ther.* (2015) 20:433–40. doi: 10.3851/IM P2925
121. De Bruijn RF, Ikram MA. Cardiovascular risk factors and future risk of Alzheimer's disease. *BMC Med.* (2014) 12:130. doi: 10.1186/s12916-014-0130-5

Conflict of Interest Statement: The authors declare that the research was conducted in the absence of any commercial or financial relationships that could be construed as a potential conflict of interest.

Copyright © 2018 Zipeto, Serena, Mutascio, Parolini, Diani, Guizzardi, Muraro, Lattuada, Rizzardo, Malena, Lanzafame, Malerba, Romanelli, Tamburin and Gibellini. This is an open-access article distributed under the terms of the Creative Commons Attribution License (CC BY). The use, distribution or reproduction in other forums is permitted, provided the original author(s) and the copyright owner(s) are credited and that the original publication in this journal is cited, in accordance with accepted academic practice. No use, distribution or reproduction is permitted which does not comply with these terms.



TRAF3 Is Required for NF- κ B Pathway Activation Mediated by HTLV Tax Proteins

Stefania Fochi¹, Elisa Bergamo¹, Michela Serena¹, Simona Mutascio¹, Chloé Journo², Renaud Mahieux², Vincenzo Ciminale^{3,4}, Umberto Bertazzoni¹, Donato Zipeto¹ and Maria Grazia Romanelli^{1*}

¹ Department of Neurosciences, Biomedicine and Movement Sciences, Section of Biology and Genetics, University of Verona, Verona, Italy, ² Retroviral Oncogenesis Laboratory, Centre International de Recherche en Infectiologie (CIRI), INSERM U1111 – Université Claude Bernard Lyon 1, CNRS, Equipe Labellisée “Fondation pour la Recherche Médicale”, UMR5308, Ecole Normale Supérieure de Lyon, Université Lyon, Lyon, France, ³ Department of Surgery, Oncology and Gastroenterology, University of Padua, Padua, Italy, ⁴ Veneto Institute of Oncology IOV – IRCCS, Padua, Italy

OPEN ACCESS

Edited by:

Louis M. Mansky,
University of Minnesota Twin Cities,
United States

Reviewed by:

Edward Harhaj,
Penn State Milton S. Hershey Medical
Center, United States
Jean-Marie Peloponese,
UMR9004 Institut de Recherche en
Infectiologie de Montpellier (IRIM),
France

*Correspondence:

Maria Grazia Romanelli
mariagrazia.romanelli@univr.it

Specialty section:

This article was submitted to
Virology,
a section of the journal
Frontiers in Microbiology

Received: 28 February 2019

Accepted: 24 May 2019

Published: 12 June 2019

Citation:

Fochi S, Bergamo E, Serena M, Mutascio S, Journo C, Mahieux R, Ciminale V, Bertazzoni U, Zipeto D and Romanelli MG (2019) TRAF3 Is Required for NF- κ B Pathway Activation Mediated by HTLV Tax Proteins. *Front. Microbiol.* 10:1302. doi: 10.3389/fmicb.2019.01302

Human T-cell leukemia viruses type 1 (HTLV-1) and type 2 (HTLV-2) share a common genome organization and expression strategy but have distinct pathological properties. HTLV-1 is the etiological agent of Adult T-cell Leukemia (ATL) and of HTLV-1-Associated Myelopathy/Tropical Spastic Paraparesis (HAM/TSP), whereas HTLV-2 does not cause hematological disorders and is only sporadically associated with cases of subacute myelopathy. Both HTLV genomes encode two regulatory proteins that play a pivotal role in pathogenesis: the transactivating Tax-1 and Tax-2 proteins and the antisense proteins HBZ and APH-2, respectively. We recently reported that Tax-1 and Tax-2 form complexes with the TNF-receptor associated factor 3, TRAF3, a negative regulator of the non-canonical NF- κ B pathway. The NF- κ B pathway is constitutively activated by the Tax proteins, whereas it is inhibited by HBZ and APH-2. The antagonistic effects of Tax and antisense proteins on NF- κ B activation have not yet been fully clarified. Here, we investigated the effect of TRAF3 interaction with HTLV regulatory proteins and in particular its consequence on the subcellular distribution of the effector p65/RelA protein. We demonstrated that Tax-1 and Tax-2 efficiency on NF- κ B activation is impaired in TRAF3 deficient cells obtained by CRISPR/Cas9 editing. We also found that APH-2 is more effective than HBZ in preventing Tax-dependent NF- κ B activation. We further observed that TRAF3 co-localizes with Tax-2 and APH-2 in cytoplasmic complexes together with NF- κ B essential modulator NEMO and TAB2, differently from HBZ and TRAF3. These results contribute to untangle the mechanism of NF- κ B inhibition by HBZ and APH-2, highlighting the different role of the HTLV-1 and HTLV-2 regulatory proteins in the NF- κ B activation.

Keywords: HTLV, NF- κ B, Tax, HBZ, APH-2, TRAF3

INTRODUCTION

Human T-cell leukemia virus type 1 (HTLV-1) was the first human retrovirus discovered. It is estimated that 10–20 million people are infected worldwide by this oncogenic virus. The majority of infected carriers remain asymptomatic, but 5–10% of infected subjects are at risk of developing either Adult T-cell Leukemia (ATL), a highly aggressive peripheral T-cell malignancy, or a chronic

neurodegenerative disorder called HTLV-1-Associated Myelopathy/Tropical Spastic Paraparesis (HAM/TSP) (Kannian and Green, 2010; Ishitsuka and Tamura, 2014; Bangham et al., 2015). HTLV-1 is genetically related to HTLV type 2 (HTLV-2), which is associated with lymphocyte proliferation and rare cases of subacute myelopathy but does not cause hematological disorders (Araujo and Hall, 2004; Bartman et al., 2008). The difference in the pathobiology of HTLV-1 and HTLV-2 might provide important clues to further understand the mechanisms leading to their distinct clinical outcomes. HTLV-1 and HTLV-2 express the transactivating proteins Tax-1 and Tax-2, respectively, which can immortalize human CD4+ T-cell (Cheng et al., 2012; Ciminale et al., 2014; Ma et al., 2016). Both Tax proteins activate viral RNA transcription from the LTR promoter (Journo et al., 2009), interact and modulate the expression of a wide range of cellular proteins and deregulate multiple cellular pathways (Romanelli et al., 2013). Among them, Tax proteins induce the hyper-activation of NF- κ B transcription factors, thus altering the control mechanisms of cell proliferation and survival (Harhaj et al., 2007; Kfoury et al., 2012; Fochi et al., 2018). The mechanism of Tax-mediated NF- κ B activation has been intensively studied in the past years showing that Tax-1 interacts with the regulatory IKK- γ subunit of I κ B kinase complex, also known as NF- κ B essential modulator (NEMO). This interaction results in the constitutive activation of IKK α and IKK β , that leads to degradation of the inhibitor I κ B and activation of the canonical NF- κ B pathway (Xiao et al., 2006; Sun, 2017). Several other factors involved in the persistent activation of the NF- κ B pathway have been found to interact with Tax-1, including TAB2 (TAK1 binding protein 2), TAX1BP (Tax1 binding protein 1), NRP/Optineurin, TRAF6 and CADM1 (cell adhesion molecule 1) (Avesani et al., 2010; Journo et al., 2013; Pujari et al., 2015). It has been demonstrated that persistent NF- κ B activation by Tax-1 induces cell senescence (Kuo and Giam, 2006; Zhi et al., 2011) and this effect may be counteracted by the expression of the HTLV-1 antisense protein HTLV-1 bZIP factor (HBZ). HBZ is an inhibitor of the activation of 5'LTR promoter and of Tax-1-mediated transcription. HBZ is constitutively expressed in most ATL cases and enhances the proliferation of T-cells *in vitro* and *in vivo* (Satou et al., 2006). The combined action of Tax-1 and HBZ is considered relevant for the proliferation of HTLV-1 infected cells and persistent infection (Barbeau et al., 2013; Zhao, 2016). Several studies have demonstrated that HBZ and Tax-1 exert opposite functions in the deregulation of cellular signaling pathways that may help the virus to escape from immune surveillance (Gaudray et al., 2002; Zhao, 2016; Bangham and Matsuoka, 2017; Baratella et al., 2017; Karimi et al., 2017). HBZ selectively inhibits the canonical NF- κ B pathway activated by Tax-1 together with the host transcription factor p65, by repressing the p65 ability to bind DNA (Zhao et al., 2009). Furthermore, HBZ reduces p65 acetylation and enhances its degradation through the PDLIM2 E3 ubiquitin ligase, resulting in the reduction of the expression of several NF- κ B target genes (Zhao et al., 2009; Wurm et al., 2012). Recently, Ma et al. (2017) have demonstrated that HBZ-mediated NF- κ B inhibition contributes to the suppression of cyclin D1 gene expression, favoring the G1/S phase transition of the cell cycle.

HTLV-2 also expresses an antisense transcript, encoding APH-2 (antisense protein of HTLV-2) (Halin et al., 2009), which is widely expressed *in vivo* (Douceron et al., 2012). Unlike Tax-1 and Tax-2, which show a high degree of conservation, APH-2 shows less than 30% similarity to HBZ and does not contain a conventional basic leucine zipper domain. APH-2 is likewise able to inhibit Tax-2-mediated viral transcription by interacting with CREB (Halin et al., 2009; Yin et al., 2012), but its repressive activity is weaker compared to HBZ. It was recently reported that APH-2, like HBZ, represses p65 transactivation. However, APH-2 does not reduce the level of p65 expression nor induces its ubiquitination (Panfil et al., 2016). It is not yet established whether APH-2 inhibits Tax-2-mediated NF- κ B activation. Of note, while both Tax-1 and Tax-2 activate the canonical NF- κ B pathway, only Tax-1 activates the non-canonical one by recruiting NEMO and IKK α to p100 and promoting the release of p52/RelB active heterodimers into the nucleus (Shoji et al., 2009; Motai et al., 2016). These different mechanisms still need to be adequately addressed. We have recently demonstrated that both Tax-1 and Tax-2 interact with the TNF-receptor associated factor 3 (TRAF3), an adaptor protein that participates in the crosstalk between the type I interferon (IFN-I), the mitogen-activated protein kinase (MAPK) and the NF- κ B pathways (Diani et al., 2015). TRAF3 positively regulates IFN-I production, while it inhibits the MAPK pathway and the non-canonical NF- κ B pathway (Häcker et al., 2011). TRAF3 is a component of a multiprotein complex containing TRAF2 and the cellular inhibitor of apoptosis proteins cIAP1 and cIAP2, which restrict the activation of the non-canonical NF- κ B pathway. TRAF3 also participates in the degradation of the alternative NF- κ B inducing kinase NIK (Hauer et al., 2005; Vallabhapurapu et al., 2008; Zarnegar et al., 2008; Hildebrand et al., 2011), acting as a negative regulator of the non-canonical NF- κ B pathway (Yang and Sun, 2015). The accumulation of NIK leads to IKK α activation and p100 processing to yield p52 (Sun, 2017). We have also demonstrated that the IFN- β promoter activation is increased when Tax-1 and TRAF3 are co-expressed with IKK ϵ or TBK1 (Diani et al., 2015). The impact of TRAF3 on HTLV-mediated NF- κ B activation has not yet been understood. In the present study, we demonstrate that TRAF3 plays a critical role in Tax-mediated NF- κ B activation. We further show that APH-2, unlike HBZ, may form complexes with Tax-2 and key factors of the NF- κ B signaling pathway, decreasing p65 nuclear translocation. These results can contribute to highlight a novel regulatory mechanism of NF- κ B activation mediated by HTLV proteins.

MATERIALS AND METHODS

Cell Lines and Transfection

HeLa, HEK293T, TRAF3 knock-out (TRAF3-KO) and U2OS cells were maintained in Dulbecco's modified Eagle's Medium (DMEM) supplemented with 10% fetal calf serum (FCS), L-glutamine (2 mM), and Penicillin G (100 U/L)/Streptomycin (100 mcg/L). Jurkat T-cells (clone E6-1) were grown to a density of 5×10^5 cells/mL in RPMI-1640 medium supplemented

with 10% FCS, L-glutamine (2 mM) and Penicillin G (100 U/L)/Streptomycin (100 mcg/L). All cell lines were grown at 37°C in a humidified atmosphere with 5% CO₂. For immunoprecipitation and confocal analysis, 4 × 10⁵ HEK293T and HeLa cells were seeded in 6-well plates. For transactivation studies, 2 × 10⁵ HEK293T cells were seeded in 12-well plates and transfected using TransIT[®]-LT1 transfection reagent (MIR2300, Mirus Bio), following the manufacturer's protocol. For confocal and transactivation analysis of Jurkat cells, 2 × 10⁶ cells were transfected by electroporation using the Neon Transfection System (Thermo Fisher Scientific), applying three pulsations of 10 ms at 1,325 V.

CRISPR/Cas9 Knockout of TRAF3

To induce the TRAF3 knockout, two guide RNA (gRNA) sequences 5'-AGCCCGAAGCAGACCGAGTG-3' and 5'-TCTTGACACGCTGTACATTT-3' were designed to target exon 1 and exon 2 of the TRAF3 gene, respectively. gRNAs were selected using online tools¹ (Ran et al., 2013). A third gRNA sequence, 5'-CCAGTTTTGTCCCTGAACA-3' was selected to target exon 1 of TRAF3 gene (Chen et al., 2015). Potential off-target sites were predicted using the online tool "CHOPCHOP"² (Labun et al., 2016). Each selected gRNA was cloned independently, using the T4 DNA ligase (Promega) into the BbsI restriction sites of the pSpCas9(BB)-2A-Puro (PX459) V2.0 vector (#62988, Addgene) and transfected in HEK293T cells using the TransIT[®]-LT1 transfection reagent (MIR2300, Mirus Bio), following the manufacturer's protocol. Cells were selected using 0.5 μg/ml puromycin for 3 days after transfection. Clonal cell lines were isolated by limiting dilution and the absence of the TRAF3 protein was tested by western blot using an anti-TRAF3 specific antibody.

Plasmids

pJFE-Tax-1, pJFE-Tax-2B full length expression vectors and the plasmid constructs expressing Tax-M22 and Tax-1 K1-10R mutants have been previously described (Turci et al., 2006, 2012). pFlag-APH-2, pGFP-APH-2, pFlag-HBZ, expression plasmids were kindly provided by Dr. Sheehy (Marban et al., 2012). pRSV-RelA/p65, pCMVF-TAB2 and Flag-TRAF3, HA-TRAF3 expression vectors have been previously described (Avesani et al., 2010; Diani et al., 2015). pEF-p52 was kindly provided by Dr. Matsuoka. pcDNA3-VSV-APH-2, pSG5M-Tax2-His, His-HBZ have been previously described (Journo et al., 2013; Dubuisson et al., 2018). pSpCas9(BB)-2A-Puro (PX459) V2.0 vector was purchased from Addgene. NF- κ B-Luc and pHRG-TK plasmids have been previously described (Bergamo et al., 2017).

Antibodies

The following primary antibodies were used: mouse monoclonal anti-Flag M2 (F3165, Sigma-Aldrich), rabbit polyclonal anti-Flag (F7425, Sigma-Aldrich), mouse monoclonal anti-VSV (V5507, Sigma-Aldrich), rabbit polyclonal anti-VSV (V4888, Sigma-Aldrich), goat polyclonal anti-His (ab9136, Abcam), rabbit

polyclonal anti-HA (H6908, Sigma-Aldrich), mouse monoclonal anti-HA (16B12, Covance), rabbit polyclonal anti I κ B- α (#9242, Cell Signaling), rabbit polyclonal anti-TRAF3 (18099-1-AP, ProteinTech), mouse monoclonal anti-p65 (C-20) (sc-372, Santa Cruz), rabbit polyclonal anti-p65 (MAB3026, Merck Millipore), mouse monoclonal anti-IKK γ (611306, BD Bioscience), rabbit monoclonal anti-NF- κ B2 p100/p52 (#3017, Cell Signaling Technology), mouse monoclonal anti- β -tubulin (bsm-33034M, Bioss Antibodies), mouse monoclonal anti-Tax-1 derives from hybridoma 168-A51 (AIDS research and Reagent Program, National Institutes of Health), rabbit polyclonal anti-Tax-2 has been previously described (Turci et al., 2012). Horseradish peroxidase-conjugated secondary antibodies anti-mouse IgG (31430, Thermo Fisher Scientific) and anti-rabbit IgG (31460, Thermo Fisher Scientific) were used in western blotting. The secondary antibodies anti-rabbit488 (ab98488, Abcam), anti-goat488 (ab150129, Abcam), anti-mouse549 (DI-2549, Vector Lab), anti-goat TexasRed (705-075-147, Jackson Imm. Res.), (ab150107, Abcam), anti-rabbit649 (STAR36D649, AbD serotec) were used in immunofluorescence.

Co-immunoprecipitations

HEK293T cells were harvested 24 h after transfection with 1 μg of each expression vector. Cells were lysed in non-denaturing buffer (10 mM Tris-HCl pH 7.5, 5 mM EDTA, 150 mM NaCl, 1% TritonX-100) supplemented with protease inhibitors Complete Protease Inhibitor Cocktail EDTA-free (Roche). Lysates were sonicated twice for 5 s, frozen at -80°C for 1 h and then centrifuged for 30 min at 14000 rpm at 4°C. Proteins were subjected to co-immunoprecipitation with the appropriate primary antibodies overnight at 4°C. Immunocomplexes were linked to magnetic beads of Dynabeads Protein G or A (LifeTechnologies) for 30 min at 4°C. The beads were then washed 3 times and resuspended in elution buffer containing NuPAGE loading buffer (LifeTechnologies) and 0.25 mM DTT.

Western Blotting

Total protein concentration in cell lysates was determined by Bradford Coomassie brilliant blue assay (Sigma-Aldrich). Equal amounts of cellular proteins were resolved in SDS polyacrylamide gel electrophoresis (SDS-PAGE) and transferred to a PVDF membrane (GE Healthcare). Membranes were first saturated in TBS solution containing 5% non-fat milk and 0.1% Tween20, and then incubated with specific primary and secondary antibodies. Anti- β -tubulin was used as loading control. Bound antibodies were revealed using ECL prime western blotting detection reagent (GE Healthcare), according to the manufacturer's instructions. Densitometry analysis of western blot protein bands was performed using the GelQuant. NET software provided by <http://biochemlabsolutions.com>.

Luciferase Reporter Assay

Luciferase functional quantitative assay was performed as previously described (Bergamo et al., 2017). Briefly, HEK293T, TRAF3-KO and Jurkat cells were transfected with 500 ng of the NF- κ B-Luc reporter plasmid together with the appropriate expression vectors or an empty vector. Transfection efficiency

¹<http://crispr.mit.edu>

²<http://chopchop.cbu.uib.no/>

was normalized using 100 ng of phRG-TK plasmid (*Renilla* luciferase vector). TNF- α -induced NF- κ B-activation was analyzed following transient expression of a NF- κ B-luciferase reporter vector and cell stimulation with 25 ng/mL TNF- α for 18 h. Luciferase activity was assayed 24 h post-transfection using the Dual-Luciferase reporter assay system (Promega). Levels of Firefly and *Renilla* luciferase were measured with a 20/20n Single Tube Luminometer (Promega). Experiments were repeated at least three times and luciferase activity was measured after deduction of the activity levels with the promoter alone.

Fluorescence Microscopy

HeLa, HEK293T, TRAF3-KO, U2OS and Jurkat cells were transfected with 1 or 2 μ g of each appropriate expression vector; p65 protein nuclear translocation was analyzed following 25 ng/mL TNF- α cell stimulation for 20 min. Cells were seeded on cover glasses and 24 h post-transfection HeLa, HEK293T, TRAF3-KO, and U2OS cells were fixed with 4% paraformaldehyde/PBS, whereas Jurkat cells were fixed with formalin (HT5011, Sigma-Aldrich), for 20 min. Cells were then permeabilized with 0.5% Triton X-100/PBS for 20 min, blocked with a 5% milk/PBS solution and incubated with appropriate primary and conjugated secondary antibodies. The cover glasses were then mounted in DAPI-containing Fluoromount-G (Southern Biotech). For confocal analyses, slides were examined under a LSM800 (Carl Zeiss MicroImaging) confocal microscope equipped with 63 \times 1.4 plan apochromat oil-immersion objective using the ZEN software. For epifluorescence imaging, slides were examined under an AxioImager.Z1 microscope (Zeiss) using the Methamorph software. To quantify p65 nuclear translocation, the ratios of the nuclear/total p65 mean brightness staining were calculated using ImageJ software. RGB profiles were calculated using the RGB profiler plugin.

RNA Isolation and Quantitative Real-Time PCR

Total RNA was extracted from HEK293T and TRAF3-KO cells using TRIzolTM (Invitrogen), according to the manufacturers' recommendations. RNA was quantified by NanoDrop 2000 Spectrophotometer (Thermo Fisher Scientific) and absorbance ratio at 260/280 and 260/230 were measured. Total RNA (1 μ g) was reverse transcribed at 50°C for 45 min using oligo

dT primers and the SuperScriptTM III First-Strand Synthesis System (Invitrogen).

PCR reactions were performed using the Power SYBR[®] Green PCR Master Mix (Applied Biosystems) and ran on CFX ConnectTM Real-Time Detection System (Bio-Rad). Primer pairs for TNF Alpha Induced Protein 3 (TNFAIP3/A20), Apoptosis Regulator Bcl-2 (BCL2), Interleukin 6 (IL-6), and Ribosomal Protein Lateral Stalk Subunit P0 (RPLP0) gene expression analysis are listed in **Table 1**. PCR cycles included an initial step of 10 min at 95°C required for enzyme activation, followed by 40 cycles of amplification: denaturation for 15 s at 95°C, annealing and extension for 60 s at 60°C. The relative fold change values were calculated using the $2^{-\Delta\Delta C_t}$ method (Livak and Schmittgen, 2001). RPLP0 was used as internal reference gene.

Statistical Analyses

All data are presented as the means \pm standard deviation from at least three independent experiments. Statistical significance was assessed by the Student's *t*-test. Differences were considered to be significant when $P < 0.05$ (*), and strongly significant when $P < 0.01$ (**), and $P < 0.001$ (***)

RESULTS

TRAF3 Is Required for an Efficient Activation of NF- κ B Mediated by Tax

It has been shown that ATL cells exhibit high expression levels of NIK, a positive regulator of the NF- κ B pathway and that NIK turnover is regulated by protein complexes that contain the E3 ubiquitin ligase TRAF3 (Chan and Greene, 2012). Based on our previous data showing that TRAF3 interacts with both Tax-1 and Tax-2 (Diani et al., 2015), we investigated the contribution of TRAF3 in the modulation of NF- κ B mediated by the viral regulatory proteins. We produced TRAF3-KO HEK293T cell lines introducing insertion/deletion (*indel*) mutations by transfection of TRAF3 RNA-guided Cas9 nuclease expressing plasmid. TRAF3-KO clones were first characterized for their ability to activate an NF- κ B promoter. Using the luciferase reporter assay, we first found that in the absence of any stimulus, the basal NF- κ B promoter activity was increased 50 folds in TRAF3-KO cell lines as compared to wild type cells (WT) (**Figure 1A**). The luciferase activity was restored by the rescue of TRAF3 expression in transfected TRAF3-KO

TABLE 1 | qRT-PCR primer sequences.

Gene	Accession no.	Primer sequence (5' -> 3')	PCR product (pb)
<i>TNFAIP3 (A20)</i>	NM_001270507.1	F: CTGGGACCATGGCACAACCTC R: CGGAAGGTTCCATGGGATTC	182
<i>BCL2</i>	NM_000633.2	F: GATGTGATGCCTCTGCGAAG R: CATGCTGATGTCTCTGGAATCT	92
<i>IL6</i>	NM_000600.4	F: TACATCCTCGACGGCATCTC R: TGGCTTGTTCTCACTACTCT	247
<i>RPLP0</i>	NM_001002.4	F: ACATGTTGCTGCGCAATAAGGT R: CCTAAGCCTGGAAAAAGGAGG	127

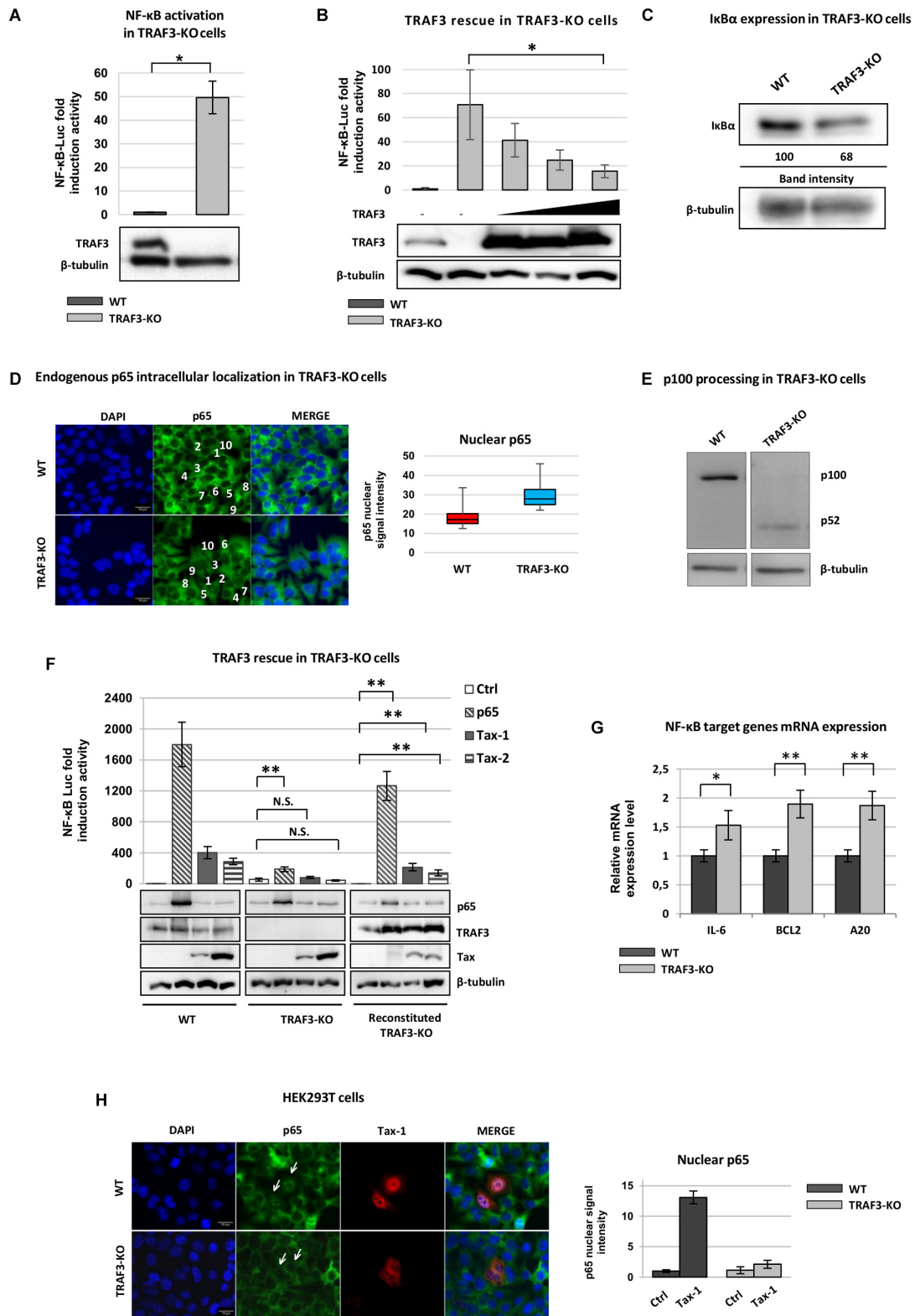


FIGURE 1 | TRAF3 is required for an efficient activation of NF- κ B mediated by Tax. **(A)** Luciferase levels were measured from HEK293T (WT) and TRAF3-KO cells transfected with pHRG-TK renilla vector (control for transfection efficiency) and NF- κ B-luciferase reporter expressing vector. **(B)** Luciferase levels were measured from HEK293T (WT) and TRAF3-KO cells transfected with pHRG-TK renilla vector, NF- κ B-luciferase reporter and increasing amount of Flag-TRAF3 expressing vector.

(Continued)

FIGURE 1 | Continued

(C) HEK293T (WT) and TRAF3-KO cells were lysed and immunoblot analysis was performed to compare the levels of endogenous I κ B. The amount of I κ B was measured relative to the amount of β -tubulin. **(D)** HEK293T (WT) and TRAF3-KO cells were stained with anti-p65 (green signal) primary antibody. Nuclei were stained with DAPI (blue signal). Scalebar, 10 μ m. Total cells and nuclei of cells ($n = 10$) indicated by a number from 1 to 10 in white were delineated using ImageJ software, and the mean brightness ratio of the nuclear RelA/p65 staining was calculated and presented as box-plot. **(E)** Immunoblot analysis of p100/p52 proteins expression levels in HEK293T (WT) and TRAF3-KO cells. **(F)** HEK293T (WT) and TRAF3-KO cells were transfected with pHRG-TK renilla vector, NF- κ B-luciferase reporter and p65, Tax-1, Tax-2, or TRAF3 expression plasmids. Cell lysates were collected and luciferase levels were measured. Immunoblot analysis was performed to detect of TRAF3, p65, Tax-1 and Tax-2 (N.S. = not significant). **(G)** RNA from HEK293T (WT) and TRAF3-KO cells were analyzed by qRT-PCR for NF- κ B-related transcripts. The values were normalized to RPLP0 and the results were expressed as relative fold change of expression levels. **(H)** HEK293T (WT) and TRAF3-KO cells were transfected with Tax-1 encoding vector and stained with anti-p65 (green signal) and anti-Tax-1 (red signal) primary antibody. Nuclei were stained with DAPI (blue signal). Total cells and nuclei were delineated using ImageJ software, and the mean brightness ratio of the nuclear p65 staining was calculated (right panel). Scalebar, 10 μ m. $P < 0.05$ (*) and $P < 0.01$ (**).

cells (**Figure 1B**). The basal activation of NF- κ B in TRAF3-KO cells was further confirmed by analyzing I κ B protein level. As expected, we measured a reduced amount of I κ B (30% decrease) in TRAF3-KO cells as compared to WT cells (**Figure 1C**). When the basal endogenous p65 distribution was analyzed in TRAF3-KO cells, the presence of p65 in the nucleus, even if limited to a weak signal, was observed (**Figure 1D**). The mean brightness ratio of the nuclear p65 staining was increased 1.5 fold in the TRAF3-KO cells compared to the WT. This indicates that the canonical NF- κ B pathway is constitutively although partially activated in the absence of TRAF3. To define if the alternative NF- κ B pathway is also activated in the absence of TRAF3, the processing of the p100 protein was analyzed. As shown in **Figure 1E**, accumulation of p52 was detectable in the TRAF3-KO cell line, but not in the WT cells. These results showing that the depletion of TRAF3 enables detectable translocation of p65 into the nucleus, as well as p100 processing, suggest that both the canonical and non-canonical NF- κ B may be partially activated.

When we analyzed the NF- κ B activation induced by the expression of p65 in TRAF3-KO cells, we unexpectedly measured a limited induction compared to WT cells (about 9-fold decrease). A similar dramatic reduction of NF- κ B induction by Tax-1 or Tax-2 was observed in TRAF3-KO cells compared to WT cells (about 5-fold and 6-fold decrease, respectively) (**Figure 1F**). Reconstituted TRAF3 expression restored the efficiency of p65- and Tax-mediated activation. In order to explore the mechanism that impairs the full activation of NF- κ B mediated by p65 in the absence of TRAF3, we analyzed TNF- α -mediated induction of the NF- κ B promoter in TRAF3-KO cells. After TNF- α stimulation, we measured a significant NF- κ B activation in TRAF3-KO cells, although lower when compared to WT cells (**Supplementary Figure 1A**). When we analyzed p65 nuclear translocation induced by TNF- α , we observed p65 nuclear translocation in WT and TRAF3-KO cells (**Supplementary Figure 1B**), indicating that the NF- κ B pathway was activated, although the resulting transcriptional activity of p65 was reduced.

To explore the possibility that in TRAF3-KO cells the basal activation of NF- κ B may lead to the expression of NF- κ B target genes that control p65 activity by negative feedback loops, we analyzed the expression of A20 and BCL2 genes, which are well known negative regulators of NF- κ B (Grimm et al., 1996; Pujari et al., 2013). We found that both genes were significantly more expressed in TRAF3-KO cells compared to WT suggesting

that limited p65-mediated induction of NF- κ B in TRAF3-KO cells can be due to negative feedback mechanisms (**Figure 1G**). Furthermore, the results showed an increased expression of IL-6, an NF- κ B target gene (Liebermann and Baltimore, 1990) (**Figure 1G**) compared to the WT cells.

In agreement with the results showing that Tax-1 mediated NF- κ B activation is impaired in TRAF3-KO cells, we observed that Tax-1 failed to induce endogenous p65 nuclear translocation in transfected cells (**Figure 1H**). Taken together, these results strongly suggest that NF- κ B hyper-activation by Tax is strictly dependent upon TRAF3 expression.

HBZ and APH-2 Interact With p65 and Suppress the NF- κ B Pathway

Since our results indicate that TRAF3 is involved in Tax-induced NF- κ B hyper-activation, and it is known that HBZ and APH-2 interfere with NF- κ B signaling, we aimed to analyze whether the antisense proteins might interfere with TRAF3 functions. Before analyzing the specific interplay of HBZ and APH-2 with TRAF3, we first aimed at precisely comparing their ability of antagonize Tax-induced NF- κ B activation.

HEK293T cells transfected with increasing amounts of Tax proteins in the presence or absence of HBZ or APH-2 were analyzed by luciferase assay (**Figures 2A,B**). As expected, when HBZ was present together with low levels of Tax-1, the NF- κ B activation was significantly reduced (**Figure 2A**, lanes 2 vs. 5), whereas no HBZ inhibitory effect was evident when Tax-1 was expressed at high levels in transfected cells (**Figure 2A**, lane 3 vs. 6). APH-2 effect on Tax-mediated NF- κ B activation was then analyzed (**Figure 2B**). Similar to HBZ, APH-2 inhibited Tax-2-induced NF- κ B activity, but unexpectedly and unlike Tax-1, high expression of Tax-2 did not restore the activation of NF- κ B (**Figure 2B**). Of note, this inhibitory effect of APH-2 was evident despite the fact that APH-2 was less expressed than HBZ in transfected cells, as previously reported (Panfil et al., 2016; Dubuisson et al., 2018). Because APH-2 appeared to be more potent than HBZ in the inhibition of Tax-mediated NF- κ B activation, the effect of HBZ and APH-2 expression on the NF- κ B promoter activation mediated by p65 over-expression was then compared in HEK293T cells. The inhibition was statistically significant for both proteins and reached similar levels (**Figures 2C,D**). The results were also reproduced in Jurkat cells in the presence of APH-2 (**Supplementary Figure 2A**).

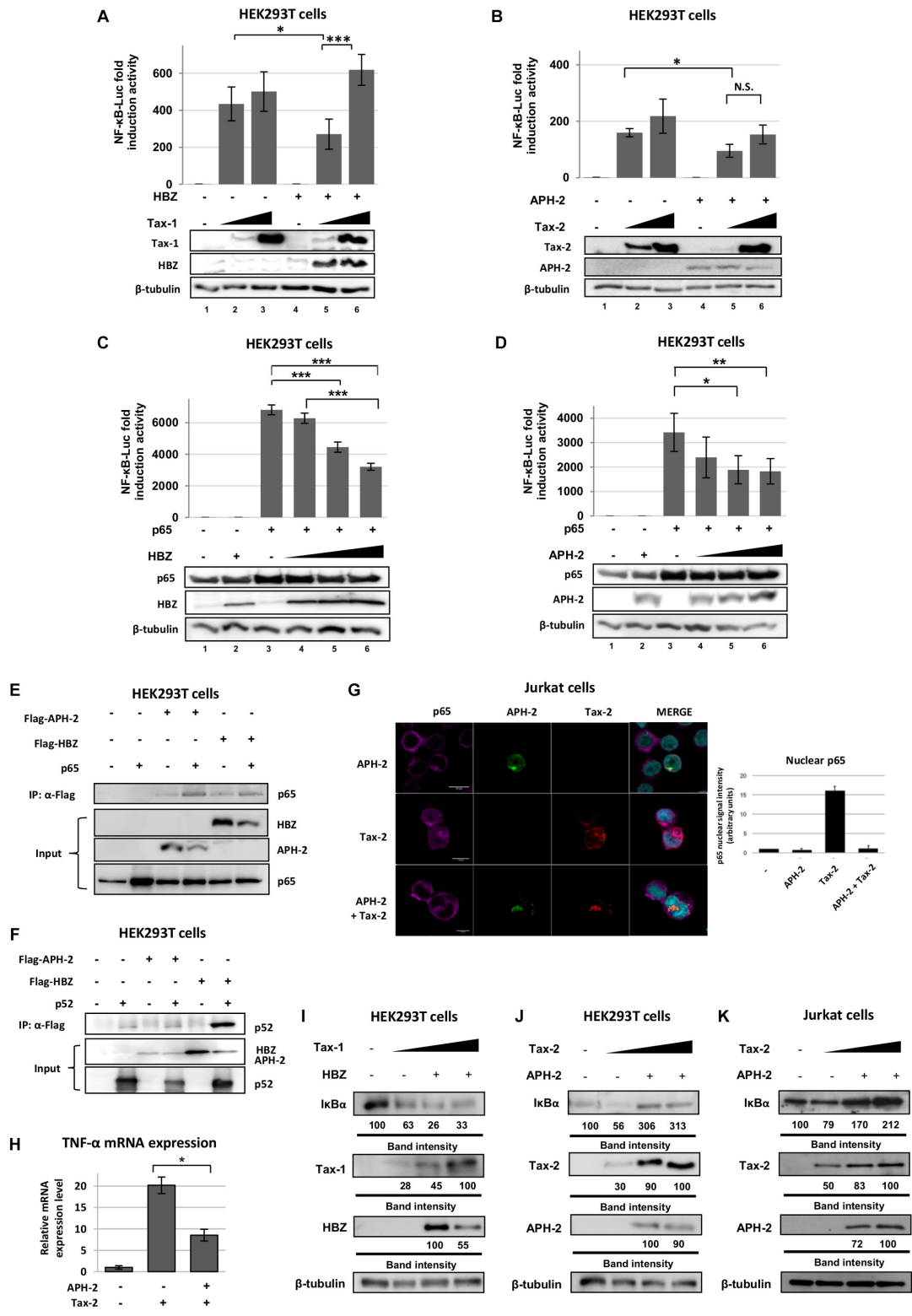


FIGURE 2 | HBZ and APh-2 interact with p65 and suppress the NF-κB pathway. HEK293T cells were transfected with pHRG-TK renilla vector, NF-κB-luciferase reporter, Flag-HBZ and increasing amounts of Tax-1 (A) or Flag-APH-2 and increasing amounts of Tax-2 expression plasmids (B) (N.S. = not significant). HEK293T cells were transfected with pHRG-TK renilla vector, NF-κB-luciferase reporter, p65 expression plasmid, and increasing amounts of Flag-HBZ (C) or Flag-APH-2 (D) expression vectors. Cell lysates were collected and luciferase levels were measured (Top). Immunoblot analysis was performed to detect the expression levels of the (Continued)

FIGURE 2 | Continued

transfected proteins (Bottom). **(E,F)** HEK293T cells were transfected with p65 or p52, Flag-APH-2, or Flag-HBZ expression vectors. Tagged proteins were immunoprecipitated with an anti-Flag antibody and the presence of the p65 or p52 proteins was examined by western blot. **(G)** Jurkat cells were transfected with VSV-APH-2 and Tax-2 expression vectors. Samples were stained with anti-VSV, anti-Tax-2 and anti-p65 primary antibodies to detect APH-2 (green signal), Tax-2 (red signal), and endogenous p65 (magenta signal), respectively. Total cells and nuclei were delineated using ImageJ software, and the mean brightness ratio of the nuclear p65 staining was calculated (right panel). Values obtained in non-transfected cells were then subtracted from those for APH-2, Tax or APH-2+Tax-expressing cells. Scalebar, 10 μ m. **(H)** TNF- α expression was analyzed by qRT-PCR from RNA of HEK293T cells transfected with VSV-APH-2 and Tax-2. The values were normalized to RPLP0 and the results were expressed as relative fold change of expression levels. **(I-K)** HEK293T and Jurkat cells were co-transfected with Flag-HBZ and increasing amount of Tax-1 or with Flag-APH-2 and increasing amount of Tax-2. Immunoblot analysis was performed to compare the levels of endogenous I κ B in the presence of the viral regulatory proteins. The amount of I κ B was measured relative to the amount of β -tubulin. $P < 0.05$ (*), $P < 0.01$ (**), and $P < 0.001$ (***)

To further compare the mechanism of NF- κ B inhibition by both antisense proteins, we then analyzed the interaction of HBZ and APH-2 with the transcription factors p65 and p52 by immunoprecipitation. **Figure 2E** shows that p65 was detected in complexes with both proteins, indicating that both antisense proteins interact with the classical transcription factor p65. When HBZ and APH-2 interaction with p52 was analyzed, it revealed that HBZ was present in complex with p52, unlike APH-2 (**Figure 2F**). These results suggested that HBZ and APH-2 share the ability to form complexes with p65, but they differ in their interaction with p52, the final effector of the alternative NF- κ B signaling. Given that p65 translocates into the nucleus when Tax is expressed, the cellular localization of p65 in the presence of APH-2 and/or Tax-2 was analyzed. The results showed that endogenous p65 localized in the cytoplasm in the presence of APH-2 (**Figure 2G**). Interestingly, it was found that the co-expression of APH-2 and Tax-2 resulted in their cytoplasmic co-localization and in the impairment of p65 nuclear translocation (5-fold decrease) (**Figure 2G**). The same results were observed in U2OS cells (**Supplementary Figure 2B**). We performed qRT-PCR analysis in the presence of Tax-2 and APH-2, analyzing the expression of TNF- α as an example of an NF- κ B target gene. In the presence of APH-2 and Tax-2, TNF- α expression was reduced more than 10-fold (**Figure 2H**). We then analyzed the effect of HBZ and APH-2 on I κ B degradation, which allows p65 nuclear translocation and which is known to be induced by Tax (Harhaj and Harhaj, 2005). As expected, the expression of I κ B was reduced to about 40% in the presence of Tax-1 and 80% in the presence of both Tax-1 and HBZ proteins (**Figure 2I**), whereas in the presence of both APH-2 and Tax-2 proteins, an increase in I κ B expression was observed (**Figure 2J**). A similar result was obtained in Jurkat cells (**Figure 2K**). Taken together, these results suggest that while HBZ and APH-2 both inhibit Tax- and p65-mediated NF- κ B activation, they may differ in their inhibition mechanism. APH-2 may inhibit p65 translocation by affecting I κ B degradation, thus limiting Tax-2-mediated NF- κ B activation.

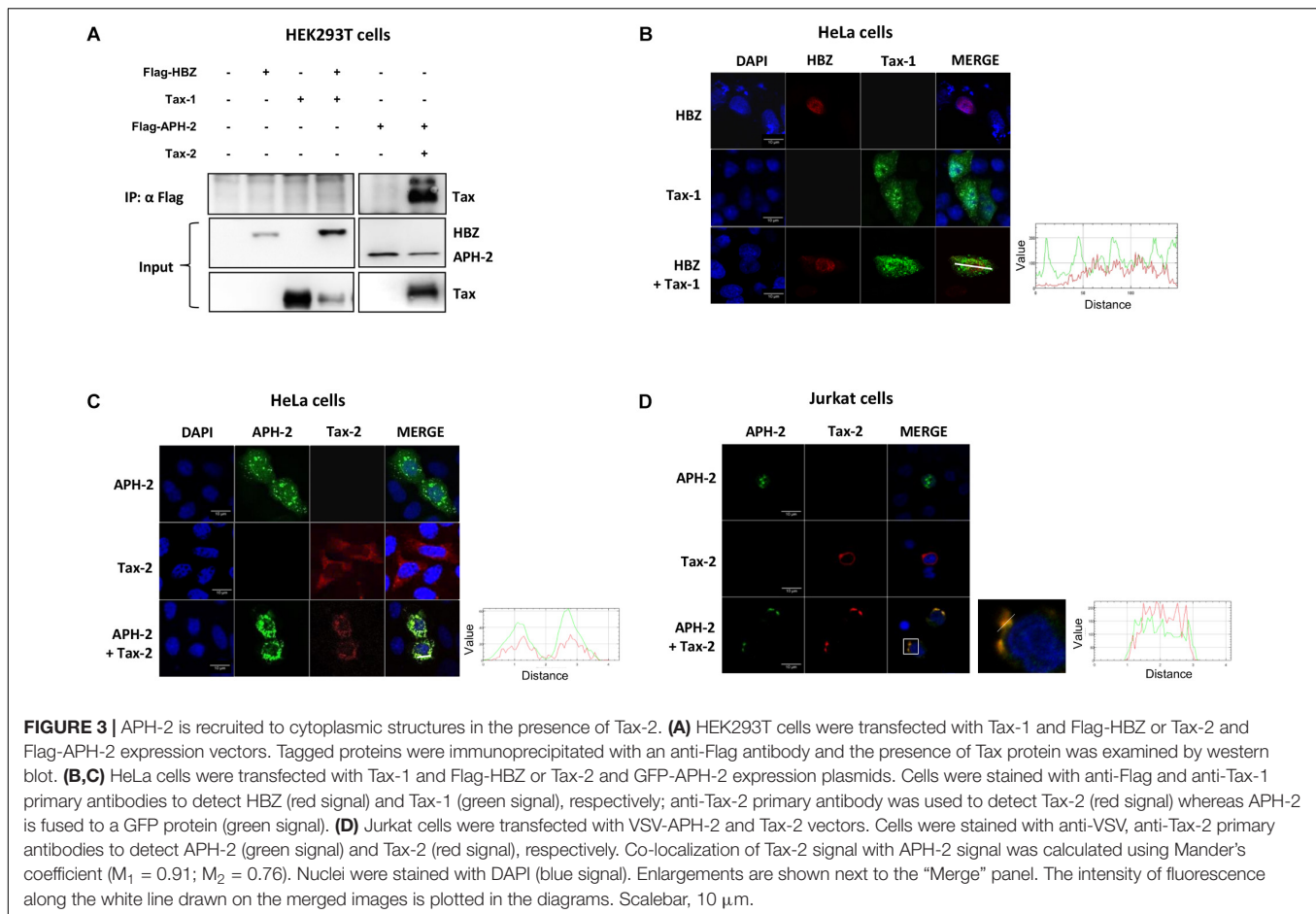
APH-2 Is Recruited to Cytoplasmic Structures in the Presence of Tax-2

To investigate how APH-2 might inhibit NF- κ B activity upstream of I κ B degradation, we analyzed APH-2 subcellular localization. Indeed, it has previously been reported that while Tax-1 does not interact with HBZ, Tax-2 does interact with APH-2 (Zhao et al., 2009; Marban et al., 2012). Given the different

cellular distribution of Tax-1 and Tax-2 (Meertens et al., 2004; Bertazzoni et al., 2011), it is possible that HBZ and APH-2 differ in the mechanism of NF- κ B inhibition due to their differential recruitment by host factors in subcellular compartments. To test this hypothesis, HEK293T cells were transfected with Tax-1 or Tax-2 and Flag-HBZ or Flag-APH-2 expressing vectors, and the presence of Tax in the immunocomplexes precipitated with an anti-Flag antibody was analyzed (**Figure 3A**). The results, as expected, confirmed that Tax-2 formed complexes with APH-2, but no interaction of Tax-1 with HBZ was observed. Confocal microscopy analyses in transfected HeLa cells showed that HBZ alone localized in the nucleus and that when Tax-1 was co-expressed with HBZ, no co-localization was observed (**Figure 3B**). Interestingly, the co-expression of APH-2 and Tax-2 resulted in APH-2 redistribution and its co-localization with Tax-2 in cytoplasmic structures (**Figure 3C**). This result was also reproduced in Jurkat cells (**Figure 3D**). To ensure that recruitment of APH-2 in cytoplasmic structures is a property of Tax-2 but not of Tax-1, HEK293T cells were transfected with both APH-2 and Tax-1, or with both HBZ and Tax-2 vectors and their intracellular localization was analyzed by fluorescent microscopy. We observed that Tax-1 and APH-2 did not co-localize in the cytoplasm (**Supplementary Figure 3A**). In the presence of HBZ, Tax-2 was mainly distributed in the cytoplasm and HBZ in the nucleus (**Supplementary Figure 3B**). Taken together, these results suggest that HBZ and APH-2 differ in their subcellular distribution when Tax proteins are expressed and that the cytoplasmic co-localization occurs only in the presence of Tax-2 and APH-2. This might explain how HBZ and APH-2 differ in the mechanism of NF- κ B inhibition.

APH-2 Is Present in Cytoplasmic Complexes With TAB2, NEMO, and Tax-2

We have previously shown that Tax-2 co-localizes in the cytoplasm with the NF- κ B pathway factors TAB2, NEMO and p65 (Avesani et al., 2010). Given that APH-2 co-localizes with Tax-2 in the cytoplasm, we speculated that APH-2 may be recruited in complexes containing these NF- κ B factors. To test this hypothesis, the co-localization of APH-2 with TAB2 and NEMO in Jurkat cells was analyzed by confocal microscopy (**Figure 4**). The results showed a redistribution of TAB2 in cytoplasmic structures in the presence of Tax-2 and APH-2. TAB2 partially co-localized with APH-2 in the absence of Tax-2 (**Figure 4A**). APH-2 co-localized with NEMO only in the presence of Tax-2 (**Figure 4B**). The co-localization of



Tax-2 and APH-2 with NEMO was also reproduced in U2OS cells (**Supplementary Figure 4A**). Taken together, these results suggest that in the presence of Tax-2, APH-2 localized in the cytoplasm with TAB2 and NEMO.

HBZ and APH-2 Interfere With TRAF3 Functions

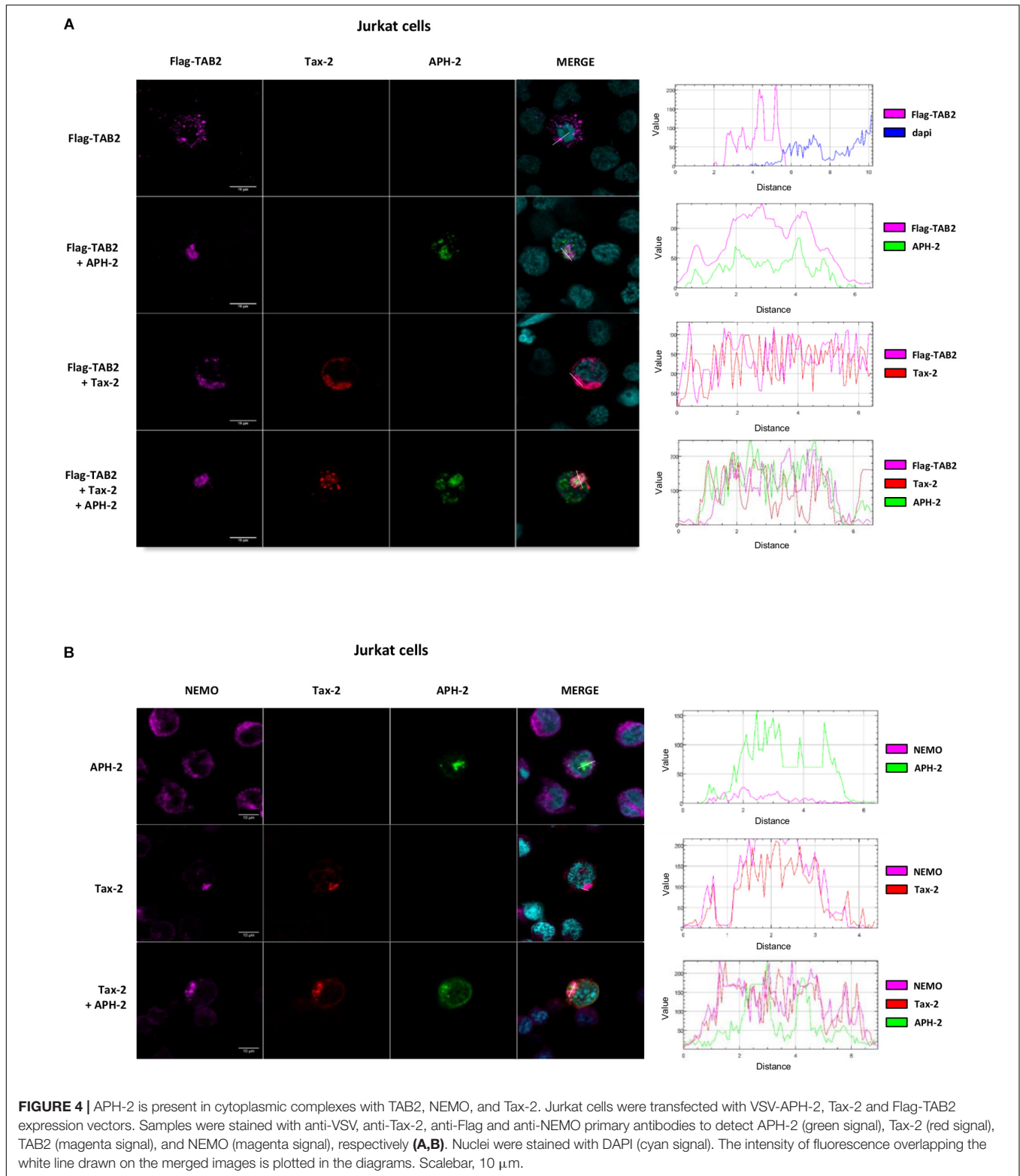
Since the antisense proteins HBZ and APH-2 both repress NF- κ B activity, we investigated the possible recruitment of HBZ and APH-2 in cytoplasmic complexes containing TRAF3. We analyzed TRAF3 distribution in the presence of viral antisense proteins by confocal microscopy in Jurkat cells. We found that HBZ (green signal) and TRAF3 (magenta signal) did not co-localize, whereas TRAF3 partially co-localized with APH-2 in the cytoplasm (**Figure 5A**). We confirmed that TRAF3 is present in immunocomplexes containing APH-2 by co-immunoprecipitation (**Figure 5B**). Furthermore, we detected TRAF3 in complexes containing both APH-2 and Tax-2 (**Figure 5B**). We analyzed by confocal microscopy TRAF3 distribution in the presence of APH-2 and Tax-2, and we found that APH-2 (green signal), TRAF3 (magenta signal) and Tax-2 (red signal) co-localized in the cytoplasm (**Figure 5C**). Co-localization of Tax-2 and APH-2 with TRAF3 was also observed in U2OS cells (**Supplementary Figure 4B**). This

indicates that APH-2, but not HBZ, could modulate Tax-2 induced NF- κ B activation by associating with Tax-2 and TRAF3 complexes.

To assess whether HBZ may deregulate the NF- κ B pathway by affecting the expression of TRAF3, as it was previously shown with p65, HEK293T cells were transfected with increasing amounts of HBZ and the expression levels of TRAF3 was evaluated. The results demonstrated a reduction of the expression of TRAF3 protein in the presence of HBZ and APH-2 (**Figure 5D**). A reduced expression of endogenous TRAF3 was also found in the presence of increasing amounts of HBZ and APH-2 (**Supplementary Figures 5A,B**). These results suggest that TRAF3 may be involved in the mechanisms of NF- κ B deregulation mediated by HTLV proteins and that its expression may be altered by both HBZ and APH-2 proteins.

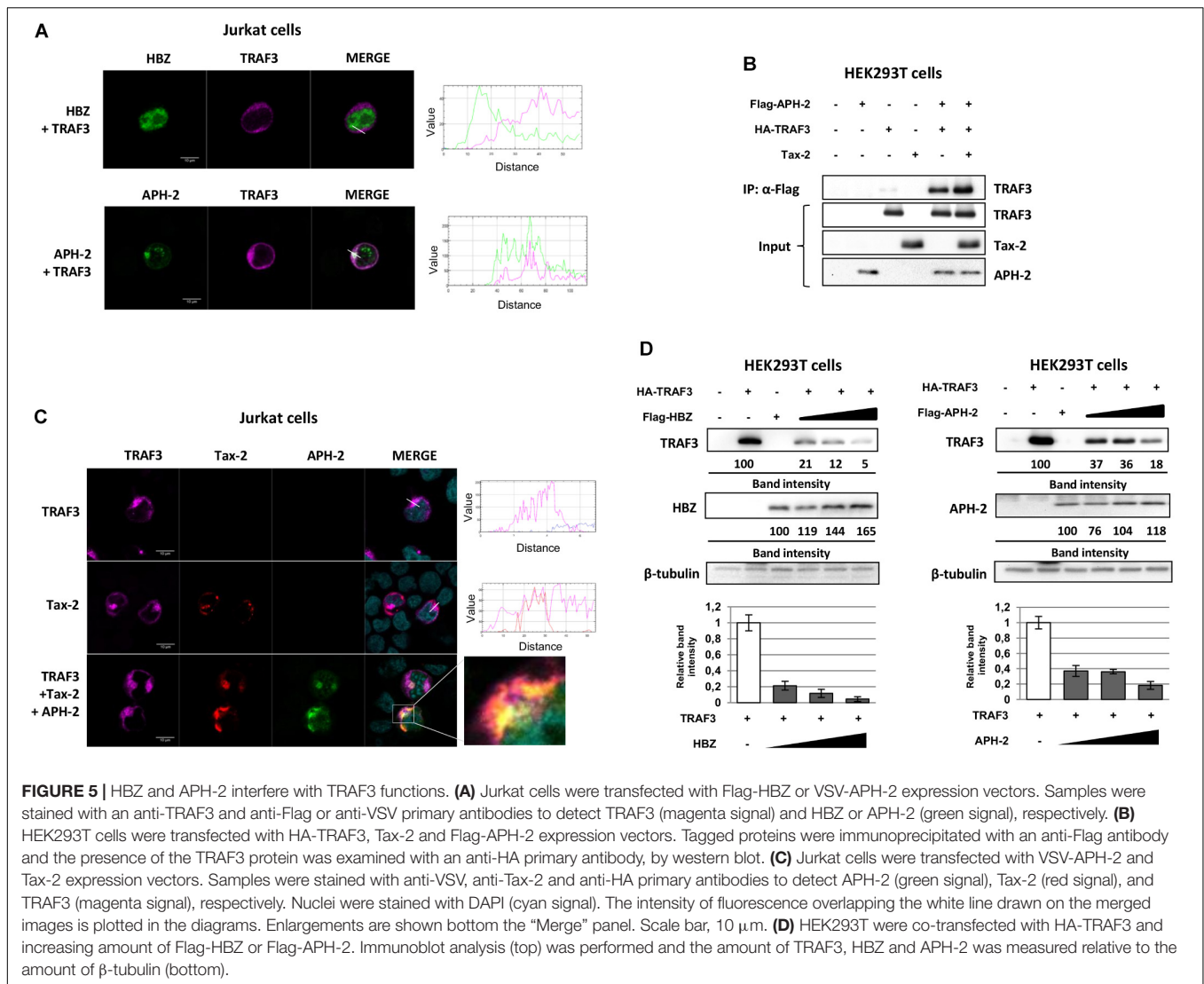
DISCUSSION

Dysregulation of the NF- κ B pathway can induce alterations of physiological cellular responses and can lead to oncogenesis (Park and Hong, 2016). It has been demonstrated that persistent NF- κ B activation derived from Tax expression induces cell senescence, and the inhibitory effect of the antisense protein HBZ on NF- κ B may represent an adaptation of HTLV-1 that contributes to



viral persistence and, in the long term, to ATL development (Giam and Semmes, 2016). It has also been reported that the inhibition of the NF- κ B pathway results in the induction of apoptosis of ATL cells (Watanabe et al., 2005). The HTLV

regulatory proteins interaction with canonical NF- κ B factors leading to NF- κ B dysregulation has been intensively investigated, but limited information is available about the interaction with factors that play a critical role in the non-canonical pathway



(Schmitz et al., 2014; Fochi et al., 2018). We focused our attention on TRAF3, a ubiquitin ligase that controls the expression levels of the NIK kinase and that has been demonstrated to be abnormally expressed in freshly isolated ATL cells (Watanabe, 2017). TRAF3-deficient mice display increased non-canonical NF- κ B activation as well as increased B cell survival, suggesting that TRAF3 may act as a negative regulator of the NF- κ B signaling *in vivo* (Gardam et al., 2008). It has been demonstrated that TRAF3 knockout results in NIK stabilization, inducing p100 processing (Liao et al., 2004; He et al., 2006). In TRAF3-deficient cell lines, we found that the NF- κ B pathway is activated and that both a partial nuclear distribution of the transcriptional factor p65 and p100 processing are taking place. These results confirm that TRAF3 is a negative regulator of the NF- κ B pathway, but it may also participate to the functional regulation between the two NF- κ B pathways. We also found that p65 and TNF- α partially induced NF- κ B activation in TRAF3-KO cell lines. This effect may be explained by negative feedback loop mechanisms derived by the expression of NF- κ B target genes

acting as negative regulators. This hypothesis is supported by the qRT-PCR analyses of A20 and BCL-2 genes in TRAF3-KO cells, showing that they are over-expressed as compared to WT cells. It is known that A20 mediates a negative regulation of the canonical NF- κ B pathway (Pujari et al., 2013) and BCL-2 overexpression specifically represses NF- κ B-dependent transactivation by attenuating the transactivation potential of p65 (Grimm et al., 1996). These results are consistent with previous data showing that TRAF3 depletion causes an accumulation of distinct subsets of NF- κ B inhibitors, including A20 (Bista et al., 2010).

We have previously shown that Tax interacts with TRAF3 and here we demonstrate for the first time that the TRAF3 factor is required for an efficient NF- κ B activation by both Tax-1 and Tax-2.

Unlike Tax-1, Tax-2 cannot induce p100 processing to p52, but can activate the canonical NF- κ B pathway as well as Tax-1 (Xiao et al., 2001; Higuchi et al., 2007). We found that Tax-mediated activation of NF- κ B is impaired in TRAF3-deficient cells and

that it is restored only after rescuing TRAF3 expression. A similar essential role of TRAF3 has been demonstrated for the Epstein-Barr virus-encoded oncoprotein latent membrane protein 1 (LMP1). In fact, LMP1 alone can transform rodent fibroblasts and activate NF- κ B (Cahir McFarland et al., 1999), but in the absence of TRAF3, LMP1-induced activation of JNK, p38, and NF- κ B are impaired (Xie et al., 2004). It has been also demonstrated that the vFlip protein expressed by Kaposi's sarcoma-associated herpesvirus (KSHV/HHV8) activates NF- κ B interacting with the IKK complex and the TRAF2/3 complex (Field et al., 2003). Interestingly, we found that TRAF3 is required not only for Tax-1, but also for Tax-2 NF- κ B activation, supporting a mechanism in which TRAF3 may be involved in the association with factors that cooperate in the canonical and non-canonical NF- κ B pathway.

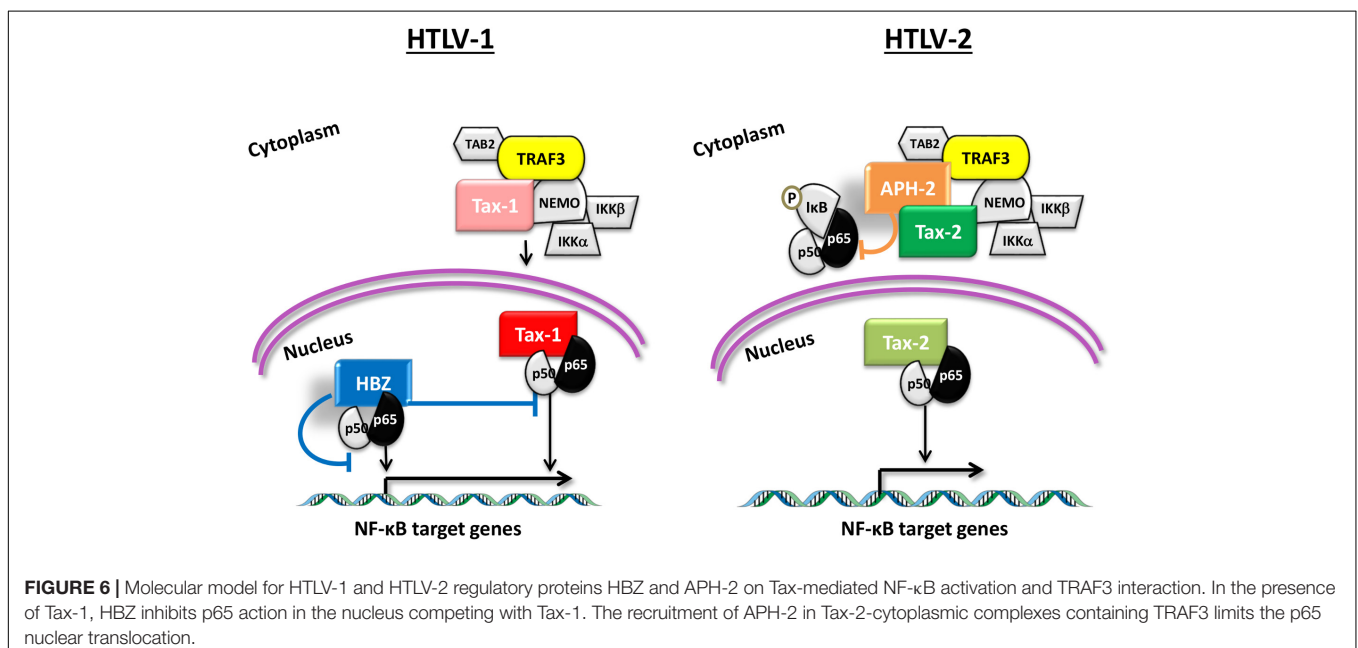
We report here a reduction of TRAF3 expression in the presence of the antisense proteins. We would have expected an activation of the non-canonical NF- κ B pathway, but we have not observed an accumulation of p52 in the presence of HBZ (data not shown). This result is in agreement with data demonstrating a lowered expression of p100 in the presence of HBZ that leads to lowered amounts of the non-canonical transcription factor p52 (Zhi et al., 2011). The HBZ effect in the non-canonical NF- κ B activation still remains controversial since Zhao et al. (2009) suggest that HBZ inhibits selectively the canonical NF- κ B pathway in the presence of Tax-1.

Zhao et al. (2009) and Panfil et al. (2016) demonstrated that both HBZ and APH-2 interact with p65 and reduce p65-mediated NF- κ B promoter activity. We show here that HBZ and APH-2 may exert a different molecular mechanism in the down-modulation of the NF- κ B pathway. We found that HBZ is less efficient in dampening Tax-mediated NF- κ B activity compared to APH-2 and that co-expression of HBZ and high levels of Tax-1 results in restoring NF- κ B activation,

whereas APH-2 maintains its inhibitory effect despite high expression levels of Tax-2. We also observed that APH-2 inhibits p65-induced NF- κ B activation in both HEK293T and Jurkat cell models. This is in contrast to the previous report showing that APH-2 inhibits the p65-induced NF- κ B activation only in HEK293T cells (Panfil et al., 2016). This discrepancy may be due to differences in the efficiency of cell transfection, as declared by the authors.

By analyzing the subcellular distribution of the protein complexes formed by Tax and the host interacting proteins, we observed that APH-2, but not HBZ, is recruited in the cytoplasmic structures containing NEMO and TAB2. We have also demonstrated that the co-expression of Tax-2 and APH-2 results in the accumulation of the NF- κ B inhibitor I κ B and in a partial impairment of p65 nuclear translocation, whereas I κ B expression is reduced when Tax-1 and HBZ are co-expressed. From the results obtained, we propose a model in which the recruitment of HBZ and APH-2 within the protein complexes formed by Tax follows different patterns. While APH-2 is partially retained in the cytoplasmic compartments, HBZ translocates more efficiently into the nucleus, thus inhibiting the transcription factor activity of p65 (Figure 6). This model is also supported by the results of Marban et al. (2012) that demonstrate a redistribution of APH-2 in the cytoplasm in the presence of Tax-2, preventing APH-2 from activating AP-1 transcription.

Our results clearly demonstrate that TRAF3 is required for NF- κ B dysregulation mediated by Tax, thus representing a novel factor recruited by the viral regulatory proteins to alter cell pathways. In fact, TRAF3 not only acts on NF- κ B pathway, but also plays significant roles in the immunity-related signal transduction (Häcker et al., 2011). Cells lacking TRAF3 are defective in IFN-I responses activated by different TLRs (Oganessian et al., 2006). The induction of IFN-I elicits the



activation of the antiviral cellular gene expression that coincides with the inhibition of viral replication. The key role of TRAF3 in promoting antiviral signaling is supported by a recent study demonstrating that the deletion of TRAF3 in adult mice attenuated their host defense against vesicular stomatitis virus (VSV) infection (Xie et al., 2019). In the non-canonical NF- κ B pathway, TRAF3, in concert with TRAF2, cIAP1 and cIAP2, promotes the constitutive degradation of NIK that in turn serves as negative regulator of IFN (Jin et al., 2014; Parvatiyar et al., 2018). A feedback inhibition mechanism has been also proposed to induce TRAF3 degradation, affecting IFN production and NIK accumulation (Nakhaei et al., 2009). Recent evidence demonstrates that the HTLV antisense proteins interact with IRF-1, a transcriptional regulator of IFN-I pathway. In particular, APH-2 enhances IRF-1 DNA binding and steady-state expression levels, whereas HBZ interacts with IRF-1 and causes its degradation (Panfil et al., 2016). The loss of IRF-1 expression has been observed in several cases of leukemia (Alsamman and El-Masry, 2018). It is reasonable to think that the recruitment of APH-2 and Tax-2 in complexes with TRAF3 may positively affect IFN response. This hypothesis could be linked to the demonstration that in rabbits, the lack of APH-2 increases the infection rate of HTLV-2 mutants in comparison to HTLV-2 WT (Yin et al., 2012). Further studies will be required to analyze the interplay of TRAF3 and the HTLV antisense proteins in deregulating the type I IFN induction.

CONCLUSION

In summary, we demonstrated that TRAF3 cell factor is required for Tax-mediated NF- κ B activation. Our findings allow to further understand the roles of host factors that may be targeted by HTLV regulatory proteins and participate in the crosstalk between IFN and NF- κ B pathway. We also found that APH-2 is more effective than HBZ in the inhibition of Tax-mediated NF- κ B activation. We suggest that the recruitment of APH-2 in Tax-2-cytoplasmic structures with NF- κ B factors that affect

REFERENCES

- Alsamman, K., and El-Masry, O. S. (2018). Interferon regulatory factor 1 inactivation in human cancer. *Biosci. Rep.* 38:BSR20171672. doi: 10.1042/BSR20171672
- Araujo, A., and Hall, W. W. (2004). Human T-lymphotropic virus type II and neurological disease. *Ann. Neurol.* 56, 10–19. doi: 10.1002/ana.20126
- Avesani, F., Romanelli, M. G., Turci, M., Di Gennaro, G., Sampaio, C., Bidoia, C., et al. (2010). Association of HTLV tax proteins with TAK1-binding protein 2 and RelA in calreticulin-containing cytoplasmic structures participates in tax-mediated NF- κ B activation. *Virology* 408, 39–48. doi: 10.1016/j.virol.2010.08.023
- Bangham, C. R., Araujo, A., Yamano, Y., and Taylor, G. P. (2015). HTLV-1-associated myelopathy/tropical spastic paraparesis. *Nat. Rev. Dis. Primers* 1:15012. doi: 10.1038/nrdp.2015.12
- Bangham, C. R., and Matsuoka, M. (2017). Human T-cell leukaemia virus type 1: parasitism and pathogenesis. *Philos. Trans. R. Soc. Lond. B Biol. Sci.* 372:20160272. doi: 10.1098/rstb.2016.0272

the p65 nuclear translocation may explain the different effects of APH-2 and HBZ. This work allows to shed light on the role of HTLV-induced NF- κ B pathway activation and ultimately in the identification of potential therapeutic targets.

DATA AVAILABILITY

The datasets generated for this study are available on request to the corresponding author.

AUTHOR CONTRIBUTIONS

SF, MS, SM, and EB performed the study and contributed to manuscript discussion. SF contributed to manuscript drafting and writing. RM, CJ, VC, DZ, and UB provided intellectual input and contributed to manuscript drafting. MR conceived and designed the experiments, coordinated the study, and contributed to manuscript drafting and writing.

FUNDING

This work was supported by grants from University of Verona – Veneto Institute of Oncology (IOV) IRCCS, Padua, Italy Joint Project (MR and VC) and from the Department of Neuroscience, Biomedicine and Movement Sciences.

ACKNOWLEDGMENTS

SF conducted this study as fulfillment of her Ph.D. degree.

SUPPLEMENTARY MATERIAL

The Supplementary Material for this article can be found online at: <https://www.frontiersin.org/articles/10.3389/fmicb.2019.01302/full#supplementary-material>

- Baratella, M., Forlani, G., and Accolla, R. S. (2017). HTLV-1 HBZ viral protein: a key player in HTLV-1 mediated diseases. *Front. Microbiol.* 8:2615. doi: 10.3389/fmicb.2017.02615
- Barbeau, B., Peloponese, J. M., and Mesnard, J. M. (2013). Functional comparison of antisense proteins of HTLV-1 and HTLV-2 in viral pathogenesis. *Front. Microbiol.* 4:226. doi: 10.3389/fmicb.2013.00226
- Bartman, M. T., Kaidarova, Z., Hirschhorn, D., Sacher, R. A., Frisley, J., Garratty, G., et al. (2008). HTLV outcomes study (HOST) investigators. Long-term increases in lymphocytes and platelets in human T-lymphotropic virus type II infection. *Blood* 112, 3995–4002. doi: 10.1182/blood-2008-05-155960
- Bergamo, E., Diani, E., Bertazzoni, U., and Romanelli, M. G. (2017). A luciferase functional quantitative assay for measuring NF- κ B promoter transactivation mediated by HTLV-1 and HTLV-2 tax proteins. *Methods Mol. Biol.* 1582, 79–87. doi: 10.1007/978-1-4939-6872-5_6
- Bertazzoni, U., Turci, M., Avesani, F., Di Gennaro, G., Bidoia, C., and Romanelli, M. G. (2011). Intracellular localization and cellular factors interaction of HTLV-1 and HTLV-2 Tax proteins: similarities and functional differences. *Viruses* 3, 541–560. doi: 10.3390/v3050541

- Bista, P., Zeng, W., Ryan, S., Bailly, V., Browning, J. L., and Lukashev, M. E. (2010). TRAF3 controls activation of the canonical and alternative NF- κ B by the lymphotoxin beta receptor. *J. Biol. Chem.* 285, 12971–12978. doi: 10.1074/jbc.M109.076091
- Cahir McFarland, E. D., Izumi, K. M., and Mosialos, G. (1999). Epstein-barr virus transformation: involvement of latent membrane protein 1-mediated activation of NF- κ B. *Oncogene* 18, 6959–6964. doi: 10.1038/sj.onc.1203217
- Chan, J. K., and Greene, W. C. (2012). Dynamic roles for NF- κ B in HTLV-I and HIV-1 retroviral pathogenesis. *Immunol. Rev.* 246, 286–310. doi: 10.1111/j.1600-065X.2012.01094.x
- Chen, H., Yang, Y., Xu, H., Yang, W., Zhai, Z., and Chen, D. (2015). Ring finger protein 166 potentiates RNA virus-induced interferon- β production via enhancing the ubiquitination of TRAF3 and TRAF6. *Sci. Rep.* 5:14770. doi: 10.1038/srep14770
- Cheng, H., Ren, T., and Sun, S. (2012). New insight into the oncogenic mechanism of the retroviral oncoprotein Tax. *Protein Cell.* 3, 581–589. doi: 10.1007/s13238-012-2047-0
- Ciminale, V., Rende, F., Bertazzoni, U., and Romanelli, M. G. (2014). HTLV-1 and HTLV-2: highly similar viruses with distinct oncogenic properties. *Front. Microbiol.* 29:398. doi: 10.3389/fmicb.2014.00398
- Diani, E., Avesani, F., Bergamo, E., Cremonese, G., Bertazzoni, U., and Romanelli, M. G. (2015). HTLV-1 Tax protein recruitment into IKK ϵ and TBK1 kinase complexes enhances IFN-I expression. *Virology* 476, 92–99. doi: 10.1016/j.virol.2014.12.005
- Douceron, E., Kaidarova, Z., Miyazato, P., Matsuoka, M., Murphy, E. L., and Mahieux, R. (2012). HTLV-2 APH-2 expression is correlated with proviral load but APH-2 does not promote lymphocytosis. *J. Infect. Dis.* 205, 82–86. doi: 10.1093/infdis/jir708
- Dubuisson, L., Lormières, F., Fochi, S., Turpin, J., Pasquier, A., Douceron, E., et al. (2018). Stability of HTLV-2 antisense protein is controlled by PML nuclear bodies in a SUMO-dependent manner. *Oncogene* 37, 2806–2816. doi: 10.1038/s41388-018-0163-x
- Field, N., Low, W., Daniels, M., Howell, S., Daviet, L., Boshoff, C., et al. (2003). KSHV vFLIP binds to IKK- γ to activate IKK. *J. Cell Sci.* 116, 3721–3728. doi: 10.1242/jcs.00691
- Fochi, S., Mutascio, S., Bertazzoni, U., Zipeto, D., and Romanelli, M. G. (2018). HTLV deregulation of the NF- κ B pathway: an update on Tax and antisense proteins role. *Front. Microbiol.* 9:285. doi: 10.3389/fmicb.2018.00285
- Gardam, S., Sierro, F., Basten, A., Mackay, F., and Brink, R. (2008). TRAF2 and TRAF3 signal adapters act cooperatively to control the maturation and survival signals delivered to B cells by the BAFF receptor. *Immunity* 28, 391–401. doi: 10.1016/j.immuni.2008.01.009
- Gaudray, G., Gachon, F., Basbous, J., Biard-Piechaczyk, M., Devaux, C., and Mesnard, J. M. (2002). The complementary strand of the human T-cell leukemia virus type 1 RNA genome encodes a bZIP transcription factor that down-regulates viral transcription. *J. Virol.* 76, 12813–12822. doi: 10.1128/jvi.76.24.12813-12822.2002
- Giam, C. Z., and Semmes, O. J. (2016). HTLV-1 infection and adult T-cell leukemia/lymphoma-A tale of two proteins: tax and HBZ. *Viruses* 8:E161. doi: 10.3390/v8060161
- Grimm, S., Bauer, M. K., Baeuerle, P. A., and Schulze-Osthoff, K. (1996). Bcl-2 down-regulates the activity of transcription factor NF- κ B induced upon apoptosis. *J. Cell Biol.* 134, 13–23. doi: 10.1083/jcb.134.1.13
- Häcker, H., Tseng, P. H., and Karin, M. (2011). Expanding TRAF function: TRAF3 as a tri-faced immune regulator. *Nat. Rev. Immunol.* 11, 457–468. doi: 10.1038/nri2998
- Halin, M., Douceron, E., Clerc, I., Journo, C., Ko, N. L., Landry, S., et al. (2009). Human T-cell leukemia virus type 2 produces a spliced antisense transcript encoding a protein that lacks a classic bZIP domain but still inhibits Tax2-mediated transcription. *Blood* 114, 2427–2438. doi: 10.1182/blood-2008-09-179879
- Harhaj, E. W., and Harhaj, N. S. (2005). Mechanisms of persistent NF- κ B activation by HTLV-I tax. *IUBMB Life* 57, 83–91. doi: 10.1080/15216540500078715
- Harhaj, N., Sun, S., and Harhaj, E. (2007). Activation of NF- κ B by the human T cell leukemia virus type I Tax oncoprotein is associated with ubiquitin-dependent relocalization of I kappa B kinase. *J. Biol. Chem.* 282, 4185–4192. doi: 10.1074/jbc.M611031200
- Hauer, J., Püschner, S., Ramakrishnan, P., Simon, U., Bongers, M., Federle, C., et al. (2005). TNF receptor (TNFR)-associated factor (TRAF) 3 serves as an inhibitor of TRAF2/5-mediated activation of the noncanonical NF- κ B pathway by TRAF-binding TNFRs. *Proc. Natl. Acad. Sci. U.S.A.* 102, 2874–2879. doi: 10.1073/pnas.0500187102
- He, J. Q., Zarnegar, B., Oganessian, G., Saha, S. K., Yamazaki, S., and Doyle, S. E. (2006). Rescue of TRAF3-null mice by p100 NF- κ B deficiency. *J. Exp. Med.* 203, 2413–2418. doi: 10.1084/jem.20061166
- Higuchi, M., Tsubata, C., Kondo, R., Yoshida, S., Takahashi, M., and Oie, M. (2007). Cooperation of NF- κ B2/p100 activation and the PDZ domain binding motif signal in human T-cell leukemia virus type 1 (HTLV-1) Tax1 but not HTLV-2 Tax2 is crucial for interleukin-2-independent growth transformation of a T-cell line. *J. Virol.* 81, 11900–11907. doi: 10.1128/jvi.00532-07
- Hildebrand, J. M., Yi, Z., Buchta, C. M., Poovassery, J., Stunz, L. L., and Bishop, G. A. (2011). Roles of tumor necrosis factor receptor associated factor 3 (TRAF3) and TRAF5 in immune cell functions. *Immunol. Rev.* 244, 55–74. doi: 10.1111/j.1600-065X.2011.01055.x
- Ishitsuka, K., and Tamura, K. (2014). Human T-cell leukaemia virus type I and adult T-cell leukaemia-lymphoma. *Lancet Oncol.* 15, e517–e526. doi: 10.1016/S1470-2045(14)70202-5
- Jin, J., Hu, H., Li, H. S., Yu, J., Xiao, Y., Brittain, G. C., et al. (2014). Noncanonical NF- κ B pathway controls the production of type I interferons in antiviral innate immunity. *Immunity* 40, 342–354. doi: 10.1016/j.immuni.2014.02.006
- Journo, C., Bonnet, A., Favre-Bonvin, A., Turpin, J., Viner, J., Côté, E., et al. (2013). Human T cell leukemia virus type 2 tax-mediated NF- κ B activation involves a mechanism independent of Tax conjugation to ubiquitin and SUMO. *J. Virol.* 87, 1123–1136. doi: 10.1128/JVI.01792-12
- Journo, C., Douceron, E., and Mahieux, R. (2009). HTLV gene regulation: because size matters, transcription is not enough. *Future Microbiol.* 4, 425–440. doi: 10.2217/fmb.09.13
- Kannian, P., and Green, P. L. (2010). Human t lymphotropic virus type 1 (HTLV-1): molecular biology and oncogenesis. *Viruses* 2, 2037–2077. doi: 10.3390/v2092037
- Karimi, M., Mohammadi, H., Hemmatzadeh, M., Mohammadi, A., Rafatpanah, H., and Baradaran, B. (2017). Role of the HTLV-1 viral factors in the induction of apoptosis. *Biomed. Pharmacother.* 85, 334–347. doi: 10.1016/j.biopha.2016.11.034
- Kfoury, Y., Nasr, R., Journo, C., Mahieux, R., Pique, C., and Bazarbachi, A. (2012). The multifaceted oncoprotein Tax: subcellular localization, posttranslational modifications, and NF- κ B activation. *Adv. Cancer Res.* 113, 85–120. doi: 10.1016/B978-0-12-394280-7.00003-8
- Kuo, Y. L., and Giam, C. Z. (2006). Activation of the anaphase promoting complex by HTLV-1 tax leads to senescence. *EMBO J.* 25, 1741–1752. doi: 10.1038/sj.emboj.7601054
- Labun, K., Montague, T. G., Gagnon, J. A., Thyme, S. B., and Valen, E. (2016). CHOPCHOP v2: a web tool for the next generation of CRISPR genome engineering. *Nucleic Acids Res.* 44, W272–W276. doi: 10.1093/nar/gkw398
- Liao, G., Zhang, M., Harhaj, E. W., and Sun, S. C. (2004). Regulation of the NF- κ B-inducing kinase by tumor necrosis factor receptor-associated factor 3-induced degradation. *J. Biol. Chem.* 279, 26243–26250. doi: 10.1074/jbc.M403286200
- Libermann, T. A., and Baltimore, D. (1990). Activation of interleukin-6 gene expression through the NF- κ B transcription factor. *Mol. Cell Biol.* 10, 2327–2334. doi: 10.1128/mcb.10.5.2327
- Livak, K. J., and Schmittgen, T. D. (2001). Analysis of relative gene expression data using real-time quantitative PCR and the 2⁻(Delta Delta C(T)) Method. *Methods* 25, 402–408. doi: 10.1006/meth.2001.1262
- Ma, G., Yasunaga, J., and Matsuoka, M. (2016). Multifaceted functions and roles of HBZ in HTLV-1 pathogenesis. *Retrovirology* 13:16. doi: 10.1186/s12977-016-0249-x
- Ma, Y., Zhang, B., Wang, D., Qian, L., Song, X., Wang, X., et al. (2017). HTLV-1 basic leucine zipper factor downregulates cyclin D1 expression via interactions with NF- κ B. *Int. J. Mol. Med.* 39, 764–770. doi: 10.3892/ijmm.2017.2868
- Marban, C., McCabe, A., Bukong, T. N., Hall, W. W., and Sheehy, N. (2012). Interplay between the HTLV-2 Tax and APH-2 proteins in the regulation of the AP-1 pathway. *Retrovirology* 9:98. doi: 10.1186/1742-4690-9-98
- Meertens, L., Chevalier, S., Weil, R., Gessain, A., and Mahieux, R. (2004). A 10-amino acid domain within human T-cell leukemia virus type 1 and type 2 tax










- protein sequences is responsible for their divergent subcellular distribution. *J. Biol. Chem.* 279, 43307–43320. doi: 10.1074/jbc.M400497200
- Motai, Y., Takahashi, M., Takachi, T., Higuchi, M., Hara, T., Mizuguchi, M., et al. (2016). Human T-cell leukemia virus type 1 (HTLV-1) Tax1 oncoprotein but not HTLV-2 Tax2 induces the expression of OX40 ligand by interacting with p52/p100 and RelB. *Virus Genes* 52, 4–13. doi: 10.1007/s11262-015-1277-7
- Nakhaei, P., Mesplede, T., Solis, M., Sun, Q., Zhao, T., Yang, L., et al. (2009). The E3 ubiquitin ligase Triad3A negatively regulates the RIG-I/MAVS signaling pathway by targeting TRAF3 for degradation. *PLoS Pathog.* 5:e1000650. doi: 10.1371/journal.ppat.1000650
- Oganesyan, G., Saha, S. K., Guo, B., He, J. Q., Shahangian, A., Zarnegar, B., et al. (2006). Critical role of TRAF3 in the Toll-like receptor-dependent and independent antiviral response. *Nature* 439, 208–211. doi: 10.1038/nature04374
- Panfili, A. R., Dissinger, N. J., Howard, C. M., Murphy, B. M., Landes, K., Fernandez, S. A., et al. (2016). Functional comparison of HBZ and the related APH-2 protein provide insight into HTLV-1 pathogenesis. *J. Virol.* 90, 3760–3772. doi: 10.1128/JVI.03113-15
- Park, M. H., and Hong, J. T. (2016). Roles of NF- κ B in cancer and inflammatory diseases and their therapeutic approaches. *Cells* 5:E15. doi: 10.3390/cells5020015
- Parvatiyar, K., Pindado, J., Dev, A., Aliyari, S. R., Zaver, S. A., Gerami, H., et al. (2018). A TRAF3-NIK module differentially regulates DNA vs RNA pathways in innate immune signaling. *Nat. Commun.* 9:2770. doi: 10.1038/s41467-018-05168-7
- Pujari, R., Hunte, R., Khan, W. N., and Shembade, N. (2013). A20-mediated negative regulation of canonical NF- κ B signaling pathway. *Immunol. Res.* 57, 166–171. doi: 10.1007/s12026-013-8463-2
- Pujari, R., Hunte, R., Thomas, R., van der Weyden, L., Rauch, D., Ratner, L., et al. (2015). Human T-cell leukemia virus type 1 (HTLV-1) tax requires CADM1/TSLC1 for inactivation of the NF- κ B inhibitor A20 and constitutive NF- κ B signaling. *PLoS Pathog.* 11:e1004721. doi: 10.1371/journal.ppat.1004721
- Ran, F. A., Hsu, P. D., Wright, J., Agarwala, V., Scott, D. A., and Zhang, F. (2013). Genome engineering using the CRISPR-Cas9 system. *Nat. Protoc.* 8, 2281–2308. doi: 10.1038/nprot.2013.143
- Romanelli, M. G., Diani, E., Bergamo, E., Casoli, C., Ciminale, V., Bex, F., et al. (2013). Highlights on distinctive structural and functional properties of HTLV Tax proteins. *Front. Microbiol.* 4:271. doi: 10.3389/fmicb.2013.00271
- Satou, Y., Yasunaga, J., Yoshida, M., and Matsuoka, M. (2006). HTLV-I basic leucine zipper factor gene mRNA supports proliferation of adult T cell leukemia cells. *Proc. Natl. Acad. Sci. U.S.A.* 103, 720–725. doi: 10.1073/pnas.0507631103
- Schmitz, M. L., Kracht, M., and Saul, V. V. (2014). The intricate interplay between RNA viruses and NF- κ B. *Biochim. Biophys. Acta* 1843, 2754–2764. doi: 10.1016/j.bbamcr.2014.08.004
- Shoji, T., Higuchi, M., Kondo, R., Takahashi, M., Oie, M., Tanaka, Y., et al. (2009). Identification of a novel motif responsible for the distinctive transforming activity of human T-cell leukemia virus (HTLV) type 1 Tax1 protein from HTLV-2 Tax2. *Retrovirology* 6:83. doi: 10.1186/1742-4690-6-83
- Sun, S. C. (2017). The non-canonical NF- κ B pathway in immunity and inflammation. *Nat. Rev. Immunol.* 17, 545–558. doi: 10.1038/nri.2017.52
- Turci, M., Lodewick, J., Di Gennaro, G., Rinaldi, A. S., Marin, O., Diani, E., et al. (2012). Ubiquitination and sumoylation of the HTLV-2 Tax-2B protein regulate its NF- κ B activity: a comparative study with the HTLV-1 Tax-1 protein. *Retrovirology* 9:102. doi: 10.1186/1742-46909-102
- Turci, M., Romanelli, M. G., Lorenzi, P., Righi, P., and Bertazzoni, U. (2006). Localization of human T-cell lymphotropic virus type II Tax protein is dependent upon a nuclear localization determinant in the N-terminal region. *Gene* 365, 119–124. doi: 10.1016/j.gene.2005.09.043
- Vallabhapurapu, S., Matsuzawa, A., Zhang, W., Tseng, P. H., Keats, J. J., Wang, H., et al. (2008). Nonredundant and complementary functions of TRAF2 and TRAF3 in a ubiquitination cascade that activates NIK-dependent alternative NF- κ B signaling. *Nat. Immunol.* 9, 1364–1370. doi: 10.1038/ni.1678
- Watanabe, M., Ohsugi, T., Shoda, M., Ishida, T., Aizawa, S., Maruyama-Nagai, M., et al. (2005). Dual targeting of transformed and untransformed HTLV-1-infected T cells by DHMEQ, a potent and selective inhibitor of NF- κ B, as a strategy for chemoprevention and therapy of adult T-cell leukemia. *Blood* 106, 2462–2471. doi: 10.1182/blood-2004-09-3646
- Watanabe, T. (2017). Adult T-cell leukemia: molecular basis for clonal expansion and transformation of HTLV-1-infected T cells. *Blood* 129, 1071–1081. doi: 10.1182/blood-2016-09-692574
- Wurm, T., Wright, D. G., Polakowski, N., Mesnard, J. M., and Lemasson, I. (2012). The HTLV-1-encoded protein HBZ directly inhibits the acetyl transferase activity of p300/CBP. *Nucleic Acids Res.* 40, 5910–5925. doi: 10.1093/nar/gks244
- Xiao, G., Cvjic, M. E., Fong, A., Harhaj, E. W., Uhlik, M. T., and Waterfield, M. (2001). Retroviral oncoprotein Tax induces processing of NF- κ B2/p100 in T cells: evidence for the involvement of IKK α . *EMBO J.* 20, 6805–6815. doi: 10.1093/emboj/20.23.6805
- Xiao, G., Rabson, A. B., Young, W., Qing, G., and Qu, Z. (2006). Alternative pathways of NF- κ B activation: a double-edged sword in health and disease. *Cytokine Growth Factor Rev.* 17, 281–293. doi: 10.1016/j.cytogfr.2006.04.005
- Xie, P., Hostager, B. S., and Bishop, G. A. (2004). Requirement for TRAF3 in signaling by LMP1 but not CD40 in B lymphocytes. *J. Exp. Med.* 199, 661–671. doi: 10.1084/jem.20031255
- Xie, X., Jin, J., Zhu, L., Jie, Z., Li, Y., Zhao, B., et al. (2019). Cell type-specific function of TRAF2 and TRAF3 in regulating type I IFN induction. *Cell Biosci.* 9:5. doi: 10.1186/s13578-018-0268-5
- Yang, X. D., and Sun, S. C. (2015). Targeting signaling factors for degradation, an emerging mechanism for TRAF functions. *Immunol. Rev.* 266, 56–71. doi: 10.1111/imr.12311
- Yin, H., Kannian, P., Dissinger, N., Haines, R., Niewieski, S., and Green, P. L. (2012). Human T-cell leukemia virus type 2 antisense viral protein 2 is dispensable for in vitro immortalization but functions to repress early virus replication in vivo. *J. Virol.* 86, 8412–8421. doi: 10.1128/JVI.00717-12
- Zarnegar, B. J., Wang, Y., Mahoney, D. J., Dempsey, P. W., Cheung, H. H., He, J., et al. (2008). Noncanonical NF- κ B activation requires coordinated assembly of a regulatory complex of the adaptors cIAP1, cIAP2, TRAF2 and TRAF3 and the kinase NIK. *Nat. Immunol.* 9, 1371–1378. doi: 10.1038/ni.1676
- Zhao, T. (2016). The role of HBZ in HTLV-1-induced oncogenesis. *Viruses* 8, 1–12. doi: 10.3390/v8020034
- Zhao, T., Yasunaga, J., Satou, Y., Nakao, M., Takahashi, M., Fujii, M., et al. (2009). Human T-cell leukemia virus type 1 bZIP factor selectively suppresses the classical pathway of NF- κ B. *Blood* 113, 2755–2764. doi: 10.1182/blood-2008-06-161729
- Zhi, H., Yang, L., Kuo, Y. L., Ho, Y. K., Shih, H. M., and Giam, C. Z. (2011). NF- κ B hyperactivation by HTLV-1 tax induces cellular senescence, but can be alleviated by the viral anti-sense protein HBZ. *PLoS Pathog.* 7:e1002025. doi: 10.1371/journal.ppat.1002025

Conflict of Interest Statement: The authors declare that the research was conducted in the absence of any commercial or financial relationships that could be construed as a potential conflict of interest.

Copyright © 2019 Fochi, Bergamo, Serena, Mutascio, Journo, Mahieux, Ciminale, Bertazzoni, Zipeto and Romanelli. This is an open-access article distributed under the terms of the Creative Commons Attribution License (CC BY). The use, distribution or reproduction in other forums is permitted, provided the original author(s) and the copyright owner(s) are credited and that the original publication in this journal is cited, in accordance with accepted academic practice. No use, distribution or reproduction is permitted which does not comply with these terms.

Article

A Potential Role of RUNX2- RUNT Domain in Modulating the Expression of Genes Involved in Bone Metastases: An In Vitro Study with Melanoma Cells

Michela Deiana ^{1,2}, Luca Dalle Carbonare ^{1,*}, Michela Serena ², Samuele Cheri ^{1,2},
Simona Mutascio ², Alberto Gandini ³, Giulio Innamorati ³, Pamela Lorenzi ²,
Michela Cumerlato ², Jessica Bertacco ², Franco Antoniazzi ³, Maria Grazia Romanelli ²,
Monica Mottes ², Donato Zipeto ² and Maria Teresa Valenti ¹

- ¹ Department of Medicine, University of Verona, University of Verona, 37100 Verona, Italy; michela.deiana@univr.it (M.D.); samuele.cheri@univr.it (S.C.); mariateresa.valenti@univr.it (M.T.V.)
- ² Department of Neurosciences, Biomedicine and Movement Sciences, University of Verona, 37100 Verona, Italy; michela.serena@univr.it (M.S.); simona.mutascio@univr.it (S.M.); pamela.lorenzi@univr.it (P.L.); michela.cumerlato@studenti.univr.it (M.C.); jessica.bertacco@univr.it (J.B.); mariagrazia.romanelli@univr.it (M.G.R.); monica.mottes@univr.it (M.M.); donato.zipeto@univr.it (D.Z.)
- ³ Department of Surgery, Dentistry, Pediatrics and Gynecology, University of Verona, 37100 Verona, Italy; alberto.gandini@univr.it (A.G.); giulio.innamorati@univr.it (G.I.); franco.antoniazzi@univr.it (F.A.)
- * Correspondence: luca.dallecarbonare@univr.it

Received: 21 February 2020; Accepted: 16 March 2020; Published: 19 March 2020



Abstract: Ectopic expression of RUNX2 has been reported in several tumors. In melanoma cells, the RUNT domain of RUNX2 increases cell proliferation and migration. Due to the strong link between RUNX2 and skeletal development, we hypothesized that the RUNT domain may be involved in the modulation of mechanisms associated with melanoma bone metastasis. Therefore, we evaluated the expression of metastatic targets in wild type (WT) and RUNT KO melanoma cells by array and real-time PCR analyses. Western blot, ELISA, immunofluorescence, migration and invasion ability assays were also performed. Our findings showed that the expression levels of bone sialoprotein (BSP) and osteopontin (SPP1) genes, which are involved in malignancy-induced hypercalcemia, were reduced in RUNT KO cells. In addition, released PTHrP levels were lower in RUNT KO cells than in WT cells. The RUNT domain also contributes to increased osteotropism and bone invasion in melanoma cells. Importantly, we found that the ERK/p-ERK and AKT/p-AKT pathways are involved in RUNT-promoted bone metastases. On the basis of our findings, we concluded that the RUNX2 RUNT domain is involved in the mechanisms promoting bone metastasis of melanoma cells via complex interactions between multiple players involved in bone remodeling.

Keywords: RUNX2; RUNT domain; PTHrP; bone; metastasis

1. Introduction

Skeletal metastases occur when cancer cells from a primary tumor invade the bone. Generally, bone metastases are associated with breast, prostate and lung cancers [1]. Bone metastases were also found in patients affected by malignant melanoma (MM) [2]. Bone invasion by cancer cells disrupts the balance between osteoblasts and osteoclasts. Therefore, osteoblastic, osteolytic or mixed-bone metastases may result, depending on the phenotype of the target cell [3,4]. However, both osteoblasts and osteoclasts are affected by cancer cells in skeletal metastases. Once cancer cells invade the bone, patient survival chances decrease. In addition, as pathological fractures, pain, hypercalcemia and bone marrow aplasia occur in patients with skeletal metastases, quality of life worsens considerably. Therefore, a multidisciplinary

approach aiming to prevent skeletal metastases and identify more effective treatments is necessary [5]. In addition, new studies should be performed to deeply understand which molecular pathways are involved in the interaction between cancer cells and the bone microenvironment. This aim is particularly relevant since the molecular mechanisms involved in the metastatic progression of melanoma are complex. In, M.M.; mutations in transcription regulators, such as BRAF, MITF, KIT, NRAS, PTEN and P53, as well as in TERT, occur frequently [6]. Several studies demonstrated the involvement of RUNX2, the master transcription factor of osteogenic differentiation, in the development of melanoma [7,8]. In fact, besides inducing osteogenic differentiation through mesenchymal stem cell commitment to pre-osteoblasts, RUNX2 is involved in many cellular transformation pathways, such as apoptosis, epithelial–mesenchymal transition (EMT), angiogenesis and metastatic processes [7]. RUNX2 overexpression has been reported in breast cancer, pancreatic cancer, prostate cancer, lung cancer, ovarian epithelial cancer and melanoma. In previous studies, we identified RUNX2 as a stemness marker for cancer [9,10] and observed higher levels of RUNX2 expression in thyroid cancer patients with bone metastases [11]. RUNX2 appears to be involved in the osteolytic process [7,12]. Importantly, the bone sialoprotein (IBSP) and osteopontin (SPP1) coding genes, which are regulated by RUNX2, play important roles in bone metastases derived from osteotropic cancers [13]. In particular, BSP is associated with adhesion, proliferation, invasion, angiogenesis and metastasis [13,14]. Similarly, the *SPP1* (secreted phosphoprotein 1) gene product, OPN(osteopontin), was observed in bone metastases [15]; it was also reported that reduced expression of SPP1 in melanoma cells is associated with a lower incidence of bone metastases [16]. Importantly, overexpression of parathyroid hormone-related protein (PTHrP) was observed in tumors with metastasized bone tissue [17]. In particular, PTHrP exerts its role in cancer progression and metastases in autocrine (enhancing proliferation, survival and apoptosis resistance), paracrine (inducing RANKL(Receptor Activator of Nuclear Factor Kappa B Ligand) expression in osteoblasts to activate bone resorption) and intracrine (promoting survival, anoikis evasion and cell invasion) manners [17]. PTHrP was demonstrated to be regulated by RUNX2 [18] in head and neck squamous cell carcinoma, and it was also shown that transient exposure to PTHrP increases VEGFR2 expression through pERK stimulation [19]. In addition, RUNX2 promotes esophageal carcinoma by activating the AKT and ERK signaling pathways [20]. Recently, we demonstrated that the RUNT domain, namely the RUNX2 DNA binding domain, is involved in different pathways leading to melanoma transformation [21]. Considering that RUNX2 induces osteogenic genes expression through the RUNT DNA binding domain, we hypothesized that the RUNT domain might also be responsible for the bone tropism of cancer. With this aim, we analyzed the effects of RUNT domain in melanoma cells, focusing on the modulation of metastatic gene expression and the activity of factors that promote osteotropic ability.

2. Materials and Methods

2.1. Cell Cultures

We used A375 (American Type Culture Collection; ATCC: CTRL-1619TM) and MELHO (DSMZ-Deutsche Sammlung von Mikroorganismen und Zellkulturen) human melanoma cells. The RUNT KO cells were obtained using CRISPR/Cas9 as we previously described [21]. Cell lines were cultured under 5% CO₂ and in RPMI (1640 (Roswell Park Memorial Institute) growth medium (Sigma-Aldrich, St. Louis, MO, USA) containing 10% fetal bovine serum (FBS) (Sigma-Aldrich), supplemented with antibiotics (1% penicillin/streptomycin) and 1% glutamine. All cell lines were tested negative for mycoplasma using the LookOut Mycoplasma PCR Detection Kit (Sigma-Aldrich).

Once 80% confluence was reached, cells were harvested, washed and counted using a Burker haemocytometer for all experiments.

2.2. Construction of RUNX-2 Expression Vector

The RUNX-2 gene was cloned into the pcDNA3 vector as previously described [22,23]. Briefly, the full-length human RUNX-2 open-reading frame (accession number NM_001024630 transcript variant 1) was amplified by polymerase chain reaction (PCR) from the pCMV6 Runx-2 Myc-DDK plasmid (OriGene Technologies, Inc. Rockville, MD, USA#:RC212884,) using the forward primer Runx2F-EcoRV (5'-gcggatattTCGCCTCACAACAACC-3') and the reverse primer Runx2R-XhoI (5'-ggacctcgagATATGGTCGCCAAACAGAT-3'); underlined nucleotides represent the restriction sites. The amplified fragment was inserted in the pCRTM2.1 cloning vector (Invitrogen, Thermo Fischer Scientific, Waltham, MA, USA), then excised by EcoRV/XhoI digestion and finally cloned in pcDNA3-Flag-HA vector (Addgene, Watertown, MA, USA, #10792, Watertown, MA, USA). The cloned fragment was sequenced at the BMR Genomics facility (<http://www.bmr-genomics.it>). RUNX-2 expression was validated by Western blot.

2.3. Exogenous PTHrP Supplementation

The exogenous PTHrP peptide (PeproTech, Rocky Hill, NJ, USA) was added to A375, 3G8, MELHO and 1F5 melanoma cells seeded into 24-well plates at a concentration of 100 µg and incubated for 24 h. Treated cells were then harvested to perform expression analyses.

2.4. AKT and ERK Inhibition

A375 and MELHO melanoma cells were plated in 96-well plates at a density of 1000 cells per well and incubated overnight. Cells were then treated with ERK1/2 and AKT inhibitors (SCH772984 and GSK690693, Selleckchem, Houston, TX, USA) for 24 h at a final concentration of 2 µM in RPMI1640 10% FBS. Cultured media were collected to perform ELISA assays, while cells were stored for gene expression analysis.

2.5. PCR Array

PCR arrays were performed using a TaqManTM Human Tumor Metastasis Array (Thermo Fisher Scientific, Waltham, MA USA) according to the manufacturer's instructions. The amplification reaction and the results analysis were carried out using a QuantStudioTM 3 Real-Time PCR System equipped with QuantStudio[®] Design and Analysis desktop software (Thermo Fisher Scientific).

2.6. Real-Time RT-PCR

Total RNA extraction and RT were performed as previously reported [21]. PCRs were performed in a total volume of 25 µl using 20 ng of cDNA for each sample. Real-time PCR was performed using TaqMan Universal PCR Master Mix (ThermoFisher Corporation, Waltham, MA, USA) and TaqMan pre-designed probes for each gene (*VEGFA*, Hs00900055_m1; *VEGFR*, Hs01052961_m1; *CD31*, Hs01065279_m1; *IBSP*, Hs00173720, *OPN*, Hs00167093_m1). Gene expression for *MMP9* (FW AGACCTGGGCAGATTCCAAC, RV CGGCAAGTCTCCGAGTAGT, Sigma-Aldrich) was tested using the Power SYBR[®] Green PCR Master Mix (Thermo Fisher Scientific). Gene expression was normalized to the housekeeping β 2-microglobulin (β 2M, Hs99999901_s1) gene, and the relative fold expression differences were calculated. TaqMan SDS analysis software was used to analyze the Ct values. Three independent experiments with three replicates for each sample were performed.

2.7. Western Blot Analysis

RIPA buffer was used for protein extraction (Thermo Fisher Scientific) and protein concentrations were determined by BCA assay (Thermo Fisher Scientific). Protein samples were separated by sodium dodecyl sulfate-polyacrylamide gel electrophoresis (SDS-PAGE) using mini-PROTEAN[®] TGXTM precast gradient 4–20% gels (BioRad, Hercules, CA, USA) and transferred onto polyvinylidene

difluoride (PVDF) membranes (Thermo Fisher Scientific). PVDF membranes were then probed with the primary and secondary antibodies reported in Table 1.

Table 1. Antibodies used in this study.

Antibody	Ab Dilution	Origin	Secondary Antibody
BSP (Bone Sialoprotein) II	1:1000	(Cell Signaling, 5486)	Anti-rabbit (Cell Signaling, 7074)
AKT (C67E7)	1:1000	(Cell Signaling, 4691)	Anti-rabbit (Cell Signaling, 7074)
p_AKT (193H12)	1:1000	(Cell Signaling, 4058)	Anti-rabbit (Cell Signaling, 7074)
ERK (13F5)	1:1000	(Cell Signaling, 4695)	Anti-rabbit (Cell Signaling, 7074)
p_ERK (D13.14.4E)	1:2000	(Cell Signaling, 4370)	Anti-rabbit (Cell Signaling, 7074)
PTHrP (1D1)	1:1000	(SantaCruz Biotech., Dallas, TX, USA)	Anti-mouse (Cell Signaling, 7076)
β ACTIN (BA3R)	1:5000	(Thermo Scientific)	Anti-mouse (Cell Signaling, 7076)

Signals were detected using a chemiluminescence reagent (ECL, Millipore, Burlington, MA, USA), and images were acquired using an LAS4000 Digital Image Scanning System (GE Healthcare, Little Chalfont, UK). Densitometric analyses were performed using the ImageJ software, and the relative protein band intensity was normalized to β-actin and expressed as the optical density (OD) ratio. The data were obtained from three independent experiments.

2.8. Immunofluorescence

Cells were fixed and processed according to the manufacturer's protocols. BSP primary antibodies (Abcam, Cambridge, UK) were diluted (as reported in the datasheet) in Antibody Dilution Buffer and incubated overnight at 4 °C. The slides were then incubated with the Alexa Fluor[®] 488 anti-rabbit (Cat. #A-11034) secondary antibody, and nuclear staining was performed by using ProLong[™] Gold Antifade Mountant with DAPI (Thermo Fisher Scientific). Images were captured using a Leica DM2500 microscope (Leica Microsystem, Wetzlar, Germany). In particular, four different fields were measured for each sample in three independent experiments, and each field contained approximately 80–100 total cells.

2.9. Migration to Bone Ability

To assess bone tropism, we first compared cells' ability to migrate in the presence or absence of a bone fragment. Therefore, cells were seeded on a 6-well plate at a density of 500,000 per well. After adhesion, half of each well was scratched using a cell scraper, and the relative migration distance (RMD) was calculated in the absence or presence of a bovine bone slice (Nøddevænget 3, DK-7300 Jelling, Denmark) placed at the same distance in all samples. Cultures were carried out for 2 days using DMEM (Dulbecco's Modified Eagle Medium) supplemented with 10% FBS and Glutamax (all from Thermo Fisher Scientific) at 37 °C and 5% CO₂. The migration ability assay was conducted with an EVOS[™] FL Auto Imaging System (Thermo Fisher Scientific) under time-lapse protocol for 48 h. Distances between the cell front and the bone slice or the signed blank space for every well were measured at the beginning and at the end of each experiment. Relative migration distances (RMDs) were calculated using the following formula: $RMD = (t_0 - t_1)/t_0$, where t_0 is the distance between the cell front and the bone slice at time zero of the assay and t_1 is the same distance at the end, as previously reported [21]. The RMD of WT cells was normalized to the RMD of RUNX2 KO cells to evaluate the role of RUNX2 in migration in the presence or absence of bone fragments. In addition, we performed experiments with the transwell system to further analyze migration and evaluate invasion ability, as previously described [24]. For both migration and invasion assays, 1×10^4 cells were seeded onto the upper chamber of transwell plates of 8 μm diameter (Corning Incorporated, NY) in the presence of RPMI supplemented with 1% FBS for 24 h (migration assay) or 48 h (invasion assay). The invasion assays were performed by coating the upper chamber with Matrigel. The lower chamber was filled with medium with or without bone fragments (Nøddevænget 3, DK-7300 Jelling, Denmark). After 48 h, cells adherent to the upper surface of the membrane were removed. Thereafter, cells in the membrane underside were fixed with 4% of

paraformaldehyde and stained with DAPI(4',6-diamidino-2-phenylindole). Cells were then visualized under a Leica DM 2500 (Leica Microsystem, Wetzlar, Germany) to take pictures and to evaluate the number of adherent cells. Cells were counted in ten random fields at 40X magnification.

2.10. ELISA

For PTHrP protein detection, we performed an ELISA (Fine Biotech Co Ltd., Wuhan, China). WT and RUNT KO cell lines were plated onto 96-well plates at a density of 10,000 cells/well. After 3 days of culture, the medium was collected and centrifuged at 1000 g for 20 min at 4 °C. Standards were prepared following the manufacturer's instructions. Samples and standards were plated into the ELISA microplate, and the assay was conducted according to the manufacturer's instructions.

2.11. Bioinformatics Analysis

RUNX2, PTHrP, AKT and ERK proteins were submitted to the STRING portal (<https://string-db.org>) for independent inspection related to their predicted connections.

2.12. Statistical Analysis

Student's paired t-test was used to compare the variation of variables between two groups. Differences were considered statistically significant at $p < 0.05$. Experiments were performed at least three times. Statistical analyses were performed using SPSS (Statistical Package for Social Science) for Windows, version 16.0 (SPSS Inc., Chicago, IL, USA).

3. Results

3.1. RUNX2 RUNT Domain Empowers RUNX2 Metastatic Ability in Melanoma Cells

Figure 1A shows a schematic representation of the RUNT domain coding region within the RUNX2 cDNA. By using the CRISPR/Cas9 technology, we partially deleted the RUNT domain or knocked out the whole RUNX2 gene containing the RUNT domain in A375 and MELHO melanoma cells (Figure 1A). Therefore, we obtained a lower and null RUNX2 proteins in KO-A375 and KO-MELHO, respectively (Figure 1B).

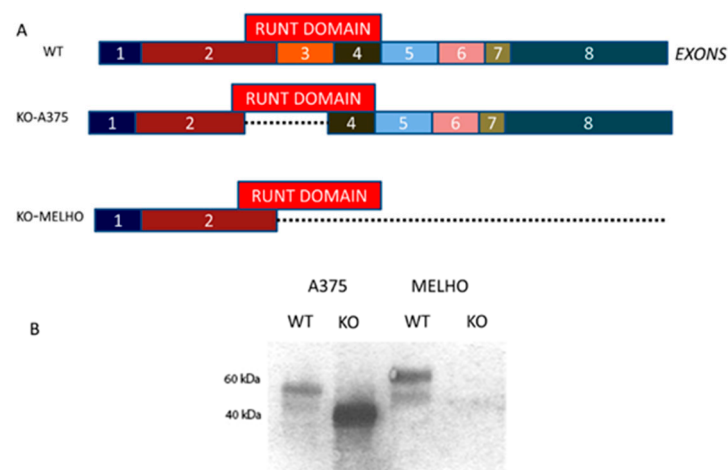


Figure 1. (A) Location of the RUNT coding domain within RUNX2 cDNA as reported in RefSeq NP 00101019801.3 (B) Western blot showing RUNX2 in A375, KO-A375, MELHO and KO-MELHO melanoma cells.

Then, we evaluated the metastatic gene expression profile in A375 and RUNX2 RUNT KO (RUNT KO) melanoma cells by using a Human Tumor Metastasis Array. The data showed lower expression of several genes involved in the metastatic process in RUNT KO cells compared to A375 cells (Figure 2A

and Table S1). To validate these findings, we performed real-time PCR assays for four selected lower expressed genes, namely, platelet and endothelial cell adhesion molecule 1 (CD31), matrix metalloproteinase 3 (MMP3), matrix metalloproteinase 9 (MMP9) and vascular endothelial growth factor A (VEGFA) in WT (A375 and MELHO) and RUNT-KO (KO-A375 and KO-MELHO) melanoma cells. The investigated genes were downregulated in both RUNT-KO cell lines, with the exception of MMP3 expression, which was unchanged in KO-A375 (Figure 2B). Gene expression was restored in all KO cells upon resetting the RUNT domain (Figure 2B). Similarly, expression levels of CD31 and VEGFA, which are genes involved in metastatic processes, were reduced in RUNT KO cells (Figure 2B), thereby confirming the array data.

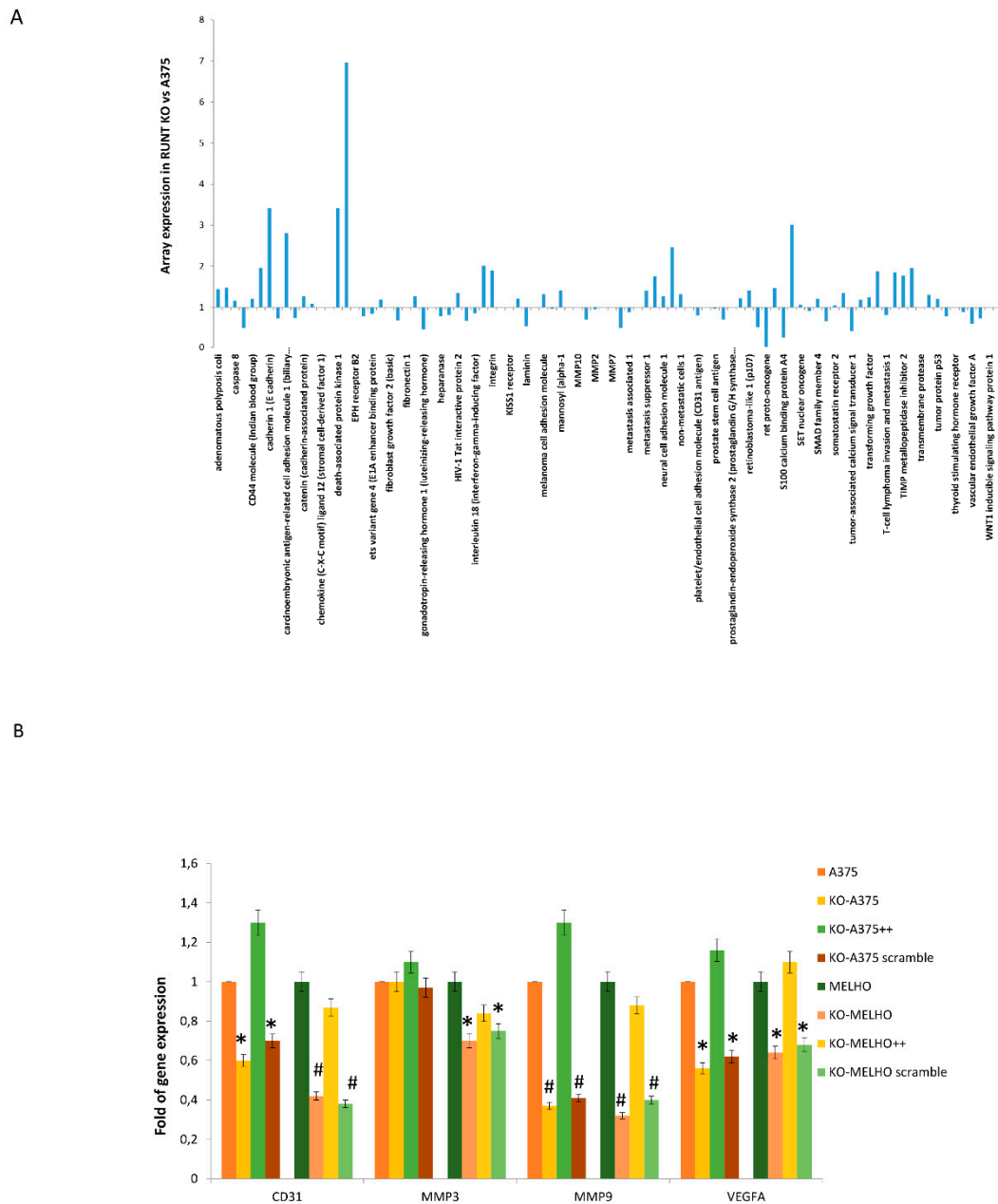


Figure 2. (A) Array PCR: Expression levels of metastatic genes evaluated by TaqMan™ Human Tumor Metastasis Array. (B) The downregulation of gene expression in RUNT-KO cells compared to wild type (WT) melanoma cells confirmed the array results. (* $p < 0.05$; # $p < 0.01$).

We then tested RUNT domain influence in driving melanoma cell migration to the bone by analyzing the expression of *IBSP* and *SPP1* genes. As shown in Figure 3A, the expression levels of *IBSP* decreased in RUNT-KO cells. We also observed a reduced number of BSP-positive cells (Figure 3B) as well as reduced BSP protein expression in RUNT-KO cells (Figure 3C) compared to WT cells. *SPP1* gene expression levels were also reduced in RUNT-KO cells (Figure 3D), which was rectified by RUNT re-expression. Interestingly, the expression of *CD44*, an osteopontin receptor which is considered a stemness marker in several kinds of cancers, was also reduced in RUNT-KO cells (Figure 3E).

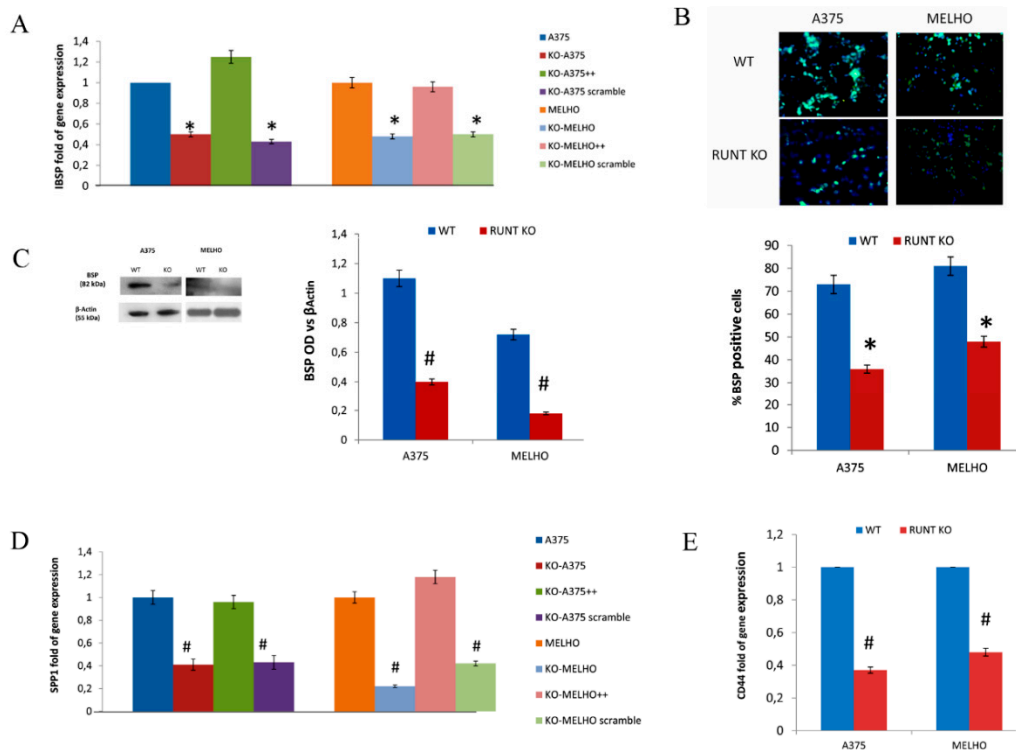


Figure 3. (A) Gene expression of the bone metastatic gene *IBSP* is lower in RUNT KO cells than in WT melanoma cells. Accordingly, there is a lower percentage of BSP-positive cells (B) and lower levels of the BSP protein (C) in RUNT KO cells compared to WT melanoma cells. Gene expression levels of the bone metastatic genes *SPP1* (D) and *CD44* (E) are lower in RUNT KO cells than in WT melanoma cells. (* $p < 0.05$; # $p < 0.01$); magnification 40X.

3.2. The RUNT Domain Increases PTHrP Levels in Melanoma and Activates AKT and ERK Pathways

As PTHrP expression is regulated by RUNX2, we measured PTHrP levels in WT and RUNT-KO melanoma cell culture media. Interestingly, we observed a significant reduction in PTHrP concentration in RUNT KO cells media compared to the WT cell media (Figure 4A), as well as a reduction in intracellular PTHrP levels (Figure 4B) in both cell lines.

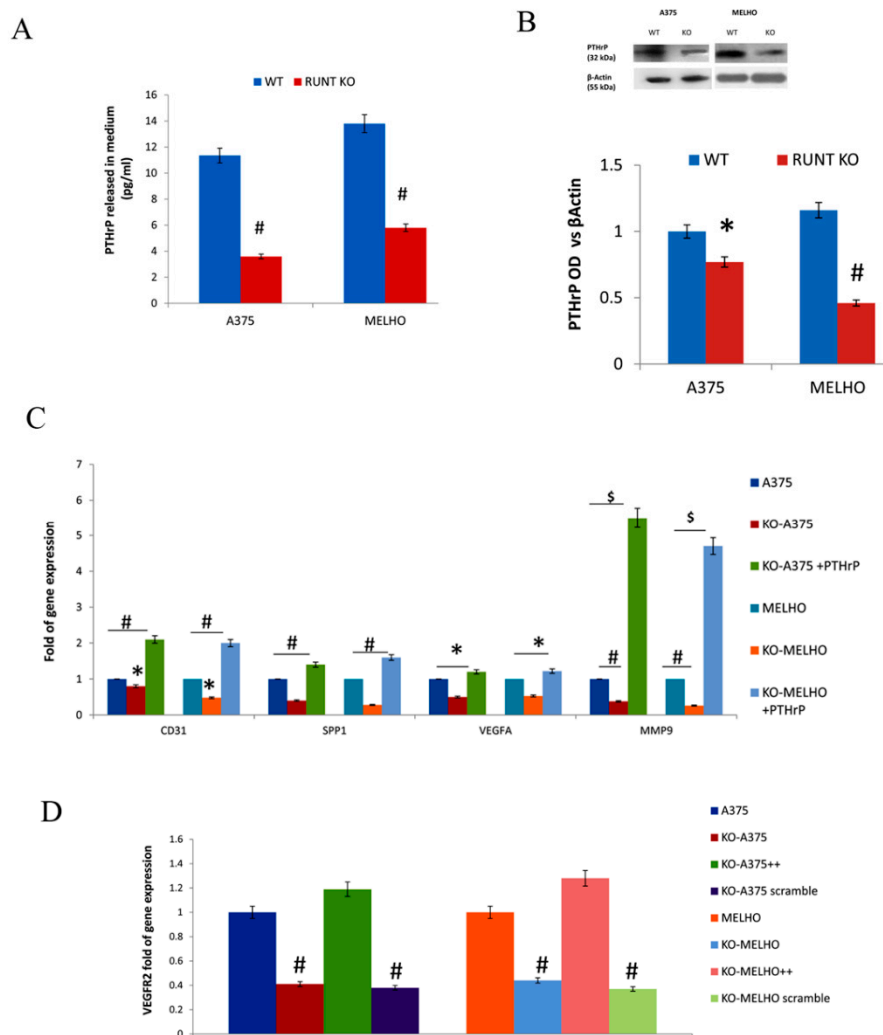


Figure 4. Both released (A) and intracellular (B) levels of parathyroid hormone-related peptide (PTHrP) are lower in RUNT KO cells than in WT cells. The addition of exogenous PTHrP restores gene expression levels in both KO-cell lines (C). (D) VEGFR2 gene fold expression is lower in RUNT-KO cells than in WT cells. Re-expression of the RUNT domain restores VEGFR2 gene expression in both cell lines. (* $p < 0.05$; # $p < 0.01$; \$ $p < 0.001$).

In order to confirm the RUNT domain role in inducing PTHrP expression, we cultured KO cells in the presence of exogenous PTHrP (+exPTHrP). As shown in Figure 4C, all investigated genes related to metastatic ability were upregulated in KO cells treated with exogenous PTHrP. In addition, we analyzed the expression of VEGFR2, which is associated with increased expression of PTHrP in other cancers. As shown in Figure 4D, downregulation of VEGFR2 expression was observed in RUNT KO cells. Restoration of the RUNT domain re-established VEGFR2 gene expression.

Considering the modulatory role of VEGFR2 in the ERK pathway, we then looked for ERK pathway modifications in KO cells. The observed reduced levels of ERK and pERK proteins expression in RUNT KO cells compared to WT cells suggested an activating role of the RUNT domain (Figure 5A). ERK and AKT pathways are strongly associated with oncogenic transformation, therefore we investigated the role of the RUNT domain in AKT pathway modulation. As shown in Figure 5B, protein expression levels of both AKT and pAKT were lower in RUNT KO cells than in WT cells in both cell lines.

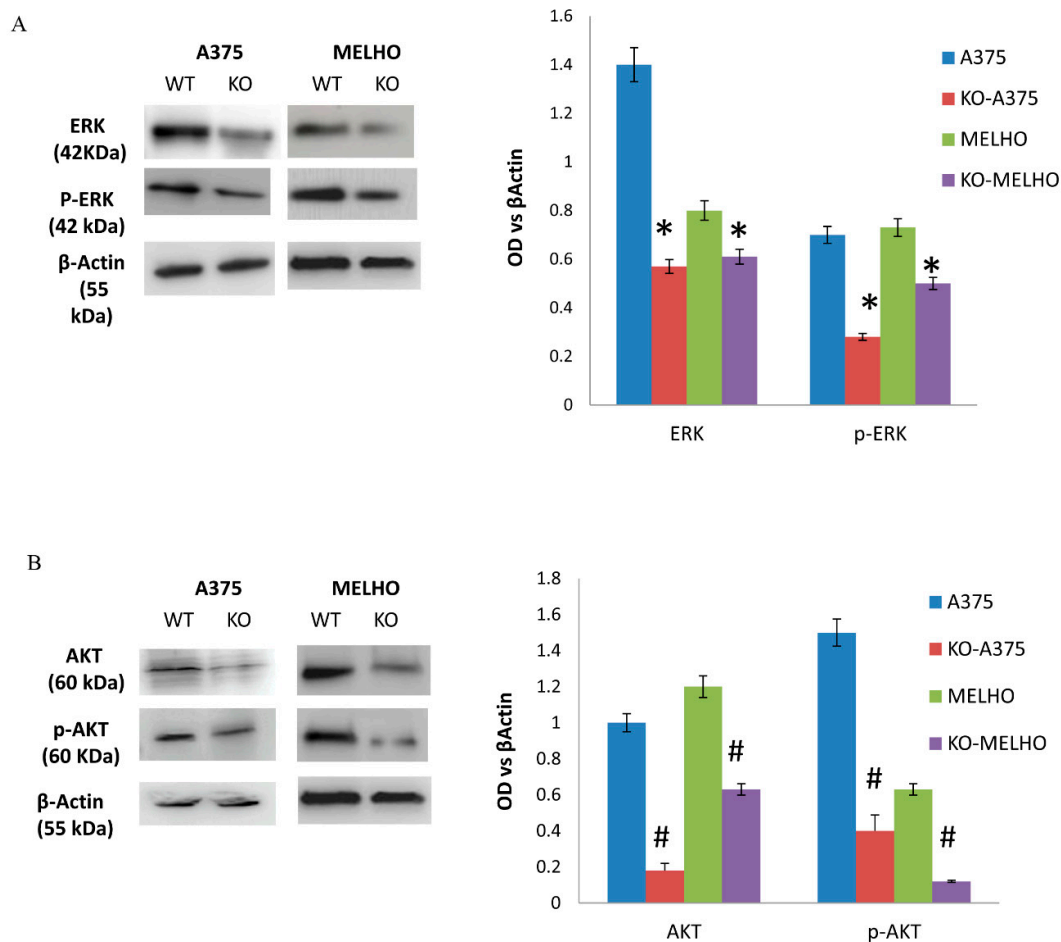


Figure 5. The expression of both ERK (A) and AKT (B) as well as the expression of the related phosphorylated proteins is lower in RUNT KO cells than in WT cells (* $p > 0.05$; # $p > 0.01$).

3.3. RUNX2 Regulates AKT and ERK in a Reciprocal Way

To evaluate the interaction between RUNT and AKT/ERK signaling pathways, we treated WT cells with either AKT or ERK inhibitors. Our data showed that the inhibition of AKT and ERK pathways did not affect RUNX2 gene expression (Figure 6A). However, the inhibition of the AKT and ERK pathways heavily reduced the expression of RUNX2-downstream genes, namely SPARC (Osteonectin), and OCN (Osteocalcin), thus demonstrating the effects of their inhibition on RUNX2 transcriptional activity (Figure 6B,C).

Importantly, inhibition of both the AKT and ERK pathways reduced the amount of PTHrP released in the WT melanoma cell medium (Figure 6D). Accordingly, bioinformatic analyses showed a fine interaction between these molecular factors (Figure 6E). For the first time in melanoma, we also observed interaction and reciprocal activation between RUNT/RUNX2 and AKT/ERK signaling (Figure 6F).

3.4. Osteotropism is Reduced in RUNT KO Melanoma Cells

At first, we evaluated the migration ability of cells either in the presence or in absence of bone fragments in vitro. In particular, we calculated the levels of the relative migration distance of WT versus RUNX2 KO cells in the presence or absence of bone fragments. We observed that RMD levels of WT, normalized with the RMD of RUNX2 KO cells, were higher in the presence of bone fragments (Figure 7). Therefore, the expression of the RUNT domain increases more cell migration in the presence of bone.

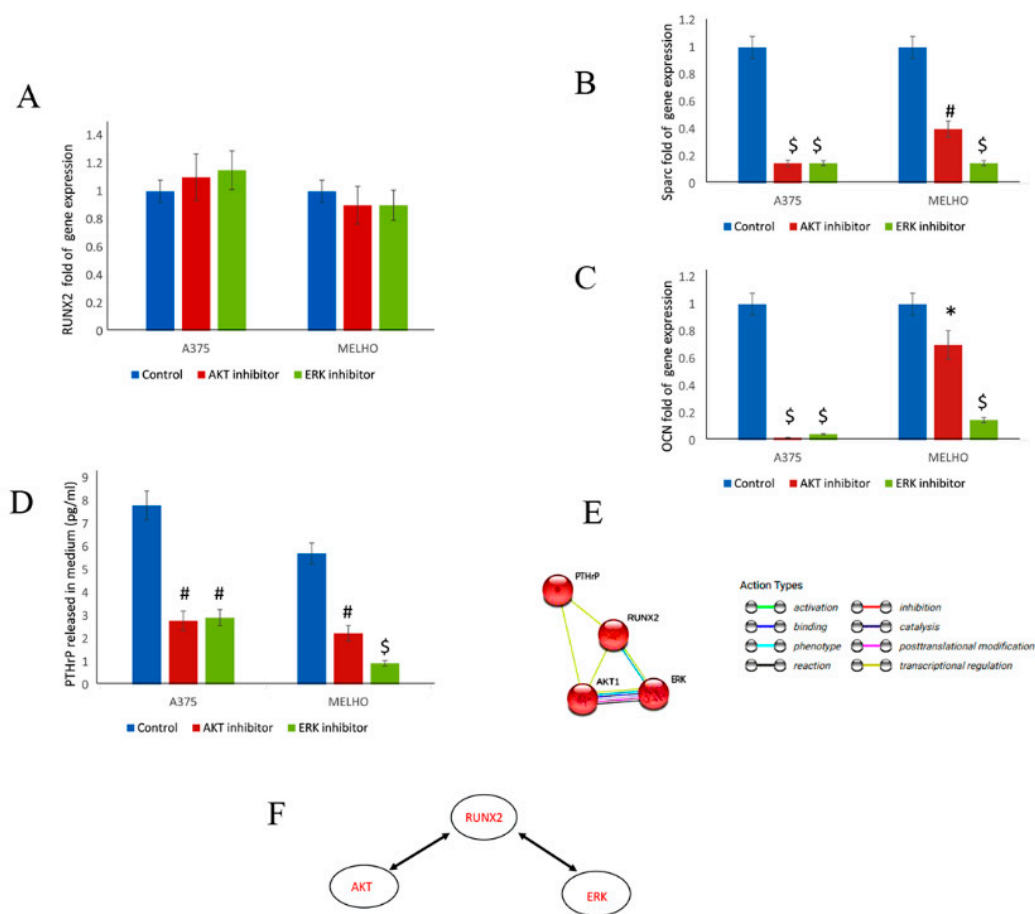


Figure 6. RUNX2 gene expression is not affected by AKT or ERK inhibitors (A) in WT melanoma cells. However, downstream target genes of RUNX2, namely Osteonectin (SPARC) (B) and Osteocalcin (OCN) (C) are downregulated by AKT or ERK inhibitor treatment. Both AKT and ERK inhibitors reduce the amount of PTHrP released by WT melanoma cells (D). Bioinformatics analyses show the interactions occurring (E). The reciprocal interaction and activation of RUNT/RUNX2 with AKT and ERK signaling (F). (* $p < 0.05$; # $p < 0.01$; \$ $p < 0.001$).

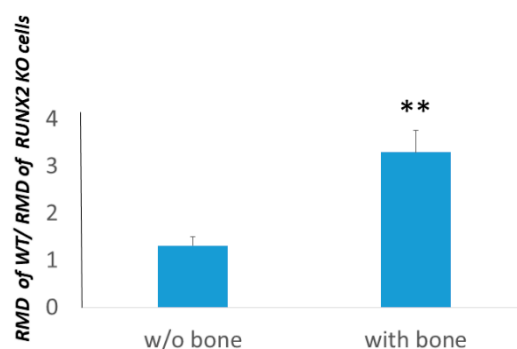


Figure 7. Relative migration distance ratio between WT and related RUNT KO cells. The presence of the RUNT domain in melanoma cells (WT) appears significantly more effective in promoting migration when bone fragments are present. ** $p < 0.01$.

To further analyze the role of the RUNT domain in driving melanoma cell migration to bone fragments, we tested the migration and invasion ability of WT and RUNT-KO melanoma cells, respectively, in a transwell system. The migration ability in the absence of bone fragments was lower for RUNT-KO cells compared to WT (Figure 8A). In the presence of bone fragments, the ability to

migrate was strongly increased in WT cells, while a comparatively lower ability to migrate was recorded for RUNT-KO cells (Figure 8B). However, the ability to migrate was restored in RUNX2-transfected RUNT KO cells (RUNT-KO++) (Figure 8B). Similarly, the invasion ability was higher in WT compared to RUNT-KO cells and the re-expression of RUNT restored this ability in both RUNT-KO cell lines (Figure 8C).

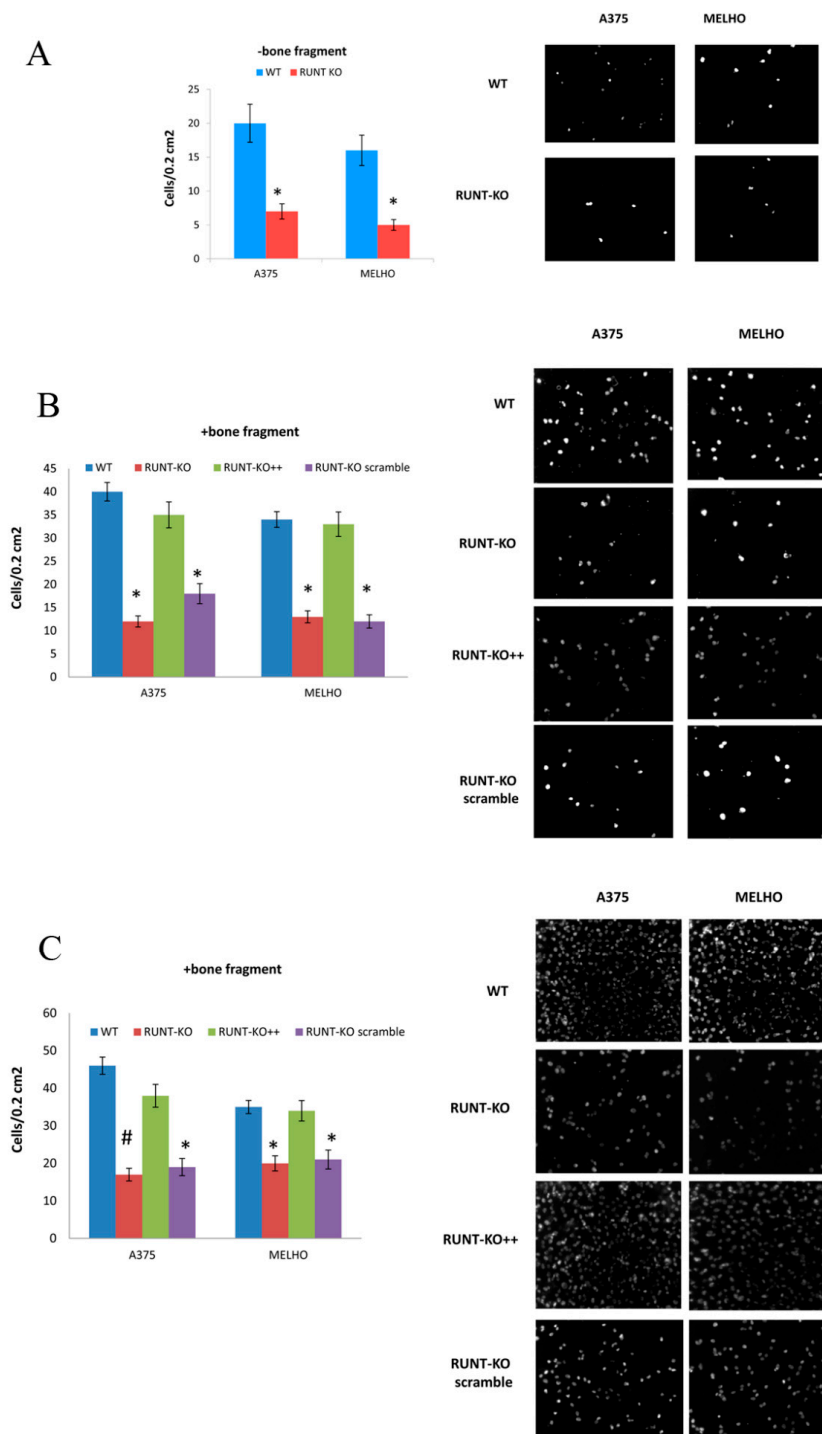


Figure 8. The ability to migrate was higher in WT compared to RUNT-KO cells (A). In addition, the presence of bone fragments increased migration (B) and invasion (C) abilities, which were greater in WT compared to RUNT-KO cells. Restored expression of RUNT domain in RUNT-KO cells re-established these abilities. Magnification 10X (* $p > 0.05$; # $p > 0.01$).

4. Discussion

The bone microenvironment regulates complex and relevant processes such as hematopoiesis, osteogenesis and osteolysis [1]. Various studies demonstrated that different molecular mechanisms are involved in promoting cancer cells residency in bone through chemotaxis in bone niches [25]. Most bone metastases occur when prostate, breast and lung primary tumors spread to the bone [26,27]. However, other primary tumors can induce bone metastases [27]. A retrospective study evaluating 98 MM patients reported that bone metastases occurred in 17.3% of cases [2,28]. Recently, radiographic imaging revealed the presence of bone metastases in 4.1% of patients at all stages of MM and in 17.2% of MM patients with metastatic disease [29]. However, as isotope bone scans may produce false-negative results [30], the actual frequency of bone metastases in metastatic MM should be considered to be higher. In post-mortem studies, bone metastases were found in 48.6% of patients with metastatic MM [31].

Transcription factor RUNX2 is the master gene of osteogenic differentiation. Its expression is high in pre-osteoblasts and in early osteoblasts, but decreases in mature osteoblasts [32]. However, RUNX2 is involved also in cellular transformation and appears upregulated in different solid tumors [9]. RUNX2 is ectopically expressed in melanoma and plays an important role in progression [7,8,33,34]. It belongs to the RUNX family, which includes also RUNX1 and RUNX3. These are RUNT-related heterodimeric transcription factors consisting of a DNA-binding “A” subunit and a non-DNA-binding “B” subunit, which enhances its affinity with DNA [35]. Among other domains, RUNX2 protein has a conserved 128-amino acid RUNT domain encoded by exons 2 to 4, which is necessary for DNA binding and heterodimerization with the non-DNA binding “B” subunit [32].

RUNX2 involvement in regulating the epithelial–mesenchymal transition (EMT) process has been demonstrated in melanoma [14]. Recently, we demonstrated that the RUNX2 RUNT domain affects EMT by increasing the expression of N-cadherin and reducing the expression of E-cadherin [21]. In addition, we found that the RUNT domain also promotes EMT by upregulating the expression of vimentin [21]. This is a noteworthy finding, considering vimentin correlation with high tumor growth rate, invasiveness and poor prognosis [35].

In lung cancers, RUNX2 overexpression was shown to promote EMT via direct regulation of vimentin along with other proteins [36,37]. Recently, it was demonstrated that RUNX2 participates in the transcriptional regulation of vimentin [38]. Yet, specific mechanisms related to RUNX2-dependent transcriptional regulation of vimentin need to be further explored in detail.

We demonstrated that the RUNT domain promotes melanoma cell proliferation and migration [21]. Accordingly, being aware of the strong association between RUNX2 and bone remodeling agents, we hypothesized that the RUNX2 RUNT domain is involved in mechanisms that promote bone metastasis in melanoma cells. With the aim to understand the molecular mechanisms modulated by RUNX2 RUNT domain in promoting bone metastasis, we performed gene expression analyses and cell signaling investigations in vitro. We obtained RUNT KO melanoma cell lines using CRISPR/Cas9-mediated gene editing. In RUNT KO melanoma cells, reduced expression of genes involved in metastatic processes (e.g., CD31, MMP9 and VEGFA) was observed, and genes involved in promoting bone metastasis, such as IBSP (coding for bone sialoprotein) and SPP1 (coding for osteopontin) [15], were downregulated. Notably, in RUNT KO melanoma cells, the expression of CD44 was also reduced. CD44 was identified as a receptor for hyaluronic acid, as well as for osteopontin, collagens and matrix metalloproteinases [39]. CD44 is a stemness marker associated with cancer metastatic progression [39]. The intracellular domain of CD44 can act as a co-transcription factor for RUNX2, inducing MMP-9 expression in breast carcinoma cells [40]. Recently, Senbanjo et al. demonstrated that RUNX2 complexes with the CD44 intracellular domain, thus inducing the expression of metastasis-related genes and increasing migration ability, as well as the formation of tumorspheres in prostatic cancer cells [41]. Notably, targeting of osteopontin or its receptors (e.g., CD44 and Integrin $\alpha\beta 3$) was suggested as a strategy to reduce carcinogenesis [42]. Gupta and coworkers demonstrated that Integrin $\alpha\beta 3$ and

CD44 are involved in prostate cancer patients bone loss by promoting osteoclastogenesis through the RUNX2/Smad 5/receptor activator of NF- κ B ligand pathways [43].

We also observed a reduced expression of PTHrP, an autocrine/paracrine ligand involved in malignancy-induced hypercalcaemia and skeletal metastatic lesions, in RUNT KO cells [17]. Interestingly, the addition of exogenous PTHrP in KO-cells restored the expression of metastatic genes. It was demonstrated that ectopic expression of RUNX2 increases PTHrP expression in neck and lung cancers [18]. In addition, since the ERK/pERK and AKT/pAKT pathways are associated with both RUNX2 and PTHrP expression, we investigated the modulation of these pathways in WT and RUNT KO melanoma cells. Interestingly, we found that both ERK/pERK and AKT/pAKT signaling processes were affected, entailing lower expression in RUNT KO melanoma cells. These findings suggested that the RUNT domain is involved in PTHrP expression through the regulation of these pathways, thus promoting bone metastasis. Bioinformatic analyses confirmed the RUNX2 interaction with AKT and ERK signalling. However, for the first time, we demonstrated that a reciprocal activation between the RUNX2 and AKT/ERK pathways occurs in melanoma. In fact, by treating WT melanoma cells with AKT or ERK inhibitors, we observed reduced activity of RUNX2, although RUNX2 gene expression was not affected. RUNX2 activity reduction due to inhibition of AKT or ERK signaling decreased PTHrP production in melanoma cells in turn. Therefore, we concluded that RUNX2 is involved in mechanisms that promote bone metastasis.

To evaluate the involvement of RUNX2 in osteotropic mechanisms, we performed *in vitro* experiments by using bone fragments as previously described by Mannavola and coworkers [24]. Employment of bone fragments was also reported by Templeton and coworkers to evaluate bone colonization of breast cancer cells [44]. Our data showed that RUNX2 KO cells exhibited statistically significant reductions in migration and invasion to bone fragments compared to WT cells. The re-expression of RUNT by transfecting KO cells with RUNX2 expression vectors restored cells' ability to migrate and invade bone fragments. This finding supports the transcriptional role of the RUNT domain in binding its downstream target genes, such as IBSP and SPP1, which are involved in bone metastasis promotion [45,46]. As discussed above, we observed reduced expression of SPP1 in RUNX2 KO cells. Osteopontin, an SPP1 gene product, was demonstrated to be involved in different steps of carcinogenesis, such as cell mobility, neoangiogenesis, invasion, intravasation and extravasation, as well as bone metastasization [45,47]. In summary, our findings, including reduced osteopontin, bone sialoprotein and CD44, supported RUNX2 involvement in promoting melanoma cell osteotropism. One limitation of our study may be the lack of an *in vivo* model. However, the purpose of this study was to deepen our understanding of the role of RUNX2 in modulating the molecular mechanisms that promote bone metastasis. Our results showed that RUNX2 is involved in the expression modulation of key genes. SPP1, bone sialoprotein and molecules that enhance bone metastasis, such as PTHrP, are significant examples which could stimulate further studies. In particular, the employment of animal models could be helpful to evaluate the role of the immune system or the angiogenesis process in the metastatic niche.

Finally, since our results showed that the RUNT domain affects the expression and the activity of various molecules involved in bone metastasis, we conclude that RUNX2, via the RUNT domain, may promote bone metastasis of melanoma through a complex scenario affecting different and strongly associated pathways.

Supplementary Materials: The following are available online at <http://www.mdpi.com/2073-4409/9/3/751/s1>, Table S1: List of modulated genes in RUNT-KO.

Author Contributions: Conceptualization, D.Z. and M.T.V.; methodology, M.D., M.S., S.C., S.M., A.G., G.I., J.B., M.C. and P.L.; software, L.D.C.; validation, M.G.R. and M.M.; investigation, M.D., S.C., G.I. and F.A.; data curation, L.D.C., M.M. and D.Z.; writing—original draft preparation, D.Z. and M.T.V.; writing—review and editing, M.G.R., M.M., D.Z. and M.T.V.; supervision, L.D.C.; funding acquisition, L.D.C. and D.Z. All authors have read and agreed to the published version of the manuscript.

Funding: This research was funded by the FUR (Fondo Unico della Ricerca of University of Verona) of Dalle Carbonare.

Conflicts of Interest: The authors declare no conflict of interest.

References

1. Aielli, F.; Ponzetti, M.; Rucci, N. Bone metastasis pain, from the bench to the bedside. *Int. J. Mol. Sci.* **2019**, *20*, 280. [[CrossRef](#)] [[PubMed](#)]
2. Patten, R.M.; Shuman, W.P.; Teefey, S. Metastases from malignant melanoma to the axial skeleton: A CT study of frequency and appearance. *AJR Am. J. Roentgenol.* **1990**, *155*, 109–112. [[CrossRef](#)] [[PubMed](#)]
3. Clauser, L.C.; Tieghi, R.; Galie, M.; Carinci, F. Structural fat grafting: Facial volumetric restoration in complex reconstructive surgery. *J. Craniofac. Surg.* **2011**, *22*, 1695–1701. [[CrossRef](#)] [[PubMed](#)]
4. Rucci, N.; Teti, A. Osteomimicry: How the Seed Grows in the Soil. *Calcif. Tissue Int.* **2018**, *102*, 131–140. [[CrossRef](#)]
5. Coleman, R.E. Impact of bone-targeted treatments on skeletal morbidity and survival in breast cancer. *Oncology* **2016**, *30*, 695–702.
6. Damsky, W.E.; Bosenberg, M. Melanocytic nevi and melanoma: Unraveling a complex relationship. *Oncogene* **2017**, *36*, 5771–5792. [[CrossRef](#)]
7. Cohen-Solal, K.A.; Boregowda, R.K.; Lasfar, A. RUNX2 and the PI3K/AKT axis reciprocal activation as a driving force for tumor progression. *Mol. Cancer* **2015**, *14*, 137. [[CrossRef](#)]
8. Perduca, M.; Carbonare, L.D.; Bovi, M.; Innamorati, G.; Cheri, S.; Cavallini, C.; Scupoli, M.T.; Mori, A.; Valenti, M.T. Runx2 downregulation, migration and proliferation inhibition in melanoma cells treated with BEL beta-trefoil. *Oncol. Rep.* **2017**, *37*, 2209–2214. [[CrossRef](#)]
9. Valenti, M.T.; Serafini, P.; Innamorati, G.; Gili, A.; Cheri, S.; Bassi, C.; Dalle Carbonare, L. Runx2 expression: A mesenchymal stem marker for cancer. *Oncol. Lett.* **2016**, *12*, 4167–4172. [[CrossRef](#)]
10. Valenti, M.T.; Dalle Carbonare, L.; Mottes, M. Ectopic expression of the osteogenic master gene RUNX2 in melanoma. *World J. Stem Cells* **2018**, *10*, 78–81. [[CrossRef](#)]
11. Dalle Carbonare, L.; Frigo, A.; Francia, G.; Davi, M.V.; Donatelli, L.; Stranieri, C.; Brazzarola, P.; Zatelli, M.C.; Menestrina, F.; Valenti, M.T. Runx2 mRNA expression in the tissue, serum, and circulating non-hematopoietic cells of patients with thyroid cancer. *J. Clin. Endocrinol. Metab.* **2012**, *97*, E1249–E1256. [[CrossRef](#)] [[PubMed](#)]
12. Zhang, X.; Akech, J.; Browne, G.; Russell, S.; Wixted, J.J.; Stein, J.L.; Stein, G.; Lian, J. Runx2-Smad signaling impacts the progression of tumor-induced bone disease. *Int. J. Cancer* **2015**, *136*, 1321–1332. [[CrossRef](#)] [[PubMed](#)]
13. Kruger, T.E.; Miller, A.H.; Godwin, A.K.; Wang, J. Bone sialoprotein and osteopontin in bone metastasis of osteotropic cancers. *Crit. Rev. Oncol. Hematol.* **2014**, *89*, 330–341. [[CrossRef](#)] [[PubMed](#)]
14. Riminucci, M.; Corsi, A.; Peris, K.; Fisher, L.W.; Chimenti, S.; Bianco, P. Coexpression of bone sialoprotein (BSP) and the pivotal transcriptional regulator of osteogenesis, Cbfa1/Runx2, in malignant melanoma. *Calcif. Tissue Int.* **2003**, *73*, 28128–28129. [[CrossRef](#)]
15. Ibrahim, T.; Leong, I.; Sanchez-Sweatman, O.; Khokha, R.; Sodek, J.; Tenenbaum, H.C.; Ganss, B.; Cheifetz, S. Expression of bone sialoprotein and osteopontin in breast cancer bone metastases. *Clin. Exp. Metastasis* **2000**, *18*, 253–260. [[CrossRef](#)]
16. Nemoto, H.; Rittling, S.R.; Yoshitake, H.; Furuya, K.; Amagasa, T.; Tsuji, K.; Nifuji, A.; Denhardt, D.T.; Noda, M. Osteopontin deficiency reduces experimental tumor cell metastasis to bone and soft tissues. *J. Bone Miner. Res.* **2001**, *16*, 652–659. [[CrossRef](#)]
17. Soki, F.N.; Park, S.I.; McCauley, L.K. The multifaceted actions of PTHrP in skeletal metastasis. *Futur. Oncol.* **2012**, *8*, 803–817. [[CrossRef](#)]
18. Chang, W.M.; Lin, Y.F.; Su, C.Y.; Peng, H.Y.; Chang, Y.C.; Hsiao, J.R.; Chen, C.L.; Chang, J.Y.; Shieh, Y.S.; Hsiao, M.; et al. Parathyroid Hormone-Like Hormone is a Poor Prognosis Marker of Head and Neck Cancer and Promotes Cell Growth via RUNX2 Regulation. *Sci. Rep.* **2017**, *7*, 41131. [[CrossRef](#)]
19. De Gortazar, A.R.; Alonso, V.; Alvarez-Arroyo, M.V.; Esbrit, P. Transient exposure to PTHrP (107–139) exerts anabolic effects through vascular endothelial growth factor receptor 2 in human osteoblastic cells in vitro. *Calcif. Tissue Int.* **2006**, *79*, 360–369. [[CrossRef](#)]
20. Lu, H.; Jiang, T.; Ren, K.; Li, Z.L.; Ren, J.; Wu, G.; Han, X. RUNX2 plays an oncogenic role in esophageal carcinoma by activating the PI3K/AKT and ERK signaling pathways. *Cell. Physiol. Biochem.* **2018**, *49*, 217–225. [[CrossRef](#)]

21. Deiana, M.; Dalle Carbonare, L.; Serena, M.; Cheri, S.; Parolini, F.; Gandini, A.; Marchetto, G.; Giulio, I.; Manfredi, M.; Marengo, E.; et al. New insights into the runt domain of RUNX2 in melanoma cell proliferation and migration. *Cells* **2018**, *7*, 220. [[CrossRef](#)] [[PubMed](#)]
22. Romanelli, M.G.; Lorenzi, P.; Sangalli, A.; Diani, E.; Mottes, M. Characterization and functional analysis of cis-acting elements of the human farnesyl diphosphate synthetase (FDPS) gene 5' flanking region. *Genomics* **2009**, *93*, 227–234. [[CrossRef](#)] [[PubMed](#)]
23. Park, E.; Gong, E.Y.; Romanelli, M.G.; Lee, K. Suppression of estrogen receptor-alpha transactivation by thyroid transcription factor-2 in breast cancer cells. *Biochem. Biophys. Res. Commun.* **2012**, *421*, 532–537. [[CrossRef](#)] [[PubMed](#)]
24. Mannavola, F.; Tucci, M.; Felici, C.; Passarelli, A.; D'Oronzo, S.; Silvestris, F. Tumor-derived exosomes promote the in vitro osteotropism of melanoma cells by activating the SDF-1/CXCR4/CXCR7 axis. *J. Transl. Med.* **2019**, *17*, 230. [[CrossRef](#)]
25. Sowder, M.E.; Johnson, R.W. Bone as a preferential site for metastasis. *JBMR Plus* **2019**, *3*, e10126. [[CrossRef](#)]
26. Hofbauer, L.C.; Rachner, T.D.; Coleman, R.E.; Jakob, F. Endocrine aspects of bone metastases. *Lancet Diabetes Endocrinol.* **2014**, *2*, 500–512. [[CrossRef](#)]
27. Karim, S.M.; Brown, J.; Zekri, J. Efficacy of bisphosphonates and other bone-targeted agents in metastatic bone disease from solid tumors other than breast and prostate cancers. *Clin. Adv. Hematol. Oncol.* **2013**, *11*, 281–287.
28. Makhoul, I.; Montgomery, C.O.; Gaddy, D.; Suva, L.J. The best of both worlds - managing the cancer, saving the bone. *Nat. Rev. Endocrinol.* **2016**, *12*, 29–42. [[CrossRef](#)]
29. Zekri, J.; Marples, M.; Taylor, D.; Kandukurti, K.; McParland, L.; Brown, J.E. Complications of bone metastases from malignant melanoma. *J. Bone Oncol.* **2017**, *8*, 13–17. [[CrossRef](#)]
30. Gokaslan, Z.L.; Aladag, M.A.; Ellerhorst, J.A. Melanoma metastatic to the spine: A review of 133 cases. *Melanoma Res.* **2000**, *10*, 78–80. [[CrossRef](#)]
31. Patel, J.K.; Didolkar, M.S.; Pickren, J.W.; Moore, R.H. Metastatic pattern of malignant melanoma. A study of 216 autopsy cases. *Am. J. Surg.* **1978**, *135*, 807–810. [[CrossRef](#)]
32. Dalle Carbonare, L.; Innamorati, G.; Valenti, M.T. Transcription factor Runx2 and its Application to bone tissue engineering. *Stem Cell Rev. Rep.* **2012**, *8*, 891–897. [[CrossRef](#)] [[PubMed](#)]
33. Boregowda, R.K.; Medina, D.J.; Markert, E.; Bryan, M.A.; Chen, W.; Chen, S.; Rabkin, A.; Vido, M.J.; Gunderson, S.I.; Chekmareva, M.; et al. The transcription factor RUNX2 regulates receptor tyrosine kinase expression in melanoma. *Oncotarget* **2016**, *7*, 29689–29707. [[CrossRef](#)] [[PubMed](#)]
34. Boregowda, R.K.; Olabisi, O.O.; Abushahba, W.; Jeong, B.S.; Haenssen, K.K.; Chen, W.; Chekmareva, M.; Lasfar, A.; Foran, D.J.; Goydos, J.S.; et al. RUNX2 is overexpressed in melanoma cells and mediates their migration and invasion. *Cancer Lett.* **2014**, *348*, 61–70. [[CrossRef](#)] [[PubMed](#)]
35. Satelli, A.; Li, S. Vimentin in cancer and its potential as a molecular target for cancer therapy. *Cell. Mol. Life Sci.* **2011**, *68*, 3033–3046. [[CrossRef](#)]
36. Bradner, J.E.; Hnisz, D.; Young, R.A. Transcriptional addiction in cancer. *Cell* **2017**, *168*, 629–643. [[CrossRef](#)] [[PubMed](#)]
37. Sancisi, V.; Gandolfi, G.; Ambrosetti, D.C.; Ciarrocchi, A. Histone deacetylase inhibitors repress tumoral expression of the proinvasive factor RUNX2. *Cancer Res.* **2015**, *75*, 1868–1882. [[CrossRef](#)]
38. Herreno, A.M.; Ramirez, A.C.; Chaparro, V.P.; Fernandez, M.J.; Canas, A.; Morantes, C.F.; Moreno, O.M.; Brugués, R.E.; Mejía, J.A.; Bustos, F.J.; et al. Role of RUNX2 transcription factor in epithelial mesenchymal transition in non-small cell lung cancer lung cancer: Epigenetic control of the RUNX2 P1 promoter. *Tumour Biol.* **2019**, *41*, 1010428319851014. [[CrossRef](#)]
39. Senbanjo, L.T.; Chellaiah, M.A. CD44: A multifunctional cell surface adhesion receptor is a regulator of progression and metastasis of cancer cells. *Front. Cell Dev. Biol.* **2017**, *5*, 18. [[CrossRef](#)]
40. Milette-Gonzalez, K.E.; Murphy, K.; Kumaran, M.N.; Ravindranath, A.K.; Wernyj, R.P.; Kaur, S.; Miles, G.; Lim, E.T.; Chan, R.; Chekmareva, M.; et al. Identification of function for CD44 intracytoplasmic domain (CD44-ICD): Modulation of matrix metalloproteinase 9 (MMP-9) transcription via novel promoter response element. *J Biol Chem.* **2012**, *287*, 18995–19007. [[CrossRef](#)]
41. Senbanjo, L.T.; AlJohani, H.; Majumdar, S.; Chellaiah, M.A. Characterization of CD44 intracellular domain interaction with RUNX2 in PC3 human prostate cancer cells. *Cell Commun. Signal.* **2019**, *17*, 80. [[CrossRef](#)]

42. Zhao, H.; Chen, Q.; Alam, A.; Cui, J.; Suen, K.C.; Soo, A.P.; Eguchi, S.; Gu, J.; Ma, D. The role of osteopontin in the progression of solid organ tumour. *Cell Death Dis.* **2018**, *9*, 356. [[CrossRef](#)]
43. Gupta, A.; Cao, W.; Chellaiah, M.A. Integrin alphavbeta3 and CD44 pathways in metastatic prostate cancer cells support osteoclastogenesis via a Runx2/Smad 5/receptor activator of NF-kappaB ligand signaling axis. *Mol Cancer.* **2012**, *11*, 66. [[CrossRef](#)]
44. Templeton, Z.S.; Lie, W.R.; Wang, W.; Rosenberg-Hasson, Y.; Alluri, R.V.; Tamaresis, J.S.; Bachmann, M.H.; Lee, K.; William, J.; Maloney, W.J.; et al. Breast cancer cell colonization of the human bone marrow adipose tissue niche. *Neoplasia* **2015**, *17*, 849–861. [[CrossRef](#)]
45. Allan, A.L.; Tuck, A.B.; Bramwell, V.H.C.; Vandenberg, T.A.; Winqvist, E.W.; Chambers, A.F.; Singh, G. *Contribution of Osteopontin to the Development of Bone Metastasis*; Singh, G., Rabbani, S.A., Eds.; Humana Press: Totowa, NJ, USA, 2005.
46. Wang, L.; Song, L.; Li, J.; Wang, Y.; Yang, C.; Kou, X.; Xiao, B.; Zhang, W.; Li, L.; Liu, S.; et al. Bone sialoprotein-alpha3 integrin axis promotes breast cancer metastasis to the bone. *Cancer Sci.* **2019**, *110*, 3157–3172. [[CrossRef](#)]
47. Shevde, L.A.; Samant, R.S. Role of osteopontin in the pathophysiology of cancer. *Matrix Biol.* **2014**, *37*, 131–141. [[CrossRef](#)]



© 2020 by the authors. Licensee MDPI, Basel, Switzerland. This article is an open access article distributed under the terms and conditions of the Creative Commons Attribution (CC BY) license (<http://creativecommons.org/licenses/by/4.0/>).